R80-45

OSP 85052
89965

WATER BALANCE STUDIES OF THE BAHR EL GHAZAL SWAMP

by
Siu-On Chan
and
Peter S. Eagleson

MIT

DEPARTMENT
OF
CIVIL
ENGINEERING

RALPH M. PARSONS LABORATORY
FOR
WATER RESOURCES AND HYDRODYNAMICS

Department of Civil Engineering
Massachusetts Institute of Technology

SCHOOL OF ENGINEERING
MASSACHUSETTS INSTITUTE OF TECHNOLOGY
Cambridge, Massachusetts 02139

Report No. 261

Prepared under the Support of
The Agency for International Deveopment
The United States Department of State
and the
Technology Adaptation Program

December 1980

R80-45

OSP 85052
89965

WATER BALANCE STUDIES OF THE BAHR EL GHAZAL SWAMP

by

SIU-ON CHAN

and

PETER S. EAGLESON

RALPH M. PARSONS LABORATORY

FOR WATER RESOURCES AND HYDRODYNAMICS

Department of Civil Engineering

MASSACHUSETTS INSTITUTE OF TECHNOLOGY

Report No. 261

Prepared under the Support of

The Agency for International Development

The United States Department of State

December 1980

ABSTRACT

Future increases in Egyptian and Sudanese water resources may come from reduction of the large water losses of the Upper White Nile's swampy regions, particularly from the Bahr el Ghazal swamp. In this work, new methods of water balance estimation which incorporate the dynamic interaction of climate, soil and vegetation are applied to the Bahr el Ghazal basin in order to study its contribution to the flow of the White Nile, and to estimate the potential water recovery through drainage of this swamp.

ACKNOWLEDGEMENTS

This work was sponsored by the M.I.T. Technology Adaptation Program which is funded through a grant from the Agency for International Development, United States Department of State.

The work was performed by Siu-On Chan, Research Assistant, and essentially as given here, constitutes his thesis presented in partial fulfillment of the requirements for the degree of Civil Engineer in the field of Water Resources. The work was supervised by Dr. Peter S. Eagleson, Professor of Civil Engineering

The authors wish to thank the many persons who made contributions to this work.

They are very grateful to Dr. Romas Krzysztofowicz, Mr. Fabio Ramos and Dr. Dick K. Yue for their many helpful discussions.

Particular thanks are due to Mr. Pedro Restrepo who provided technical assistance on computer work, and to Mrs. Anne L. Clee, who typed this report.

TABLE OF CONTENTS

Page No.

Page No.

Page No.

Page No.

LIST OF PRINCIPAL SYMBOLS

NOTE:

1) Symbols not included in the list are defined in the text wherever they are used.

2) In cases if a single notation represents more than one quantity in the text, it should be self-evident from the context to which it implies.

3) In the text, overhead bar normally indicates time average and underbar, areal average.

A	catchment area, km^2
A_s	shortwave albedo of wet soil surface
A_w	space-time average wetted surface area in a catchment, km^2
a_i, a_j	monthly proportionality factor
b_i	ratio of gaged mean monthly yield to gaged mean annual monthly yield for the i^{th} month
c	pore disconnectedness index
C_L	total canal construction cost, U.S. $
D_o	deep seepage at Central Swampland, md
D_B	deep seepage at the Bahr el Ghazal basin, md
d	diffusivity index
E	evaporation effectiveness
E_{p_A}	annual (seasonal) total potential evapotranspiration, cm
E_{r_A}	annual (seasonal) surface retention, cm
E_{rs}	surface retention loss from bare soil fraction, cm
E_{rv}	surface retention loss from vegetated fraction, cm
E_r	surface retention loss, cm
E_s	soil moisture evaporation from bare soil fraction, cm
E_v	transpiration from vegetated fraction of surface, cm

E_{T_A}	annual (seasonal) evapotranspiration, cm
e_p	potential evaporation rate of wet soil surface, cm/day
e_{pw}	potential evaporation rate of water surface, cm/day
e_p^*	weighted potential evapotranspiration rate, cm/day
e_p'	Piche tube water evaporation rate, cm/day
G	gravitational infiltration parameter
G_L	ungaged inflow to Central Swampland, md
H	mean residual sensible heat flux, ly/min
H	depth of channel, m
h	storm depth, cm
h_o	surface retention capacity, cm
J_o	annual Jebel spillage, md
$K(1)$	saturated hydraulic conductivity, cm/sec
k_v	potential transpiration efficiency
k_v'	plant coefficient
L_e	latent heat of vaporization, $\cong$ 597 cal/g
M	vegetated fraction of surface (vegetal canopy density)
M_o	equilibrium vegetal canopy density
m	pore size distribution index
m_ν	mean annual (seasonal) number of storms
m_ν'	mean annual (seasonal) number of rainy days
$m_{\nu c}$	mean annual (seasonal) number of catchment storms
m_τ	mean length of rainy season, days
m_H	mean storm depth, cm
m_i	mean storm intensity, cm/sec

m_{t_r} mean storm duration, days

m_{t_b} mean time between storms, days

N cloud cover

n effective medium porosity

P_A annual precipitation, cm

P_o annual precipitation at Central Swampland, md

P_s annual seasonal precipitation, cm

q canal flow, md/yr

q_i insolation rate on a unit surface of the catchment, ly/min

q_i monthly canal flow, md/month

q_b net outgoing longwave radiation rate, ly/min

q_c canal capacity, md/yr, Mm^3/day

q_{cm} monthly canal capacity, md/mo, Mm^3/mo

q_A annual canal flow, md/yr

q_N annual canal flow from the north-going canal, md/yr

q_S annual canal flow from the south-going canal, md/yr

q_T total annual potential water recovery at Malakal, md/yr

q_{CS} capacity of south-going canal, md/yr

q_{CN} capacity of north-going canal, md/yr

R_{g_A} annual (seasonal) groundwater runoff, cm

R_{s_A} annual (seasonal) surface runoff, cm

S relative humidity

s_o space-time average soil moisture in surface boundary layer

T_A air temperature, °C

T_S wet season air temperature, °C

w	capillary rise from water table, cm/sec
w	top width of canal, m
x	normalized annual canal flow
x_c	normalized annual canal capacity
x_{ci}, x_{cj}	normalized monthly canal capacity
x_i	normalized monthly canal flow
x_N	normalized annual canal flow from the north-going canal
x_S	normalized annual canal flow from the south-going canal
x_T	normalized total annual potential water recovery at Malakal
x_{CS}	normalized annual canal capacity of the south-going canal
x_{CN}	normalized annual canal capacity of the north-going canal
Y_A	annual catchment yield, cm
y	normalized annual catchment yield
Z	depth to water table, cm
α	reciprocal of m_i, sec/cm
β	reciprocal of m_{t_b}, days^{-1}
δ	reciprocal of m_{t_r}, day^{-1}
η	reciprocal of m_H, cm^{-1}
κ	parameter of Gamma distribution of storm depth
λ	parameter of Gamma distribution of storm depth, equal to κ/m_H, cm^{-1}
Δ	slope of vapor pressure-temperature curve
Δ	relative error term

ν	counting variable for number of storms
σ	capillary infiltration parameter
σ_x	standard deviation of x
μ_x	mean of x
τ	length of rainy season, days
ϕ_e	dimensionless desorption diffusivity
ϕ_i	dimensionless sorption diffusivity
$\psi(1)$	saturated soil matrix potential, cm (suction)
E[ ]	expected value of [ ]
J[ ]	evapotranspiration function
P[a, x]	Pearson's incomplete Gamma function
Var[ ]	variance of [ ]
Γ[ ]	Gamma function
γ[a, x]	incomplete Gamma function

LIST OF TABLES

LIST OF FIGURES

Chapter 1

INTRODUCTION

1.1 The Nile System

The river Nile flows a distance of 6680 kilometers from its source in the equatorial lakes to the Mediterranean Sea. It is the second longest river in the world, shorter than the Mississippi-Missouri (6823 km), but longer than the Amazon (6437 km). Except for its headwaters, the Nile flows through only two countries, the Republic of the Sudan and Egypt. Figure 1.1 shows the Nile system. The numbers in brackets are the mean annual discharges in milliards* of cubic meters along its course.

The waters of the lower Nile come from two main sources - the Blue Nile in the east and the White Nile in the south. The White Nile originates in a series of equatorial lakes lying astride several international boundaries. These lakes include Lake Albert, Lakes Edward and George, Lake Kioga and Lake Victoria. The last is the largest and contributes more than 90% of the total headwaters flow (23 md). Most of the lakes are within the boundaries of Uganda, while the southern-half of Lake Victoria is in the territory of Tanzania.

The upper White Nile is known as the Albert Nile from Lake Albert to Nimule, and as the Bahr el Jebel from Nimule to Lake No. At Lake No, the White Nile receives a very minor inflow from the Bahr el Ghazal (0.6 md). Between Lake No and Malakal, it is joined by two more tributaries, the Bahr el Zeraf (4 md) and the Sobat (13 md), all of which

*1 milliard (md) $\equiv 10^9$. When used by itself hereafter, the term will refer to the number of cubic meters annually.

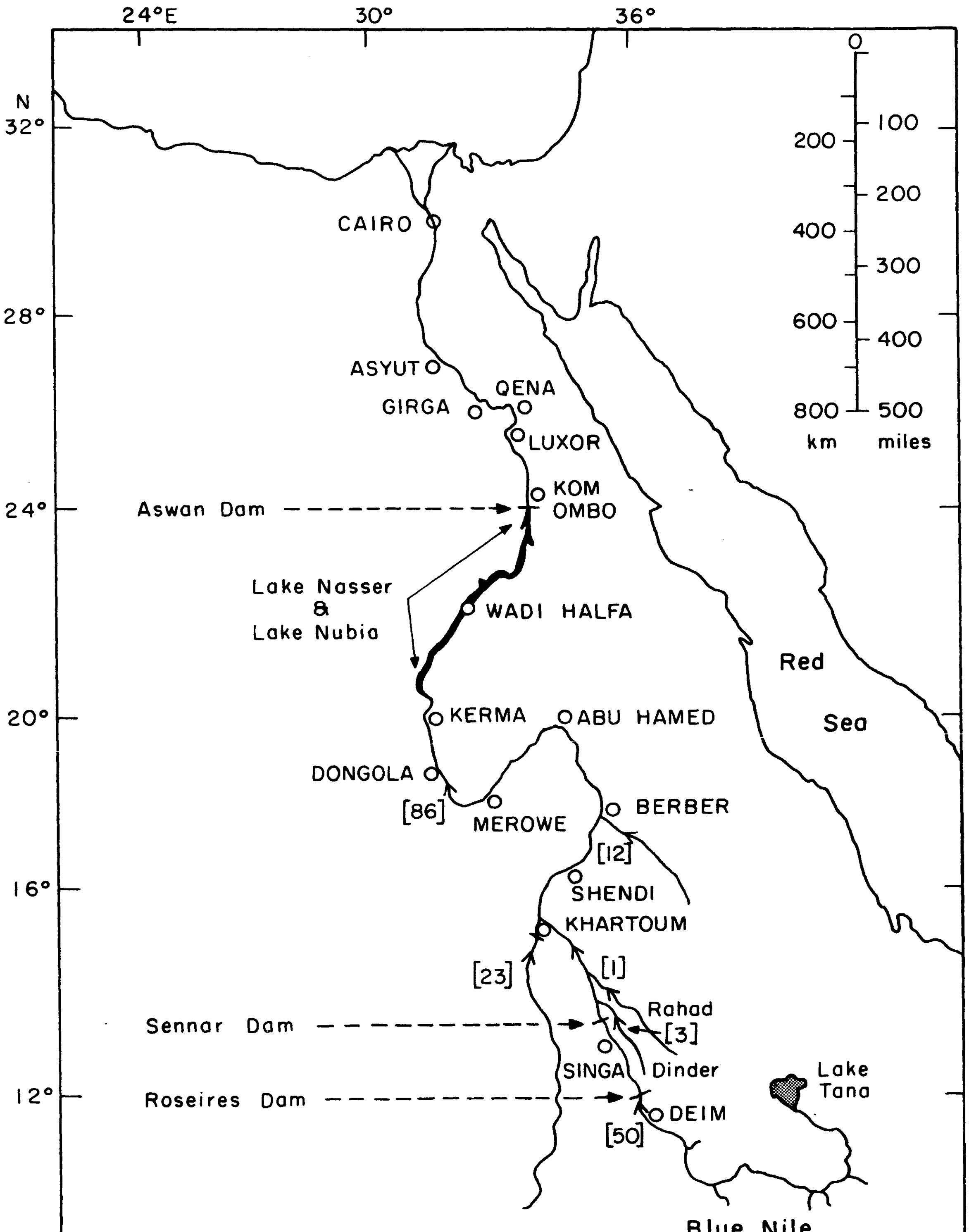

FIGURE 1.1a

THE NILE SYSTEM — THE BLUE NILE AND THE JOINT NILE (1)

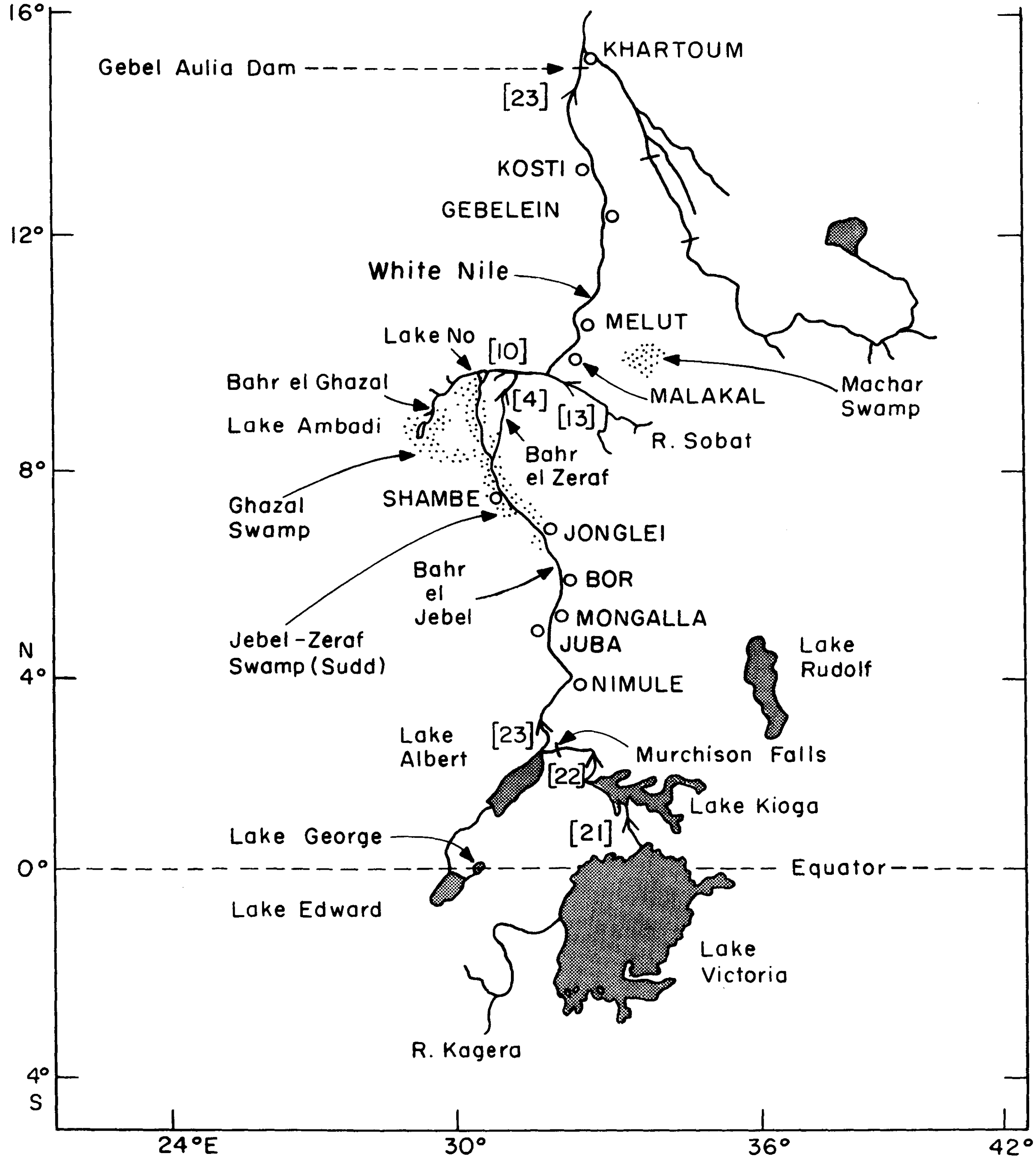

FIGURE 1.1b

THE NILE SYSTEM — THE HEADWATER LAKES AND THE WHITE NILE (1) give the White Nile a combined flow of 27 md at Malakal. It then flows from Malakal to Khartoum, where it is joined by the Blue Nile flowing from the east.

The Blue Nile, starting from Lake Tana in Ethiopia, receives its water from numerous streams along its course, and by the time it gets to the Roseires Dam, the discharge amounts to 50 md - the largest among all tributaries of the Nile. It then receives two more tributaries, the Dinder (3 md) and Rahad (1 md) before joining the White Nile at Khartoum.

The last tributary, the Atbara (12 md), enters the Nile 322 km downstream from Khartoum. This is an ephemeral river, active only during the July to October rainy season.

The White Nile, the Blue Nile and the Atbara jointly give the Nile a total natural discharge of 86 md, which is the approximate mean annual inflow to Lake Nasser at Dongola. According to the Nile Water Agreement concluded between Egypt and Sudan in 1959, 55.5 md of water is allocated to Egypt at the Aswan Dam and 18.5 md is allocated to Sudan (2). The remaining 12 md is accounted for by evaporation and seepage at Lake Nasser.

The longitudinal profiles of the White and Main Nile are shown in Figure 1.2, and the distribution of rainfall along the Nile system is shown in Figure 1.3.

1.2 Apparent Water Losses in the Swampy Region of the Upper Nile Basin

Before reaching Mongalla, the Bahr el Jebel is joined by numerous streams contributing 4.3 md, so that at Mongalla the total discharge is 27 md (see Figure 1.4).

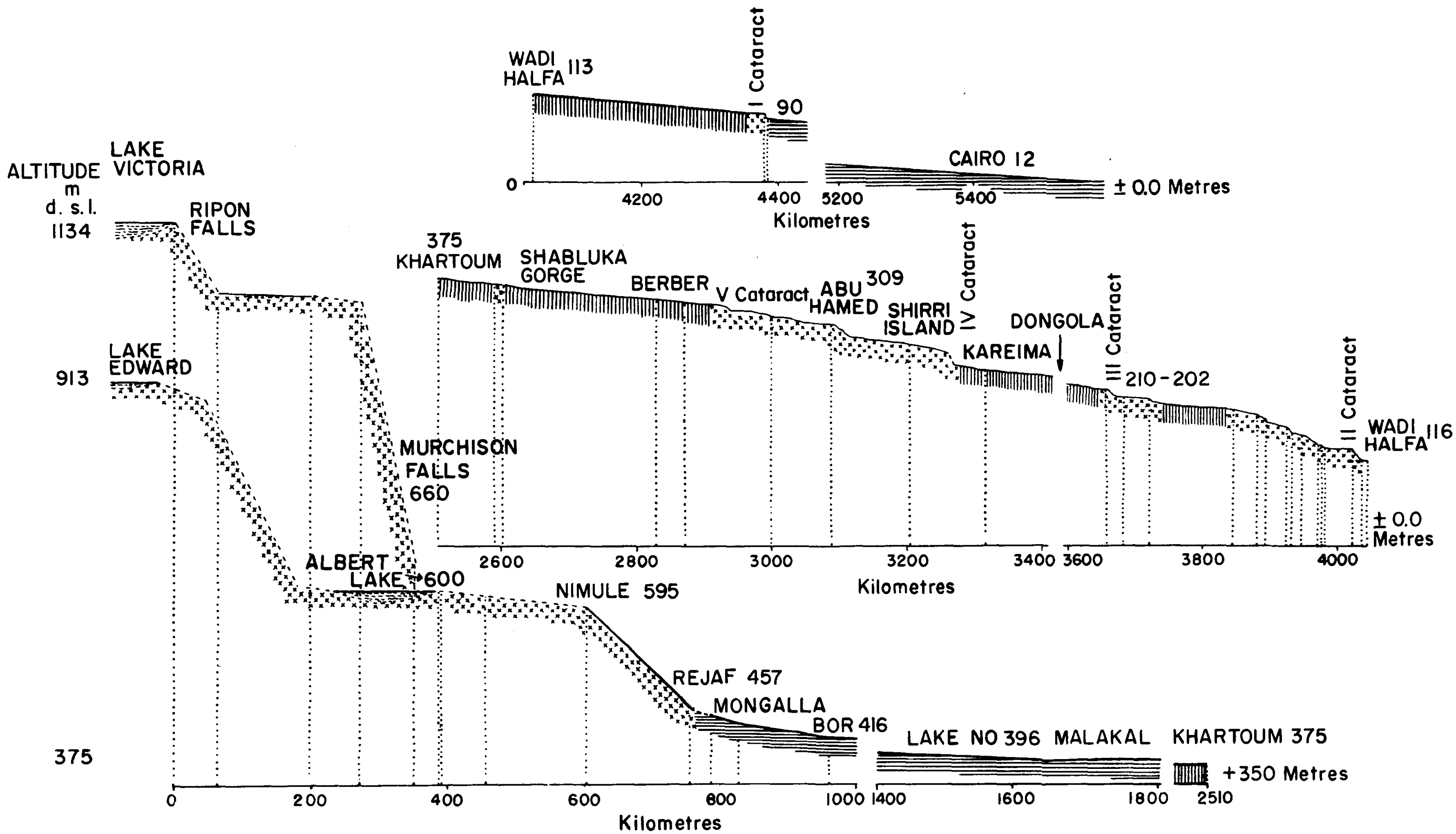

FIGURE 1.2

LONGITUDINAL PROFILE OF WHITE AND MAIN NILE (1)

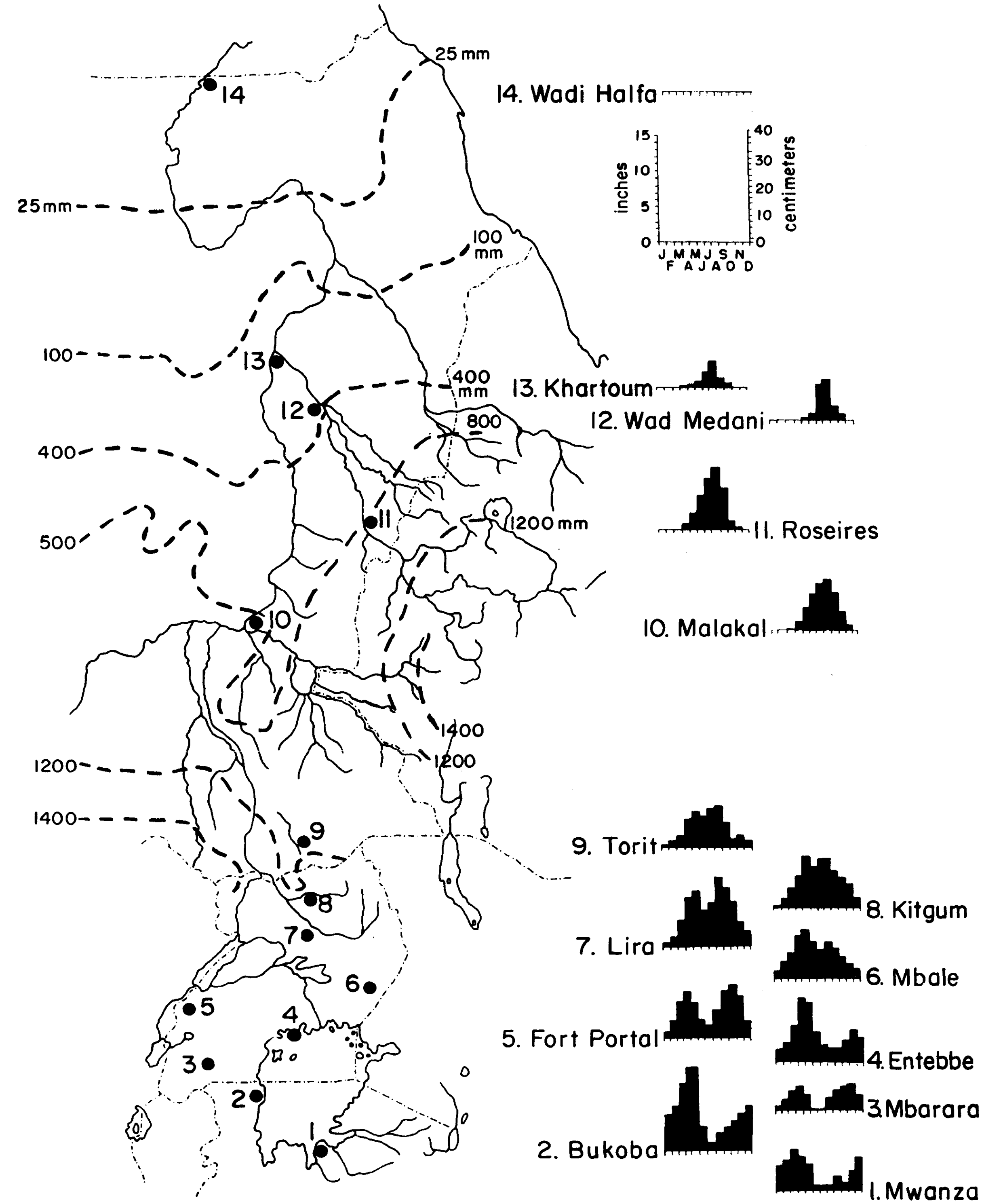

FIGURE 1.3

RAINFALL DISTRIBUTION ALONG THE NILE SYSTEM (1)

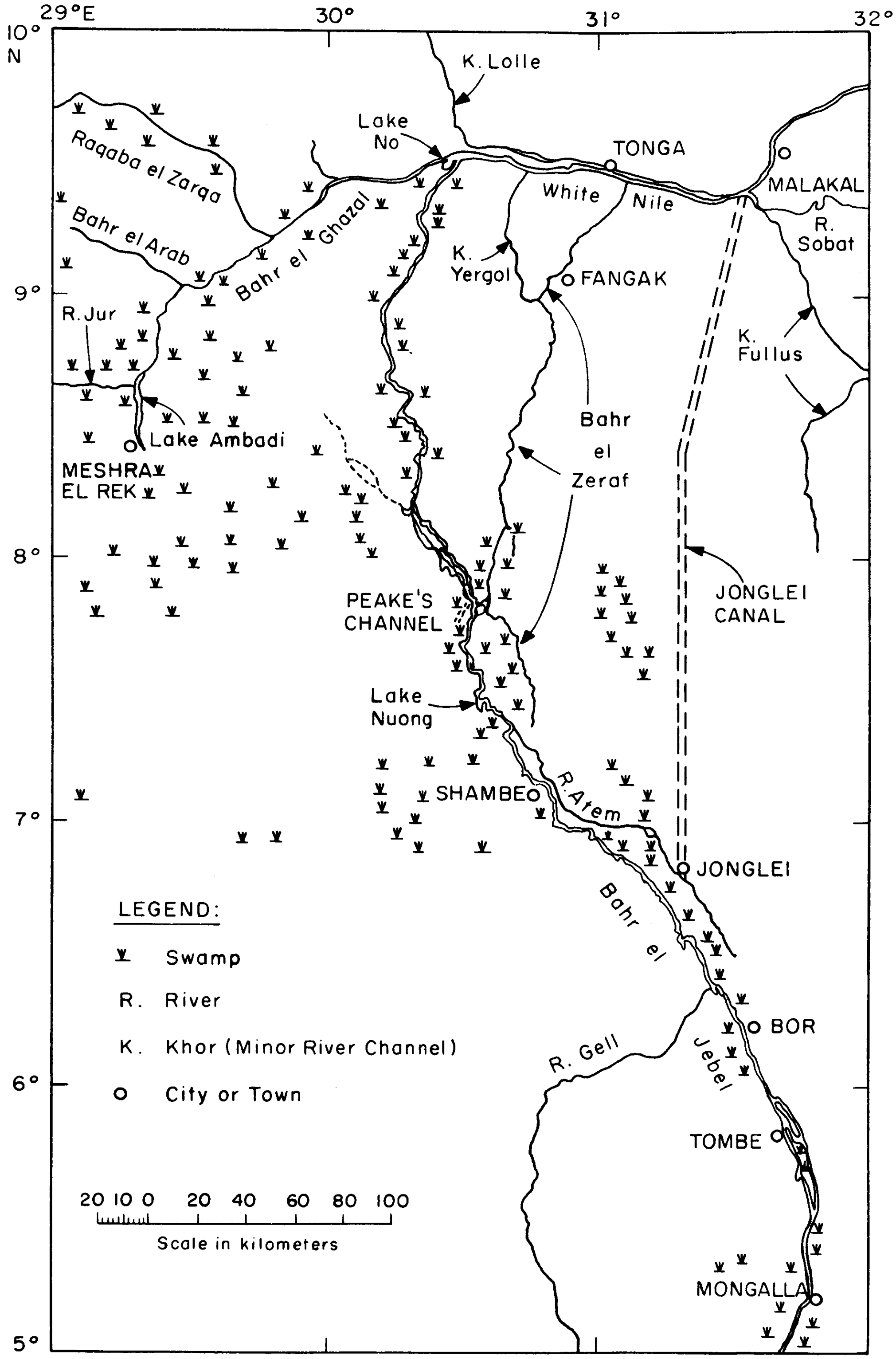

FIGURE 1.4

JEBEL-ZERAF SWAMP (THE SUDD) (3)

From Mongalla to Lake No, along the river on both sides are mostly papyrus swamps and savanna grasslands.

Between Mongalla and Bor, the river spills more-or-less equally over both banks in times of flood. The spillage losses in this reach are not as large as those farther north because the extent of the swamps is bounded here by high ground on both sides. On the east bank, high ground ends 15 km north of Bor (612 km from Lake No), whereas on the west, it ends at Lake Nuong (356 km from Lake No). The land levels between Jonglei and Peake's Latitude are such that about 25% of the river spill of this reach goes to the east, occurring in the first 100 km north of Jonglei, while 75% goes to the west, occurring north of Lake Nuong (4). This westward spill migrates toward the Bahr el Ghazal. North of Peake's Latitude, the river spills over both banks, with the west side probably receiving the larger portion.

In a normal year, the 27 milliards passing Mongalla are reduced by spillage to 23.4 md at Jonglei, and to 14.3 md (Jebel and Zeraf) below Lake No. It is estimated (4) that 6 md from the Jebel are spilled westward between Lake Nuong and Buffalo Cape, divided into 4.6 md between Lake Nuong and Peake's Latitude and 1.4 md between Peake's Latitude and Buffalo Cape.

It is surprising that the Jebel, in flowing through this swampy region, loses almost half of its discharge. But it is even more surprising that the Bahr el Ghazal, which receives a total discharge of about 12.7 md from its eight tributaries, loses practically everything while passing through the central swampy region bounded more-or-less by the 400 meter contour line (see Figure 3.3). The Bahr el Ghazal Basin, with an area of 500,000 km^2, will be fully described in Chapter 3.

The total area of permanent swamps in connection with the Bahr el Jebel and the Bahr el Zeraf is estimated to be 8300 km^2 (5). For the Bahr el Ghazal, it is estimated to be 16,600 km^2 (5). The mean annual precipitation on the swampy areas is about 900 mm, which produces inputs of 7.5 md to the Jebel and Zeraf swamps and 15 md to the Ghazal swamps.

In order to have some idea of how much water is lost in the swampy region of the Upper Nile, an approximate water balance of the swamps is necessary.

The above flows can be combined to give the mean annual water balance of the Jebel and Zeraf swamps as illustrated schematically in Figure 1.5. For these swamps, the mean total annual water loss is 14.2 md on 8300 km^2, which is about 1.7 meters.

In a similar water balance for the Ghazal swamp, we must realize that the gaged surface inflows from the tributaries of the Bahr el Ghazal do not discharge directly into the permanent swamp (see Figure 3.3). Instead they discharge into the surrounding toich lands.* To the first approximation, the annual precipitation in this region (900 mm) is matched by the open water potential evaporation during the wet season (7 months). If we assume that the vegetation in the toich lands, which is mainly grass, transpires at the same rate as the open water evaporation during the wet season, we may perform a crude water balance of the permanent Ghazal swamp which is independent of the toich lands. This is indicated schematically in Figure 1.6, where we see the water losses in the Ghazal Swamp alone to be 33.1 md over an area of 16,600 km^2, which is about 2.0 meters.

*'Toich lands', a common Nilotic word meaning lands seasonally flooded by spill-water from rivers. Vegetation is mainly open grassland.

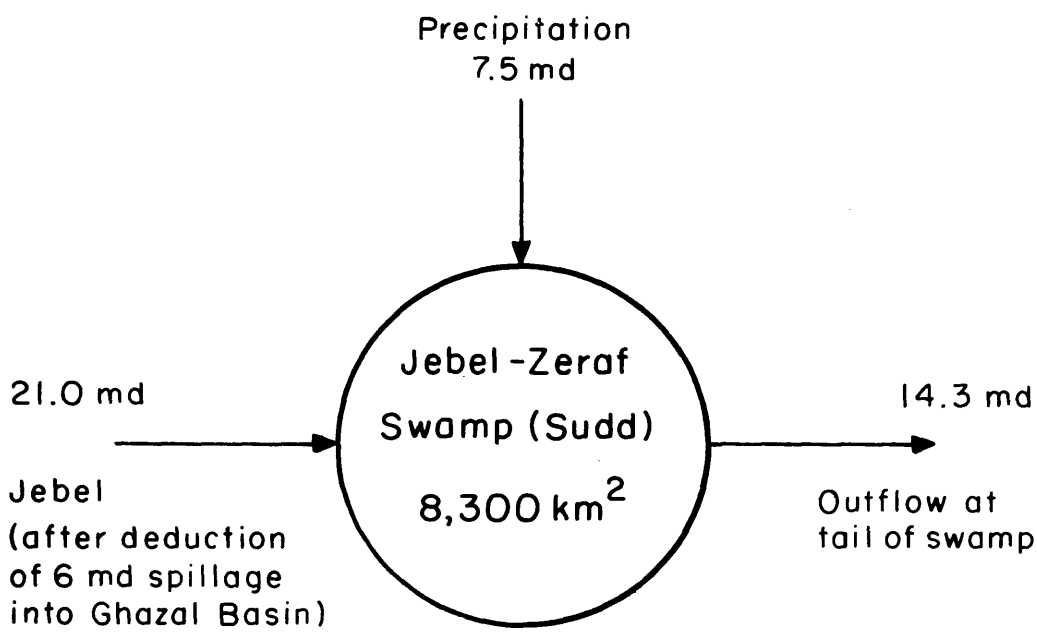

$$1 \text{ md} = 1 \text{ km}^3 = 10^9 \text{ m}^3$$

Apparent Water Loss at the Jebel-Zeraf Swamp

$$= \text{Input} - \text{Output} = (21.0 + 7.5 - 14.3) \text{ md}$$

$$= 14.2 \text{ md} \equiv \underline{1.7 \text{m}}$$

FIGURE 1.5

A CRUDE ANNUAL WATER BALANCE

(JEBEL-ZERAF SWAMP)

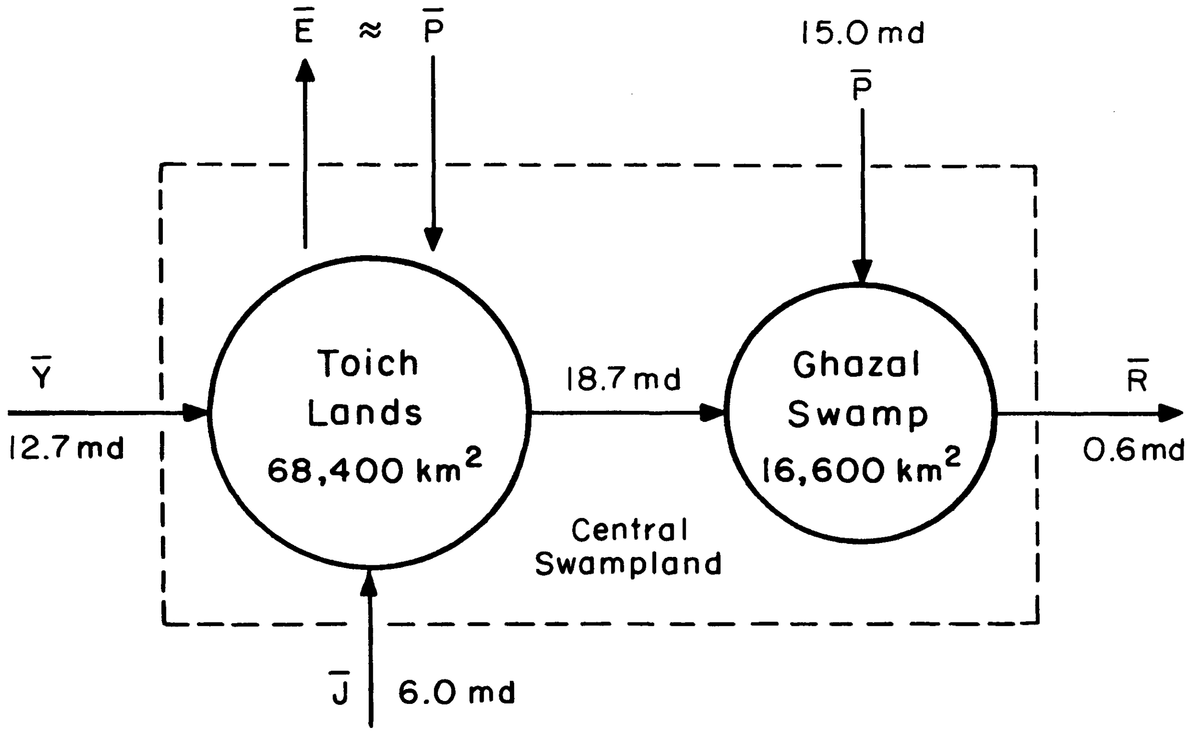

P : Precipitation

E : Actual Evapotranspiration

Y : Gaged Discharges

J : Jebel Spillage

R : Outflow at Lake No

Overbar denotes mean annual values

1 md = 1 km^3 = 10^9 m^3

Apparent Water Loss at the Ghazal Swamp

= Input − Output = (18.7 + 15.0 − 0.6) md

= 33.1 md ≡ 2.0 m

FIGURE 1.6

A CRUDE ANNUAL WATER BALANCE

(GHAZAL SWAMP)

The total water loss of all the swamps (Jebel and Zeraf, and Ghazal) thus amounts to 47.3 md over an area of 24,900 km^2, which is about 1.9 meters.

If we compare the apparent water losses (47.3 md) in all the swamps (Jebel and Zeraf, and Ghazal) with the flow of the White Nile at Malakal (27 md) and with that of the total Nile at Dongola (86 md), the ratios are 1.75 and 0.55, respectively. In other words, more than one and a half times the flow of the White Nile, or half the discharge of the total Nile, disappears in the swamps.

What happens to this water? There are only two practical possibilities - evapotranspiration and deep groundwater seepage. What is the magnitude of the actual evapotranspiration? Could evapotranspiration alone explain most of the losses, or is there appreciable leakage through the aquiclude on which the swamp is founded? These are some of the questions which we hope to answer in this report.

1.3 Evapotranspiration of Papyrus Swamps and Grasslands

From May 1947 to April 1948, Migahid (6) performed a lysimeter experiment to measure the evapotranspiration of papyrus swamps near the Zeraf Cuts. The average result was 6.5 mm per day or 2.4 meters per year.

For the papyrus swamps in the region of Lake Victoria, Vowinckel and Orvig (7) used an energy budget to estimate an evapotranspiration rate of 2.2 meters per year.

For papyrus swamps in Bangweulu, Zambia, Balek (8) used the water balance method to estimate an evapotranspiration rate of 2.1 meters per year.

Based on the above consistent findings, the mean annual potential evapotranspiration of papyrus swamps in tropical Africa is taken to be 2.2 meters per year.

Considering next the potential evapotranspiration of grasslands, experimental values for standard grasses around Lake Victoria (9) indicate a rate of 1496 mm per year (125 mm per month).

For Nigeria (10), experimental values for short grass cover give 1366 mm per year (114 mm per month).

For natural savanna grasslands with forest glades in the Congo Basin (11), water balance estimates show that the mean annual evapotranspiration is 1082 mm. Since the rainy season there is about 9 months, the mean annual potential evapotranspiration is estimated to be 120 mm per month in the wet season.

From the above values, the mean annual potential evapotranspiration for grasslands in tropical Africa is taken to be 120 mm per month during the wet season.

It is instructive to compare the above average annual rate of evapotranspiration from papyrus swamps (2.2m) with the apparent annual water losses of the major Nile swamps obtained from the crude water balance computations summarized in Table 1.1. Discounting the Machar marshes due to the high uncertainty of the water balance components, the areally-weighted average annual loss for the Ghazal and Jebel-Zeraf is 1.9 meters. The closeness of these two values indicates the likelihood that the swamp water losses are due primarily if not entirely to evapotranspiration rather than to ungaged outflows such as surface spillage or deep seepage. This result confirms the earlier conclusion of others (5), (11), (12).

We must remember, however, that there may be ungaged inflows to the swamps, both surface and groundwater, which could greatly increase the apparent water loss. These inflows must be estimated and included in a refined water balance before we can eliminate the possibility of significant deep groundwater seepage.

1.4 Projects for Conserving Water for Egypt and the Sudan

Anticipating full utilization of the current annual Nile flow, Egyptian and Sudanese water resource planners have sought upstream development projects on the White Nile which give promise of increasing the available water. Among these projects are:

1. Mutir dam to regulate Lake Albert
2. Nimule dam on the Bahr el Jebel between Lake Albert and Mongalla
3. Jonglei Canal to channelize the Bahr el Jebel between Mongalla and Malakal
4. Gambeila dam in the headwaters of the Sobat River
5. Drainage and land reclamation in the Machar marshes along the lower reaches of the Sobat.
6. Drainage and land reclamation in the swamps contiguous to the Bahr el Jebel
7. Drainage and land reclamation in the huge swamp area from which the Bahr el Ghazal flows to join the Bahr el Jebel at Lake No to form the White Nile.

Of all these projects, the largest potential return in terms of increased water yield would seem to come from the last three which involve drainage of the large swamp areas. Indeed, without reducing the water lost in passage of the flow through these swamps, any upstream projects would be of limited utility.

Table 1.1 gives a comparison of the apparent water losses of major Nile swamps. These losses are compared in the last column with 27 md*, the mean annual flow of the White Nile downstream of the swamps at Malakal.

Clearly, the Ghazal area has the greatest development potential, and we will limit this study to that region.

Table 1.1

Apparent Water Losses of Major Nile Swamps

Location	Area of Permanent Swamp	Inputs			Output	Losses		Loss / White* Nile
		Prec.	Gaged inflow	Estimated Spillage	Gaged			
	km^2	md	md	md	md	md	m	
Machar( )	8,700	7.3	2.0	3.5	0.1	12.8	1.5	0.47
Jebel-Zeraf	8,300	7.5	27.0	-6.0	14.3	14.2	1.7	0.53
Ghazal	16,600	15.0	12.7	6.0	0.6	33.1	2.0	1.23

By preventing spillage and tributary inflows by appropriate channelization, water which is now transpired will be retained in the Nile for downstream use. Due to reduced water supply in the swamps after channelization, a new equilibrium vegetal system will be reached which transpires at a lower level than that before channelization.

1.5 The Objective of this Work

The objective of this work is to estimate the potential water recovery by alternative drainage projects in the Bahr el Ghazal Basin.

Since precipitation is probabilistic in nature, we can only define the basin yield in statistical terms. The methodology used in achieving this objective will be fully described in Chapter 2.

Chapter 2

METHODOLOGY

2.1 Introduction

In the previous chapter we used gross estimates from the literature to perform a preliminary overall water balance for the permanent and semi-permanent swamplands of the White Nile. These analyses confirmed earlier findings that the observed water losses of the White Nile in the region may be accounted for by evapotranspiration.

In this chapter we will introduce new techniques which will be used later in a more detailed analysis of sub-catchments of the Bahr el Ghazel Basin in order to refine estimates of the water yield and of the other water balance components. This approach should also indicate whether or not deep groundwater seepage is currently taking place and hence whether proposed swamp drainage might seriously reduce regional groundwater recharge.

2.2 Water Balance Model*

The water balance of a catchment can be formulated, from conservation of mass principles, assuming groundwater seepage is negligible.

as

$$\int_0^t [i(t) - e_T(t) - V_s(t)]\, dt$$

$$= \int_0^t [r_s(t) + r_g(t)]\, dt \equiv \int_0^t y(t)\, dt \qquad (2.1)$$

*Sections 2.2 and 2.3 are from Eagleson 1978 where $i(t)$ = precipitation rate

$e_T(t)$ = evapotranspiration rate

$V_s(t)$ = rate of moisture storage in soil, vegetation, snow, lakes, etc.

$r_s(t)$ = surface runoff rate

$r_g(t)$ = groundwater runoff rate

$y(t)$ = yield rate

By fixing the time interval of the integration, o to t, to correspond exactly with the annual water year, and assuming the system is stationary in the mean, we may take the expected value, term by term, of equation (2.1), and write the long-term mean annual water balance equation as

$$E[P_A] - E[E_{T_A}] = E[R_{S_A}] + E[R_{g_A}] = E[Y_A] \tag{2.2}$$

where by the stationarity assumption,

$$E[\int_o^{1\ \text{year}} V_S(t)\ dt] \equiv 0 \tag{2.3}$$

and where

$E[\ ]$ ≡ Expected value of [ ]

P_A = Annual precipitation

E_{T_A} = Annual evapotranspiration

R_{S_A} = Annual surface runoff

R_{g_A} = Annual groundwater runoff

Y_A = Annual water yield

A qualitative representation of equation 2.2 is shown in Figure 2.1, and a schematic representation of the soil column is shown in Figure 2.2.

The annual potential evapotranspiration may be computed from the conservation of energy principle, as a function of the insolation, the longwave back radiation and the sensible heat transfer of the surface considered.

Each component of the water balance model is formulated from accepted physical laws as a function of the climate, soil and vegetation parameters of the basin. The inclusion of these parameters in the water balance elements is extremely important because it is only through changes in such real parameters that we may study the effects of any man-induced alteration of the system.

For notational simplicity we will now drop the expectation signs in Equation 2.2, replacing them by overbars (e.g. $\bar{P}_A$). All water balance elements, except for the mean annual precipitation, are functions of the average moisture content of the catchments surface soils. This space-time average soil moisture is shown in Figure 2.3 as "s_o".

Equation 2.2 may now be written as,

$$\bar{P}_A - \bar{E}_{T_A}(s_o) = \bar{R}_{S_A}(s_o) + \bar{R}_{g_A}(s_o) = \bar{Y}_A(s_o) \qquad (2.4)$$

Given the mean annual precipitation, and all the climatic, soil and vegetation parameters, the above equation contains one unknown, s_o, which may be obtained by trial and error solution. Once "s_o" is known it can be back substituted to obtain the individual water balance components.

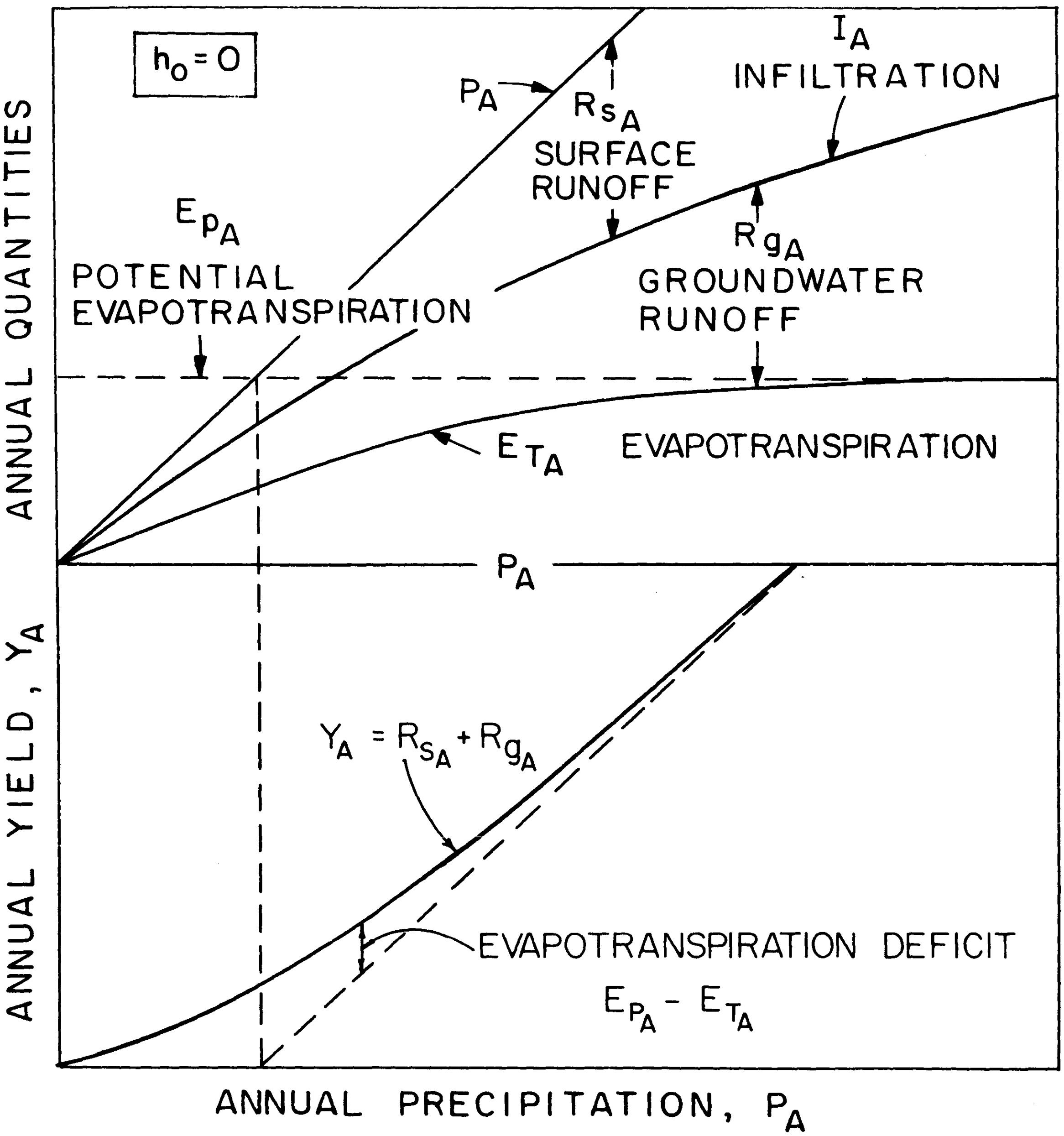

FIGURE 2.1

CLIMATIC INFLUENCE ON THE ANNUAL WATER BALANCE

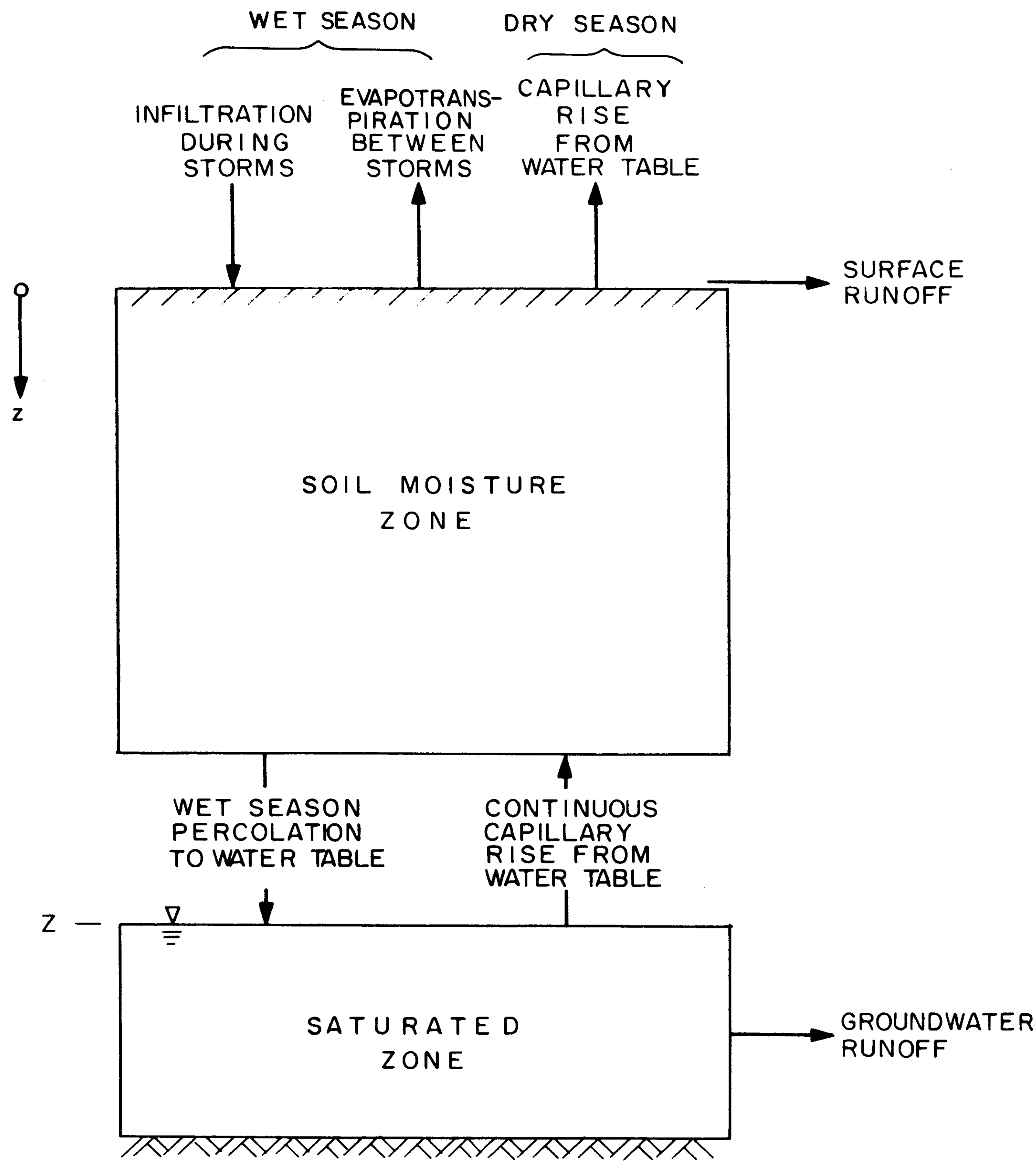

FIGURE 2.2
SCHEMATIC REPRESENTATION OF SOIL COLUMN

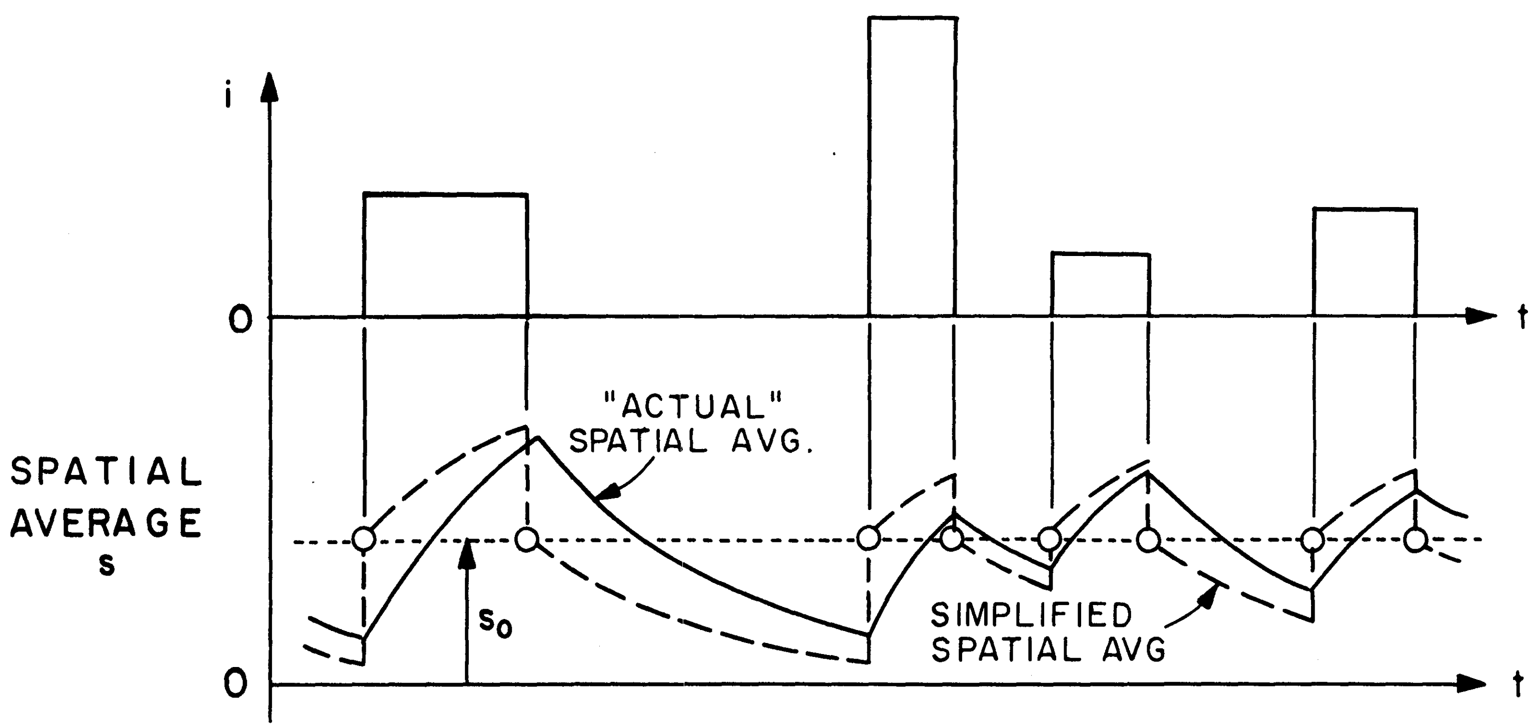

FIGURE 2.3

SOIL MOISTURE REPRESENTATION

In the above formulation of the water balance, deep underground and lateral water seepages are assumed neglegible. Wherever there is a large discrepancy between the computed mean annual basin yield and that obtained from a long series of historical records of discharge, the groundwater seepage term or the ungaged discharge has to be included. This modification will be discussed in Chapter 4, where the water balance of each sub-catchment is considered.

2.3 Hydrologic Parameters and Distributions

2.3.1 Introduction

In the previous section a brief account of the water balance model is given. In this section the formulations of the individual water balance element are presented along with the probability distributions of the precipitation and yield components. For a detailed derivation of all the formulas, refer to (13 through 20).

The processes which operate in the vertical direction on a unit horizontal area of a catchment, namely precipitation, infiltration and evapotranspiration, are considered separately, and then are combined to formulate the water balance of the catchment.

2.3.2 Point Precipitation and Its Probability Distribution

Point precipitation is represented by Poisson arrivals of rectangular intensity-pulses having random depth and duration (Figure 2.4). Assuming the storm depths to be independent and identically gamma-distributed, the cumulative distribution function (CDF) for normalized annual precipitation is derived in terms of two parameters of the storm sequence; the mean number of storms per annual rainy season, m_ν, and the shape parameter, κ, of the gamma distribution of storm depths. This derived CDF is

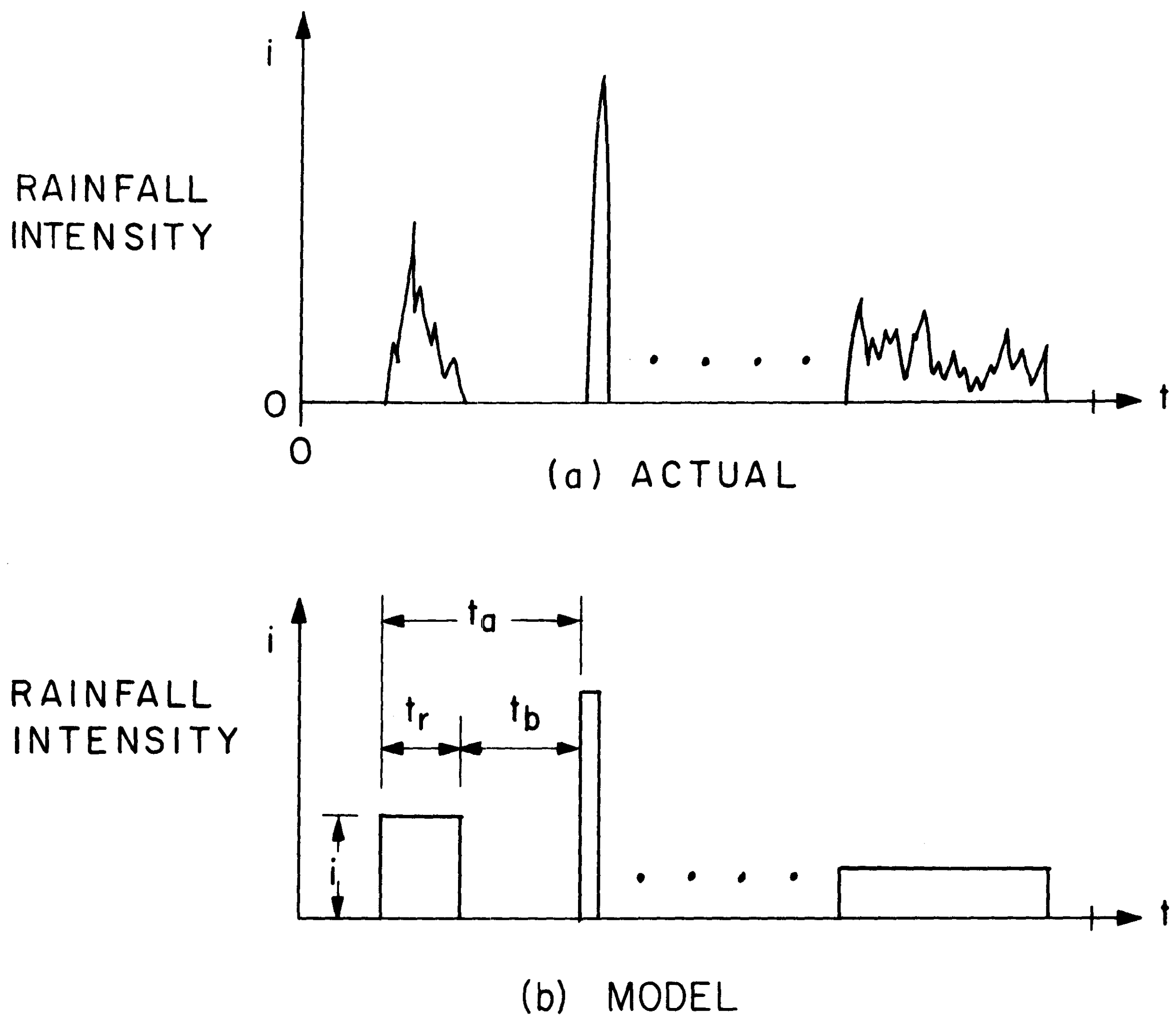

FIGURE 2.4

MODEL OF PRECIPITATION EVENT SERIES

$$\text{Prob}\left[\frac{P_A}{\bar{P}_A} < z\right] = e^{-m_\nu}\left\{1 + \sum_{\nu=1}^{\infty} \frac{m_\nu^\nu}{\nu!} \cdot P[\nu\kappa,\ m_\nu \kappa z]\right] \qquad (2.5)$$

where P[a, x] is Pearson's incomplete gamma function, as

$$P[a,\ x] = \frac{\gamma[a,\ x]}{\Gamma(a)} \qquad (2.6)$$

and

$\gamma[a, x]$ = the incomplete gamma function

$\Gamma(a)$ = the gamma function

with P_A = annual precipitation

$\bar{P}_A$ = mean annual precipitation

ν = counting variable for number of storms

Comparisons of this Poisson precipitation distribution with observations (using the Thomas (1948) plotting position) (21) are shown in Figure 2.5 and 2.6. The Thomas relation is given as

$$\text{Prob}\left[\frac{P_A}{\bar{P}_A} < z\right] = \frac{m_z}{N + 1} \qquad (2.7)$$

where m_z = rank order of observation of magnitude z

N = number of years of record

The agreement is remarkable even though the parameters of Equation 2.5 were evaluated using only 5 years of storm data. Other comparisons are made by Eagleson (15), and the conclusion is that the precipitation distribution function is applicable in general to both arid and humid climates, provided that the storms are independent and come

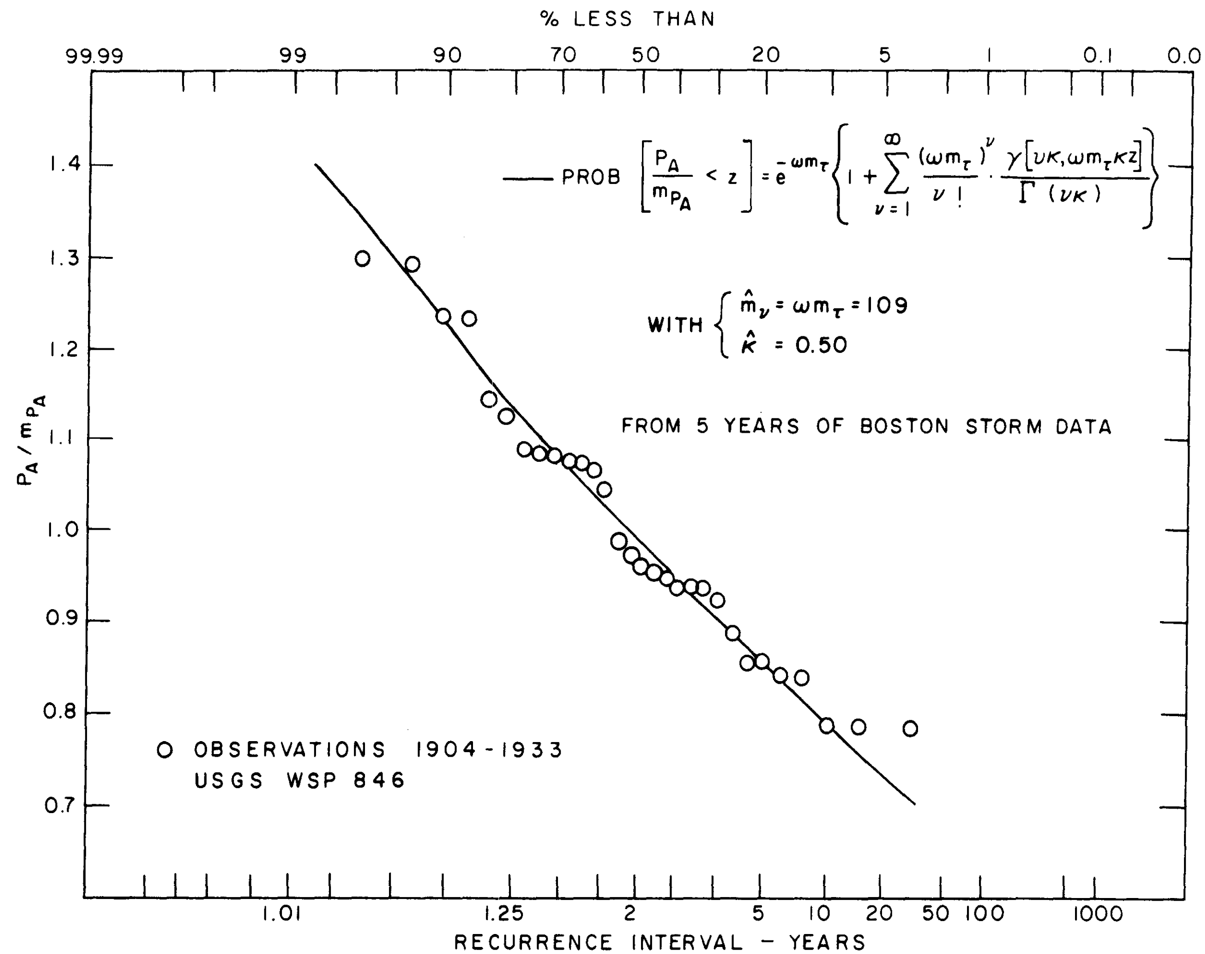

ANNUAL PRECIPITATION NASHUA RIVER BASIN AT CLINTON, MASS

FIGURE 2.5

FREQUENCY OF ANNUAL PRECIPITATION, CLINTON, MA.

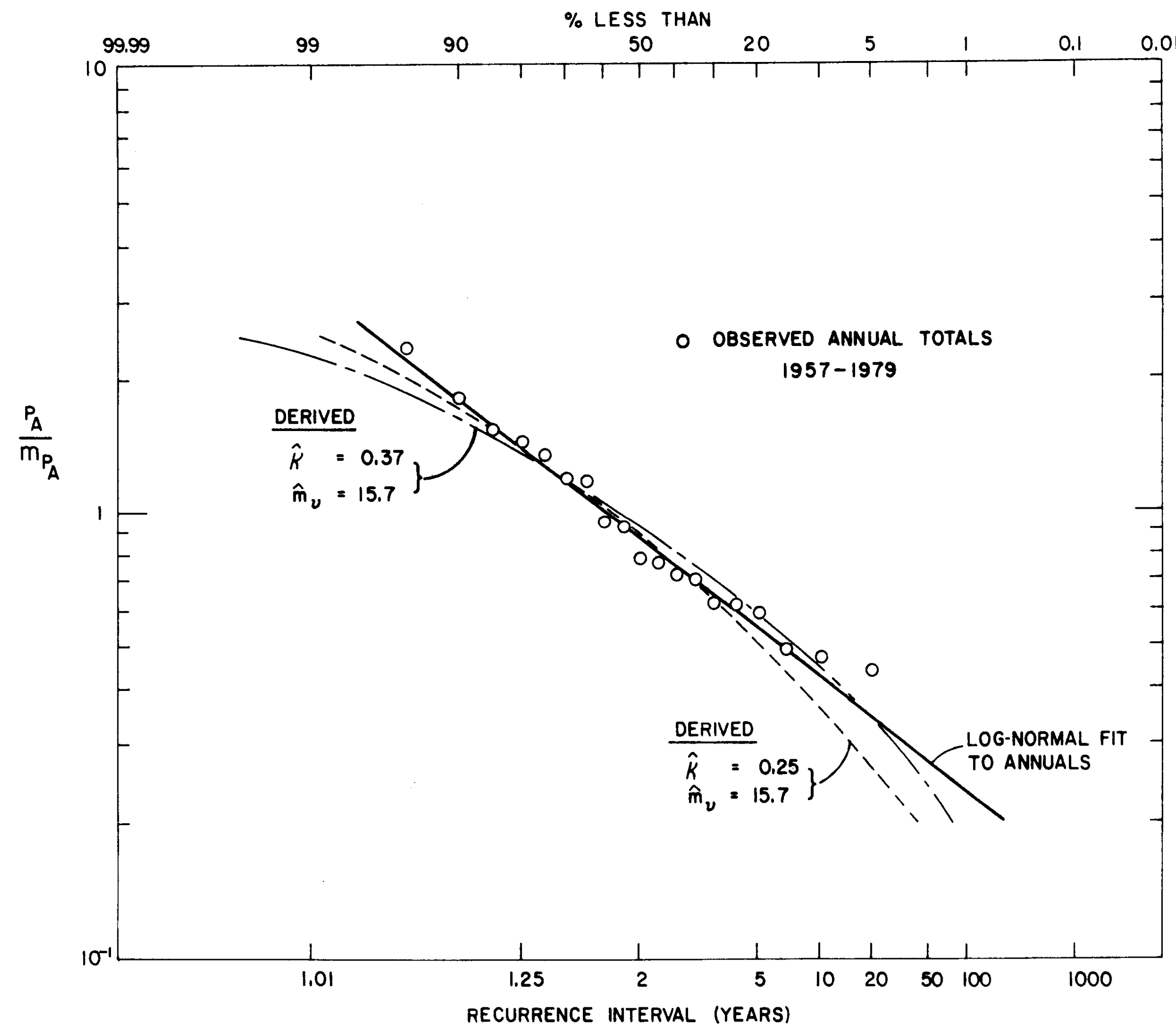

FIGURE 2.6

FREQUENCY OF ANNUAL PRECIPITATION, SANTA PAULA, CA.

from a single, homogenous population.

2.3.3 Evapotranspiration

For permeable natural surfaces comprising a homogeneous mixture of vegetated and bare soil fractions, the evapotranspiration process can be separated into three components, namely the surface retention loss, E_r, the bare soil evaporation, E_s, and the vegetal transpiration, E_v.

The surface retention loss is the depth of free-standing water left on all surfaces at the conclusion of precipitation and surface runoff. This is comprised of retention loss on the bare soil part, E_{rs}, and that on the vegetation part, E_{rv}. They are assumed to be evaporated in between storms at the wet soil surface potential rate e_p, and the vegetal potential rate e_{pv}, respectively. Neglecting carryover unevaporated retention from storm to storm, the bare soil retention loss is given as (17)

$$\beta \, \bar{E}_{rs}/\bar{e}_p = 1 - e^{-\beta h_o/\bar{e}_p} \, \frac{\Gamma(\kappa, \lambda h_o)}{\Gamma(\kappa)} - \left(1 + \frac{\beta h_o/\bar{e}_p}{\lambda h_o}\right)^{-\kappa} \cdot \frac{\gamma[\kappa, (\lambda h_o + \beta h_o/\bar{e}_p)]}{\Gamma(\kappa)} \tag{2.8}$$

The vegetation retention loss is

$$\beta \bar{E}_{rv}/\bar{e}_p = k_v \left\{ 1 - e^{-\beta h_o/\bar{e}_p} \, \frac{\Gamma[\kappa, \lambda k_v h_o]}{\Gamma(\kappa)} - \left(1 + \frac{\beta h_o/\bar{e}_p}{\lambda k_v h_o}\right)^{-\kappa} \cdot \frac{\gamma[\kappa, (\lambda k_v h_o + \beta h_o/\bar{e}_p)]}{\Gamma(\kappa)} \right\} \tag{2.9}$$

And the mean annual surface retention loss, $\bar{E}_{r_A}$, as

$$\frac{\bar{E}_{r_A}}{\bar{E}_{p_A}} = \frac{(1 - M)\ \beta \bar{E}_{rs}/\bar{e}_p + M \beta \bar{E}_{rv}/\bar{e}_p}{(1 - M + Mk_v)} \tag{2.10}$$

where the overbars again denote the expected value, or the long-term mean value and

E_{r_A} = annual surface retention loss, mm

E_{p_A} = annual potential evapotranspiration, mm

E_{rs} = surface retention loss from bare soil fraction, mm

E_{rv} = surface retention loss from vegetated fraction, mm

e_p = potential evaporation rate of wet soil surface, mm/day

h_o = surface retention capacity, mm

k_v = ratio of potential rates of transpiration and wet soil surface evaporation

M = vegetal canopy density

β = reciprocal of average time between storms, equal to $m_{t_b}^{-1}$, days^{-1}.

κ = parameter of gamma distribution of storm depth

λ = parameter of gamma distribution of storm depth, equal to κ/m_H, mm^{-1}

m_H = mean storm depth, mm

The interstorm evaporation from a unit area of bare soil, E_s, is

$$\beta \bar{E}_s/\bar{e}_p = \Bigg\{ \frac{\gamma[\kappa, \lambda h_o]}{\Gamma(\kappa)} - [1 + \frac{\beta h_o/\bar{e}_p}{\lambda h_o}]^{-1} \cdot \frac{\gamma[\kappa, \lambda h_o + \beta h_o/\bar{e}_p]}{\Gamma(\kappa)} \cdot e^{-BE}$$

$$+ [1 - \frac{\gamma[\kappa, \lambda h_o]}{\Gamma(\kappa)}] \cdot \Big[1 - e^{-BE - \beta h_o/\bar{e}_p} \cdot (1 + Mk_v + (2B)^{1/2} \cdot E - w/\bar{e}_p)$$

$$+ e^{-CE - \beta h_o/\bar{e}_p} \cdot (M k_v + (2C)^{1/2} \cdot E - w/\bar{e}_p)$$

$$+ (2E)^{1/2} \cdot e^{-\beta h_o/\bar{e}_p} \cdot [\gamma(\tfrac{3}{2}, CE) - \gamma(\tfrac{3}{2}, BE)] \Big]$$

$$+ [1 + \frac{\beta h_o/\bar{e}_p}{\lambda h_o}]^{-\kappa} \cdot \frac{\gamma[\kappa, \lambda h_o + \beta h_o/\bar{e}_p]}{\Gamma(\kappa)} \Big[(2E)^{1/2} \cdot [\gamma(\tfrac{3}{2}, CE) - \gamma(\tfrac{3}{2}, BE)]$$

$$+ e^{-CE} [Mk_v + (2C)^{1/2} \cdot E - w/\bar{e}_p]$$

$$- e^{-BE} [Mk_v + (2B)^{1/2} \cdot E - w/\bar{e}_p] \Big] \Bigg\} \qquad (2.11)$$

Here
$$B = \frac{1 - M}{1 + Mk_v - w/\bar{e}_p} + \frac{M^2 k_v + (1 - M)\, w/\bar{e}_p}{2(1 + Mk_v - w/\bar{e}_p)^2} \qquad (2.12)$$

$$C = \frac{1}{2} (Mk_v - w/\bar{e}_p)^{-2} \qquad (2.13)$$

$$E = [2\ \beta n\ K(1)\ \psi(1)/\pi m \bar{e}_p^{\,2}]\ \phi_e\ s_o^{\,d+2} \qquad (2.14)$$

where E is the evaporation effectiveness

and n = effective medium porosity

m = pore size distribution index

$K(1)$ = saturated effective hydraulic conductivity, cm/sec

$\psi(1)$ = soil matrix potential (suction), cm

ϕ_e = dimensionless exfiltration diffusivity

s_o = time and spatial average soil moisture concentration in surface boundary layer

w = capillary rise from water table, cm/sec

d = diffusivity index

For a vegetal surface, assuming that the mean interstorm transpiration, $\bar{E}_v$, is always at the potential rate, $k_v \bar{e}_p$, we have

$$\bar{E}_v/\bar{e}_p = k_v \tag{2.15}$$

Finally the mean annual evapotranspiration for a unit surface of homogenous soil and vegetation fractions, $\bar{E}_{T_A}$, is

$$\frac{\bar{E}_{T_A}}{\bar{E}_{p_A}} = J(E, M, k_v, h_o) = \frac{(1 - M)\ \beta\ \bar{E}_s/\bar{e}_p + M\beta\ \bar{E}_v/\bar{e}_p}{(1 - M + Mk_v)} \tag{2.16}$$

The mean potential evaporation rate of the wet soil surface, $\bar{e}_p$, may be estimated by the modified combination Penman equation (13) ,

$$\bar{e}_p = \frac{\bar{q}_i\ (1 - A_s) - \bar{q}_b + H}{\rho_e\ L_e\ (1 + \gamma/\Delta)} \tag{2.17}$$

where $\bar{q}_i$ = mean insolation rate on a unit surface of the catchment $\ell y/min$

$\bar{q}_b$ = mean net outgoing long wave radiation rate, $\ell y/min$

H = mean residual sensible heat flux, $\ell y/min$

A_s = shortwave albedo of wet soil surface

ρ_e = mass density of evaporating water ($\cong 1\ g/cm^3$)

L_e = latent heat of vaporization ($\cong$ 597 cal/g)

$\frac{\gamma}{\Delta}$ = atmospheric parameter

$\bar{q}_b$, H, γ/Δ may be estimated by the following empirical relations (13),

$$\bar{q}_b = (1 - 0.8N)\ [0.245 - 0.145 \times 10^{-10}\bar{T}_A] \quad , \quad \ell y/min \qquad (2.18)$$

$$\frac{\bar{q}_b}{H} = 0.25 + 1/(1 - \bar{S}) \qquad (2.19)$$

$$1/(1 + \frac{\gamma}{\Delta}) = 0.42 + 0.013\ \bar{T}_A \qquad (2.20)$$

and

N = mean annual seasonal cloud cover fraction

$\bar{S}$ = mean annual seasonal relative humidity

$\bar{T}_A$ = mean annual seasonal air temperature,

^oK in Equation (2.18) , ^oC in Equation (2.20)

$\bar{e}_p$ as obtained from Equation 2.17 is in cm per minute. A conversion factor is needed to convert it into mm per day.

Assuming evapotranspiration to be significant only during interstorm periods in the rainy season, the mean annual potential evapotranspiration may be estimated by

$$\bar{E}_{p_A} = m_\nu \, m_{t_b} \, \bar{e}_p^{\,*} \qquad (2.21)$$

where

$$\begin{aligned} \bar{e}_p^{\,*} &= (1 - M)\bar{e}_p + M\bar{e}_{pv} \qquad (2.22) \\ &= [1 - M + Mk_v]\bar{e}_p \end{aligned}$$

with $\bar{e}_p^{\,*}$ = weighted mean potential evapotranspiration rate, mm/day

m_{t_b} = mean time between storms, days.

m_ν = mean number of storms per rainy season

Equation (2.16) is represented in Figure 2.7, evaluated over the practical ranges of the parameters; $h_o = 0(1)\text{mm}^*$, $\beta = 0(10^{-1} - 10^{-2})\text{days}^{-1}$, $\lambda = 0(10^{-1} - 10^{-2})\text{mm}^{-1}$, and $\bar{e}_p = 0(1)$ mm/day.

For bare soil conditions, M = 0 and $w/\bar{e}_p << 1$ (Figure 2.7a), the results indicate that surface retention makes an appreciable difference in the annual evaporation only in the very arid climate where the evaporation effectiveness, E, is small; and that J(E) is very insensitive even at small E, to variations in the relative surface retention, λh_o, but is quite sensitive there to changes in $\beta h_o/\bar{e}_p$.

---

* 0( ) ≡ the order of magnitude

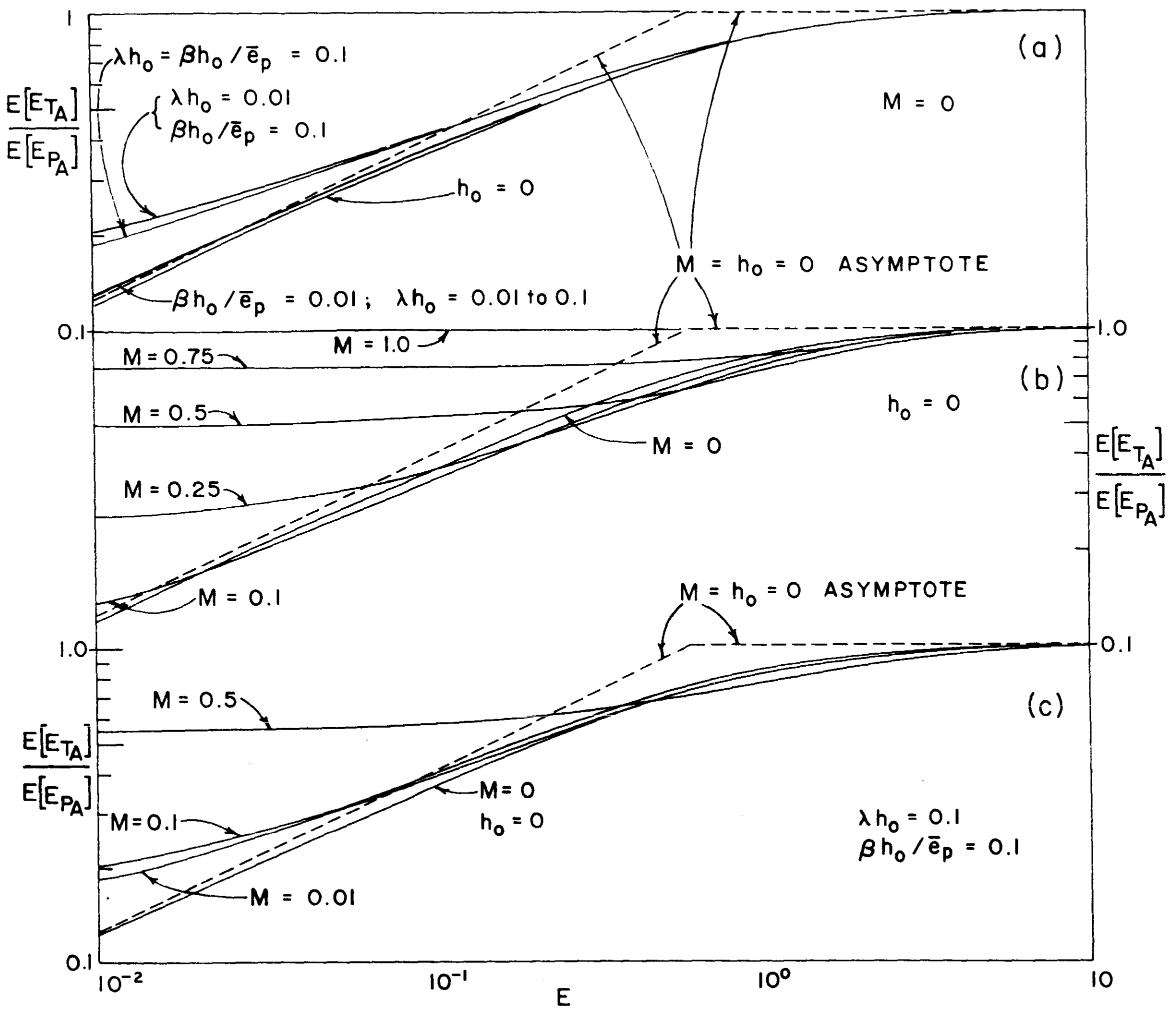

FIGURE 2.7

EVAPOTRANSPIRATION FUNCTION

($\kappa = 0.5$, $k_v = 1$, $w/\bar{e}_p << 1$)

For mixed vegetation and bare soil conditions (Figure 2.7b,c) with $k_v = 1$ and $w/\bar{e}_p << 1$, vegetal cover apparently has a strong effect on annual evapotranspiration particularly for small E.

2.3.4 Storm Surface Runoff

The Philip infiltration equation and the joint distribution of rainfall intensity and duration are used to derive the distribution of the annual storm surface runoff volume, and hence, its expected value (18).

The expected annual surface runoff volume, $\bar{R}_{s_A}$, is given as

$$\frac{\bar{R}_{s_A}}{\bar{P}_A} = e^{-G - 2\sigma} \cdot \Gamma(\sigma + 1) / \sigma^{\sigma} - \bar{E}_r/m_H \qquad (2.23)$$

$$\text{if} \qquad e^{-G - 2\sigma}\, \Gamma(\sigma + 1)/\sigma^{\sigma} > \bar{E}_r/m_H$$

$$\text{otherwise} \qquad \bar{R}_{s_A}/\bar{P}_A = 0$$

The first term on the right side of Equation (2.23) represents the rainfall excess and the second, the mean interstorm surface retention, $\bar{E}_r$.

Here, G is the gravitational infiltration parameter and σ, the capillary infiltration parameter, as

$$G = \frac{\alpha K(1)}{2} [1 + s_o^c] = \alpha w \qquad (2.24)$$

$$\sigma = \left[\frac{5\, n\, \eta^2\, K(1)\, \psi(1)\, (1 - s_o)^2\, \phi_i(d,\, so)}{6\, \pi\, \delta\, M}\right]^{\frac{1}{3}} \qquad (2.25)$$

with

α = reciprocal of average rainstorm intensity, equal to m_i^{-1}, sec/cm

m_i = average rainstorm intensity

η = reciprocal of mean storm depth,
equal to m_H^{-1}, days^{-1}

m_H = mean storm depth

δ = reciprocal of average storm duration,
equal to $m_{t_r}^{-1}$, days^{-1}

m_{t_r} = average storm duration, days

ϕ_i = dimensionless infiltration parameter

The mean interstorm surface retention $\bar{E}_r$ is related to the mean annual interstorm surface retention $\bar{E}_{T_A}$ by $\bar{E}_{r_A} = m_\nu \bar{E}_r$

The fraction of mean annual precipitation becoming mean annual surface runoff is sensitive to the gravitational and capillary infiltration potentials, $G(s_o = 0)$ and $\sigma(s_o = 0)$, respectively, and to the average soil moisture s_o. Values of this fraction evaluated for typical climate and soil properties compare favorably with observations. (18)

To facilitate computations, values of σ versus $e^G \bar{R}_{s_A}/\bar{P}_A$ are plotted in Figure 2.8.

2.3.5 Groundwater Runoff

The annual groundwater runoff is taken as the difference between percolation to the water table during the wet season and capillary rise from the water table over the year.

The mean annual groundwater runoff is given as

$$\bar{R}_{g_A} = m_\tau K(1) s_o^c - Tw \qquad (2.26)$$

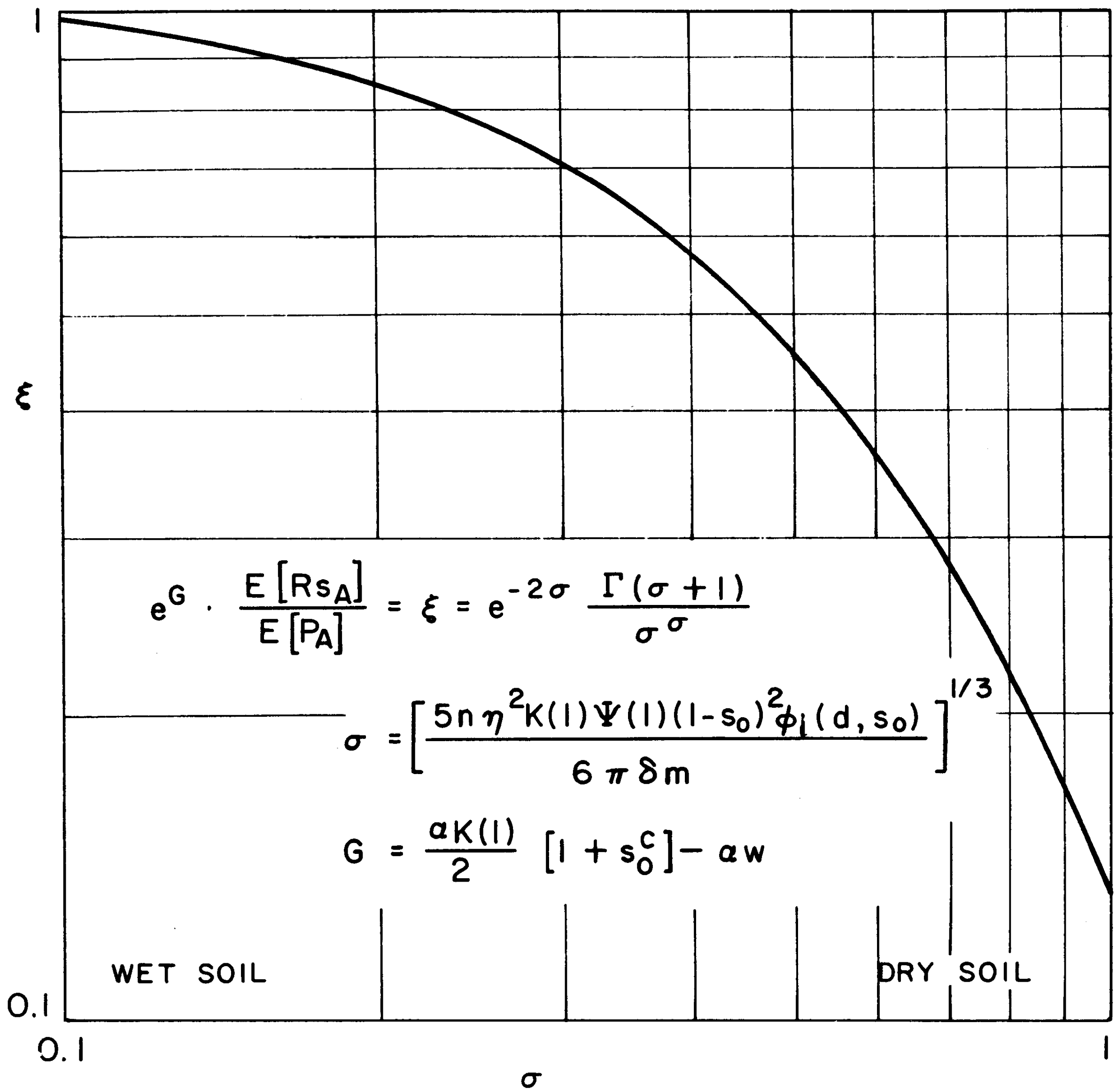

SURFACE RUNOFF FUNCTION

FIGURE 2.8

PLOT OF SURFACE RUNOFF FUNCTION ($h_o = 0$)

where

m_τ = mean length of rainy season, days

c = pore disconnectedness index

T = 1 year = 365 days

2.3.6 Yield of a Catchment and its Distribution

From Equation 2.4, the mean annual water budget is

$$\bar{P}_A - \bar{E}_{T_A}(s_o) = \bar{R}_{s_A}(s_o) + \bar{R}_{g_A}(s_o) = \bar{Y}_A(s_o) \qquad (2.27)$$

For non-zero surface runoff it can be written as

$$\bar{P}_A - \bar{E}_{p_A} \cdot J(E, M, k_v, h_o) = \bar{P}_A\, e^{-G-2\sigma}\, \Gamma(\sigma + 1)\, \sigma^{-\sigma} - \bar{E}_{r_A} + m_\tau K(1) s_o^{\,c} - Tw \qquad (2.28)$$

where E, G, and σ are functions of s_o.

Equation 2.28, from left to right, represents the precipitation, the actual evapotranspiration including surface retention, the rainfall excess, the surface retention, the groundwater recharge and the groundwater loss.

With the climatic, soil and vegetation parameters known, the above function contains only one unknown, the long-term space-time average soil moisture, s_o, which can be solved to obtain the mean annual water budget of the catchment. Once s_o is known, each water balance element is known, giving the mean annual yield of the catchment.

In order to introduce uncertainty into the catchment yield to a first order approximation, we will replace the mean annual values of Equation (2.27) by their respective annual values. This assumes small annual deviations from their mean annual values. The annual water budget now becomes

$$P_A - E_{T_A} = R_{s_A} + R_{g_A} = Y_A \qquad (2.29)$$

or

$$P_A - E_{p_A} \cdot J\,(E,\, M,\, k_v,\, h_o) = P_A\, e^{-G-2\sigma}\, \Gamma(\sigma + 1)\sigma^{-\sigma} - E_{r_A} + \tau\, K(1)\, s_o^c - Tw \qquad (2.30)$$

To facilitate analytical derivation of the distribution of the annual yield, the seasonal length, τ, the annual potential evapotranspiration, E_{p_A}, and the annual surface retention loss, E_{r_A}, are held at their respective mean annual values. This forces all yield variance to originate with precipitation variance. In computer application of course we can retain the appropriate distribution for τ and E_{p_A} and derive the distribution of Y_A through Monte Carlo simulation.

Equation (2.30) can now be rewritten (after rearranging) as

$$P_A\,[1 - e^{-G-2\sigma}\, \Gamma(\sigma + 1)\sigma^{-\sigma}] = \bar{E}_{p_A}\, J(E,M,k_v,h_o) - \bar{E}_{r_A} + M_\tau K(1) s_o^c - Tw \qquad (2.31)$$

i.e. Infiltration = Total Evapotranspiration - surface retention + Groundwater discharge

and

$$Y_A = P_A - \bar{E}_{p_A} \cdot J(E,M,k_v,\, h_o) \qquad (2.32)$$

which is in a form

$$Y_A = g(P_A) \qquad (2.33)$$

or

$$P_A = g^{-1}\,(Y_A) \qquad (2.34)$$

For each annual precipitation, Equation (2.31) is used to determine the space-time average soil moisture for the year. Substituting the annual precipitation and the corresponding space-time average soil moisture into Equation (2.32) then gives the annual yield of the catchment.

Since from Equation (2.32) the annual yield is a monotonic increasing function of the annual precipitation, we may derive the distribution of the annual yield from the distribution of precipitation. From Equations (2.5) and (2.34) we obtain

$$\text{Prob}\ [\frac{Y_A}{\bar{P}_A} < z] = e^{-m_\nu}\ \{1 + \sum_{\nu=1}^{\infty} \frac{m_\nu^\nu}{\nu!} P[\nu\kappa,\ m_\nu\ \kappa g^{-1}(z)]\ \} \tag{2.35}$$

The derived yield distribution is compared with historical data (using the Thomas plotting relation) for two catchments, one in Clinton, Massachusetts, and the other in Santa Paula, California, as shown in Figure (2.9) and (2.10). The κ values are from Figure (2.5) and (2.6). A detailed discussion of the procedures used in obtaining the soil parameters, and the sets of values of the optimal vegetation canopy density, M_o, and potential transpiration efficiency, k_v, is given in (19). From the comparison on the figures, the agreements are remarkable, which justifies the gross approximations in our model assumptions and indicates the general validity of applying such a technique to different catchments.

In the original development of the water balance model (19), the storm surface runoff is obtained, as herein, by subtracting the surface retention from the rainfall excess. However, later development (22) shows that it is more appropriate (though still only approximate) to subtract the surface retention at the beginning of the rainfall period, than to discount it against those events producing rainfall excess.

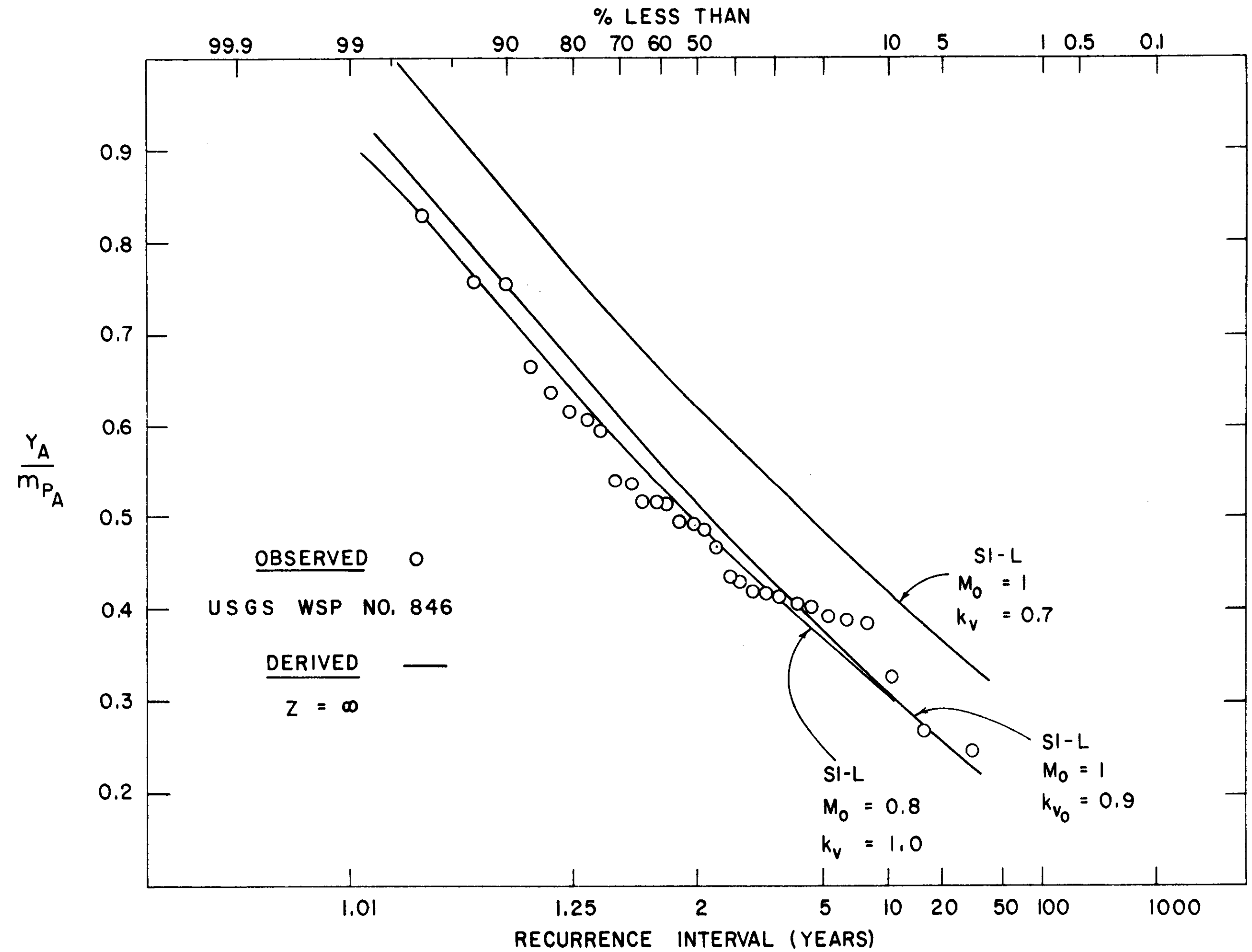

FIGURE 2.9
FREQUENCY OF ANNUAL BASIN YIELD WITH SUB-OPTIMAL VEGETAL COVER
(SOUTH BRANCH OF THE NASHUA RIVER AT CLINTON, MA., AREA = 174 km^2)

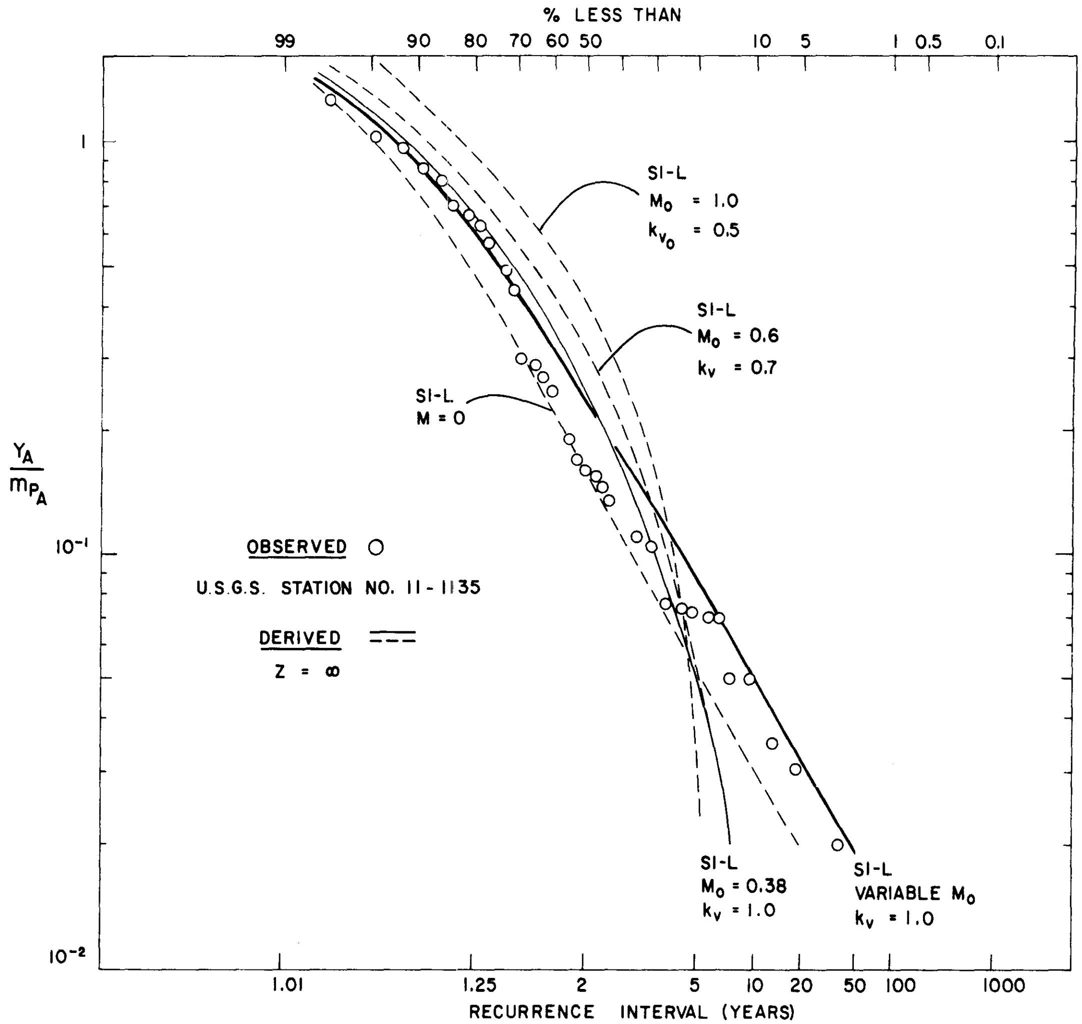

FIGURE 2.10

FREQUENCY OF ANNUAL BASIN YIELD WITH SUB-OPTIMAL VEGETAL COVER

(SANTA PAULA CREEK NEAR SANTA PAULA, CA., AREA = 64 km^2, κ = 0.25)

With this modification, Equation 2.23 is reduced to

$$\frac{\bar{R}_{s_A}}{\bar{P}_A} = e^{-G - 2\sigma} \Gamma(\sigma + 1)/\sigma^{\sigma} \tag{2.36}$$

and the water balance (Equation 2.28 and 2.31) becomes

$$\bar{P}_A \, [1 - e^{-G-2\sigma} \Gamma(\sigma + 1)\sigma^{-\sigma}] = \bar{E}_{p_A} \cdot J(E,M,k_v,h_o) + m_\tau K(1) \; s_o{}^c - Tw \tag{2.37}$$

and

$$P_A \, [1 - e^{-G-2\sigma} \Gamma(\sigma + 1)\sigma^{-\sigma}] = \bar{E}_{p_A} \cdot J(E,M,k_v,h_o) + m_\tau K(1) \; s_o{}^c - Tw \tag{2.38}$$

This modification will be used throughout this work and the effect of it on the CDF of yield is only significant in the dry years, when the surface retention becomes relatively important.

The water balance model is derived for the rainy season only and it is more correct to use the annual seasonal precipitation in the water balance equations than of the annual total precipitation. This assumes that the rainfall in the dry season is too small to have any appreciable effects on the annual catchment yield, and will be evaporated.

2.4 Remote Sensing as a Tool to Define Basin Parameters

In studying a large basin like the Bahr el Ghazal, which consists of eight subcatchments, occupying an area of five hundred thousand square kilometers (close to the size of France), it is extremely difficult, if not impossible, to know the distribution of vegetation and soil types over the entire basin. Remote sensing, one of the best tools available to the water resource planner, is especially effective in studying such a large scale system particularly because of the system's diversity of habitat, variability of hydrologic regime and inaccessibility of terrain.

The Landsat satellite, for example, employs an optical-mechanical multispectral scanner (MSS) to acquire data in four spectral band widths in the visible and the near-infra red portions of the electromagnetic spectrum. Each band emphasizes different surface or subsurface features of the land. Together with ground control observations they allow one to define the swamp areas and the extent of surface water, drainage patterns, vegetation and soil types, and surface geological information such as landform.

Satellite mappings of the whole basin in the wet and dry season are crucial to understanding the dynamic physical processes governing the swamps, for they indicate the extent of permanently-flooded and seasonally-flood areas.

Simultaneous ground observations and aerial data (i.e., ground truth) are needed to confirm the Landsat data interpretations.

Chapter 3

GENERAL DESCRIPTION OF THE BAHR EL GHAZAL BASIN

3.1 Introduction

The Bahr el Ghazal Basin is located in the southwestern part of the Sudan. It lies between latitudes 4° and 14° North and between longitudes 23° and 31° East. Its area is about half a million square kilometers (5×10^5 km^2) (see Figure 3.1).

Topographically, the area approximates a funnel having eight tributary streams leading to a central swampy region which occupies the extremely flat lands at the mouth. The peculiarity of this basin lies in its enormous loss of water in the central swampy region.

The output from the basin measured at Lake No remains more or less a constant from year to year, despite large yearly variations in precipitation, and hence in the streamflow of each sub-catchment. The variability of precipitation and of streamflow within the basin is reflected in the area of the swampy region, rather than in the streamflow output of the basin. Because of its funnel-like shape with an extremely flat bottom (slope: 1 cm/km), heavy rainfall and high input streamflows will cause the flooded area to expand considerably, thus making available a huge area for evapotranspiration and groundwater seepage, while at the same time causing only a relatively small change in water surface elevation and hence in output streamflow. When rainfall is scanty and runoffs are low, the flooded area will contract, thus reducing the water loss considerably, but not greatly lowering the output streamflow. Such a

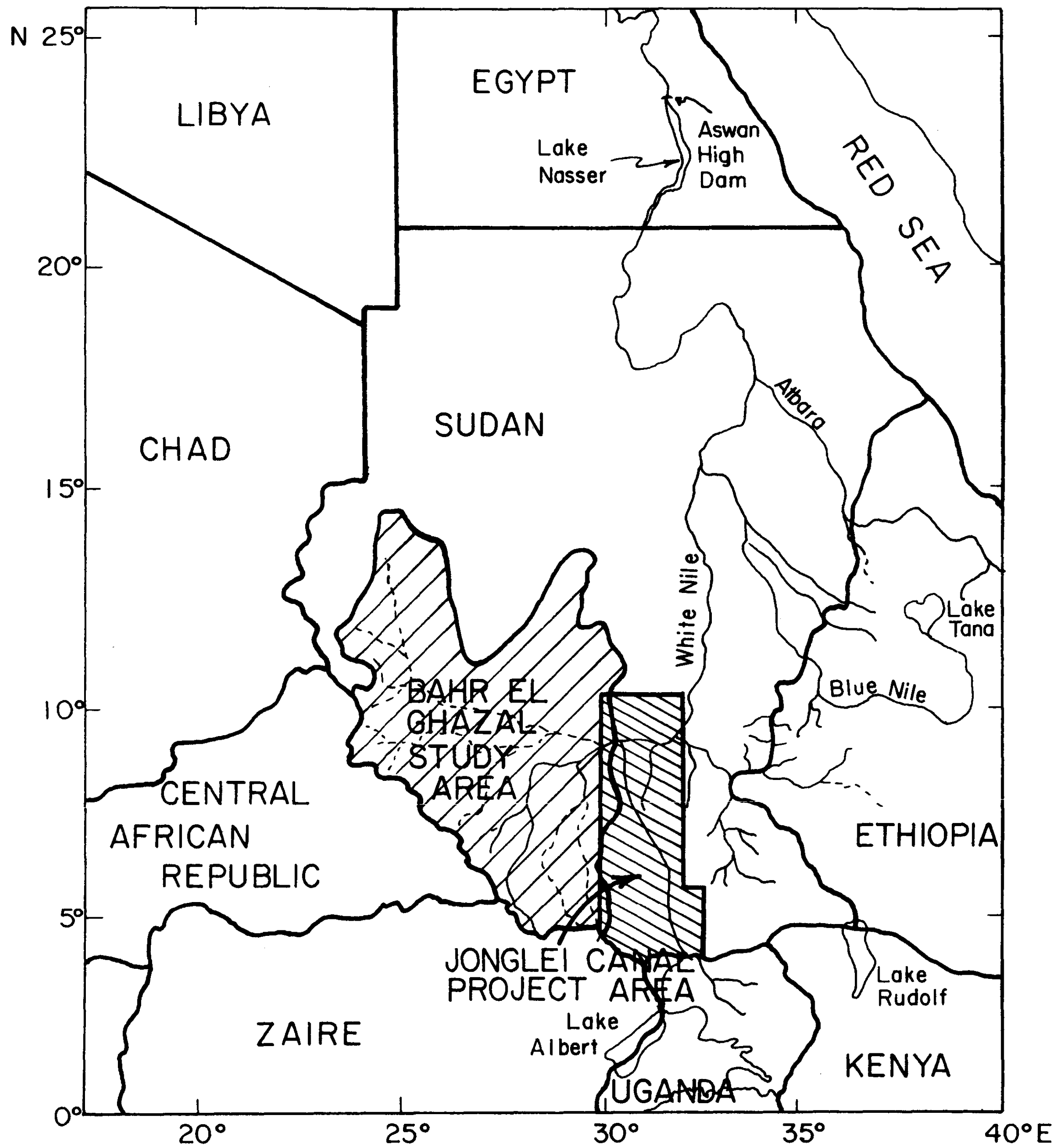

Figure 3.1 GENERAL LOCATION OF THE STUDY AREA

mechanism explains the relative constancy of the basin output. The evapotranspiration and groundwater seepage in the swampy region are so high that the basin output amounts to only a few percent of the total input.

3.2 Demarcation of Boundaries of Sub-catchments

The boundary of the basin is shown in Figure 3.2. The boundaries in the north and in the south follow the water-dividing lines of the "Operational Navigation Charts" (23), while in the east, it goes southward from Lake No to Lake Nuong, then follows the water-dividing line separating the catchments of River Naam and River Lau. River Lau is excluded in this investigation because from the drainage map of the Jonglei Canal project area (obtained from Landsat satellite images), there is a strong indication that its water is flowing into the Bahr el Jebel near Lake Nuong. The boundary between Lake No and Lake Nuong is adjacent to the Bahr el Jebel, since the Bahr el Jebel is known to spill its water westward into the Bahr el Ghazal swamp along this line (4).

The boundaries for each sub-catchment can be traced along its drainage divide from available maps. At the lower end of the tributaries, however, the boundaries are rather vague because the drainage divides as well as the tributary stream channels (River Jur excepted) disappear as they merge with the central swampy region. The latter is more or less bounded by the 400 meter contour (Figure 3.3).

The central swampy region can be roughly divided into two parts -- the papyrus swamp and the open grassland. The two intermingle.

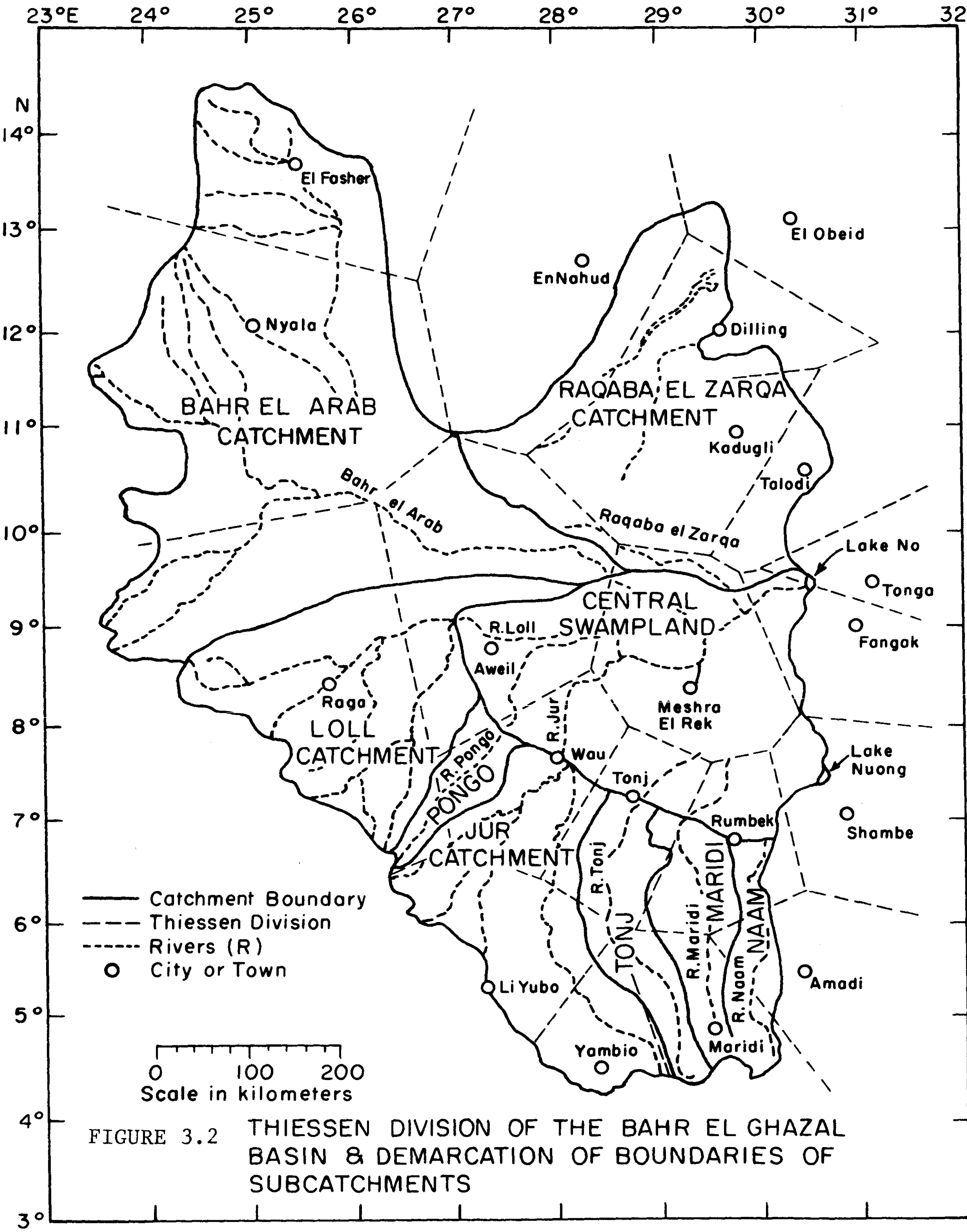

FIGURE 3.2 THIESSEN DIVISION OF THE BAHR EL GHAZAL BASIN & DEMARCATION OF BOUNDARIES OF SUBCATCHMENTS

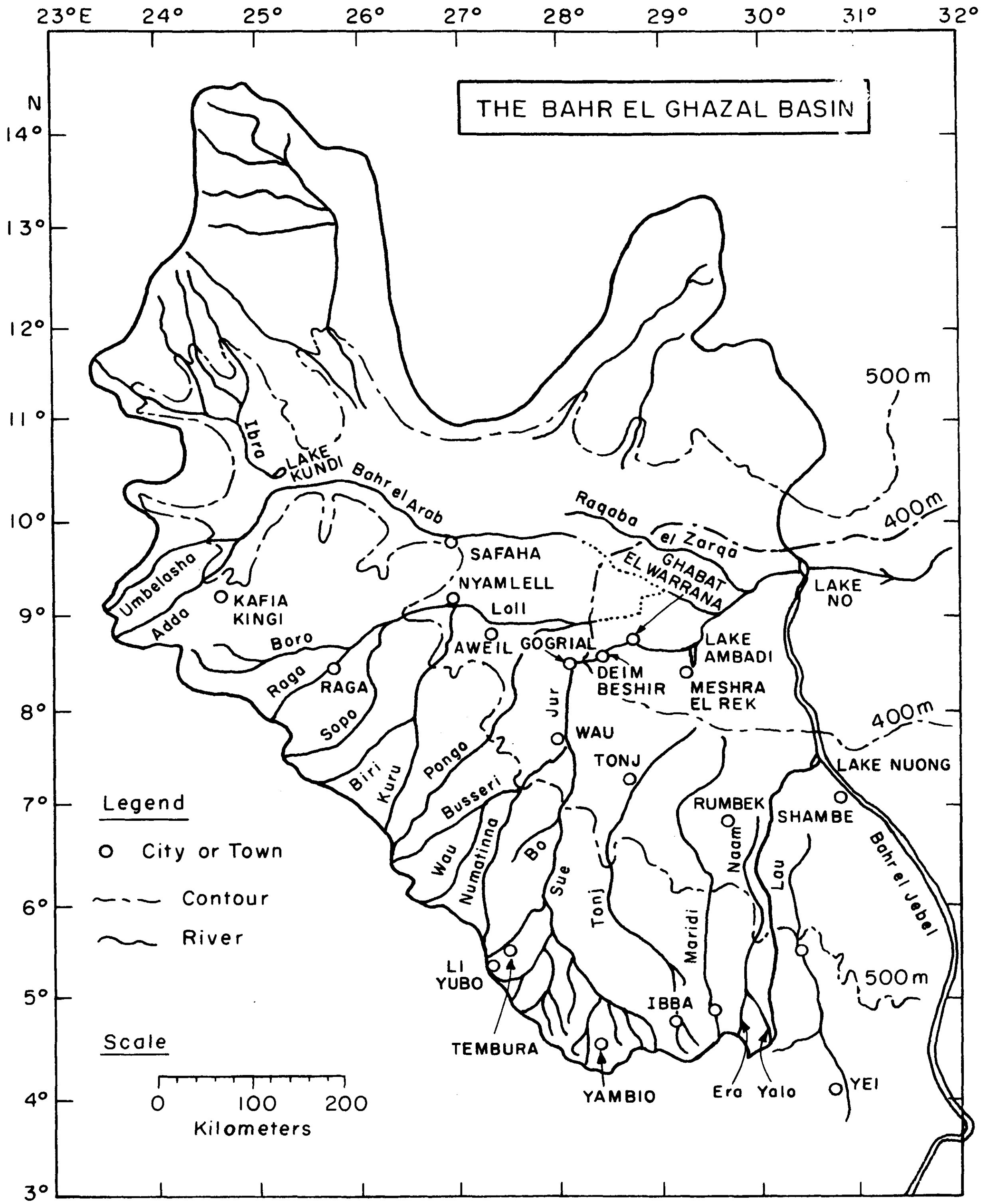

FIGURE 3.3

TRIBUTARIES OF THE BAHR EL GHAZAL BASIN

For simplicity, we will use the words "Central Swampland" to represent the sum of these two regions, as shown on Figure 3.2. In order to define the tributary inputs to the Central Swampland, we will choose the boundary of the Central Swampland as the line crossing all the downstream gaging stations of the sub-catchments. With the system boundaries so defined, Table 3.1 gives the area of each sub-catchment, and of the Central Swampland.

3.3 The River System (26)

3.3.1 A Typical River

Most of the important rivers in this basin are torrents originating in the southwest where the rainfall is heaviest. As shown in Figure 3.2, the main tributaries of the Bahr el Ghazal include the rivers Jur, Loll, Tonj, Pongo, Maridi, Naam, Raqaba el Zarqa and Bahr el Arab. The rivers Jur and Loll contribute about 70% of the total discharge of the basin while Raqaba el Zarqa and Bahr el Arab contribute only 3%. Table 3.1 shows the gaged discharge of the rivers. The monthly discharges of the rivers (Raqaba el Zarqa and Bahr el Arab excepted) are plotted in Appendix A.

All the rivers in the southwest show a strong resemblance to one another in their stages of development.

The typical river begins at the Nile-Congo Divide and flows through a steep area of rapid runoff where drainage is good and small streams are numerous. Rapids occur in this region. It then flows into an area of well-defined flood plains where the reduction in channel

Table 3.1

PRECIPITATION AND DISCHARGE FOR BAHR EL GHAZAL BASIN

Catchment Name	Catchment Number	Mean Annual Precipitation* mm	Catchment Area** km^2	Mean Annual Precipitation $10^9\ m^3$ (md)	Mean Gaged Discharge (24) $10^9\ m^3$ (md)
Naam	1	1224	11,962	14.6	0.476[a]
Maridi	2	1120	15,390	17.2	0.520[b]
Tonj	3	1255	21,708	27.2	1.600 (D.S.R.B. Tonj)
Jur	4	1371	54,705	75.0	5.220 (at Wau)
Pongo	5	1173	8,428	9.9	0.575 (D.S.R.B.)
Loll	6	1128	65,338	73.7	3.900 (at Nyamlell)
Bahr el Arab	7	653	157,397	102.8	0.300
Raqaba el Zarqa	8	689	92,508	63.7	0.100
Sum or Average		899	427,436	384.1	12.7
Central Swampland		917	84,949	77.9	-
Bahr el Ghazal Basin		902	512,385	462	12.7

* by Thiessen method, using precipitation values on Table 3.2.
**above gage at edge of Central Swampland
D.S.R.B. = Downstream of Road Bridge
a: From (25), for the period (1942 - 1952), at Mvolo.
b: From (25), for the period (1942 - 1960), through Road Bridge.

slope causes the river to spill and deposit the suspended material carried down from above, forming alluvial banks alongside the channel. The sandy river bed in this region takes up much of the dry season flow through seepage. Going downstream, the river enters the Central Swampland where flooding is unrestricted. The impermeable clay plain together with the extremely small gradient (1 cm/km) accounts for the eventual disappearance of the river identity (River Jur excepted) in this region. Swamp formation occurs locally where the land level is depressed.

3.3.2 Naam

Starting in a clockwise direction from the Southeastern catchment boundary, River Naam is the first river encountered within the basin. It has two tributaries, the Era and the Yalo, which rise from the Nile-Congo Divide. About 50 kilometers north of the road from Shambe to Rumbek, the Naam is lost in swamp (see Figure 3.3).

3.3.3 Maridi

The second river is the Maridi. Its flood plain begins about 50 kilometers upstream of the Tonj-Mvolo road-bridge. South of Meshra El Rek (around latitude 8° North), it disappears in the swamp.

3.3.4 Tonj

The third river is the Tonj. It is also known as the Ibba in its southern reaches. The river begins to spill at about latitude 6°40' (80 kilometers south of Tonj) and at about 7°40', it is lost in the swamp.

3.3.5 Jur

The Jur is the fourth and the largest river. It has two major tributaries, River Sue and River Busseri, which join just south of Wau. Rivers Wau and Numatinna are tributaries of the Busseri, and River Bo is a tributary of the Sue. Definite spills occur downstream of Deim Beshir. Beyond Ghabat el Warrana, the river narrows with many square miles of swampy area bordering it on both sides. At the end of its journey, the Jur empties into Lake Ambadi.

3.3.6 Pongo

The fifth river is the Pongo. In the literature, it is considered to be a tributary of the Loll. Since it joins the Loll north of Deim Beshir, which is well inside the Central Swampland, it will be considered, for modeling purposes, as a separate river feeding the Central Swampland.

3.3.7 Loll

The sixth river is the Loll, which is the second largest river of the basin. It is fed by four tributaries (Pongo excluded). In a clockwise direction, they are the Kuru, (Biri, a Kuru tributary), Sopo, Raga and Boro. They all join to form the Loll before Nyamlell is reached. Below Nyamlell, the Loll starts to spill into swamps and it eventually disappears about 180 kilometers downstream of Nyamlell.

3.3.8 Bahr el Arab

The seventh river is the Bahr el Arab. This river has the largest catchment in the basin and yet the smallest discharge due to its lower precipitation and flatter land slope. Its two most important tributaries come from the extreme southwestern part of the catchment, with River Adda being the first and River Umbelasha the second. Most of the streams in the north do not reach the Bahr el Arab, instead, they terminate in swamps connected with the Arab. For example, the principal stream, Ibra, ends in a swamp near Lake Kundi.

It is possible that the Bahr el Arab starts spilling near Kafia Kingi because of some swamp formation along that reach. When the river reaches Safaha due north of Nyamlell, much of its water has already been lost by spilling, and further losses occur downstream. In the dry season, there is practically no flow at Safaha. Further downstream at about latitude 9°18'N and longitude 29°E, it splits up into many small channels and is eventually lost in a swampy region where the Bahr el Arab and Loll are believed to merge.

3.3.9 Raqaba el Zarqa

The eighth river is the Raqaba el Zarqa. There is practically no information on this river. Only some meteorological data are available for a few stations within this catchment.

3.3.10 Bahr el Ghazal

The outflow from Lake Ambadi is known as the Bahr el Ghazal. Flowing north, it is joined by the Bahr el Arab which is now a stream emerging from the swamps of Loll and Arab. From the mouth of the Bahr el Arab to Lake No, the Ghazal breaks into many parallel channels, spreading out and rejoining the main stream along its course. Towards

Lake No, the defined river banks give way to many channels and lagoons. The Bahr el Ghazal terminates in Lake No.

3.4 Hydrological Zones

3.4.1 Introduction

A hydrological map of the Bahr el Ghazal basin is shown in Figure 3.4, as obtained from Reference (26). Information is available only to about 10° North latitude, however, this includes most of the important sub-catchments of the basin. We will ignore the Bahr el Arab and Raqaba el Zarqa catchments in the following descriptions since they apparently make a negligible contribution to the hydrology of the Bahr el Ghazal.

The Bahr el Ghazal basin has been divided hydrologically into two zones (26): the Flood Region and the Equatorial Region (Figure 3.4).

3.4.2 The Flood Region

The Flood Region has a mean annual rainfall of 750 to 1000 mm during the rainy season of 6 to 7 months. The lands are extremely flat, with a general slope of about 10 cm per kilometer. Because of the impermeable soils in this region, heavy flooding and waterlogging occur during rains. According to the level of flooding, it can be further subdivided into four land types, the High land, the Intermediate land, the Toich land and the Sudd land.

The "High land" is about one meter higher than the surrounding areas but is relatively flood-free even at the peak of the rainy season. Vegetation is mainly woodland of the thorn type or open-mixed woodland.

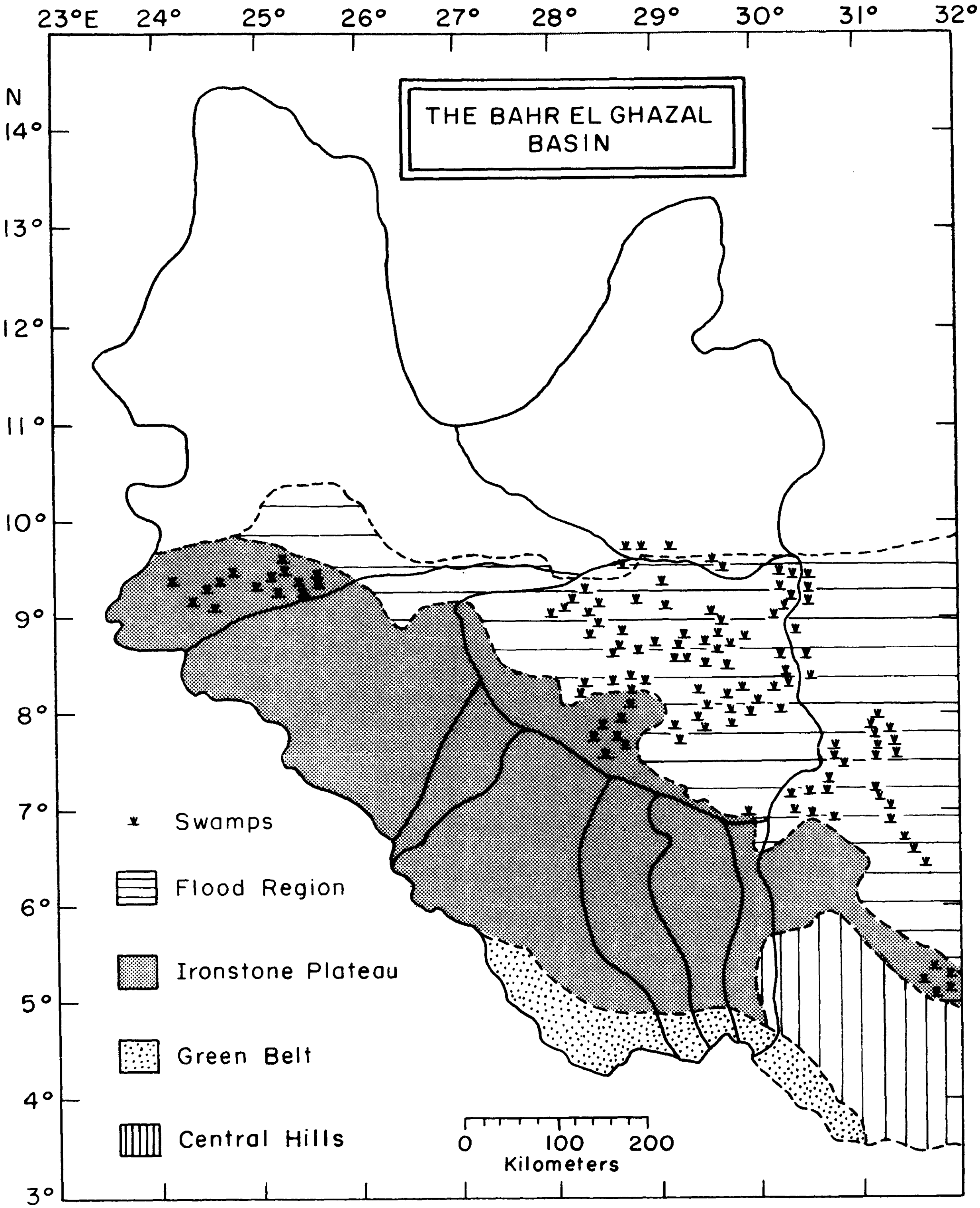

FIGURE 3.4

HYDROLOGIC MAP, BAHR EL GHAZAL BASIN

Soils vary from clay to loose sands.

The Intermediate land is subjected to heavy flooding during rains but remains dry during the dry season. The land level is lower than the High land but higher than the Toich land. Vegetation is predominantly open perennial grassland with some areas of acacia woodland. Soils vary from clay to heavy loam.

The Toich land is seasonally flooded by spill-water from the rivers. Vegetation is mainly grasses and few trees exist. The soil retains sufficient moisture to support active grass growth even in the dry season. Soils vary from sandy-clay to heavy clay.

The Sudd land is permanent or semi-permanent swamp where the soil moisture is always at saturation. Vegetation is predominantly *Cyperus papyrus*. This land type is usually at the lowest level in the Flood Region where it is inundated most of the year. The soils contain a fairly high percentage of clays which swell when wet inhibiting infiltration (12).

3.4.3 The Equatorial Region

The Equatorial Region contains the Ironstone Plateau, the Green Belt and the Central Hills.

The Ironstone Plateau has a mean annual precipitation of 900 to 1300 mm during the rainy season of 6 to 8 months. Vegetation is mainly broad-leaved woodland and savanna grasslands. The soils are predominantly shallow, reddish, sandy loams.

The Green Belt has the highest mean annual precipitation in the basin, receiving 1350 to 1600 mm during the rainy season of 8 to 9 months. Vegetation is similar to the Ironstone Plateau but the woodland is more luxuriant, with forests along perennial streams. Soils are similar to the Ironstone Plateau.

The Central Hills have a mean annual precipitation of 900 to 1200 mm during the rainy season of 7 to 8 months. Vegetation is similar to the Ironstone Plateau, but with less developed woodland and denser grasses. Soils are usually red loams with frequent rock exposure.

3.5 Soils and Vegetation Distribution (26)

3.5.1 Soils and Vegetation Distribution in the Central Swampland

The Central Swampland lies almost entirely within the Flood Region, with only a narrow strip of Ironstone Plateau intruding along its southwestern boundary (Figure 3.4). Within the Flood Region, four land types have been identified, namely, the "High land," the Intermediate land, the Toich land and the Sudd land. The soils and vegetation are highly specific according to different land types. They are described as follows:

3.5.1.1 On the "High land"

The soils of the "High land" vary from clay to loose sands.

Sandy soils generally occur as outcrops on flat clay plains. Flooding is uncommon due to free soil drainage. The coarse sand content is high (25 to 60%) and the clay content is usually below 15%. Because of free drainage, crops grown on these soils may be susceptible to drought.

Clay soils are found on flat ground slightly higher than the surrounding lands, or on sloping ground on the banks of watercourses. Flooding is also uncommon. Clay content ranges from 25 to 60%. These soils are often intensively cultivated.

The predominant vegetation types on the "High land" are the woodlands. They are generally of the thorn type, including *Acacia seyal*, *Acacia fistula*, *Balanites aegyptiaca*, and *Acadia sieberiana*.

In the northern Central Swampland, the shorter annual grasses, *Eragrostis spp.* and *Aristida spp.* occur frequently, but in areas of dense *Acacia seyal-Balanites aegyptiaca* woodland, the taller annual grasses, *Rottboellia exaltata* and *Leptochloa chinensis*, are more common.

In the southern Central Swampland, the grasses *Hyparrhenia dissoluta*, *Hyparrhenia filipendula*, and some *Andropogon gayanus*, are more common.

Close to the edge of the Ironstone Plateau, mixed woodland of the broad-leaved and the thorn type usually occurs on sandy soils (see also Section 3.5.1.5).

In many areas, numerous trees have been cut down for fuel and building purposes.

3.5.1.2 On the Intermediate land

The soils in this region vary from clay to heavy loams. They both occur on flat plains and are subjected to heavy flooding during the rainy season. The clay content of the loam soils ranges from 25 to 50%, with a coarse sand content of over 20%. The clay content of the clay soils is much higher, from 40 to 75%. Both soils are fertile, but their agricultural value is limited by poor drainage.

The vegetation on the open plains is predominantly grassland, with species *Setaria incrassata* dominating areas of lesser flooding and *Hyparrhenia rufa* dominating other areas.

On higher ground, acacia woodlands occur, mainly a mixture of *Acacia seyal* and *Balanites aegyptiaca*.

Most of the open grassland in the region is purposely burned off in the dry season to stimulate regrowth for cattle feeding.

3.5.1.3 On the Toich land

The predominant vegetation on this land is grass. Few trees exist. The distribution of grasses is largely governed by the depth and duration of flooding, by the soil type, and to a lesser degree, by the extent of grazing and burning. Three types of grassland are of major importance -- *Echinochloa toiches*, *Phragmites toiches* and *Hyparrhenia toiches*.

The dominant grass species on the *Echinochloa toiches* are *Echinochloa stagnina* and *Echinochloa pyramidalis*. They are generally found on riverain flood-plains where flooding occurs from 3 to 6 months of the year and where the soils do not dry out completely throughout the year. *E. stagnina* usually stands on lower flood-plain levels while *E. pyramidalis* appears on the higher. The clay content of the soils is high (40 to 70%). The soils are fertile and they provide excellent dry season grazing.

The dominant grass on the *Phragmites toiches* is *Phragmites communis*. It occurs on riverain flood-plains where flooding lasts 2 to 4 months of the year, with the soils drying out completely toward the end of the dry season. The clay content of the soil is between 25 to 60%. The soils are only of moderate fertility and support moderate dry season grazing.

The dominant grass on the *Hyparrhenia toiches* is *Hyparrhenia rufa*, though sometimes a considerable amount of *Vetineria nigritana* is also present. They are generally found on lands where flooding rarely exceeds a period of ten weeks and where the water table is high in the rainy season. The soils are mainly clay with sandwiched, thin, sand layers. The soils are fertile, but at present cultivation is not extensive.

3.5.1.4 On the Sudd land (permanent swamps)

The Sudd vegetation is predominantly *Cyperus papyrus*. It occurs on low-level lands adjoining the major watercourses, with a flooding period of 4 to 8 months per year, but with a waterlogging period of 9 to 12 months of the year. Clay content of the soils is usually high (up to 60%). In some areas, coarse sand content may amount to 40%. Swamp vegetation grows luxuriantly on the clay soils, but its growth is stunted on the sandy soils (12).

3.5.1.5 On the edge of the Ironstone Plateau

The dominant vegetation here is mixed woodland of the broad-leaved and the thorn type. They usually occur on sandy soils which is at most only slightly flooded during the rainy season. In many areas, the broad-leaved type is more common. The mixed woodland generally includes *Combretum sp.*, *Terminalia sp.*, *Anogeissus schimperi*, *Acacia spp.* (*A. segal*, *A. sieberiana*, *A. senegal*, *A. campylacantha*), *Balanites* *aegyptiaca, Dalbergia melanoxylon, Mitragyne sp., Kigelia aethiopica, Ficus sp., Bauhinia reticulata, Dichrostachys glomerata* and other broad-leaved types.

The grass may include *Hyparrhenia dissoluta, H. barteri var. calvescens, H. rufa* and *Andropogon gayanus,* and *Setaria incrassata.*

3.5.2 Soils and Vegetation of the Sub-catchments

The six sub-catchments in the south lie almost entirely on the Ironstone Plateau, only a small part in the southern-most region of the catchments* Jur, Tonj, Maridi and Naam is within the Green Belt, and a small part of Naam is in the Central Hills zone (Figure 3.2 and 3.4). The soils and vegetation of these regions are described as follows.

3.5.2.1 On the Ironstone Plateau

The major part of this area is covered by shallow reddish sandy loam overlying hard ironstone. The depth of soil is generally much shallower than 2 feet.

At the highest elevations where the soils are shallow, coarse and very well drained, broad-leaved woodland exists. The common tree species are *Khaya senegalensis, Anogeissus schimperi, Lannea kerstingii, Burkea africana, Combretum ghasalense, Prosopis africana, Boscia senegalensis, Grewia mollis* and *Terminalia mollis.* Grasses in this area are not well-developed, with perennial *Hyparrhenia spp.* (*H. barteri var.*

*For simplicity, the words "catchment" and "sub-catchment" will be used interchangeably throughout this work.

calvescens and *H. dissoluta*) being the dominant type.

Along the slopes where the soils are deeper and better drained, the grass cover is better developed than the woodland. Here fewer tree species exist.

On the low-level land, the deeper, heavier and less freely drained soils are subject to seasonal flooding. Grass growth is luxurious and many areas are treeless. Major grasses are *Hyparrhenia spp.* (*H. rufa* and *H. filipendula*). In areas where woodland occurs, the tree species include *Terminalia spp.*, *Anogeissus schimperi*, *Acacia seyal* and *Mitragyne sp.*

Two factors which may be important in the redistribution of vegetation on the Ironstone Plateau are the annual fires and the shifting pattern of cultivation. Where grass growth is dense, the annual fires are severe and the development of woodland is stunted. In shifting cultivation, new lands are periodically cleared while the old sites are allowed to regenerate. However, the regeneration of trees is much slower than that of grasses, and the regeneration of non-fire-resistant tree species is almost impossible.

3.5.2.2 On the Green Belt

The soils in this region are similar to those of the Ironstone Plateau. Because of the heaviest rainfall and smaller land slopes in this region, the broad-leaved woodland here is more luxuriant, with additional species of *Chlorophora sp.*, *Anona sp.*, *Lophira sp.*, *Sterculia sp.* and *Crossopteryx sp.*

Fully-developed forests occur alongside River Sue, and in the southwestern part of Yambio District. Tree species in these forests include *Khaya grandifoliola, Chlorophora excelsa, Canarium schweinfurthii, Ceiba pentandra, Erythrophleum guineense,* and *Mitragyne stipulosa.*

3.5.2.3 On the Central Hills

The soils here are similar to those of the Ironstone Plateau. However, due to high erosion in this region, they are generally very shallow and lateritic, with frequent rock exposure. Deeper red loams are found only in the valleys and local depressions. Vegetation is similar to that of the Ironstone Plateau, but with less developed woodland and denser grasses. In addition to the broad-leaved woodland, woodland of the thorn type also occurs.

This region is just outside of the Bahr el Ghazal basin and appears to be of minor importance to the hydrology of the basin. Thus, no further description of it will be given.

3.6 Groundwater Table

Available information on the groundwater table in the Bahr el Ghazal basin is very limited. The following description comes from Reference (26).

On the lower ironstone peneplain (close to the Central Swampland), the water table is generally high.

At Rumbek, water is found as little as 10 feet below the land surface (see Figure 3.3).

In Tonj District, 90 government wells have depths ranging from 20 to 100 feet, and more than 180 other wells have depths down to 15 feet.

Along the Wau-Aweil-Raga road, close to the edge of the ironstone, depth of well is generally found to be between 15 to 20 feet.

Along the direct Wau-Raga road, water is easily found at depths of up to 30 feet.

In the Gogrial area of the Central Swampland, 60 government wells have an average depth of 25 feet.

In the southern and southwestern part of the ironstone areas and in the Green Belt, wells in general have not been successful. An exception is at Tembura (close to Li Yubo), where a well at 40 feet strikes water, yet another well 10 meters away remains dry in the dry season.

Most of the information available comes from the northern-most part of the catchments at the edge of the Central Swampland where the water table should be closest to the surface. As an estimate, the areal mean depth to water table for all the catchments is taken to be 20 meters. Effects of varying this depth will be discussed in the next chapter.

3.7 Climatic Parameters

3.7.1 Rainfall Characteristics

Rainfall in the study area is generally convective in nature and occurs in violent afternoon and evening thunderstorms (26), (27). The rainy season ranges in length from 5 months (May to September) in the north to 9 months (March to November) in the south and is governed largely by the migration of the inter-tropical convergence zone (ITCZ). Within the season, monthly rainfall rises to a peak in July or August.

There are about twenty meteorological stations in the study area. Table 3.2 gives their names, locations and altitudes, together with the long-term mean annual precipitation and the mean number of rainy days.

The mean annual precipitation is lowest in the north (299 mm at El Fasher) and highest in the south (1498 mm at Li Yubo). It is linearly related to the mean annual number of rainy days (see Figure 3.5) and to the latitude (see Figure 3.6). Assuming one storm per rainy day, the former correlation implies a relatively constant average storm depth ($m_H = \overline{P}_A/m'_\nu$ = 14.3 mm) throughout the basin.

For all stations, the monthly precipitation follows a bell-shaped curve. The rainy season is determined by omitting those months in the tails having a collective precipitation no greater than 5% of the annual total. The average annual seasonal precipitation, $\overline{P}_s$, may then be estimated as 95% of the annual value. By this estimation, it is obvious that $P_s/\overline{P}_s = P_A/\overline{P}_A$ and the observed distribution for the two are the same.

To apply the Poisson model developed earlier, we need to know the mean seasonal number of storms (m_ν) and the shape parameter, κ, of the Gamma distribution of the storm depth. If a long record of the annual precipitations and the associated m_ν are available (say, more than 20 years), then κ may be obtained from these data using the Poisson definition

Table 3.2

LOCATION OF METEOROLOGICAL STATIONS AND THEIR MEAN ANNUAL PRECIPITATION DATA

Station	Latitude North (28)	Latitude East (28)	Altitude (28) (m)	Mean Annual Precipitation $\overline{P}_A$ (mm)	Standard Deviation of P_A σ_{P_A} (mm)	Mean Annual Number of Rainy Days m'_ν	Years of Observation (up to 1975)
El Fasher	13°37'	25°20'	730	299	120	34.3	58
El Obeid	13°10'	30°14'	570	371	111	34.2	73
En Nahud	12°42'	38°26'	565	396	102	33.8	64
Nyala	12°04'	24°53'	675	486	109	42.4	54
Dilling	12°02'	29°38'	670	436	127	46.2	59
Kadugli	11°00'	29°43'	500	747	144	53.2	64
Talodi	10°37'	30°24'	473	794	150	56.0	60
Tonga*	9°28'	31°03'	390	877	193	58.8	61
Fangak*	9°04'	30°53'	390	936	290	59.6	49
Aweil*	8°46'	27°24'	415	901	175	64.6	41
Raga	8°28'	25°41'	545	1183	162	79.6	63
Meshra el Rek*	8°25'	29°16'	427	836	179	49.5	53
Wau*	7°42'	28°01'	435	1126	182	82.9	72
Tonj*	7°17'	28°45'	430	1056	198	71.7	28
Shambe*	7°05'	30°46'	405	780	228	51.1	61
Rumbek*	6°48'	29°42'	420	988	217	63.9	63
Amadi	5°31'	30°20'	500	1175	185	80.6	39
Li Yubo	5°24'	27°15'	600	1498	200	104.8	34
Maridi	4°55'	29°28'	750	1385	225	100.3	55
Yambio	4°34'	28°24'	650	1429	197	110.3	52

*Station in the vicinity of the Central Swampland

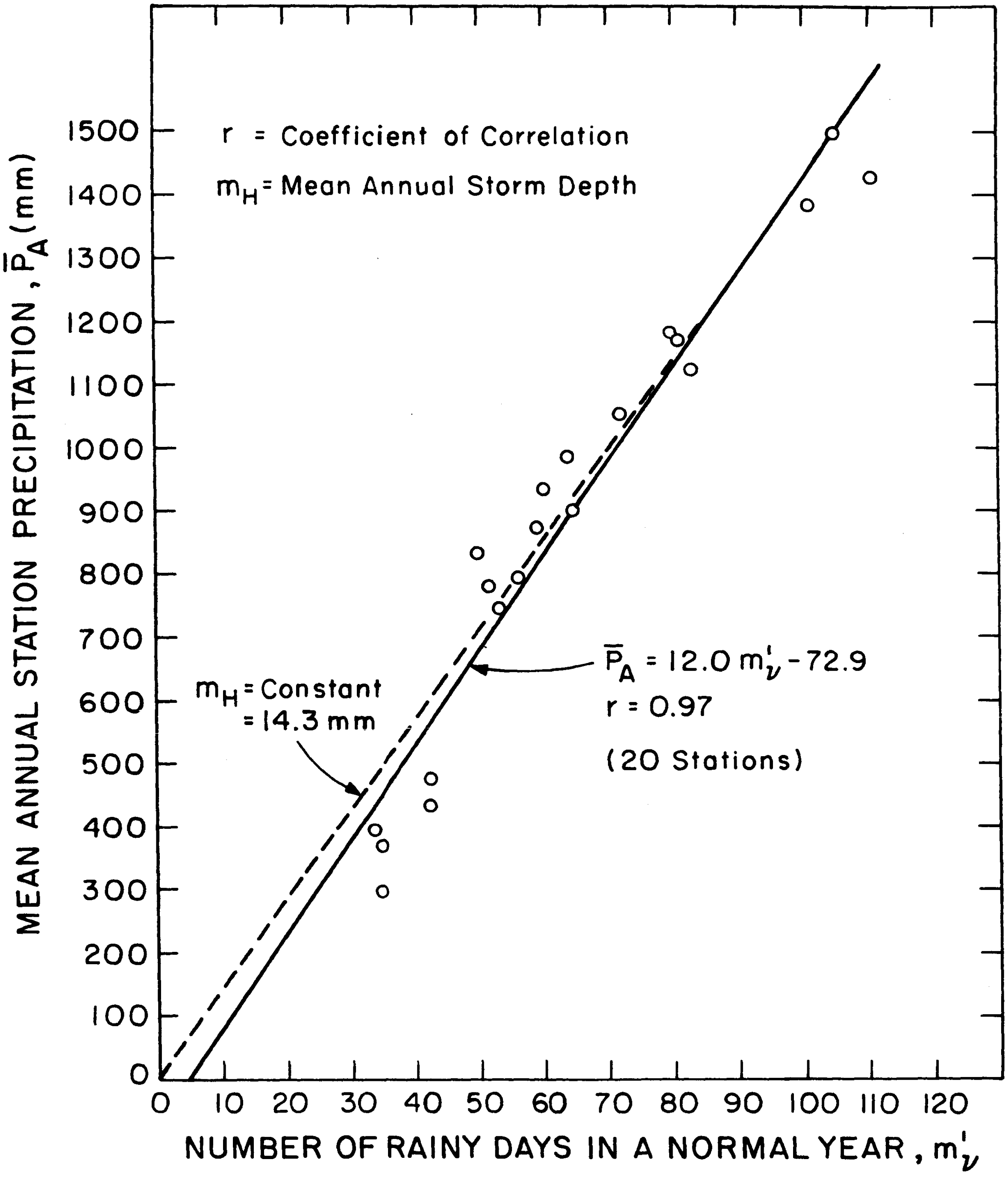

FIGURE 3.5

CORRELATION BETWEEN MEAN ANNUAL STATION PRECIPITATION AND MEAN ANNUAL NUMBER OF RAINY DAYS

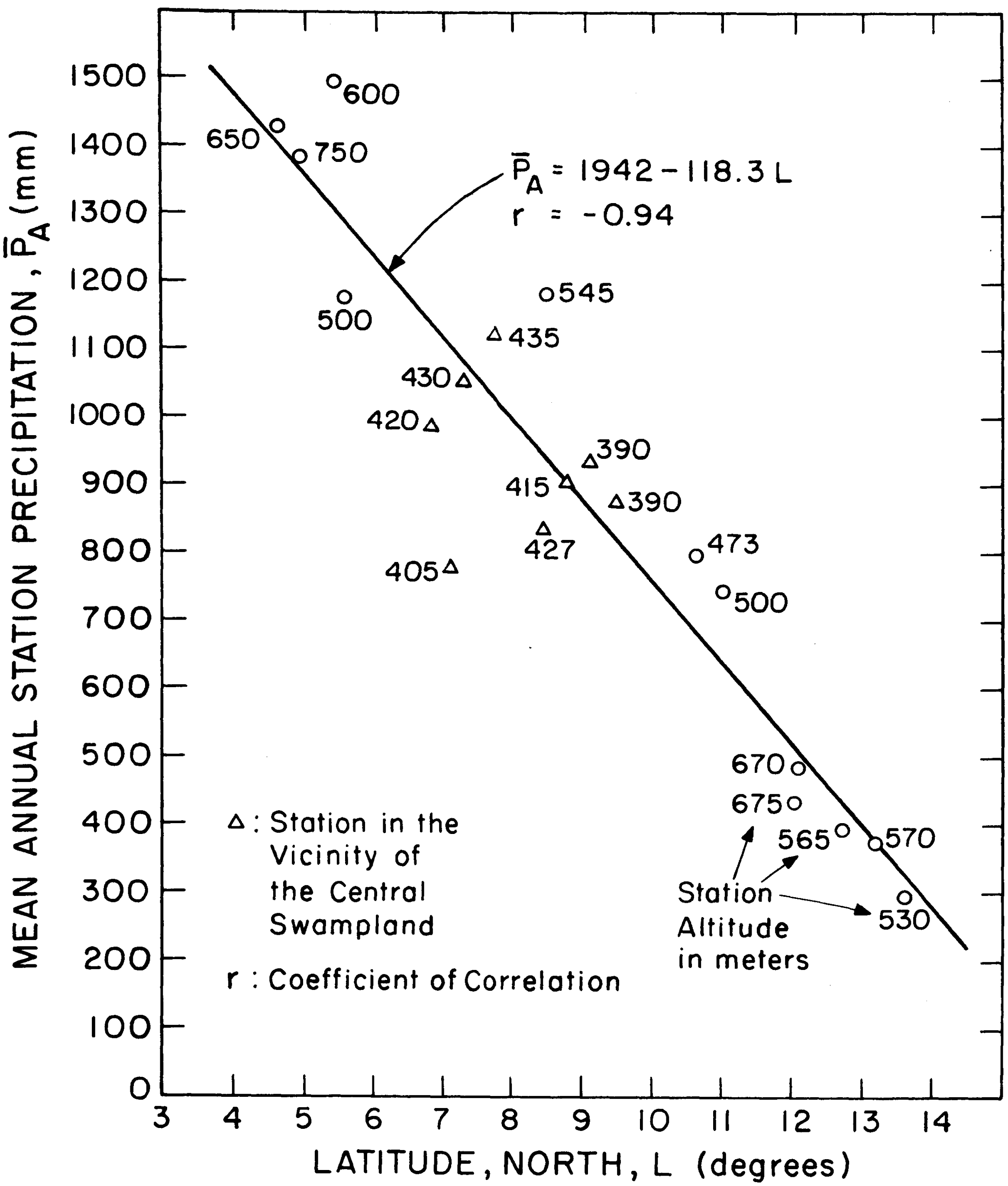

FIGURE 3.6

CORRELATION BETWEEN MEAN ANNUAL STATION PRECIPITATION AND LATITUDE

$$\kappa = \left[m_\nu \left(\frac{\sigma_{P_A}}{\bar{P}_A}\right)^2 - 1\right]^{-1} \qquad (3.1)$$

which is derived in (15).

In a long record, to facilitate the work, m_ν in Eq. (3.1) may be replaced by the mean annual number of storms, instead of the mean seasonal, since in this case the two differs by very little.

If only a few years of rainfall record are available, κ may best be determined from observations of individual storm depth (h) as follows:

By definition of the Gamma distribution

$$m_H = \kappa/\lambda = \text{mean storm depth} \qquad (3.2)$$

and

$$\sigma_H^2 = \kappa/\lambda^2 = \text{variance of storm depth} \qquad (3.3)$$

therefore

$$\kappa = \left(\frac{m_H}{\sigma_H}\right)^2 \qquad (3.4)$$

The CDF of storm depth is given in ( ), as

$$\text{Prob}(h \leq h') = \int_0^{h'} \frac{\lambda(\lambda h)^{\kappa-1} e^{-\lambda h}}{\Gamma(\kappa)} \, dh \qquad (3.5)$$

in which, as before,

$$\lambda = \kappa/m_H \qquad (3.6)$$

Storm depth data available through the Sudanese Meteorological Service consist of the average number of rainy days in the wet season having a storm depth, h, greater than 0.1 mm (X_1), greater than 1.0 mm (X_2), and greater than 10.0 mm (X_3). The station record length is from 3 to 18 years. To obtain the parameters κ and λ of the Gamma distribution fitted to these points on the CDF of storm depth (Equation 3.5), two assumptions are made:

(1) The number of storms is proportional to the number of rainy days

$$m_\nu = a\, m_\nu' \tag{3.7}$$

where

m_ν' = average number of rainy days in the wet season

and

a = constant ≥ 1.

(2) Storms with $h \leq 0.1$ mm are neglected. Then

$$\text{Prob}[h \leq 1.0 \text{ mm}] = 1 - \frac{aX_2}{aX_1} = 1 - \frac{X_2}{X_1} \tag{3.8}$$

$$\text{Prob}[h \leq 10 \text{ mm}] = 1 - \frac{aX_3}{aX_1} = 1 - \frac{X_3}{X_1} \tag{3.9}$$

Equations (3.5), (3.6), (3.8) and (3.9) define κ and λ which together give the mean storm depth from Equation (3.2). The mean number of storms in the wet season is then given by

$$m_\nu = \overline{P}_s / m_H \tag{3.10}$$

where

$\overline{P}_s$ = mean annual seasonal precipitation, cm and from Eq. (3.7),

$$a = \frac{m'_\nu}{m_\nu} \tag{3.11}$$

The values of "a" using the above solution range from 0.85 to 1.48 for the 20 stations. κ and m_ν so obtained are checked by comparing Eq. (2.5) with the CDF of observed station annual precipitation. The results in general are poor. For the three stations (Wau, Raga, Yubo) that fit well, "a" ranges from 1.03 to 1.10.

The poor results are not unexpected. Due to the practical difficulty of distinguishing between depths of 0.1 mm and 1 mm in the field, the right-hand side of Eq. (3.8) may be highly inaccurate, and, in some extreme cases, it is even driven to zero, which makes Eq. (3.5) impossible.

To circumvent this problem, Eq. (3.8) is not used. Instead, by assuming a = 1.0 in Eq. (3.7), we obtain

$$m_\nu = m'_\nu \tag{3.12}$$

which then gives the mean storm depth as

$$m_H = \overline{P}_s/m_\nu \tag{3.13}$$

Equations (3.5), (3.6), (3.9) and (3.13) now define κ. The values of κ and m_ν so defined may be checked by comparing Eq. (2.5) with the CDF of observed station annual precipitation. Figure 3.7 for station Wau gives a typical comparison. The rest of the stations are given in Appendix A. In all these figures, $\overline{P}_A = m_{P_A}$ and $\overline{P}_s = m_{P_s}$. The fit for

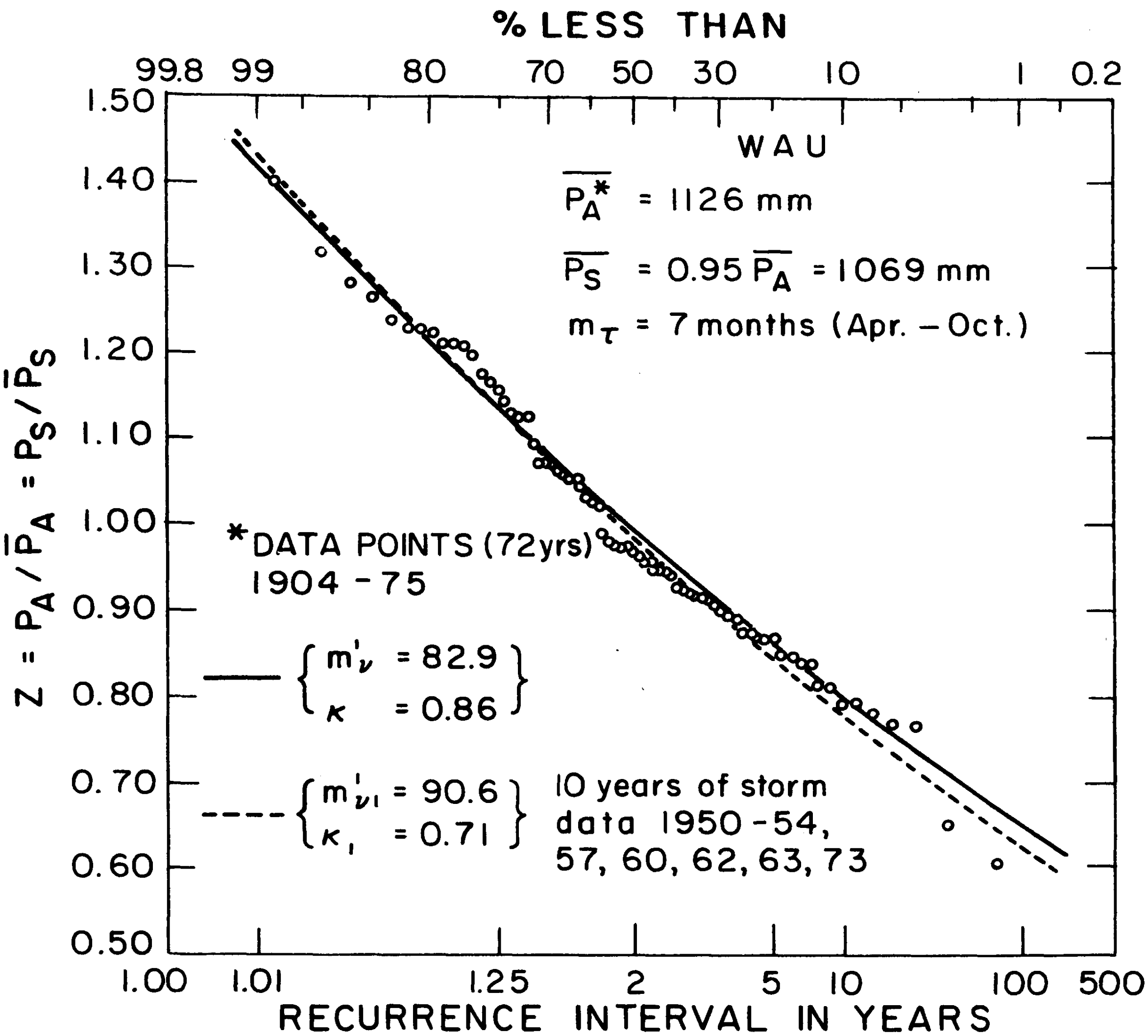

FIGURE 3.7

FREQUENCY OF ANNUAL PRECIPITATION

(STATION WAU)

most of the stations is amazingly good even using only three to eighteen years of observations for determining the parameters. There are three exceptions, stations El Fasher, El Obeid and Fangak. These are probably due to the fact that stations El Fasher and El Obeid were moved to new locations several miles away from their old sites in 1945 and 1942, respectively, while the precipitation of Fangak appears to have been experiencing a decreasing trend since 1947. Using a few years of precipitation observations at the new station sites or the observations in the low precipitation years will certainly underestimate the variance of the long-term records, thus giving a flatter CDF than the observed.

Obtaining the Poisson parameters from the entire sample of annual observations, as indicated in Eq. (3.1), gives a remarkable fit with the observations at all stations indicating that these <u>are</u> Poisson arrival processes. The above results reinforce our earlier conclusion that the precipitation distribution function is applicable in general to both arid and humid climates, provided that the storms are independent and come from a single, homogeneous population. They also show the validity of using only a few years of precipitation records to predict the long-term precipitation CDF.

The P_s, m_τ, κ and m'_ν of the stations are tabulated in Table 3.3.

Since the Bahr el Arab and Raqaba el Zarqa apparently make a negligible contribution to the hydrology of the Bahr el Ghazal because of their insignificant discharges, we will ignore the stations in these two catchments in the rest of this study.

Table 3.3

LONG-TERM AND SHORT-TERM RAINFALL PARAMETERS

	Long-term (up to 1975)			Short-term (3 to 18 years)		
	Mean Seasonal Precipitation $\overline{P}_s$ (mm) (=$0.95\overline{P}_A$)	Mean Rainy Season Length m_τ (months)	κ (Eq. 3.1)	κ (Eq. 3.5, 3.6 3.9, 3.13) κ_1	Mean Seasonal Number of Rainy Days $m'_{\nu 1}$	Years of Observation
El Fasher	284	5	0.22	0.43	39.7	6
El Obeid	353	6	0.49	0.66	40.4	8
En Nahud	377	6	0.80	0.44	39.5	6
Nyala	461	6	0.88	0.75	45.0	6
Dilling	604	6	1.19	0.96	39.6	16
Kadugli	710	6	1.02	0.77	60.0	8
Talodi	754	6	1.00	0.78	55.0	3
Tonga	833	6	0.54	0.65	59.6	15
Fangak	890	7	0.21	0.88	45.4	16
Aweil	856	7	0.70	0.73	66.4	10
Raga	1124	7	2.03	0.81	88.3	10
Meshra El Rek	794	7	0.79	1.28	45.8	11
Wau	1069	7	0.86	0.71	90.6	10
Tonj	1003	7	0.66	0.75	69.0	18
Shambe	741	7	0.30	0.50	45.4	8
Rumbek	939	7	0.48	0.67	71.2	10
Amadi	1116	9	1.00	1.38	73.9	12
Li Yubo	1423	9	1.15	0.96	100.0	6
Maridi	1315	9	0.61	1.08	108.1	3
Yambio	1357	9	0.91	0.81	117.3	7

Only nine stations in the south are needed to describe the climatic parameters of the six sub-catchments by the Thiessen's method. If a_{ij} denotes the area belonging to station i in catchment j, then the Thiessen's method gives the areal average of a parameter x for the catchment j by the following expression,

$$\underline{x}_j = \frac{\sum_{i=1}^{9} a_{ij}\ x_{ij}}{\sum_{i=1}^{9} a_{ij}} = \frac{\sum_{i=1}^{9} a_{ij}\ x_{ij}}{A_j}, \qquad j = 1, \ldots, 6 \qquad (3.14)$$

where

A_j = area of the j^{th} catchment.

For example, for annual precipitation, we have

$$\underline{\overline{P}_{A_j}} = \sum_{i=1}^{9} a_{ij}\ \overline{P}_{A_{ij}}/A_j\ , \qquad j = 1, \ldots, 6 \qquad (3.15)$$

where the overbar denotes the time average and the underbar denotes the spatial average.

The mean monthly precipitation, number of rainy days and storm depth for the 9 stations are given in Appendix A , together with the table for a_{ij} and the space-time average of the latter two parameters for the 6 sub-catchments.

The space-time mean monthly catchment precipitation is tabulated in Table 3.4. Using the rainy season criterion mentioned before, we obtain the wet season months (m_τ), and the mean seasonal precipitation, $\underline{\overline{P_s}}$. Once the wet season months are known, the mean seasonal catchment rainy days, $\underline{m}'_\nu$, and the mean seasonal catchment storm

Table 3.4

Space-time Mean Monthly Catchment Precipitation, mm/month

(Time average up to 1972)

		Naam	Maridi	Tonj	Jur	Pongo	Loll
		1	2	3	4	5	6
	Month						
January	1	6	4	8	8	2	0
	2	17	11	14	18	7	3
	3	53	40	53	65	30	15
	4	129	106	123	117	73	52
	5	172	152	161	176	145	135
	6	159	163	175	189	176	173
	7	181	178	189	171	192	215
	8	186	194	196	214	224	254
	9	156	150	170	195	180	192
	10	124	97	123	154	120	86
	11	43	29	41	46	19	8
December	12	8	4	9	13	3	1
	$\overline{P_A}$ (mm)	1235	1129	1261	1364	1171	1134
	m_I (months)	9	8	9	9	8	7
	$\overline{P_s}$ (mm)	1204	1081	1230	1325	1140	1107
	$\overline{P_A}/\overline{P_s}$	0.975	0.958	0.975	0.971	0.974	0.976

depth, $\underline{m}_H$, can be evaluated.

Observations of storm durations are few. The closest stations to the Tonj catchment with such information are Juba (27) (4°51'N, 31°37'E) where the mean storm duration m_{t_r} = 1.1 hr., Bata (2°3'N, 33°12'E) where m_{t_r} = 1.2 hr. and Bugunese (1°9'N, 34°14'E) where m_{t_r} = 1.2 hr. (9). Based on these findings, the mean storm duration (m_{t_r}) for the six catchments in the south is taken to be 1.2 hr.

The mean time between storms, $\underline{m}_{t_b}$, is computed by the following equation,

$$\underline{m}_{t_b} = \frac{\underline{m}_\tau}{\underline{m}'_\nu} - m_{t_r} \tag{3.16}$$

The mean storm intensity, $\underline{m}_i$, is computed by

$$\underline{m}_i = \frac{\underline{m}_H}{m_{t_r}} \tag{3.17}$$

Extensive plots of station κ versus station precipitation parameters, station longitudes, latitudes and altitudes show that there are hardly any correlations, so we assume κ is a random variable and use the Thiessen's method to obtain the areal average $\underline{\kappa}$ for each sub-catchment.

All the important catchment precipitation parameters are summarized in Table 3.5.

3.7.2 Potential Evaporation and Evapotranspiration

3.7.2.1 Potential evaporation

The average wet season monthly evaporation rates for a water

Table 3.5: Important Catchment precipitation parameters

(Space-time Averages)

		Naam	Maridi	Tonj	Jur	Pongo	Loll
		1	2	3	4	5	6
Area	km^2	11962	15390	21708	54705	8428	65338
$\overline{P}_s$	mm	1204	1081	1230	1325	1140	1107
m'_ν		82.4	72.1	86.4	93.3	80.3	74.1
m_H	mm	14.1	14.5	13.6	13.7	13.4	14.3
m_{t_r}	hrs	1.2	1.2	1.2	1.2	1.2	1.2
m_{t_b}	days	3.29	3.33	3.13	2.90	2.99	2.84
m_τ	days	275	244	275	275	244	214
m_i	cm/hr	1.18	1.21	1.13	1.14	1.12	1.19
κ		0.73	0.54	0.70	1.00	1.07	1.76

surface, $\bar{e}_{pw}$, and for a wet soil surface, $\bar{e}_p$, are computed using a form of the modified Penman equation (Equation 2.17). Parameters required for evaluating $\bar{e}_{pw}$ and $\bar{e}_p$ include the insolation, surface albedo, air temperature, relative humidity and cloud cover. The last three are provided by the Sudanese Meteorological Service. The albedos for water surface and wet soil surface are assumed to be 0.05 and 0.10, respectively. Reference (29) gives the mean annual insolation across Africa. By interpolating the insolation between isolines, we obtain the station insolation as given in Table 3.6

The mean monthly insolation is obtained by proportioning the annual insolation according to the variation in monthly temperature, as

$$\bar{q}_i^j = \bar{q}_i^m \times \frac{\bar{T}_A^j}{\bar{T}_A^m} \tag{3.18}$$

where

$\bar{q}_i^j$ = the mean insolation for month j, kcal/cm^2/month

$\bar{q}_i^m$ = the mean annual monthly insolation, kcal/cm^2/month $= \frac{\bar{q}_i}{12}$

$\bar{q}_i$ = the mean annual insolation, kcal/cm^2/year

$\bar{T}_A^j$ = the mean air temperature for month j, °C

$\bar{T}_A^m$ = the mean annual monthly air temperature, °C

$= \sum_{j=1}^{12} \bar{T}_A^j/12$

The mean monthly insolation, air temperature, relative humidity and cloud cover, and the mean monthly potential evaporation for water and wet soil surface evaluated by Equations (2.17) through (2.20) for the 9 stations are all tabulated in Appendix A.

Table 3.6

Mean Annual Station Insolation $\bar{q}_i$, Kcal/cm^2/year

Station Name	Aweil	Raga	Wau	Tonj	Rumbek	Amadi	Yubo	Maridi	Yambio
Station Number	1	2	3	4	5	6	7	8	9
Mean Annual Insolation (Kcal/cm^2/yr)	164	161	159	158	156	154	153	152	151

Tables 3.7 and 3.8 give the mean monthly catchment potential evaporation for water, $\underline{\bar{e}_{pw}}$, and wet soil surface, $\underline{\bar{e}_{p}}$, respectively.

The Piche tube observations, $\bar{e}'_p$, for the 9 stations are also tabulated in Appendix A, together with the catchment areal averages, $\underline{\bar{e}'_p}$.

The Piche reduction factor (annual $\underline{\bar{e}_{pw}}/\underline{\bar{e}'_p}$) for the six catchments ranges from 0.70 to 1.00 (Table 3.9) with an overall areal average of 0.78. This result is consistent with Hurst's findings (5) that in a highly humid region, the Piche reduction factor is larger than the standard 0.5.

The mean monthly Piche tube observation and water surface evaporation are also plotted for the six catchments in Appendix A.

3.7.2.2 Potential evapotranspiration

The potential evapotranspiration rate for papyrus swamp has been estimated earlier to be 2.2 meters per year, and that for grasslands in our catchments to be 120 mm per month in the wet season. And for woodland in tropical Africa, it is estimated to be 158 mm/month in the wet season (30).

According to the vegetation distribution map for the Jonglei project area (31), the vegetation of the Ironstone Plateau is estimated to be 67% grasses and 33% deciduous trees. There is no mention of the bare soil fraction in this area, nor the actual canopy density (vegetation fraction) of the area. In a later chapter, the canopy density for each catchment will be derived from our water balance model by adopting

Table 3.7: Space-Time Mean Monthly Catchment Potential

Evaporation (Water Surface) , $\underline{\bar{e}_{pw}}$, mm/month

(Albedo = 0.05)

Month	Naam 1	Maridi 2	Tonj 3	Jur 4	Pongo 5	Loll 6
1	129	134	128	128	130	120
2	142	145	141	138	146	139
3	154	161	152	145	163	164
4	145	153	147	141	164	177
5	138	142	137	130	151	164
6	128	131	127	121	137	149
7	121	125	120	116	128	138
8	121	124	120	113	125	136
9	126	129	125	118	131	140
10	130	134	128	122	135	143
11	132	136	129	125	134	134
12	130	132	126	122	127	119
Yearly (mm/yr)	1595	1646	1582	1517	1670	1718
Seasonal (mm/month in the wet season)	133	137	132	125	142	149

Table 3.8: Space-time Mean Monthly Catchment Potential Evaporation (Wet Soil Surface), $\bar{e}_p$, mm/month (Albedo = 0.10)

Month	Naam 1	Maridi 2	Tonj 3	Jur 4	Pongo 5	Loll 6
1	121	126	120	120	122	112
2	134	137	133	129	137	130
3	144	151	142	135	153	155
4	136	144	138	132	154	167
5	130	134	129	122	142	155
6	121	124	120	113	128	140
7	114	117	113	108	120	130
8	114	116	112	106	118	128
9	119	121	118	111	123	132
10	122	126	121	114	126	134
11	124	128	121	117	125	126
12	122	124	118	113	119	112
Yearly (mm/yr)	1499	1548	1484	1420	1568	1621
Seasonal (mm/month in the wet season)	125	129	124	118	133	141

Table 3.9

Piché Reduction Factor $(\bar{e}_{pw}/\bar{e}'_p)$

	Naam	Maridi	Tonj	Jur	Pongo	Loll
Yearly $\bar{e}_{pw}$ (mm)	1595	1646	1582	1517	1670	1718
Yearly $\bar{e}_p'$ (mm)	1603	1884	2012	1880	2393	2449
Yearly $\bar{e}_{pw}/\bar{e}_p'$	1.00	0.87	0.79	0.81	0.70	0.70

the vegetal equilibrium hypothesis (19) which states that for a given climate, soil and plant coefficient, the equilibrium canopy density, M_o, is such that the space-time average soil moisture is a maximum. Under such a condition, the vegetation is only experiencing a minimum stress.

Since our six catchments lie almost entirely within the Ironstone Plateau, the composite potential evapotranspiration, $\bar{E}_v$, for the vegetation surface of the catchments will be estimated as $\bar{E}_v = 120(0.67) + 158(0.33) = 134$ mm/month in the wet season.

The potential transpiration efficiency, k_v, for the catchments is defined by

$$k_v = \frac{\bar{E}_v}{\bar{e}_p} \tag{3.19}$$

and the plant coefficient, k_v', for the catchments

$$k_v' = \frac{E_v}{\bar{e}_{pw}} \tag{3.20}$$

These values are given in Table 3.10 where, for convenience, $\bar{e}_p$ and $\bar{e}_{pw}$ are also given.

Because of the extreme closeness of the values of $\bar{E}_v$ and $\bar{e}_p$ or $\bar{e}_{pw}$ (in many cases the differences are only a few millimeters, which is well within the limits of estimation error), there is no strong evidence to indicate that k_v is greater than or less than one. In lieu of such findings, we will assume k_v to be 1.0 for all the catchments.

The surface retention capacity, h_o, of the vegetal surface is assumed to be 3 mm.

Table 3.10

Catchment Potential Transpiration Efficiency and Plant Coefficient

Catchment Name	Naam	Maridi	Tonj	Jur	Pongo	Loll	Overall Areal Thiessen's Average
$\bar{e}_p$ mm/month	125	129	124	118	133	141	
$\bar{e}_{pw}$ mm/month	133	137	132	125	142	149	
k_v	1.07	1.04	1.08	1.14	1.01	0.95	1.04
k_v'	1.01	0.98	1.02	1.07	0.94	0.90	0.98

3.8 The Inhabitants and their Living Pattern

3.8.1 On the Flood Region of the Central Swampland (Fig. 3.4)

The Flood Region is occupied almost exclusively by the Nilotic tribes -- the Dinka, Nuer and Shilluk. Cultivation in this region is extremely limited because the crops either perish from drought in the dry season or are drowned by heavy flooding during the wet season. Only the "High land" is heavily exploited for permanent dwellings and for crop production. Dura (sorghum, millet) is the only major crop. Since crop production is a precarious undertaking, cattle raising becomes the most important economic activity in this region. In some areas, fishing is also important.

During the rainy season, the river overflows its bank and the people are forced to move inland to higher ground where they cultivate their crops and graze their herds in the immediate vicinity. During the dry season, the herds are driven from the "High land" to graze first on the Intermediate land and then on the Toich land. As the rainy season comes, they return again to "High land". This annual cycle of movement shows a living pattern in which man is living in a very delicate balance with his environment.

3.8.2 On the Ironstone edge of the Central Swampland

This region includes the transition zone between the Flood Region and the Ironstone Plateau along Rumbek, Tonj, Gogrial and Aweil (Figures 3.3 and 3.4). The inhabitants in this region are mostly the Dinka tribes. Here, a mixed economy is practiced, in which animal husbandry is sometimes more important than crop production. Permanent dwellings are mainly along the edge of the Ironstone Plateau. Shifting cultivation is practiced in the vicinity of their dwellings. The fields are normally cultivated for 4 to 5 years and then rested for 3 to 5 years. After 10 to 12 years, they are abandoned and new fields and dwellings have to be found. The old fields are allowed to regenerate for a period of 20 to 30 years before they are reopened. Dura is the only important crop grown here. In the dry season, livestocks are moved for grazing to the widely dispersed toich areas in the Flood Region, and along many of the watercourses.

3.8.3 On the Ironstone Plateau of the Sub-catchments

On the Ironstone Plateau, along Wau and Raga, and south of the Green Belt, the inhabitants are composed of many small tribes of mixed origin including the western Sudanic and a few of the Shilluk-speaking Nilotic. They are all settled cultivators and the number of livestock is very small. The major crops include dura, sesame, groundnuts, beans and cassava. Lands here are cultivated continuously for 5 to 8 years and then rested for up to 30 years. People move their homes frequently and over long distances because of limited areas of fertile soils.

3.8.4 On the Green Belt of the Sub-catchments

On the Green Belt along Tembura, Yambio and Ibba, the inhabitants are mostly the Zande of western Sudanic origin. They are primarily cultivators because the presence of the tsetse fly renders cattle raising almost an impossible task. Cotton and cassava are among the important crops. There are also some minor subsidiary activities such as fishing, hunting and honey extraction.

Around the Amadi area are the Moru-Madi group. They are settled cultivators. Dura and cotton are the major crop. Some cattle of smaller stock exists, but their numbers are very limited due to the infestation of tsetse fly.

Shifting cultivation is also practiced on the Green Belt region. Lands are normally cultivated for from 3 to 5 years and then rested for a period of 5 to 10 years. Two crops a year are common.

3.8.5 Population Distribution of the Bahr el Ghazal Basin

The Sudan is politically divided into eight provinces. The Bahr el Ghazal basin lies astride five of them, namely, the Darfur, the Kordofan, the Upper Nile, the Bahr el Ghazal and the Equatoria Provinces (Figure 3.8)*. The last two cover the six sub-catchments and the major part of the Central Swampland. The remaining part of the Central Swampland and the Raqaba el Zarqa catchment are within the territory of the Upper Nile Province. The source of Bahr el Arab lies in the Bahr el Ghazal Province and the rest of it is in the Darfur Province. As our information is only available up to 10° North latitude, we will ignore the Bahr el Arab and Raqaba el Zarqa catchment in the following description.

---

*Numbers next to circles in the figure stand respectively for 1) Nyamlell, 2) Aweil, 3) Gogrial, 4) Meshra el Req, 5) Wau, 6) Deim Zubeir, 7) Raga, 8) Said Bundas, 9) Tonj, 10) Rumbek, 11) Yirol, 12) Shambe, 13) Tembura, 14) Li Yubo, 15) Yambio, 16) Maridi, 17) Amadi, 18) Juba, 19) Yei.

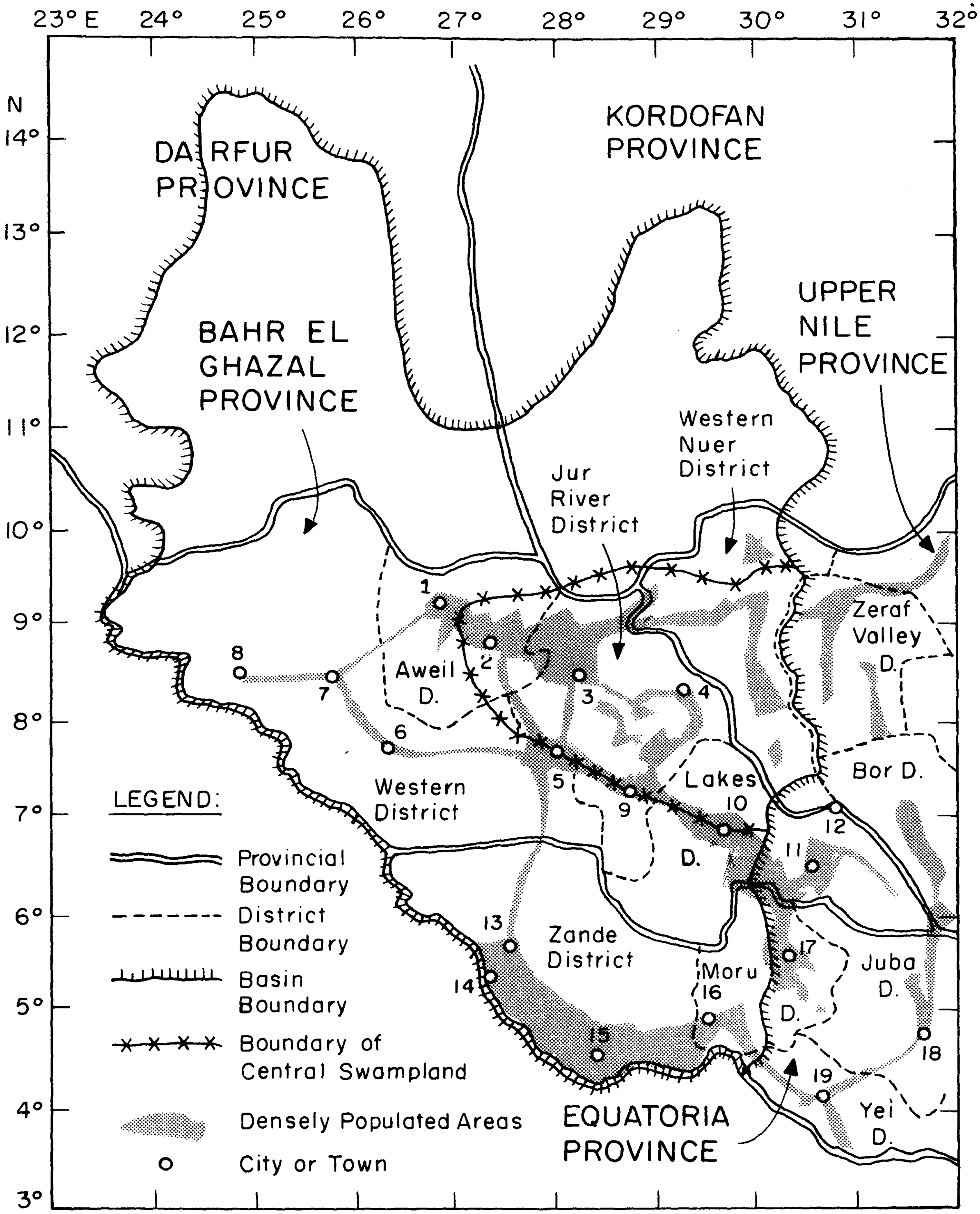

FIGURE 3.8

DISTRIBUTION OF POPULATION DURING WET SEASON (26)

Each province is sub-divided into districts. Within the Bahr el Ghazal Province, there are four districts, the Jur River, the Lakes, the Aweil and the Western District. In the Equatoria Province, only the Zande and Moru District are associated with the Bahr el Ghazal basin, and in the Upper Nile Province, it is the Western Nuer District.

Table 3.11 gives the approximate population distribution by districts of the Bahr el Ghazal basin. The "Estimated Total Population" is the number of tax-payers in the region multiplied by a factor ranging from 4 to 5. Even with such a multiplier, these figures are still probably very much less than the actual (26). The population density given in the table could be quite deceptive because hugh areas of the districts are still unexplored and uninhabited. The population are concentrated mostly in areas where water is accessible and communication possible. These areas are along the water-courses and the major roads. The "High land" and Ironstone edge of the Central Swampland, and the Green Belt of the sub-catchments have the highest population concentration.

The "Estimated Animal Population" is noticeably small in the Western, Zande and Moru Districts because they are within the tsetse fly zone where the stock can hardly survive.

Just to have a rough idea of how many people would be affected by the drainage projects of the Bahr el Ghazal swamps, we may sum the "Estimated Total Population" in the Aweil, the Jur River, the Western, the Western Nuer and the Lakes Districts. This amounts to 1,090,822.

Table 3.11: Population Statistics of the Bahr el Ghazal Basin (26)

Province	District	Estimated Total Population	Area (sq. miles)	Density (#/sq. mile)	Estimated Animal Population: cattle	Estimated Animal Population: sheep and goat	Ratio of Animal Unit to Humans
Bahr el Ghazal	Lakes	268,670	16,593	16.2	280,000	480,000	1.3
	Jur River	325,140	16,087	20.2	540,000	648,000	1.9
	Aweil	217,105	11,706	18.5	251,000	190,000	1.3
	Western	85,972	38,234	2.2	7,200	5,000	0.1
Equatoria	Zande	169,219	22,124	7.6	-	-	-
	Moru	64,555	9,210	7.0	1,600	-	-
Upper Nile	Western Nuer	193,935	14,000	13.9	257,000	111,000	1.4
	Total:	1,324,596	127,954	10.4			

Chapter 4

MODELLING THE BAHR EL GHAZAL BASIN

4.1 Introduction

The objective of this work is to model the hydrologic behavior of the Bahr el Ghazal basin in such a way as to demonstrate the effect of possible drainage and channelization projects upon the statistics of the contribution from this region to the flow of the White Nile. To achieve the objective, the water balances of the Central Swampland and of all the individual catchments have to be known. A conceptual model of the Central Swampland will be formulated for the purpose of studying its dynamic behavior in response to varying annual inputs, and in order to estimate the change in water yield which will result from swamp drainage.

In such a study, satellite mapping techniques are useful in obtaining estimates of the extent of different vegetation and soil types over the entire basin, and the extent of permanent swamps. This information is vital in the estimation of the actual evapotranspiration rate both on land and on swamp, and of other hydrologic parameters. However, at the present time, these data are not available. Without satellite mapping data for our area, we will rely heavily on available literature and on the satellite mapping information of the nearby 'Jonglei Canal Project' area in the estimation of the hydrologic, soil and vegetation parameters of the Bahr el Ghazal basin.

4.2 A Preliminary Water Balance of the Central Swampland

There are eight Bahr el Ghazal sub-catchments, producing eight tributary inputs to the Central Swampland. The Central Swampland has two constituents -- papyrus swamps and grasslands -- which are intermingled. For modelling purposes, we will concentrate the grasslands in an annulus surrounding the papyrus swamp which is the lower limit of the variable water-surface area shown in Figure 4.1.

Since we are only dealing with mean annual values in this section, for simplicity, we will drop the words 'mean annual' in the following discussion.

There are about 20 available precipitation stations scattered more or less uniformly over the entire basin. Based on Thiessen's weighting, the average annual precipitation over all the sub-catchments ($\underline{\overline{P}_L}$) amounts to 384.1 md and on the Central Swampland ($\underline{\overline{P}_o}$), to 77.9 md (Table 3.1).

For the papyrus swamps (16,600 km^2), the evapotranspiration is assumed to occur at its potential rate (2.2m) since the water supply is unlimited. This produces an annual loss of 36.5 md.

The grasslands in the Central Swampland cannot all be transpiring at the potential rate during the entire year. When flooded, we assume they will transpire at the potential rate throughout the year, but where unflooded, we assume they will transpire only during the rainy season and then at the potential rate. The area of the flooded grassland is highly variable, and is a function of the land slopes, precipitation, yearly carry-over in water storage, evapotranspiration of grassland,

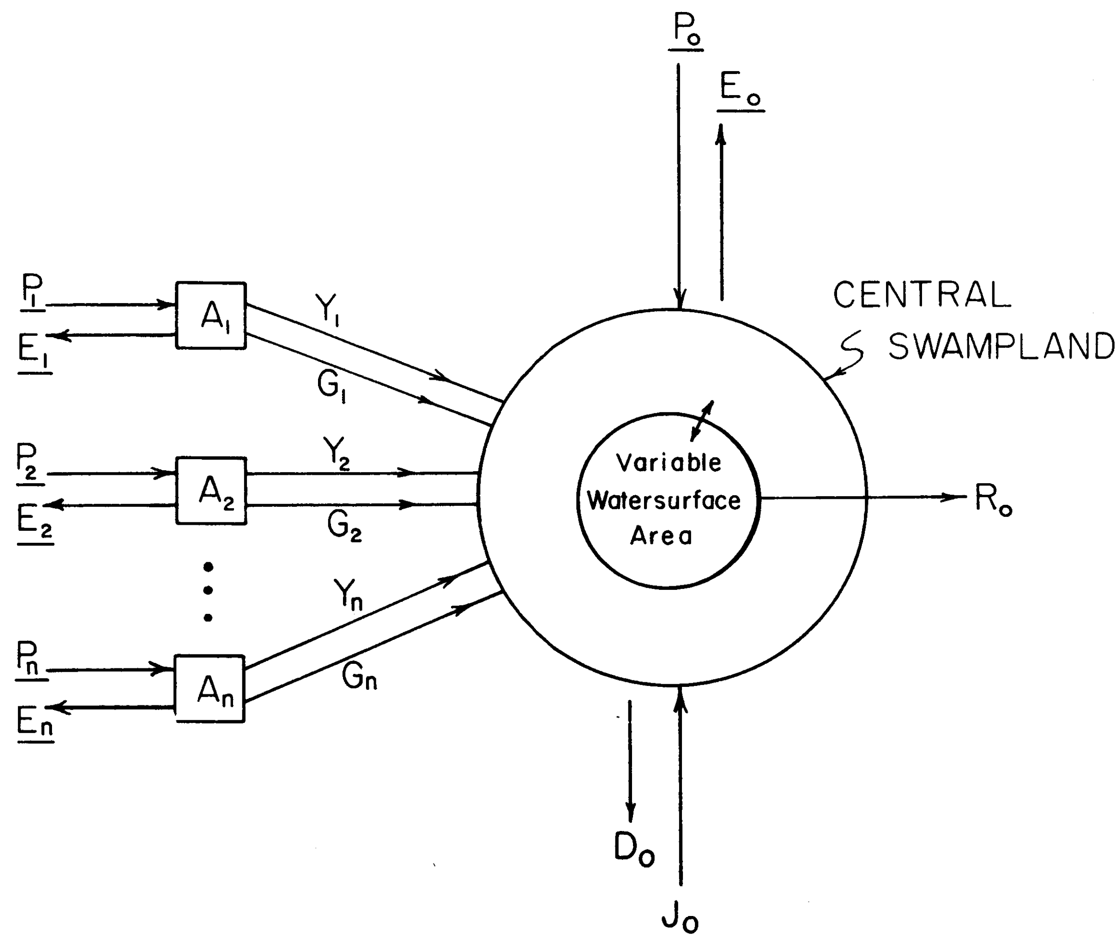

Figure 4.1 SCHEMATIC REPRESENTATION OF THE BAHR EL GHAZAL BASIN

seepage, etc. To the first approximation, we will deal only with the estimated mean annual flooded grassland area (A_F). The outer boundary of this mean flooded area is limited by the outer boundary of the Central Swampland while the inner boundary is limited by the extent of the papyrus swamps. The mean flooded area then varies between 0 and 68,400 km^2 ($A_{F_{max}}$). At the moment, detailed description of the topography of the Central Swampland is not available. In order to have some idea of the space-time average flooded area, we will assume that the random variable, A_F, follows a triangular distribution (Figure 4.2). It is more likely that the annual flooded area is closer to the inner boundary than to the outer, since it is flooding outward from the center. In order to account for the above fact, we will assume the distribution shown in Figure 4.2. Under such an assumption, the expected value of the mean unflooded grassland area is 39,900 km^2.

Assuming the unflooded grass to be dormant in the dry season and using the potential evapotranspiration rate determined earlier, we can calculate the evapotranspiration of the grassland, E_g, as

$$\begin{aligned}\bar{E}_g &= 120 \text{ mm/month} \times 12 \text{ months} \times 28{,}500 \text{ km}^2 + 120 \text{ mm/month} \\ &\quad \times 7 \text{ months} \times 39{,}900 \text{ km}^2 \\ &= 74.6 \text{ md}\end{aligned}$$

The total evapotranspiration of the Central Swampland is the sum of the evapotranspiration of the papyrus swamps and the grasslands, and amounts to 111.1 md ($\bar{E}_o$).

The total gaged discharge ($\bar{Y}_L$) from the eight tributaries amounts to 12.7 md (Table 3.1).

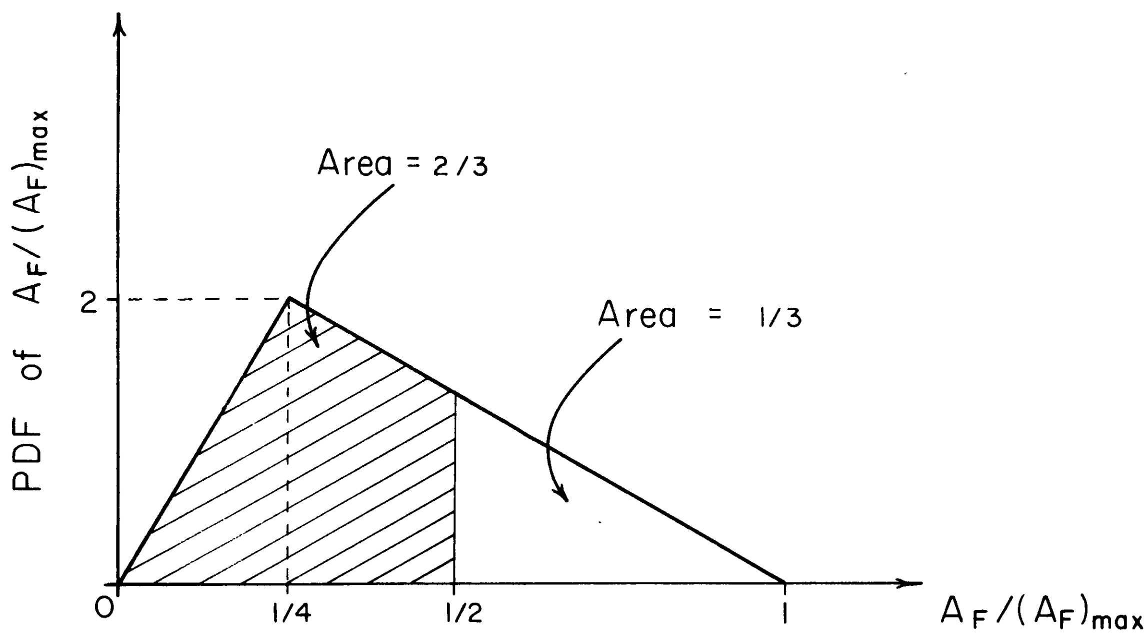

Figure 4.2 TRIANGULAR DISTRIBUTION OF THE NORMALIZED TEMPORAL MEAN FLOODED AREA

Before reaching the Central Swampland, all the tributaries start to spill onto their flood-plains during the wet season (3), (26). The sandy river bed on the Ironstone Plateau just south of the Central Swampland takes up much of the dry season flow through seepage (26). Numerous ungaged small streams, either ephemeral or perennial, flow into the Central Swampland from the sub-catchments (32). On the boundary of the Central Swampland, the water table is generally high. The average depth of well is about 10 to 25 feet along the southern boundary (page 83), which may give rise to ungaged sub-surface inflows along this boundary.

The varied evidence cited above gives a strong indication that there is a significant ungaged surface and/or sub-surface inflow ($\overline{G}_L$) to the Central Swampland. Assuming that deep seepage ($\overline{D}_o$) at the Central Swampland is negligible, a $\overline{G}_L$ of 15.1 md is required to close the water balance of this region (Fig. 4.3).

The evapotranspiration on the sub-catchments, $\overline{E}_L$, is estimated by a subsequent closure of the water balance of the lumped sub-catchments.

From the result of the above water balance, it is found that the magnitude of ungaged inflow, $\overline{G}_L$, to the Central Swampland (15.1 md) is comparable to that of the gaged discharges, $\overline{Y}_L$ (12.7 md).

In the above analysis, any sub-catchment outflow not entering the Central Swampland (such as deep seepage) is ignored.

4.3 A Refined Water Balance Model of the Central Swampland

4.3.1 The Refined Water Balance Model

In the preliminary mean annual water balance of the Central

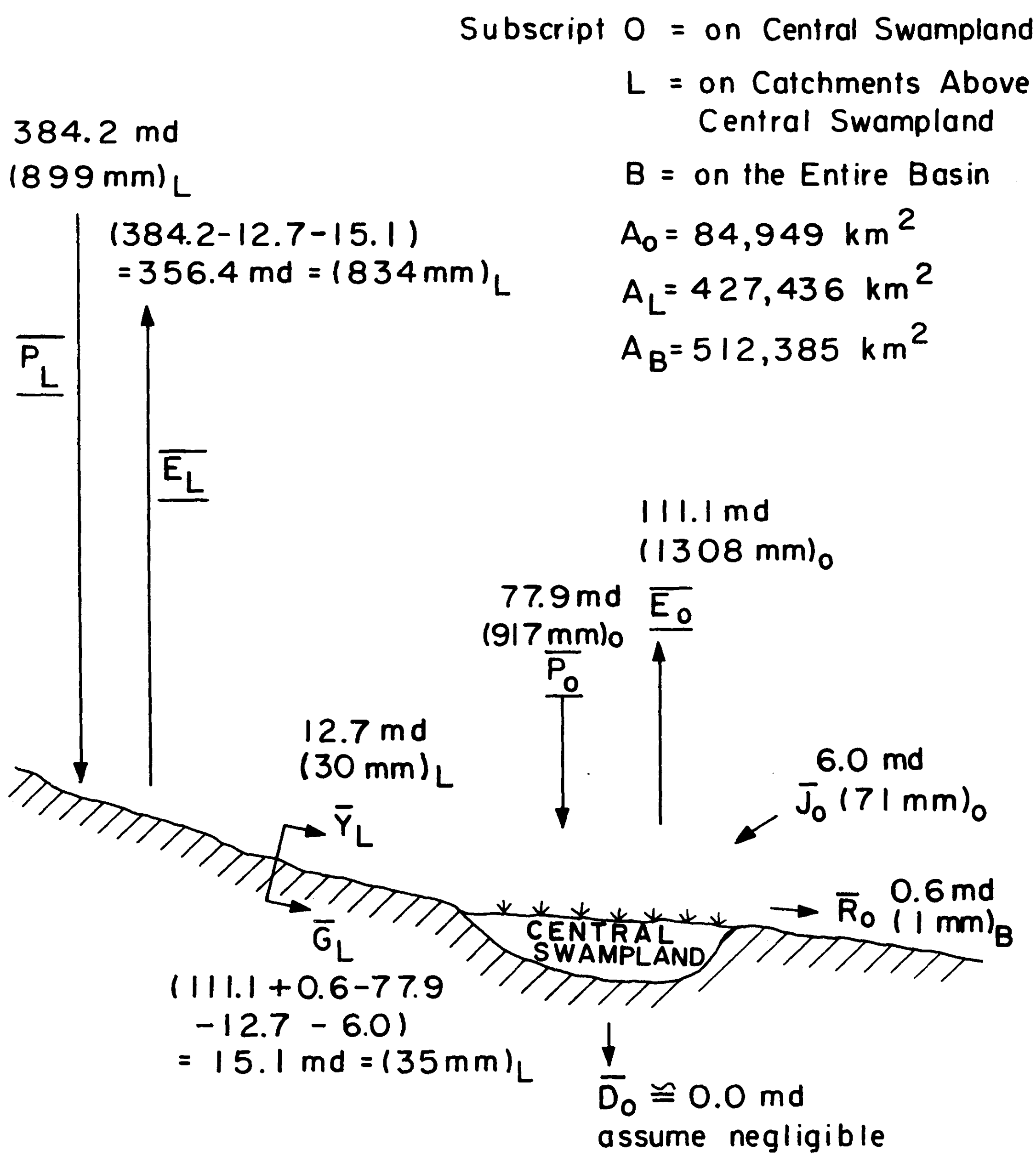

FIGURE 4.3

A PRELIMINARY MEAN ANNUAL WATER BALANCE OF THE CENTRAL SWAMPLAND

Swampland, the deep seepage at the Central Swampland ($\overline{D}_o$) and on the sub-catchments is neglected. In order to know whether deep seepage is indeed negligible, a refined water balance model is needed.

Referring to Figure 4.1, the annual water balance for the Central Swampland of the Bahr el Ghazal basin can be written as

$$\underline{P}_o + Y_L + G_L + J_o - \underline{E}_o - D_o - \Delta S_o = R_o \qquad (4.1)$$

in which

$\underline{P}_o$ = areal average annual precipitation

$Y_L = \sum_{i=1}^{n=8} Y_i$ = sum of gaged annual inflows from the n sub-catchments

$G_L = \sum_{i=1}^{n=8} G_i$ = sum of ungaged annual inflow from the n sub-catchments, including catchment deep seepage.

J_o = annual spillage from the Bahr el Jebel

$\underline{E}_o$ = areal average annual evapotranspiration

D_o = annual deep seepage

R_o = annual outflow from Lake No

ΔS_o = annual change in storage

Taking the expected value of Equation (4.1) term by term, we eliminate the troublesome change-of-storage term to obtain the average annual water balance

$$\overline{\underline{P}}_o + \overline{Y}_L + \overline{G}_L + \overline{J}_o - \overline{\underline{E}}_o - \overline{D}_o = \overline{R}_o \qquad (4.2)$$

where the underbar represents the Thiessen areal average and the overbar represents the time average.

The mean total annual outflow from the catchments ($\overline{Y}_T$) may be obtained from a similar water balance analysis for each of the tributary catchments. Since there is no spillage into these tributaries, this will be given by

$$\overline{Y}_T = \overline{Y}_L + \overline{G}_L = E[\sum_{i=1}^{n=8} (Y_i + G_i)] = E[\sum_{n=1}^{n=8} (\underline{P}_i - \underline{E}_i)] \qquad (4.3)$$

To the first order approximation (20), the cumulative distribution function (CDF) of the <u>annual</u> yield, Y_T, can be obtained from those of the <u>annual</u> tributary precipitations, $\underline{P}_i$, using Eq. (4.3) without time averaging.

The CDF of R_o may be estimated by the Monte Carlo simulation method, given the CDF's of the annual variables on the left side of Eq. (4.1).

The value of J_o will be related to the stage in the Bahr el Jebel. Its CDF may be crudely estimated from that of the observed Jebel discharge.

The value of $\underline{E}_o$, D_o and ΔS_o will be related to the flooded area of the swamp which is hydraulically related to the outflow, R_o, through the rating curve of the outlet control. In the natural state, this is the outlet of Lake No, but in a proposed drained state, this would be determined by the particular drainage scheme.

Equation (4.1) thus provides the mechanism for assessing the uncertainty of R_o both in the natural state and under various drainage schemes.

4.3.2 CDF of Catchment Precipitation

The CDF of station annual precipitation is given by Eq. (2.5), as

$$\text{Prob}\left|\frac{P_A}{\overline{P_A}} < z\right| = e^{-m_\nu}\left\{1 + \sum_{\nu=1}^{\infty} \frac{m_\nu^\nu}{\nu!} \cdot P[\nu\kappa,\ m_\nu\kappa z]\right\} \tag{2.5}$$

This is a one-dimensional model in which the annual precipitation is assumed to fall uniformly over the entire catchment. For small catchments, this assumption is rather good, as can be verified from the previous application in Chapter 2 (Santa Paula and Clinton catchments). However, for large catchments with localized thunderstorms, this one-dimensional model may not be adequate. In large catchments, high annual precipitation at one station may be offset by low annual precipitation at another station, thereby reducing the variance of the areal average annual catchment precipitation. The annual total number of storms (say rainy days) within a large catchment could, in fact, be much larger than any station's annual number of storms (rainy days) because it could rain in different portions of the catchment on different days. This two-dimensional precipitation characteristic will be reflected in the parameters of Equation (2.5), which is now rewritten as

$$\text{Prob}\left|\frac{\underline{P_A}}{\underline{\overline{P_A}}} < z\right| = e^{-m_{\nu c}}\left\{1 + \sum_{\nu=1}^{\infty} \frac{m_{\nu c}^\nu}{\nu!} \quad P[\nu\underline{\kappa},\ m_{\nu c}\underline{\kappa} z]\right\} \tag{4.4}$$

where the underbar again represents the Thiessen areal average and $m_{\nu c}$ is the mean annual number of catchment storms[1] given by Equation (3.1), as

[1]Individual "catchment storms" are defined by separation in time not space.

$$m_{\nu c} = \left(\frac{\overline{P_A}}{\sigma_{P_A}}\right)^2 [1 + \frac{1}{\kappa}] \tag{4.5}$$

Station κ is treated as a random variable and the catchment κ is represented by the Thiessen areal average of the station κ's (Chapter 3, Page 95).

To verify the two-dimensional precipitation model (Equation (4.4) and (4.5)), 32 years of synchronized station precipitations of 9 stations were areally averaged to obtain the 6 catchment annual precipitations which are tabulated in Appendix B. Table 4.1 gives the relevant parameters.

Table 4.1

CATCHMENT PRECIPITATION PARAMETERS

	Naam	Maridi	Tonj	Jur	Pongo	Loll
κ	0.73	0.54	0.70	1.00	1.07	1.76
$\overline{P_A}$ (32 yrs) mm	1199	1091	1251	1388	1198	1165
σ_{P_A} (32 yrs)	97	117	127	136	99	123
$m_{\nu c}$	362	298	236	208	283	141

Figure 4.4 illustrates a typical fitting of the two-dimensional precipitation model (solid line) to the observed CDF of catchment precipitation (circles) for the Tonj catchment. The observations are plotted using the Thomas plotting position (21), (Appendix B)

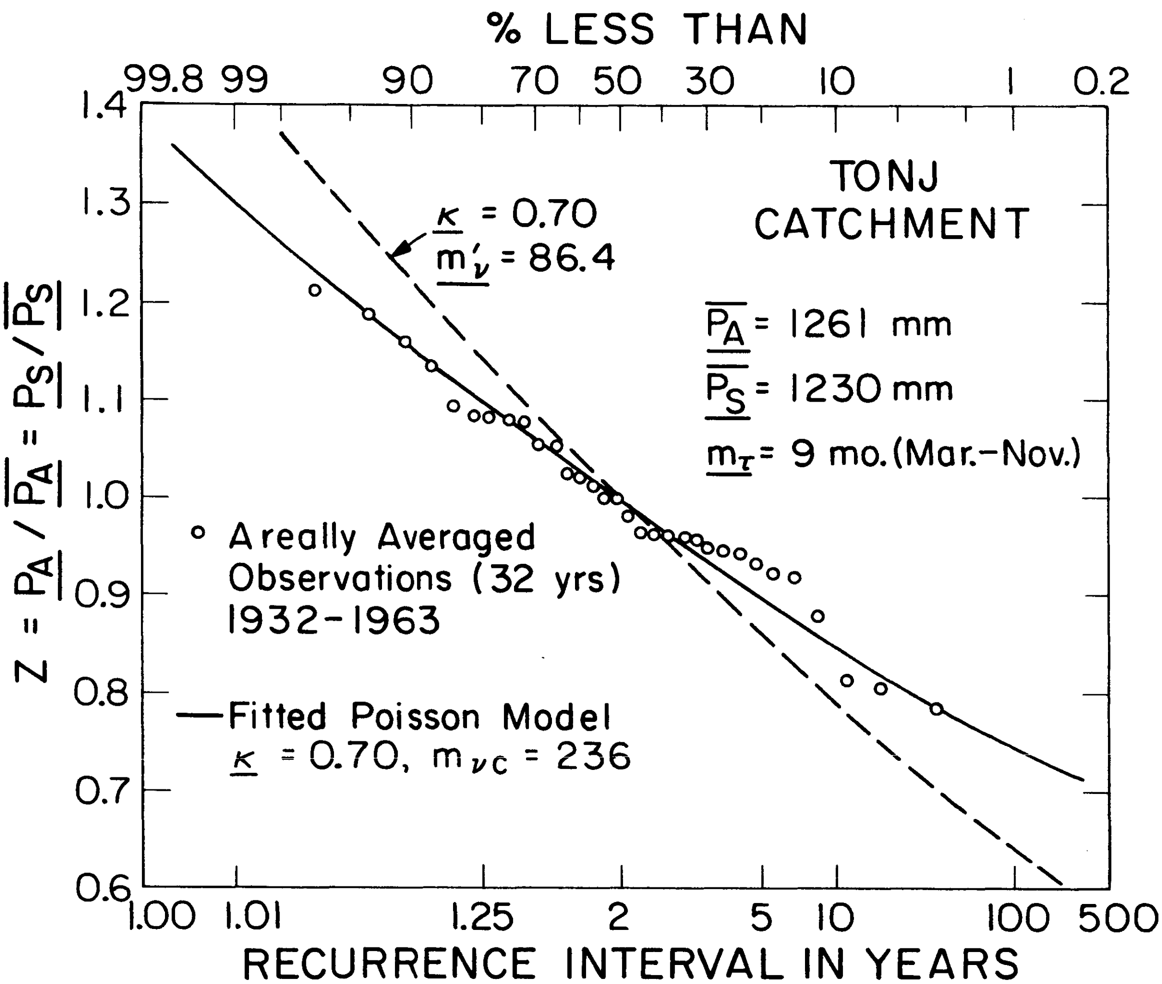

FIGURE 4.4

FREQUENCY OF ANNUAL CATCHMENT PRECIPITATION

(TONJ CATCHMENT)

$$\text{Prob}[\underline{P}_A/\overline{\underline{P}_A} < z] = \frac{m_z}{N+1} \qquad (4.6)$$

where

m_z = rank order of observation of magnitude z

N = number of years of record

The dashed line in Figure 4.4 represents the one-dimensional precipitation model, in which $m_{\nu c}$ in Equation (4.4) is replaced by the Thiessen areal average of the observed station m'_ν. It is clear from this figure that the one-dimensional precipitation model has a larger variance than that of the two-dimensional model. This illustrates the potentially large error which could be introduced by applying the one-dimensional model to such large catchments.

In Figure 4.4, the long-term mean annual and seasonal precipitation and the rainy season length are taken from Table 3.4. The CDF's of $\underline{P}_A$ for the rest of the stations are given in Appendix B.

Assuming that $m_{\nu c}$ represents the actual total number of storms falling on a catchment in a normal year, (rather than being just a fitting parameter to account for the smaller precipitation variance), we may draw some inference about average storm size. This comes from the preservation of annual precipitation volume, as given by

$$\overline{\underline{P}_A}\, A = m_{\nu c}\, \underline{m}_H\, A_w \qquad (4.7)$$

where

A = total area of the catchment

A_w = average area of the catchment that is wetted by a single storm

$\underline{m}_H$ = mean areal storm depth

But

$$\overline{P_A} = \underline{m}'_\nu \, \underline{m}_H \tag{4.9}$$

Thus

$$\frac{A_w}{A} = \frac{\underline{m}'_\nu}{m_{\nu c}} \tag{4.10}$$

which tells us on the average the percentage of wetted surface area in a catchment in a normal year. It is a measure of the "patchiness" of the storm rainfall.

This result is given in Table 4.2.

Table 4.2

SPACE-TIME AVERAGE WETTED SURFACE AREA PERCENTAGE IN A CATCHMENT

	Naam	Maridi	Tonj	Jur	Pongo	Loll
$\underline{m}'_\nu$	82.4	72.1	86.4	93.3	80.3	74.1
$m_{\nu c}$	362	298	236	208	283	141
$\frac{A_w}{A}$ %	22.8	24.2	36.6	44.9	28.4	52.6

4.3.3 Uncertainty in the Water Yield from Each Sub-catchment

The mean annual water balance of a catchment along with the CDF of annual precipitation and annual yield are derived in (19), (20) and are given in Chapter 2. Only slight modification of the above model is needed in order to apply it to each of the sub-catchments of the Bahr el Ghazal basin.

In functional form, the mean annual catchment water balance equation is

$$\overline{\underline{P_s}} = \overline{E}_{T_A}(s_o|\overline{\underline{e}}_p, \underline{m}_\tau, \underline{m}_{t_b}, n, K(1)\ \Psi(1), m, M, k_v, h_o, Z)$$

$$+ \overline{R}_{s_A}(s_o|\underline{m}_\nu, \underline{m}_H, \underline{m}_i, \underline{m}_{t_r}, \underline{m}_{t_b}, \overline{\underline{e}}_p, \underline{\kappa}, n, K(1), \Psi(1), m, M, k_v, h_o, Z)$$

$$+ \overline{R}_{g_A}(s_o|\underline{m}_\tau, K(1), \Psi(1), n, m, Z) \qquad (4.11)$$

With $\overline{\underline{P_s}}$ and the climate, soil and vegetation parameters of a catchment known, Equation (4.11) can be solved for the soil moisture, s_o, which is then back-substituted into Equation (4.11) to obtain the individual water balance elements of the sub-catchment.

The total outflow from each sub-catchment is the sum of the surface and groundwater runoffs. Assuming that the water table is a constant, then deep seepage may be considered as part of the groundwater runoff because it is coming from the water that percolates into the ground. The mean annual sub-catchment outflow is thus

$$\overline{Y}_A = \overline{R}_{s_A} + \overline{R}_{g_A} = \text{gaged outflow + ungaged outflow including deep seepage} \qquad (4.12)$$

In this application, the gaged and ungaged outflows from each sub-catchment become the gaged and ungaged inflows to the Central Swampland. Any deep seepage from the sub-catchments, however, may or may not seep into the Central Swampland. Further consideration will be given to this quantity later.

To the first order (20), we may use Equations (4.11) and (4.12) to describe the relationship among the annual quantities themselves (by removing the overhead bars). Assuming the variance in annual yield to be due solely to variance in the seasonal catchment precipitation, Equations (4.11) and (4.12) provide an approximate relation between the two annual random variables:

$$\left.\begin{aligned} Y_A &= g(\underline{P_s}) \\ &\text{or} \\ \underline{P_s} &= g^{-1}(Y_A) \end{aligned}\right\} \tag{4.13}$$

Equations (4.4) and (4.13) define the CDF of the total annual outflow from each sub-catchment as

$$\mathrm{Prob}\left|\frac{Y_A}{\underline{P_s}} < z\right| = e^{-m_{\nu c}} \left\{1 + \sum_{\nu=1}^{\infty} \frac{m_{\nu c}^{\nu}}{\nu!} \cdot P[\nu\underline{\kappa},\ m_{\nu c}\underline{\kappa} g^{-1}(z)\right\} \tag{4.14}$$

Notice that $m_{\nu c}$ is used only in the CDF of the annual catchment precipitation and yield (Equations (4.4) and (4.14)), but it is not used in the water balance equation (Equation (4.11)) because its sole purpose is to preserve the CDF of annual catchment precipitation and hence the CDF of the catchment yield or outflow. It has no physical significance in the generation of local soil moisture.

Most of the parameters in Equation (4.11) are known (Tables 3.5, 3.7 and 4.1) with the exception of the catchment vegetal density (M) and the soil parameters ($K(1)$, $\Psi(1)$, n, m).

The six sub-catchments in the south lie almost entirely within the soil zone defined as the "Ironstone Plateau." Similar soils found in the Jonglei Project area (Figure 3.1) are described (31) as well drained, moderately permeable, loaming soils which have a saturated permeability ($K(1)$) ranging from 10^{-4} to 10^{-3} cm/sec. Our analysis of the two most applicable soil profiles from the Ironstone region of the Jonglei area (31) indicates the range of the pore size distribution index (m) to be from 0.17 to 1.7 and that of the soil suction ($\Psi(1)$) to be from 30 to 150 cm. The effective porosity (n) is taken to be 0.35.

The above ranges of soil parameters are then scanned using Eq. (4.11). For each set of soil parameters (n, m, $K(1)$, $\Psi(1)$), a plot of the space-time soil moisture s_o versus the vegetal canopy, M, defines the equilibrium vegetal canopy, M_o, occurring at the maximum space-time soil moisture. It is found that M_o is a decreasing function of m and for m to be high (e.g., > 0.3), M_o is always low (e.g., < 0.7). M_o is an increasing function of both $K(1)$ and $\Psi(1)$, but m apparently sets the higher bound to which M_o can rise. Our six catchments enjoy a wet tropical climate and it is very unlikely that the vegetal canopy should fall below 0.6. Thus, we set as a criterion that M_o must be greater than 0.6. This determined m to be 0.2.

$K(1)$ largely determines the ratio of annual surface runoff

(R_{s_A}) to annual groundwater runoff (R_{g_A}). For humid regions where the soils have been described as 'well-drained, moderately permeably loamy soils,' it seems reasonable to expect the groundwater runoff component to be higher than the surface runoff component (33). For high K(1), however, the ratio ($\overline{R}_{s_A}/\overline{R}_{g_A}$) becomes so small (e.g., < 0.05) as to render it highly improbable. Thus, we set the limits of ($\overline{R}_{s_A}/\overline{R}_{g_A}$) to be between 0.05 and 1.0.

With the above two criteria for M_o and ($\overline{R}_{s_A}/\overline{R}_{g_A}$), we have effectively narrowed the range of K(1) to be from 3×10^{-4} to 6×10^{-4} cm/sec and that of $\Psi(1)$, from 100 to 150 cm.

Figures 4.5 and 4.6 illustrate the final procedure employed to obtain the parameters K(1) and $\Psi(1)$. Tonj catchment is shown as a typical example. In Figure 4.5, soils number 1 and 12 represent the just-estimated bounds of the soil parameters, K(1) and $\Psi(1)$. The CDF's of the normalized yield for these two soils are plotted on Figure 4.6, with curve 1 representing soil number 1 and curve 2, soil number 12. It is seen that in the dry year, curve 1 lies above the observed CDF while curve 2 lies below. These two curves define the estimated upper and lower limits of the derived CDF's, which also give the 'uncertainty range' of $\overline{Y}_A/\overline{P}_s$. In the dry years, we would expect the ungaged outflow from a catchment to be very much diminished, since the stream would be within its banks. Thus, the tails of the derived and the observed CDF's should match. This forms the last fitting criterion, which in turn determines the soil parameters, $\Psi(1)$ and K(1), as given by soil number 13 in Table 4.3. K(1) and $\Psi(1)$ for the remaining 5 catchments are determined by the

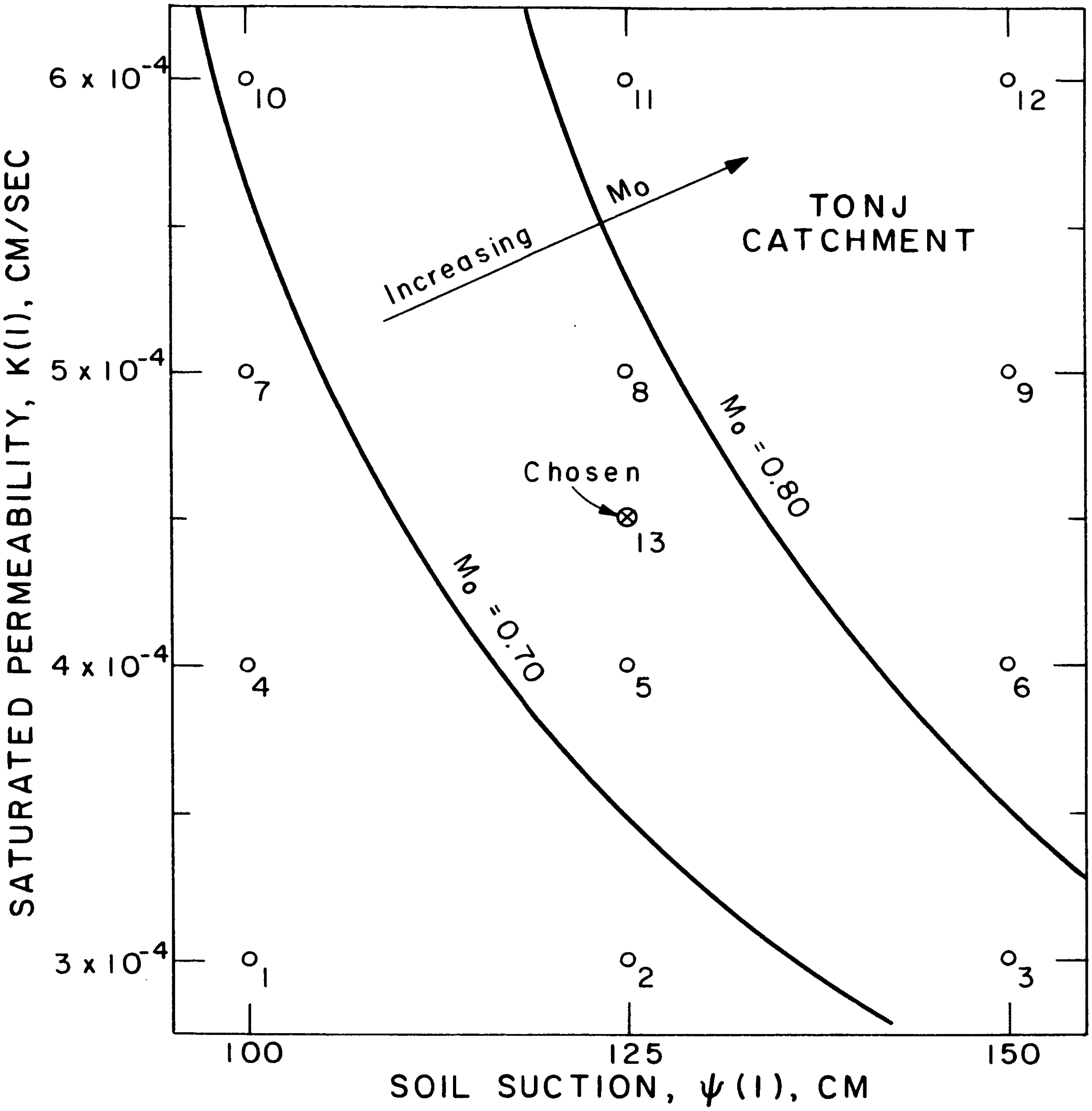

FIGURE 4.5

SOIL PARAMETER RANGE FOR THE TONJ CATCHMENT

Table 4.3: Results generated by the Soil Parameters in Figure 4.5

Number	M_o	$\bar{R}_{s_A}/\bar{R}_{g_A}$	$\bar{Y}_A/\overline{P_s}$	$w/\bar{e}_p$,%
1	0.60	0.80	0.1692	5.3
2	0.68	0.81	0.1412	8.9
3	0.77	0.81	0.1240	14.8
4	0.68	0.46	0.1510	7.1
5	0.73	0.45	0.1284	12.4
6	0.82	0.42	0.1154	19.5
7	0.70	0.29	0.1426	8.3
8	0.80	0.28	0.1187	15.4
9	0.83	0.25	0.1120	24.3
10	0.70	0.19	0.1346	10.1
11	0.80	0.18	0.1159	18.3
12	0.85	0.17	0.1084	29.6
13	0.78	0.35	0.1234	13.6

($n = 0.35$, $m = 0.2$, $Z = 20$ meters)

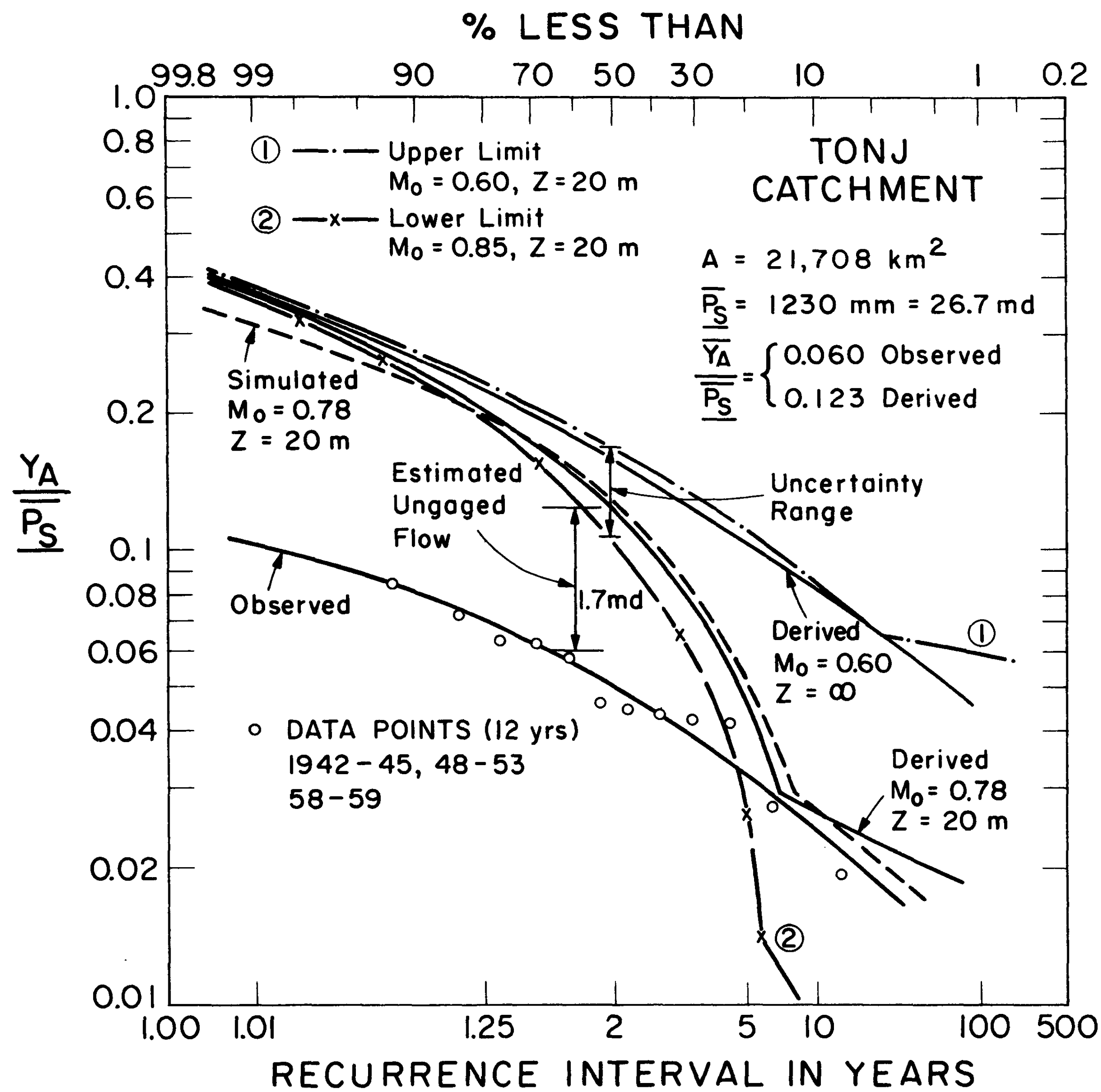

FIGURE 4.6

FREQUENCY OF ANNUAL CATCHMENT YIELD

(TONJ CATCHMENT)

same procedure. The CDF's for the 5 remaining catchments are plotted in Appendix B.

Referring to Figure 4.6, the vertical distance between the observed normalized mean annual discharge and the derived normalized mean annual discharge multiplied by the mean annual seasonal precipitation gives the so-called 'Estimated Ungaged outflow' from the catchment, including deep seepage (Fig. 4.6).

In the extremely dry years, there is an abrupt change in the slope of the derived CDF. This starts at the point where the groundwater runoff is driven to zero by the scanty rainfall. Further decrease in the rainfall does not cause a corresponding rate of decrease of surface runoff, and hence a more slowly decreasing rate of normalized yield results.

The water table effects are explored in Figure 4.7, using Tonj as a typical illustration. It is seen that the smaller the depth to the water table (Z), the higher is the equilibrium vegetal density (M_o) and the higher is the ratio of the rate of capillary rise from the water table to the rate of potential wet soil surface evaporation ($w/\bar{e}_p$).

A 'Z' of 10 meters produces a fully-vegetated cover ($M_o = 1.0$) over the entire catchment and a high ratio of $w/\bar{e}_p$ (83.4%). The tail of the derived yield CDF for this shallow water table cuts that of the observed yield sharply, violating the tail-matching criterion. All these conditions indicate the infeasibility of a 10-meter Z. Even though the 30-meter Z could be a possible candidate for matching the tails, the observed depth of wells in the area (Section 3.6) shows it to be highly

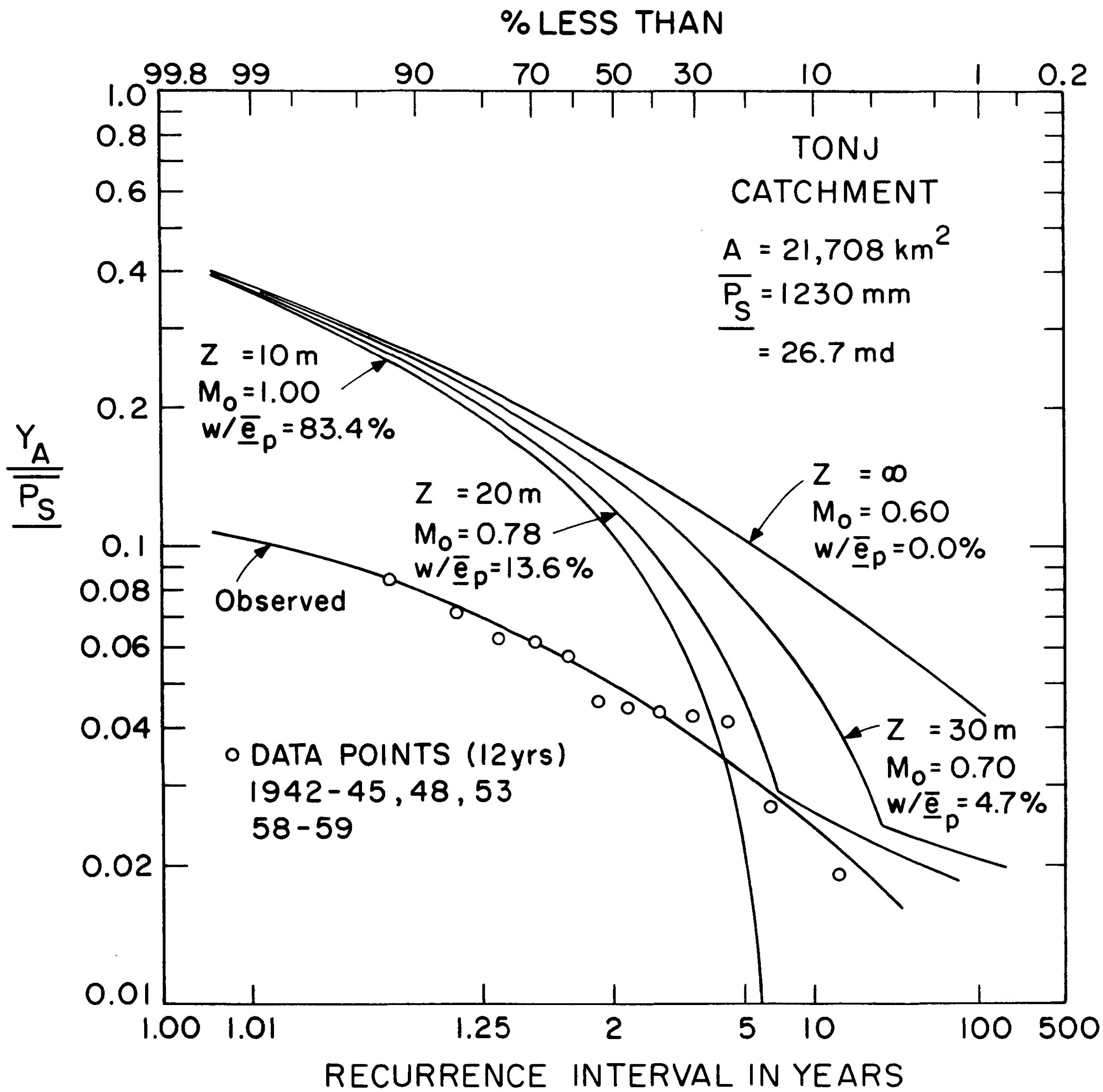

FIGURE 4.7

FREQUENCY OF ANNUAL CATCHMENT YIELD FOR TONJ CATCHMENT:

EFFECTS OF VARYING THE WATER TABLE DEPTH unlikely. Thus, it seems that the 20-meter Z should be a fairly good representation of the actual areally-averaged depth to the water table in the area.

For comparison, the CDF of the normalized yield without the water table ($Z = \infty$) is also plotted. This produces the lowest M_o and the highest normalized yield ratio, and the groundwater runoff component is never driven to zero.

For convenience, all the climatic, vegetation and soil parameters are tabulated in Table 4.4. The results generated using these parameters are given in Table 4.5.

4.3.4 A Refined Mean Annual Water Balance of the Central Swampland

In a preliminary analysis (Section 4.2), we obtained the ungaged inflows* $\overline{G}_L$ (15.1 md) required to close the water balance of the Central Swampland with deep seepage ignored. In the refined water balance model, $\overline{G}_L$ is estimated by summing the ungaged inflows from the six sub-catchments. This amounts to 19.8 md (Table 4.5).

The difference between the refined and preliminary $\overline{G}_L$ (19.8 - 15.1 = 4.7 md) may account for deep seepage on the 6 sub-catchments or it may merely reflect the uncertainty of the various estimates. This seepage, if it exists, may or may not seep into the Central Swampland. If it does, it will become the deep seepage at the Central Swampland. In either case, this 4.7 md represents the total water imbalance on the entire basin, $\overline{D}_B$.

*In this section, for simplicity, the words 'mean annual' will be dropped from all mean annual parameters.

Table 4.4: Climatic-soil-vegetal parameters of 6 sub-catchments

			Naam 1	Maridi 2	Tonj 3	Jur 4	Pongo 5	Loll 6
Climatic Parameters	$\underline{\overline{P}_s}$	cm	120.4	108.1	123.0	132.5	114.0	110.7
	$m_{\nu c}$		362	298	236	208	283	141
	$\underline{m}'_{\nu}$		82.4	72.1	86.4	93.3	80.3	74.1
	$\underline{m}_H$	cm	1.41	1.45	1.36	1.37	1.34	1.43
	$\underline{m}_{t_r}$	days	0.05	0.05	0.05	0.05	0.05	0.05
	$\underline{m}_{t_b}$	days	3.29	3.33	3.13	2.90	2.99	2.84
	$\underline{m}_{\tau}$	days	275	244	275	275	244	214
	$\underline{m}_i$	cm/hr	1.18	1.21	1.13	1.14	1.12	1.19
	$\underline{\kappa}$		0.73	0.54	0.70	1.00	1.07	1.76
Vegetation Parameters	k_v		1.0	1.0	1.0	1.0	1.0	1.0
	M_o		0.75	0.72	0.78	0.85	0.70	0.78
	$\underline{\bar{e}}_p$	cm/day	0.410	0.422	0.406	0.386	0.437	0.463
	h_o	cm	0.3	0.3	0.3	0.3	0.3	0.3
	$\underline{\overline{T}_s}$	^oC	25.8	26.6	25.8	25.8	27.2	26.8
	Z	meters	20	20	20	20	20	20
Soil Parameters	n		0.35	0.35	0.35	0.35	0.35	0.35
	m		0.20	0.20	0.20	0.20	0.20	0.20
	K(1)	cm/sec	5×10^{-4}	5×10^{-4}	4.5×10^{-4}	4×10^{-4}	3.5×10^{-4}	5×10^{-4}
	$\psi(1)$	cm	125	125	125	150	125	125

Table 4.5: Components of the Refined Water Balance for the Sub-catchments

		Naam	Maridi	Tonj	Jur.	Pongo	Loll	
		1	2	3	4	5	6	
A	km^2	11962	15390	21708	54705	8428	65338	
S_o		0.632	0.634	0.639	0.670	0.642	0.650	
$\bar{P}_S$	md	14.4	16.6	26.7	72.5	9.6	72.3	
E_{T_A}	cm	108.9	99.3	107.8	104.2	101.2	96.0	
R_{s_A}	cm	3.4	3.4	3.9	5.0	5.5	3.5	
R_{g_A}	cm	8.1	5.5	11.3	23.2	7.4	11.2	
$\bar{Y}_A/\bar{P}_S$ (Derived)		0.095	0.082	0.123	0.213	0.113	0.133	
$\bar{Y}_A/\bar{P}_S$ (Observed)		0.033	0.031	0.060	0.072	0.060	0.054	
$A * \bar{Y}_A$ (Derived)	md	1.368	1.358	3.290	15.420	1.084	9.620	
$A * \bar{Y}_A$ (Observed)	md	0.476	0.520	1.600	5.220	0.575	3.900	
$\bar{G}*$	md	0.89	0.84	1.69	10.18	0.51	5.72	Σ19.83
$\bar{G}*_{max}$	md	1.78	1.62	2.92	12.09	0.89	9.39	Σ28.68
$\bar{G}*_{min}$	md	0.64	0.54	1.29	10.10	0.20	4.83	Σ17.62
$w/\bar{e}_p$	%	15.2	14.8	13.6	20.5	9.9	13.5	
CDF (at $\bar{Y}_A/\bar{P}_S$)	%	50.9	51.0	50.9	50.6	50.9	50.9	

* $\bar{G} = [\bar{Y}_A$ (Derived) $- \bar{Y}_A$ (Observed)$]*A$
For the 'Uncertainty Range',
$\bar{G}_{max} = [\bar{Y}_{A_{max}}$(derived) $- \bar{Y}_A$ (Observed)$]*A$
$\bar{G}_{min} = [\bar{Y}_{A_{min}}$ (derived) $- \bar{Y}_A$ (Observed)$]*A$

1 md = 1 km^3 = 10^9 m^3

The refined water balance of the Central Swampland is shown in Figure 4.8. The water loss from the gaged and ungaged inflows alone amounts to at least 27.8 md*, and possibly 32.5 md**, which is comparable to the flow of White Nile at Malakal (27 md).

The deep seepage for the entire basin appears to be negligible (4.7 md). However, we must remember that the two dry sub-catchments in the north, Bahr el Arab and Raqaba el Zarqa (which we have not considered) have a combined annual precipitation of 166.5 md. Even if one percent of this quantity made its way into the Central Swampland, it would still be a huge amount (16.7 md).

Even though we cannot conclude definitely that the deep seepage at the Central Swampland is insignificant, we can be sure that the huge water loss at the Central Swampland can be explained by evapotranspiration alone.

4.4 Uncertainty in the Potential Water Yield from Swamp Drainage

4.4.1 Introduction

Planning for water resource development requires estimation of the anticipated annual basin yield. For each drainage scheme, we need to state not only the anticipated mean annual basin yield, but also the anticipated probability distribution of this basin yield.

Different drainage schemes may be devised for the Bahr el Ghazal basin, but the most obvious one is to dredge a canal surrounding

---

*Preliminary $(\overline{G}_L) + \overline{Y}_L = 15.1 + 12.7 = 27.8$ md (Figure 4.3)

**Refined $(\overline{G}_L) + \overline{Y}_L = 19.8 + 12.7 = 32.5$ md (Figure 4.8)

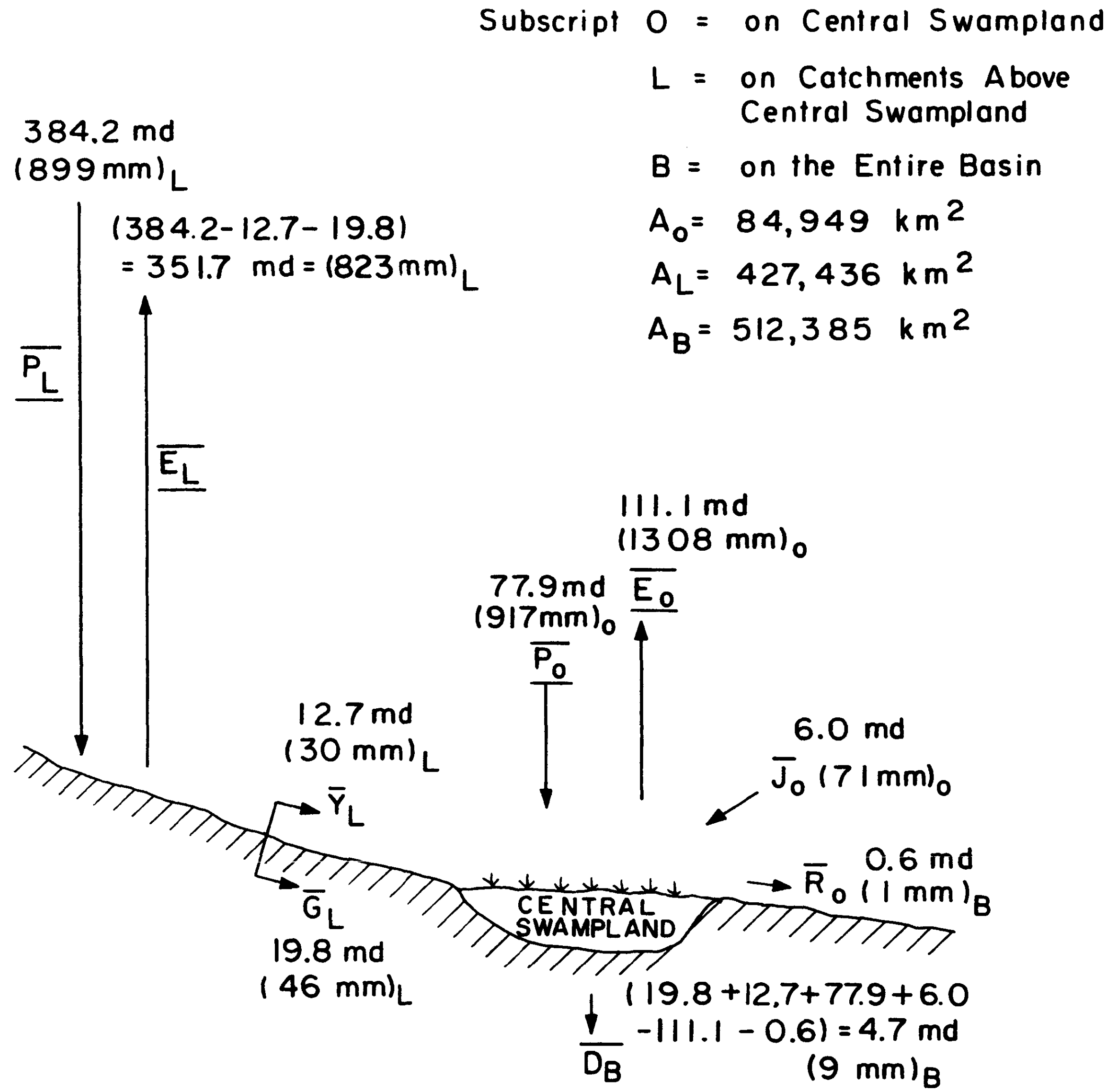

FIGURE 4.8

A REFINED MEAN ANNUAL WATER BALANCE OF THE CENTRAL SWAMPLAND the Central Swampland in the north and in the south, collecting the tributary inflows before they reach the Central Swampland.

Two drainage schemes are of particular interest (see Figure 4.9). One starts at the Tonj catchment, going east along the boundary of the Central Swampland, intercepting the Maridi and the Naam. It eventually joins the Bahr el Jebel upstream of the Jonglei Canal off-takes so that its water may reach Malakal via the Jonglei Canal. The other starts at the Jur catchment, cutting the Pongo and the Loll along the edge of the Central Swampland, going directly north at Nyamlell to cut the Bahr el Arab, then swings east to cross the Raqaba el Zarqa, and eventually reaches the White Nile south of Malakal. The north-going canal may be identified closely with the Gogrial By-pass, which is described in the literature (34), (35). The reason that River Jur should join the north-going canal is probably due to the topography of the region.

For the rivers Tonj, Jur, Pongo, Loll, based on 5 to 11 years of synchronized observations, the correlation of the annual gaged discharges between adjacent catchments ranges from 0.33 to 0.77.

Due to a lack of knowledge of the joint probability distributions of the correlated streamflows, the CDF's of their sums will not be derived analytically. Instead, they will be estimated by employing the Monte Carlo simulation technique. A model is called for to generate the six annual catchment areally-averaged precipitations, which preserves the respective catchment observed precipitation mean and variance, as well as the lag-zero and lag-one auto- and cross-

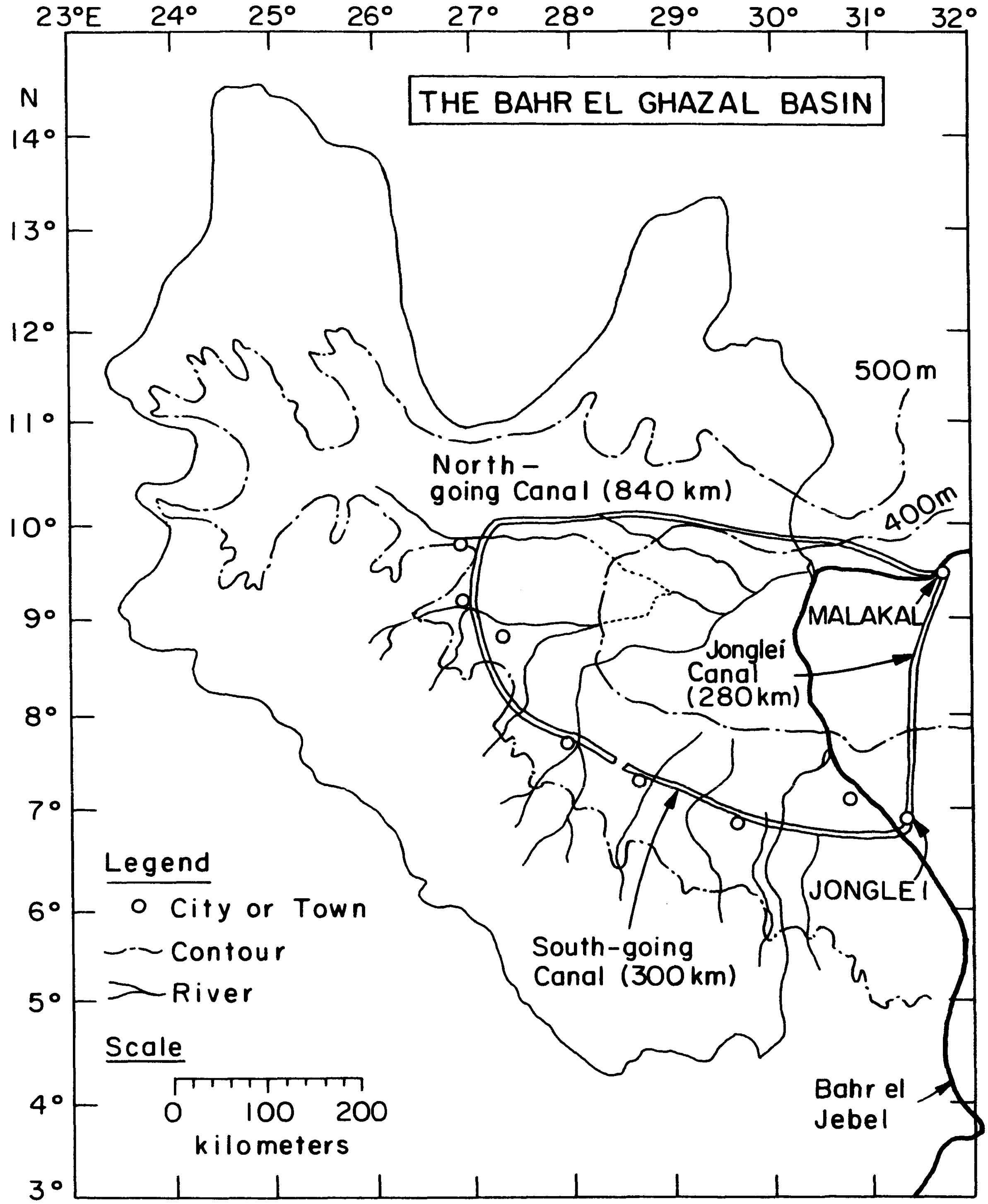

FIGURE 4.9

CANAL ROUTES

correlations. Long series of these 6 catchment correlated synthetic annual precipitations are used as the inputs to the water balance equation, which then produces long series of the corresponding 6 catchment correlated synthetic annual yields. From these synchronized synthetic yields, we may evaluate the empirical CDF's of the six separate catchment annual yields, and the empirical CDF's of the combined catchment annual yields.

After the swamps are drained, it is expected that they will be replaced naturally by grasslands which transpire at a lower rate, and that the precipitation and Jebel spillage on the Central Swampland will be matched approximately by the actual evapotranspiration of the grasslands in the region.

4.4.2 Simulation of Correlated Annual Catchment Yields

Analysis of the 32 years of the 6 catchment annual observed precipitations (Appendix B) has shown that these precipitations are correlated, with simple (lag-zero) correlations ranging from -0.10 to 0.68 among the catchments (Table 4.6). The lag-one correlations appear to be rather insignificant (Table 4.7).

A multivariate, autoregressive, Markovian model (36), (37), (38), is used to generate six synchronized long series of catchment annual precipitation, which preserves the observed historical catchment annual precipitation means, variances, lag-zero and lag-one auto- and cross-correlations. This model is applicable to a weakly-stationary process and is described as follows:

Table 4.6: Simple (Lag-zero) Correlations* of the Annual Observed Catchment Precipitations (32 years), $\rho^{(ij)}_{\underline{P_A}}(0)$

		Naam	Maridi	Tonj	Jur	Pongo	Loll
		1	2	3	4	5	6
Naam	1	1					
Maridi	2	0.50 (0.63)**	1				
Tonj	3	0.55 (0.49)	0.33 (0.34)	1			
Jur	4	0.39 (0.28)	0.21 (0.18)	0.68 (0.61)	1		
Pongo	5	0.49 (0.44)	0.25 (0.29)	0.57 (0.56)	0.60 (0.57)	1	
Loll	6	0.06 (0.03)	-0.19 (-0.19)	-0.20 (-0.25)	-0.10 (-0.11)	0.27 (0.35)	1
$\overline{\underline{P_A}}$ (32 yrs)	mm	1199	1091	1251	1387	1198	1165
$\sigma_{\underline{P_A}}$ (32 yrs)	mm	97	117	127	136	99	123

* This is a symmetric matrix, with

$$\rho^{(ij)}_{\underline{P_A}}(0) = \rho^{(ji)}_{\underline{P_A}}(0)$$

** Lag-zero correlations of the annual synthetic catchment precipitations (2,000 years)

Table 4.7: Lag-one correlations of annual observed Catchment precipitations (32 yrs), $\rho^{(ij)}_{\underline{P_A}}$ (1)

		Naam 1	Maridi 2	Tonj 3	Jur 4	Pongo 5	Loll 6
Naam	1	0.00 (0.02)*	-0.36 (0.00)	0.06 (-0.02)	-0.09 (-0.02)	-0.02 (0.00)	0.20 (0.03)
Maridi	2	-0.11 (0.02)	0.04 (0.02)	-0.24 (-0.01)	-0.32 (-0.02)	-0.11 (-0.01)	0.27 (0.01)
Tonj	3	0.17 (0.01)	-0.13 (-0.01)	0.17 (0.01)	0.05 (-0.03)	0.14 (-0.02)	0.35 (-0.01)
Jur	4	0.17 (-0.01)	-0.10 (-0.03)	0.14 (-0.02)	-0.02 (-0.03)	0.08 (-0.01)	0.27 (0.01)
Pongo	5	0.08 (-0.03)	-0.12 (-0.05)	0.07 (-0.03)	-0.02 (-0.05)	-0.14 (-0.04)	0.10 (0.01)
Loll	6	-0.02 (-0.04)	-0.12 (-0.04)	-0.03 (-0.05)	0.07 (-0.01)	0.16 (-0.01)	0.14 (0.02)

* Lag-one correlations of the annual synthetic catchment precipitations (2,000 years)

Consider a linear relationship expressed by

$$\underline{\underline{P}}_A(k+1) = A\underline{\underline{P}}_A(k) + B\underline{V}(k+1) \qquad (4.15)$$

with

$$\underline{\underline{P}}_A(k+1) = [\underline{P}_A^{(1)}(k+1),\ \underline{P}_A^{(2)}(k+1),\ \ldots,\ \underline{P}_A^{(6)}(k+1)]^T \qquad (4.16)$$

Here, $\underline{\underline{P}}_A(k+1)$ is a vector (6x1) denoting the annual six sub-catchment precipitations in the $(k+1)^{th}$ year. A(6x6) and B(6x6) are the generation matrices for the annual catchment precipitations. $\underline{V}(k+1)$ is a random vector (6x1) independent of $\underline{\underline{P}}_A(k)$.

This is a one-step Markov process in which the current precipitation depends probabilistically on only the immediately preceding precipitation. It is assumed that $\underline{\underline{P}}_A(k+1)$ and $\underline{\underline{P}}_A(k)$ are both internally correlated (lag-zero correlations) and that they are externally correlated at lag-one.

To facilitate the determination of matrices A and B, the vectors in Equation (4.15) are reduced by their respective means, as

$$\left.\begin{aligned}
\underline{x}_{k+1} &= \underline{\underline{P}}_A(k+1) - E\{\underline{\underline{P}}_A(k+1)\} = \underline{\underline{P}}_A(k+1) - \overline{\underline{\underline{P}}_A} \\
\underline{x}_k &= \underline{\underline{P}}_A(k) - E\{\underline{\underline{P}}_A(k)\} = \underline{\underline{P}}_A(k) - \overline{\underline{\underline{P}}_A} \\
\underline{v}_{k+1} &= \underline{V}(k+1) - E\{\underline{V}(k+1)\} \\
\text{and} \qquad & \\
\overline{\underline{\underline{P}}_A} &= [\overline{\underline{P}}_A^{(1)},\ \overline{\underline{P}}_A^{(2)},\ \ldots,\ \overline{\underline{P}}_A^{(6)}]^T
\end{aligned}\right\} \qquad (4.17)$$

Now,

$$\underline{x}_{k+1} = A\underline{x}_k + B\underline{v}_{k+1} \tag{4.18}$$

Taking the expected values on both sides of Eq. (4.18),

$$E\{\underline{x}_{k+1}\} = A\ E\{\underline{x}_k\} + B\ E\{\underline{v}_{k+1}\} \equiv \underline{0} \tag{4.19}$$

Post-multiplying Equation (4.18) by the transpose of $\underline{x}_k$ gives

$$\underline{x}_{k+1}\underline{x}_k^T = A\ \underline{x}_k\underline{x}_k^T + B\underline{v}_{k+1}\underline{x}_k^T \tag{4.20}$$

Taking the expected value of the above equation,

$$E\{\underline{x}_{k+1}\underline{x}_k^T\} = A\ E\{\underline{x}_k\underline{x}_k^T\} + B\ E\{\underline{v}_{k+1}\underline{x}_k^T\} \tag{4.21}$$

But, $\underline{v}_{k+1}$ and $\underline{x}_k$ are independent, which implies

$$E\{\underline{v}_{k+1}\ \underline{x}_k^T\} = \underline{\underline{0}} \tag{4.22}$$

Let

$$\left.\begin{aligned} S_{\underline{xx}} &= E\{\underline{x}_k\underline{x}_k^T\} \\ \text{and} \qquad & \\ S_{\underline{x'x}} &= E\{\underline{x}_{k+1}\underline{x}_k^T\} \end{aligned}\right\} \tag{4.23}$$

Then, Equation (4.21) becomes

$$\left.\begin{aligned} S_{\underline{x'x}} &= A\ S_{\underline{xx}} \\ \text{or} \qquad & \\ A &= S_{\underline{x'x}}\ S_{\underline{xx}}^{-1} \end{aligned}\right\} \tag{4.24}$$

Matrix A is defined because $S_{\underline{xx}}$ is the variance-covariance matrix which is nonsingular and hence its inverse exists.

$S_{\underline{xx}}$ and $S_{\underline{x'x}}$ are estimated by

$$S_{\underline{xx}} \cong \begin{vmatrix} \frac{1}{N}\sum_{k=1}^{N} x_k^{(1)}\ x_k^{(1)} & \frac{1}{N}\sum_{k=1}^{N} x^{(1)}\ x_k^{(2)} & \cdots & \frac{1}{N}\sum_{k=1}^{N} x_k^{(1)}\ x_k^{(6)} \\ \frac{1}{N}\sum_{k=1}^{N} x_k^{(2)}\ x_k^{(1)} & \ddots & & \vdots \\ \vdots & & \ddots & \vdots \\ \frac{1}{N}\sum_{k=1}^{N} x_k^{(6)}\ x_k^{(1)} & \cdots & \cdots & \frac{1}{N}\sum_{k=1}^{N} x_k^{(6)}\ x_k^{(6)} \end{vmatrix} \qquad (4.25)$$

= a symmetric matrix

$$S_{\underline{x'x}} \cong \begin{vmatrix} \frac{1}{N}\sum_{k=1}^{N-1} x_{k+1}^{(1)}\ x_k^{(1)} & \frac{1}{N}\sum_{k=1}^{N-1} x_{k+1}^{(1)}\ x_k^{(2)} & \cdots & \frac{1}{N}\sum_{k=1}^{N-1} x_{k+1}^{(1)}\ x_k^{(6)} \\ \frac{1}{N}\sum_{k=1}^{N-1} x_{k+1}^{(2)}\ x_k^{(1)} & \ddots & & \vdots \\ \vdots & & \ddots & \vdots \\ \frac{1}{N}\sum_{k=1}^{N-1} x_{k+1}^{(6)}\ x_k^{(1)} & \cdots & \cdots & \frac{1}{N}\sum_{k=1}^{N-1} x_{k+1}^{(6)}\ x_k^{(6)} \end{vmatrix} \qquad (4.26)$$

where N, the number of years of observed precipitation records, is 32.

Post-multiplying Equation (4.18) by its transpose yields

$$\underline{x}_{k+1}\ \underline{x}_{k+1}^T = (A\underline{x}_k + B\underline{v}_{k+1})(A\underline{x}_k + B\underline{v}_{k+1})^T$$

$$= A\underline{x}_k\underline{x}_k^T A^T + A\underline{x}_k\underline{v}_{k+1}^T B^T + B\underline{v}_{k+1}\underline{x}_k^T A^T + B\underline{v}_{k+1}\underline{v}_{k+1}^T B^T \quad (4.27)$$

Taking the expected values of Equation (4.27), and simplifying, gives

$$\underline{S_{x'x'}} = A\ \underline{S_{xx}}\ A^T + B\ \underline{S_{v'v'}}\ B^T \quad (4.28)$$

where

$$\underline{S_{x'x'}} = E\{\underline{x}_{k+1}\ \underline{x}_{k+1}^T\}$$

$$\underline{S_{v'v'}} = E\{\underline{v}_{k+1}\ \underline{v}_{k+1}^T\}$$

For annual precipitations, $\underline{S_{x'x'}} = \underline{S_{xx}}$. By defining the random process to be of unit variance, that is, $\underline{S_{v'v'}} = I$, where 'I' is the identity matrix, we may now combine Equations (4.28) and (4.24) to yield

$$BB^T = \underline{S_{xx}} - \underline{S_{x'x}}\ \underline{S_{xx}}^{-1}\ \underline{S_{x'x}}^T \quad (4.29)$$

where BB^T is a known positive semi-definite matrix. One of the techniques in recovering matrix B from BB^T employs the principal component analysis which is fully described in Reference (37) (including computer programs), so it will not be repeated here.

It is possible to state at this point that using this model the observed precipitation means are preserved by Equation (4.19), without any restrictions on matrices A and B.

However, to preserve the second moments (the observed precipitation lag-zero and lag-one variance-covariances), matrices A and B have to be chosen in such a way as to satisfy Equation (4.24) and (4.29). Notice that the only conditions imposed on the random variate, $\underline{v}_{k+1}$ are that its elements are independently identically distributed with zero means, zero covariances and unit variances, and that it is independent of $\underline{x}_k$. There is no restriction on the underlying distribution of $\underline{v}_{k+1}$. In this work, it will be sampled from a normal distribution. A discussion of using the normal distribution in this model is also given in References (37) and (38).

After matrices A and B are determined, the generation of synthetic rainfall series proceeds by first setting the initial values $\underline{x}_1 = \underline{0}$ in Equation (4.18) and then using the same equation recursively, each time feeding in a new set of random normal variates (zero means, unit variances). To these generated annual precipitation residues ($\underline{x}_k$'s) are added the long-term observed mean annual catchment precipitation from Table 3.4, instead of the short-term (32 years) observed mean values. These synthetic correlated annual records are further discounted by multiplying by the factor, $\underline{\overline{P}_s}/\underline{\overline{P}_A}$, (Table 4.8) to reduce them to the synthetic seasonal catchment precipitation. The synthetic seasonal records are then used as the inputs to the annual water balance model (Equations (4.11) and (4.12) without time averaging) to

Table 4.8: Comparison of the observed* and the generated Catchment precipitation means and variances

		Naam	Maridi	Tonj	Jur	Pongo	Loll
		1	2	3	4	5	6
$\overline{P_A}$ (Observed)	mm	1235	1129	1261	1364	1171	1134
$\overline{P_A}$ (Generated)	mm	1234	1128	1261	1363	1171	1136
σ_{P_A} (Observed)	mm	97	117	127	136	99	123
σ_{P_A} (Generated)	mm	86	103	112	124	91	115
$\overline{P_S}/\overline{P_A}$ (Observed)		0.975	0.958	0.976	0.971	0.974	0.976
$[\overline{P_A}$(Gen) $-$ $\overline{F_A}$ (Obs)$]/\overline{P_A}$(obs)	%	-0.1	-0.1	0.0	-0.1	0.0	0.2
$[\sigma_{P_A}$(Gen) $-$ σ_{P_A}(obs)$]/\sigma_{P_A}$(obs)	%	-11.3	-12.0	-11.8	-8.8	-8.1	-6.5

* From Table 3.4 long term records up to 1972

generate six series of correlated annual catchment yields. After some trials, it is concluded that synthetic series of 2000 years are sufficient to generate reliable empirical catchment yield CDF's.

From Table 4.8, it is seen that the generated precipitation means are almost identical with the observed, with a maximum absolute value of the relative error of only 0.2%. The standard deviation of the generated precipitation is consistently below that of the observed, with a relative error ranging from 6.5% to 12.0%. The reason for this underestimation is not clear; but a maximum relative error of 12% in the variance is still a good indication of the validity of the generating model. The lag-zero correlations of the synthetic precipitations are given under that of the observed in Table 4.6 for comparison. The results are quite satisfactory when considering the preservation of 15 correlations. The lag-one correlations comparison is dismissed because the lag-one correlations of the observed catchment precipitation appear to be quite insignificant (Table 4.7).

Preservation of the observed annual catchment precipitation CDF's can be demonstrated by comparing the empirical CDF's of the catchment's synthetic records with those of the observed records. This may also be demonstrated by comparing the derived CDF's of the catchment yield with the empirical CDF's of the catchment synthetic yield.

The comparison of the CDF's of the simulated normalized catchment annual yields with that of the derived are seen in Figure 4.6, Table 4.9 and in Appendix B. In all the comparisons, the simulated curve is slightly flatter than the derived (ignoring the bending of the

Table 4.9: Simulated Mean Annual Catchment Yield Data

Catchment			Naam	Maridi	Tonj	Jur	Pongo	Loll
Catchment Number			1	2	3	4	5	6
Mean Seasonal Precipitation (Observed)	$\overline{P_s}$	mm	1024	1081	1230	1325	1140	1107
	$A*\overline{P_s}$	md	14.40	13.64	26.70	72.48	9.61	72.33
Mean Annual Yield (Observed)	$\overline{Y}_A$	mm	119	101	159	283	135	156
	$A*\overline{Y}_A$	md	1.42	1.56	3.45	15.48	1.14	10.17
Mean Annual Yield (Derived)	$\overline{Y}_A$	mm	115	89	152	282	129	147
	$A*\overline{Y}_A$	md	1.34	1.36	3.29	15.42	1.08	9.62
Standard Deviation of Y_A (Simulated)	σ_{Y_A}	mm	70	74	93	118	70	97
	$A*\sigma_{Y_A}$	md	0.84	1.14	2.02	6.46	0.59	6.34
Coefficient of variation (Simulated)	$\frac{\sigma_{Y_A}}{\overline{Y}_A}$		0.588	0.733	0.585	0.417	0.519	0.622
Normalized Mean Annual	$\frac{Y_A}{\overline{P_s}}$		0.0988	0.0938	0.1291	0.2136	0.1183	0.1407
CDF at $\overline{Y}_A/\overline{P_s}$ (simulated)	%		53	56	51	50	52	52

tail where the groundwater runoff component is zero), indicating a smaller variance in the simulated case. This is due to the fact that the synthetic catchment precipitation has a smaller variance than the observed. However, despite this small deviation, all the simulated curves match closely with the observed.

As a result of the simulation, we also derive the lag-zero correlation structure of the simulated annual catchment yields as tabulated in Table 4.10.

4.4.3 Uncertainty in the Potential Water Yield from Swamp Drainage

In this section, the empirical CDF's of the estimated potential water yield from different drainage schemes (canals) will be given for the ideal case of unlimited canal capacities. This assumes that all yields from the sub-catchments are fully intercepted by the canals and that no spillage, evaporation or seepage losses occur. In reality, the amount of water to be recovered depends critically on the design of the interception system, and of the canal capacity. Because of the various ways in which the ungaged inflows to the Central Swampland can occur (page 118), without any on-site investigation, it is impossible at this stage of our work to speculate on the efficiency of the interception system. The seepage loss may be significant if the soils along the canal routes are highly permeable. At the moment, since no detailed soil description along the canal routes is available, we will only consider the ideal case. In the next chapter, the CDF's of the yield from the canals given the canal capacities will be explored.

Table 4.10: Lag-Zero Correlations of the simulated annual catchment yield

(a symmetric matrix)

	Naam	Maridi	Tonj	Jur	Pongo	Loll
	1	2	3	4	5	6
1	1					
2	0.62	1				
3	0.47	0.32	1			
4	0.27	0.17	0.60	1		
5	0.43	0.27	0.54	0.56	1	
6	0.03	-0.18	-0.25	-0.12	0.34	1

For simplicity, we will use numbers one to six to represent the six catchments, with Naam as 1, Maridi, 2, Tonj, 3, Jur, 4, Pongo, 5 and Loll, 6.

For the combined catchments, we will adopt the following notations:

C12 = Catchments Naam + Maridi

C123 = Catchments Naam + Maridi + Tonj

C56 = Catchments Pongo + Loll

C456 = Catchments Jur + Pongo + Loll

C16 = Catchments Naam + Maridi + Tonj + Jur + Pongo + Loll

Due to our drainage schemes (Fig. 4.9), only the CDF's of the potential water yield from adjacent catchments are needed. The potential yield from C456, C123 and C16 are, respectively, the ideal maximum water recovery from the north-going and the south-going canal, and the maximum water gain at Malakal due to swamp drainage.

From the last section, six synchronized series of the synthetic annual catchment yields are available, each 2,000 years long. In the final analysis, these synchronized synthetic yields are combined year-by-year to give the combined catchment yields which are then normalized by their combined catchment seasonal precipitation.

For the combined catchment, k, where k = (1, 2), (1, 2, 3), (5, 6), (4, 5, 6), (1, 2, 3, 4, 5, 6), we have:

The combined catchment area:

$$A_k = \sum_{\text{all } i \varepsilon k} A_i \tag{4.30}$$

The space-time mean seasonal combined catchment precipitation,

$$\overline{\underline{P_s}}^{(k)} = \left(\sum_{\text{all } i\varepsilon k} A_i * \overline{\underline{P_s}}^{(i)} \right) / A_k \qquad (4.31)$$

The annual combined catchment yield,

$$Y_A^{(k)}(j) = \left[\sum_{\text{all } i\varepsilon k} A_i * Y_A^{(i)}(j) \right] / A_k, \qquad j = 1, \ldots, 2000 \qquad (4.32)$$

The space-time mean annual combined catchment yields,

$$\overline{Y}_A^{(k)} = \frac{1}{N} \sum_{j=1}^{N} Y_A^{(k)}(j) \quad , \qquad N = 2000 \text{ years} \qquad (4.33)$$

and the normalized annual combined catchment yield

$$[Y_A^{(k)}(j) / \overline{\underline{P_s}}^{(k)}] \quad , \qquad j = 1, \ldots, 2000 \qquad (4.34)$$

with its mean at $\overline{Y}_A^{(k)} / \overline{\underline{P_s}}^{(k)}$.

The results for the mean values are tabulated in Table 4.11 and the empirical CDF's of $Y_A^{(k)} / \overline{\underline{P_s}}^{(k)}$ are plotted on Figure 4.10. From Table 4.11, the mean yield from C456 is 26.8 md, from C123, 6.4 md, and from C16, 33.2 md. The 33.2 md is augmented by 0.4 md, the reported mean discharge of Bahr el Arab and Raqaba el Zarqa (5) to arrive at 33.6 md which is the total simulated yield from the sub-catchments of the Bahr el Ghazal basin. It compares favorably with the derived yield (12.7 + 19.8 = 32.5 md from Figure 4.8), with a difference of only 3%.

Table 4.11: Simulated Mean Annual Combined Catchment Yield Data

Combined Catchment:			C12	C56	C123	C456	C16
Area, A		km^2	27,352	73,766	49,060	128,471	177,531
Mean Seasonal Precipitation (Observed),	$\overline{P_s}$	mm	1135	1111	1177	1202	1195
	$A*\overline{P_s}$	md	31.04	81.95	57.74	154.42	212.15
Mean Annual Yield (Simulated),	$\bar{Y}_A$	mm	109	153	131	209	187
	$A*\bar{Y}_A$	md	2.98	11.31	6.43	26.79	33.22
Standard Deviation of Y_A (Simulated)	σ_{Y_A}	mm	65	86	65	69	57
	$A*\sigma_{Y_A}$	md	1.78	6.34	3.21	8.86	10.17
Coefficient of Variation	$\frac{\sigma_{Y_A}}{\bar{Y}_A}$		0.596	0.561	0.499	0.330	0.306
Mean Normalized Annual Yield	$\frac{\bar{Y}_A}{\overline{P_s}}$		0.0961	0.1380	0.1114	0.1735	0.1566
Standard Deviation of $Y_A/\overline{P_s}$,	$\sigma_{Y_A/\overline{P_s}}$		0.0573	0.0774	0.0555	0.0575	0.0480
CDF at $\bar{Y}_A/\overline{P_s}$		%	54.5	52	54	52	50

FIGURE 4.10

FREQUENCY OF ANNUAL COMBINED CATCHMENT YIELD

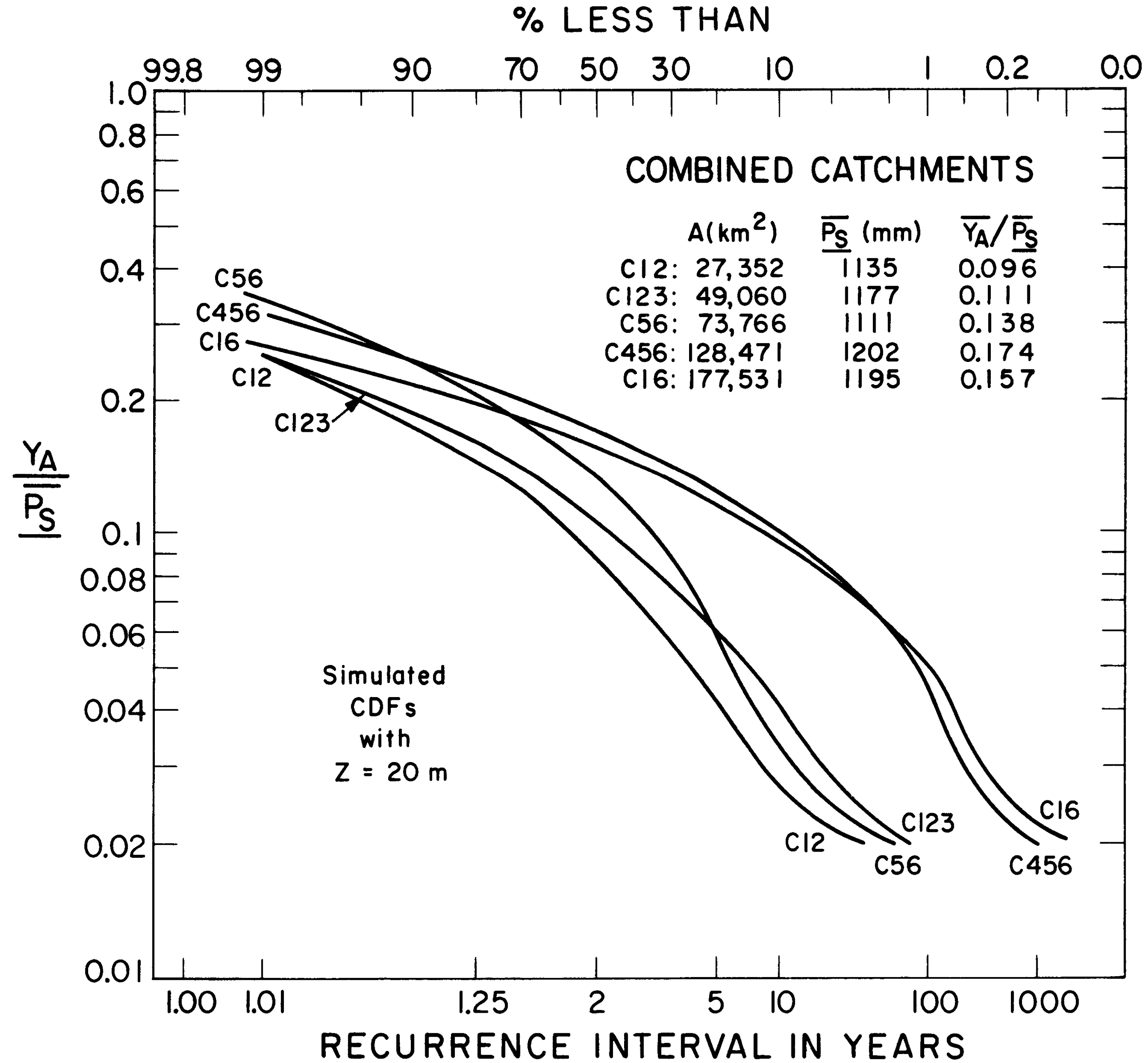

Chapter 5

CANAL COST-CAPACITY UNDER CERTAIN CANAL FLOWS

5.1 Introduction

In the previous chapter, we have obtained the simulated distributions* of the annual combined catchment yields. These distributions are identical to those of the canal flows from the combined catchments in the ideal case of unlimited canal capacities and fully-efficient interception systems. Without any on-site knowledge of the ungaged inflows and of the soil parameters along the canal routes, we will not launch a full-scale study of the interception and conveyance losses. These will be left for future research.

In this chapter, we will consider only the distribution of the maximum potential canal flow given the canal design capacity. This distribution is very important in canal capacity design, since it defines the uncertainty in the amount of potentially-available water given the canal capacity. It will be derived from the empirical distribution of the combined catchment yield. Wherever possible, we will strive for analytical solutions instead of numerical ones.

Some cost estimates of canal work are also offered. These estimates are by no means the actual construction costs and should not be used in any specific canal cost estimates. Their main purpose here is to demonstrate how the distribution of canal flow with limited canal capacity can be useful in the ultimate problem of canal cost estimation.

*'distribution' and 'CDF' are used interchangeably in this work.

5.2 Analytical Representation of the Simulated Distributions

The simulated distributions of annual combined catchment yield are given in numerical form in Appendix B. To facilitate the derivation of the distribution of the canal flow given the canal capacity, the yield distributions should be represented in functional form. For simplicity, a continuous function should be used.

Many functions can be employed to fit simulated distributions, but by far the most convenient are the polynomials, since their integrals, derivatives and products are also polynomials.

The simulated distribution may be fitted by a function of the form

$$\hat{F} = \sum_{k=0}^{N} C_k \, y^k \tag{5.1}$$

with $0 \leq y < \infty$, $0 \leq \hat{F} < 1$ or

$$\hat{y} = \sum_{k=0}^{N} C_k \, F^k \tag{5.2}$$

with $0 \leq \hat{y} < \infty$, $0 \leq F < 1$ where

$y = Y_A/\overline{P_s}$ = normalized annual combined catchment yield

$\hat{y}$ = estimate of y

F = CDF of y

$\hat{F}$ = estimate of F

C_k = coefficient of kth term

N = highest degree of the polynomials

Both forms suffer the drawback of not matching the upper tail condition ($y \to \infty$, $F \to 1$). If we set the upper limit finite at ($y = y_{max}$, $F = 0.9999$) and use a polynomial of degree $N = 10$, $\hat{F}$ can be greater than 1 when y approaches y_{max} in Eq. (5.1). Also, $\hat{y}$ in Eq. (5.2) matches poorly with the actual y when F is greater than 0.98. Equation (5.2) is easier to handle than Equation (5.1), because the independent variable F in the former lies between 0 and 1. To remedy its upper tail-matching condition, the following form is suggested,

$$\hat{y} = \sum_{k=0}^{N} C_k F^k + \frac{a}{(1 - F)^b} = G(F) \tag{5.3}$$

with

$$\begin{matrix} 0 \leq \hat{y} < \infty \\ 0 \leq F < 1 \end{matrix} \quad , \qquad a, b > 0$$

It is obvious from this formulation that $\hat{y}$ approaches infinity when F approaches one.

Referring to Fig. 5.1a, the simulated CDF curve is represented by $y = g(F)$. (F_i, y_i) is the ith discrete data point on $y = g(F)$.

The fitting procedure takes two steps.

The first step involves the determination of the constants a and b in Eq. (5.3) by employing those points (F_i, y_i) for which $0.98 \leq F_i < 1$. This is done by writing

$$y' = \frac{a}{(1 - F)^b} \tag{5.4}$$

for $0.98 \leq F < 1$, $a, b > 0$

Taking the logarithm of both sides,

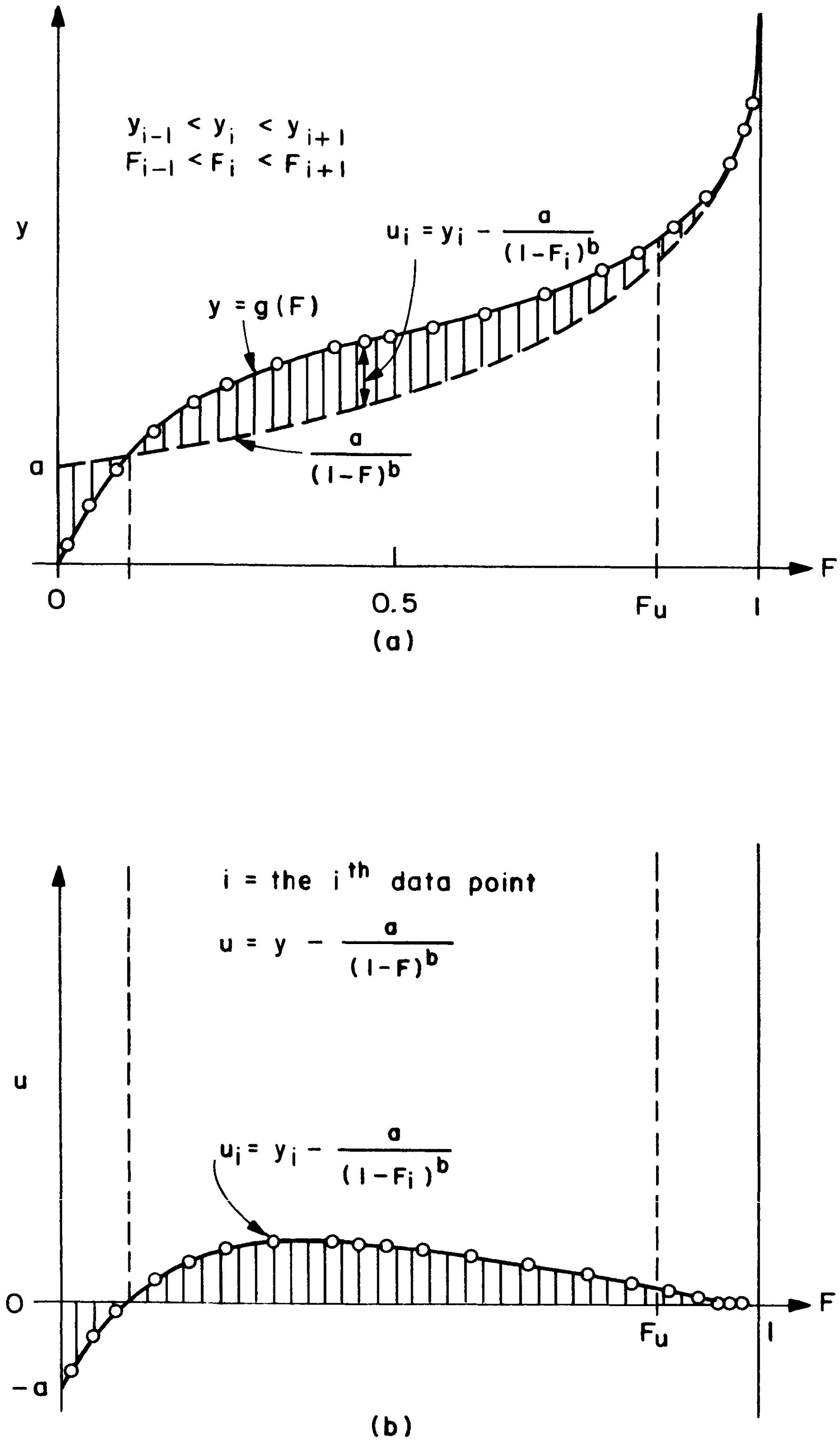

FIGURE 5.1

SIMULATED DISTRIBUTION OF ANNUAL COMBINED CATCHMENT YIELD

(FUNCTIONAL REPRESENTATION)

$$\log_{10} y' = \log_{10} a - b \log_{10}(1 - F) \tag{5.5}$$

This is a polynomial of degree one, which can be written

$$Z = a_o + a_1 v \tag{5.6}$$

where

$$Z = \log_{10}y' \quad , \qquad a_o = \log_{10}a$$

$$v = \log_{10}(1 - F) \ , \ a_1 = -b$$

The coefficients a_o and a_1 in Eq. (5.6) can be determined by a least-squares fit to the data points (Z_i, v_i). Notice that at least two points are required for the fitting. The constants a and b can then be retrieved from,

$$a = 10^{a_o} \quad , \quad b = - a_1 \tag{5.7}$$

Having determined a and b, we form the function u, as

$$u = y - \frac{a}{(1 - F)^b} \tag{5.8}$$

and for discrete points

$$u_i = y_i - \frac{a}{(1 - F_i)^b} \tag{5.9}$$

for all points (F_i, y_i) for which $0 \leq F_i < 1$ (Figure 5.1 b).

The second step requires the fitting (39) of u by $\hat{u}$ of the polynomial form

$$\hat{u} = \sum_{k=0}^{N} C_k F^k \tag{5.10}$$

The fitting error (ε) is described by

$$\varepsilon = \hat{u} - u \tag{5.11}$$

Combining Eqs. (5.8), (5.10) and (5.11) yields

$$y + \varepsilon = \sum_{k=0}^{N} C_k F^k + \frac{a}{(1 - F)^b} \tag{5.12}$$

which is identical to Eq. (5.3) for

$$\hat{y} = y + \varepsilon \quad \text{or} \quad \varepsilon = \hat{y} - y \tag{5.13}$$

The relative error, Δ, is defined by

$$\Delta = (\hat{y} - y)/y \quad , \quad y \neq 0 \tag{5.14}$$

The above fitting procedure is applied to the simulated distribution of C123, C456 and C16. It is found that with polynomials of degree N up to ten, the results are entirely satisfactory. A typical fitting result is given in Table 5.1. Here, F and Y are the simulated CDF data points (F_i, y_i) for the combined catchment C456. YFIT is given by Eq. (5.3). YERR is ε and YREL is Δ. Discard the point ($F = 0$, $y = 0$) which is of no interest. It can be seen that when F approaches zero, the absolute error $|\varepsilon|$ is in the hundredths, and when F approaches one, the maximum absolute value of the relative error Δ is about 3%. The coefficients and constants in Eq. (5.3) for C123 and C16 are given in Appendix B.

TABLE 5.1

SIMULATED DISTRIBUTION OF ANNUAL COMBINED CATCHMENT YIELD,

CATCHMENT C456 (INCLUDING POLYNOMIAL COEFFICIENTS OF EQUATION 5.3)

CATCHMENT NAME
C456

COEFF. OF POLYNOMIAL IN ASCENDING ORDER

```
C( 0)= -0.2164263E+00
C( 1)=  0.3230697E+01
C( 2)= -0.5536269E+02
C( 3)=  0.5170396E+03
C( 4)= -0.2761466E+04
C( 5)=  0.9000055E+04
C( 6)= -0.1851148E+05
C( 7)=  0.2412408E+05
C( 8)= -0.1930970E+05
C( 9)=  0.8658594E+04
C(10)= -0.1664771E+04
```

A = 0.2298366E+00   B = 0.6665868E-01

I	F(I)	Y(I)	YFIT(I)	YERR(I)	YREL(I)
1	0.0	0.0	0.0134	0.0134	
2	0.0010	0.0200	0.0166	-0.0034	-0.1699
3	0.0050	0.0300	0.0283	-0.0017	-0.0560
4	0.0080	0.0400	0.0361	-0.0039	-0.0978
5	0.0115	0.0500	0.0442	-0.0058	-0.1168
6	0.0160	0.0600	0.0531	-0.0069	-0.1146
7	0.0305	0.0700	0.0734	0.0034	0.0489
8	0.0485	0.0800	0.0865	0.0065	0.0816
9	0.0690	0.0900	0.0934	0.0034	0.0372
10	0.0905	0.1000	0.0974	-0.0026	-0.0261
11	0.1300	0.1100	0.1056	-0.0044	-0.0399
12	0.1805	0.1200	0.1200	-0.0000	-0.0003
13	0.2305	0.1300	0.1325	0.0025	0.0191
14	0.2900	0.1400	0.1415	0.0015	0.0105
15	0.3510	0.1500	0.1483	-0.0017	-0.0113
16	0.4150	0.1600	0.1581	-0.0019	-0.0117
17	0.4865	0.1700	0.1713	0.0013	0.0074
18	0.5590	0.1800	0.1817	0.0017	0.0092
19	0.6265	0.1900	0.1891	-0.0009	-0.0046
20	0.6870	0.2000	0.1976	-0.0024	-0.0121
21	0.7455	0.2100	0.2095	-0.0005	-0.0022
22	0.7900	0.2200	0.2197	-0.0003	-0.0015
23	0.8374	0.2300	0.2305	0.0005	0.0020
24	0.8729	0.2400	0.2391	-0.0009	-0.0039
25	0.9034	0.2500	0.2470	-0.0030	-0.0118
26	0.9284	0.2600	0.2595	-0.0005	-0.0020
27	0.9459	0.2700	0.2722	0.0022	0.0081
28	0.9609	0.2800	0.2828	0.0028	0.0101
29	0.9719	0.2900	0.2889	-0.0011	-0.0039
30	0.9799	0.3000	0.2966	-0.0034	-0.0112
31	0.9884	0.3100	0.3073	-0.0027	-0.0087
32	0.9944	0.3200	0.3212	0.0012	0.0037
33	0.9959	0.3300	0.3285	-0.0015	-0.0044
34	0.9969	0.3400	0.3290	-0.0110	-0.0322
35	0.9984	0.3500	0.3490	-0.0010	-0.0028
36	0.9989	0.3700	0.3596	-0.0104	-0.0281
37	0.9994	0.3800	0.3752	-0.0048	-0.0127
38	0.9999	0.4200	0.4192	-0.0008	-0.0019

5.3 Derivation of the Distribution, Mean and Variance of the Potential Canal Flow Given the Canal Capacity

5.3.1 Derivation of the Distribution of Potential Canal Flow Given the Canal Capacity

Having put the simulated distribution of the annual combined catchment yield in functional form (Appendix B), we now proceed to derive the distribution of the potential canal flow given the canal capacity. The potential canal flow is the flow from the combined catchment without taking into consideration any canal interception, seepage and conveyance losses. For simplicity, we will omit the word "potential" when discussing canal flow throughout this section.

The canal flow is limited by the canal capacity. When the catchment yield exceeds this capacity, the flow is constant at the capacity. The canal flow (q) is given by

$$q = \begin{cases} A^*Y_A \quad , & A^*Y_A < q_c \\ q_c \quad , & A^*Y_A \geq q_c \end{cases} \tag{5.15}$$

or

$$x = \begin{cases} y \quad , & y < x_c \\ x_c \quad , & y \geq x_c \end{cases} \tag{5.16}$$

where

$$y = Y_A/\overline{P_s} = AY_A/(\overline{AP_s})^{**} = \text{normalized combined catchment yield}$$

** $\overline{P_s}$ is the space-time mean seasonal precipitation falling on an unit area of the catchment (cm/yr or mm/yr). $\overline{AP_s}$ is the space-time mean seasonal precipitation falling on the entire catchment (m^3/yr, km^3/yr or md/yr) (see Table 4.11).

Y_A = annual combined catchment yield

$x = q/(A\overline{P}_s)$ = normalized canal flow

$x_c = q_c/(A\overline{P}_s)$ = normalized canal capacity

q = canal flow

q_c = canal capacity

A = area of combined catchment

$\overline{P}_s$ = space-time mean seasonal precipitation

Knowing the error of replacing y by $\hat{y}$ (Eqs. 5.3 and 5.12) is small, Eq. (5.16) may be written as

$$x = \begin{cases} \sum_{n=0}^{10} C_n F^n + \dfrac{a}{(1 - F)^b} , & 0 \le F < F_c \\ x_c , & F_c \le F \le 1 \end{cases} \tag{5.17}$$

Figures 5.2, 5.3 and 5.4 show, respectively, the relationship of x and y (Eq. 5.16), the CDF of y and the CDF of x.

In Figure 5.2, the shaded area represents the probability that x is equal to x_c, as

$$\begin{aligned} \text{Prob}[x = x_c] &= \text{Prob}[y \ge x_c] \\ &= \int_{x_c}^{\infty} f(y)\, dy = \int_{F_c}^{1} dF = (1 - F_c) \end{aligned} \tag{5.18}$$

where

$f(y)$ = probability density function (PDF) of y

In Figure 5.3, the distribution of y is given by Eq. (5.12),

FIGURE 5.2: ANNUAL CANAL FLOW AS A FUNCTION OF ANNUAL COMBINED CATCHMENT YIELD (NORMALIZED

FIGURE 5.3: CUMULATIVE DISTRIBUTION OF ANNUAL COMBINED CATCHMENT YIELD (NORMALIZED)

FIGURE 5.4: CUMULATIVE DISTRIBUTION OF ANNUAL CANAL FLOW (NORMALIZED)

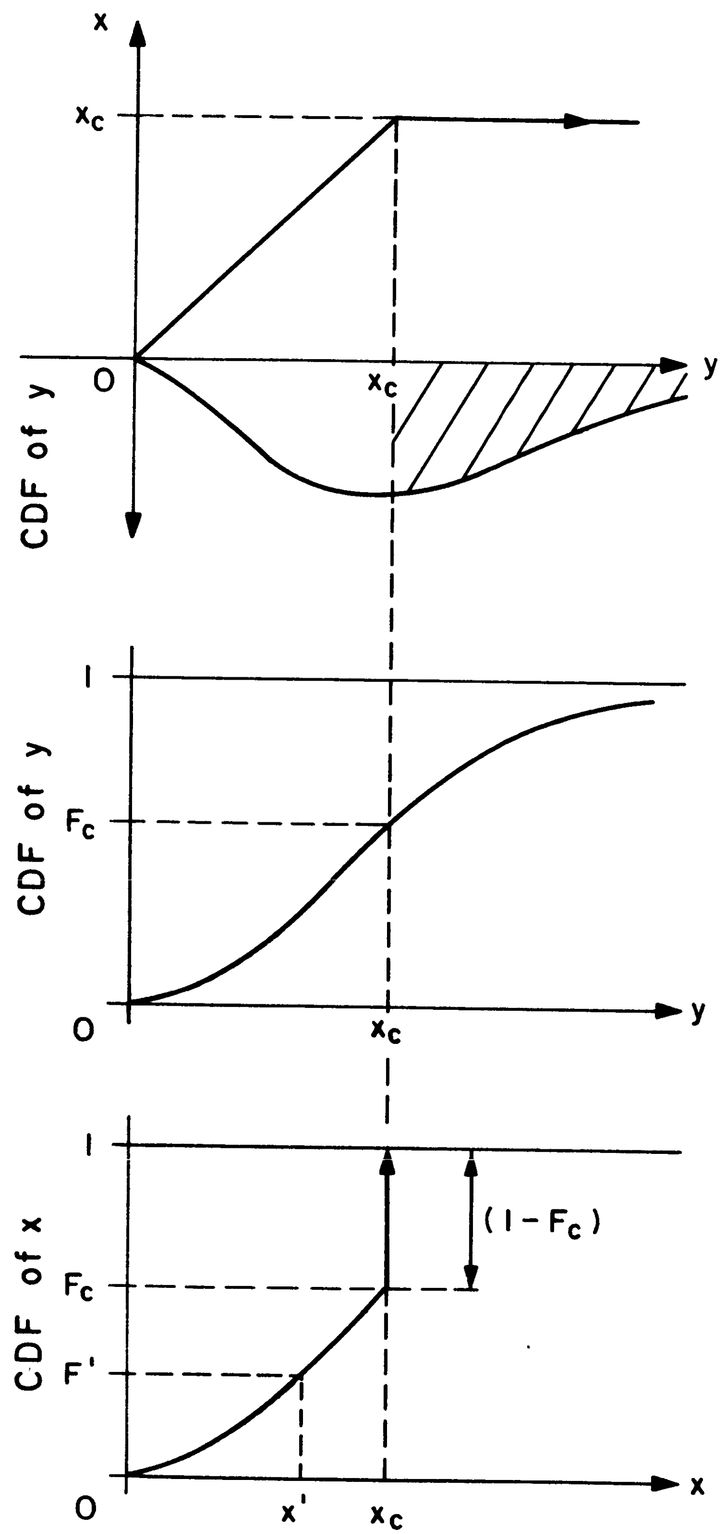

ignoring the minor fitting error (ε), that is,

$$y = G(F) = \sum_{n=0}^{10} C_n F^n + \frac{a}{(1 - F)^b} \qquad (5.19)$$

$$0 \leq F < 1$$

from which

$$x_c = G(F_c) = \sum_{n=0}^{10} C_n F_c^n + \frac{a}{(1 - F_c)^b} \qquad 5.20)$$

where

F_c = CDF of x_c

and

$$F = G^{-1}(y) \qquad (5.21)$$

Given any normalized canal capacity (x_c), Eq. (5.20) may be easily solved numerically to obtain F_c by a binary search algorithm (40).

The distribution of x is shown in Fig. 5.4. The probability impulse is given by Eq. (5.18) and

$$\text{Prob}[x < x' | 0 \leq x' < x_c] = \int_o^{x'} f(x)\, dx = \int_o^{F'} dF = F' = G^{-1}(x') \qquad (5.22)$$

where

$f(x)$ = PDF of x

and

$$\text{Prob}[x \leq x_c] = 1 \qquad (5.23)$$

5.3.2 Derivation of the Mean and Variance of the Potential Canal Flow Given the Canal Capacity

The normalized canal flow (x) with capacity constraint (x_c) is given by Eq. (5.17).

The mean of x given x_c is derived from Eq. (5.17) as follows,

$$\mu(x|x_c) = E(x|x_c)^* = \int_o^\infty x\, f(x)\, dx$$

$$= \int_o^{x_c} x\, f(x)\, dx + \int_{x_c}^\infty x_c\, f(x)\, dx$$

$$= \int_o^{F_c} [\sum_{n=0}^{10} C_n F^n + \frac{a}{(1-F)^b}]\, dF + x_c \int_{F_c}^1 dF$$

$$= \sum_{n=0}^{10} \frac{C_n F_c^{n+1}}{(n+1)} + \frac{a}{(1-b)} [1 - (1 - F_c)^{1-b}] + x_c(1 - F_c)$$

$$\text{for } a > 0,\ 0 < b < 1 \qquad (5.24)$$

The variance of x given x_c is

$$\sigma^2(x|x_c) = E(x^2|x_c) - \mu^2(x|x_c)$$

$$= \int_o^{x_c} x^2\, f(x)\, dx + \int_{x_c}^\infty x_c^2\, f(x)\, dx - \mu^2(x|x_c)$$

$$= \int_o^{F_c} (\sum_{n=0}^{10} C_n F^n)^2\, dF + 2a \sum_{n=0}^{10} C_n \int_o^{F_c} F^n(1-F)^{-b}\, dF$$

$$+ a^2 \int_o^{F_c} (1-F)^{-2b}\, dF + x_c^2(1 - F_c) - \mu^2(x|x_c)$$

---

*E( ) ≡ the expected value of ( )

$$= I_1 + 2a \sum_{n=0}^{10} C_n * I_2 + I_3 + x_c^2 (1 - F_c) - \mu^2 (x|x_c) \tag{5.25}$$

where

$$I_1 = \int_o^{F_c} \left(\sum_{n=0}^{10} C_n F^n \right)^2 dF$$

$$= \int_o^{F_c} \sum_{n=0}^{20} e_n F^n \, dF = \sum_{n=0}^{20} \frac{e_n F_c^{n+1}}{(n + 1)} \tag{5.26}$$

with

$$e_o = C_o^2, \quad e_n = \sum_{k=0}^{n} C_k * C_{n-k}, \quad n = 1, \ldots, 20$$

$$I_2 = \int_o^{F_c} F^n (1 - F)^{-b} \, dF$$

$$= B(n + 1, 1 - b) * I_{F_c}(n + 1, 1 - b), \quad 0 < b < 1 \tag{5.27}$$

where

$$B(z, w) = \text{Beta function} = \int_o^1 t^{z-1} (1 - t)^{w-1} \, dt$$

with

$$z, w > 0 \tag{5.28}$$

and

$$I_\alpha(z, w) = \text{incomplete Beta function}$$

$$= \frac{1}{B(z, w)} \int_o^\alpha t^{z-1} (1 - t)^{w-1} \, dt \tag{5.29}$$

with

$$0 \leq \alpha \leq 1$$

The Beta function can be represented by the Gamma function, $\Gamma(\cdot)$, as

$$B(z, w) = \frac{\Gamma(z)\ \Gamma(w)}{\Gamma(z + w)} = B(w, z) \tag{5.30}$$

so that I_2 can be written as (from Eq. (5.27), (5.30))

$$I_2 = \Gamma(1 - b) \left\{\frac{\Gamma(n + 1)}{\Gamma(n + 2 - b)} * I_{F_c}(n + 1, 1 - b)\right\} \tag{5.31}$$

$$0 < b < 1$$

Finally,

$$I_3 = a^2 \int_o^{F_c} (1 - F)^{-2b}\ dF$$

$$= \frac{a^2}{(1 - 2b)} [1 - (1 - F_c)^{1-2b}] \tag{5.32}$$

For $\qquad 0 < b < 1/2, \quad a > 0$

Combining Eq. (5.25) through (5.32), we arrive at

$$\sigma^2(x|x_c) = \left\{\sum_{n=0}^{20} \frac{e_n\ F_c^{n+1}}{(n + 1)} + 2a*\Gamma(1 - b) \sum_{n=0}^{10} C_n * \frac{\Gamma(n+1)}{\Gamma(n+2-b)} * I_{F_c}(n+1, 1-b) + \frac{a^2}{(1 - 2b)} [1 - (1 - F_c)^{1-2b}] + x_c^2(1 - F_c) - \mu^2(x|x_c)\right\} \tag{5.33}$$

with

$$a > 0\ , \quad 0 < b < 1/2$$

$$e_o = C_o^2\ , \quad e_n = \sum_{k=0}^{n} C_k\ C_{n-k}, \qquad n = 1, 2, \ldots, 20$$

The limits for b in Eq. (5.24) and (5.33) imply that b is in the range $0 < b < 1/2$.*

Since the combined catchment flow is the flow in a canal of infinite capacity, the validity of Eqs. (5.24) and (5.33) may be checked by comparing them with the mean and variance of the normalized annual combined catchment yield (Table 4.11) for the case $x_c \to \infty$, $F_c \to 1$.

For unlimited canal capacity, Eq. (5.20) gives

$$x_c = \lim_{F_c \to 1} \left\{ \sum_{n=1}^{10} C_n F_c^n + \frac{a}{(1 - F_c)^b} \right\} \to \infty \quad , \qquad a > 0,\ 0 < b < 1/2 \tag{5.34}$$

To evaluate $\mu(x|x_c \to \infty)$ and $\sigma^2(x|x \to \infty)$, the two terms, $x_c(1 - F_c)$ and $x_c^2(1 - F_c)$, have first to be evaluated for the limiting case ($x_c \to \infty$, $F_c \to 1$). Multiplying Eq. (5.20) by $(1 - F_c)$ on both sides and taking the limits,

$$\lim_{\substack{x_c \to \infty \\ F_c \to 1}} x_c(1 - F_c) = \lim_{F_c \to 1} \left\{ \sum_{n=0}^{10} C_n F_c^n (1 - F_c) + a(1 - F_c)^{1-b} \right\} = 0 \tag{5.35}$$

$$\text{for } 0 < b < 1/2$$

and

$$\lim_{\substack{x_c \to \infty \\ F_c \to 1}} x_c^2(1 - F_c) = \lim_{F_c \to 1} \left\{ \sum_{n=0}^{20} e_n F_c^n (1 - F_c) + 2a(1 - F_c)^{1-b} * \sum_{n=0}^{10} C_n F_c^n + a^2(1 - F_c)^{1-2b} \right\} = 0 \tag{5.36}$$

$$\text{for } 0 < b < 1/2$$

Hence, from Eqs. (5.24) and (5.35), for unlimited canal

*This range of b takes precedence over that found in Eq. (5.24).

capacity ($x_c \to \infty$, $F_c \to 1$),

$$\mu(x|x_c \to \infty) = \sum_{n=0}^{10} \frac{C_n}{(n + 1)} + \frac{a}{(1 - b)} \tag{5.37}$$

and from Eqs. (5.33) and (5.36),

$$\sigma^2(x|x_c \to \infty) = \left\{ \sum_{n=0}^{20} \frac{e_n}{(n + 1)} + 2a*\Gamma(1 - b) \sum_{n=0}^{10} C_n* \frac{\Gamma(n + 1)}{\Gamma(n + 2 - b)} \right.$$

$$\left. + \frac{a^2}{(1 - 2b)} - \mu^2(x|x_c \to \infty) \right\} \tag{5.38}$$

$$\text{for} \qquad a > 0, \quad 0 < b < 1/2$$

Equations (5.37) and (5.38) are compared with the mean and variance of the normalized combined catchment yield for C123, C456 and C16 (Table 4.11). The results are tabulated in Table 5.2. The agreement is remarkable. The absolute value of the relative error is less than 1% in μ, and it is no greater than 2% in σ. These justify our ignoring the fitting error ε in Eq. (5.12) to arrive at Eq. (5.17). It also gives us the confidence in applying Eqs. (5.24) and (5.33) to different canal capacity designs.

Tables 5.3 and 5.4 give the mean and standard deviation of the normalized canal flow given different canal capacities for the north-going and south-going canals, respectively. They are plotted on Fig. 5.5 for the north-going canal. From Table 5.3 and Figure 5.5, it can be seen that both $\mu(x|x_c)$ and $\sigma(x|x_c)$ are monotonically increasing functions of x_c. The figure implies that when the canal capacity is small, the mean canal flow is almost identical with the canal capacity, with

Table 5.2: Comparison of Empirical Results and

Derived Results of $\mu(x|x_c \to \infty)$ and $\sigma(x|x_c \to \infty)$

Catchment	Empirical μ (Table 4.11)	Derived μ (Equ. 5.37)	Relative Error %*	Empirical σ (Table 4.11)	Derived σ (Equ. 5.38)	Relative Error %**
C123	0.1114	0.1106	-0.7	0.0555	0.0544	-2.0
C456	0.1735	0.1737	0.1	0.0575	0.0579	0.7
C16	0.1566	0.1563	0.2	0.0480	0.0482	0.4

* Relative error = (Derived μ - Empirical μ)/Empirical μ

** Relative error = (Derived σ - Empirical σ)/Empirical σ

Absolute Relative error = |Relative error|

Table 5.3: $\mu(x|x_c)$ and $\sigma(x|x_c)$ for the North-going Canal

x_c	F_c	$\mu(x\|x_c)$ Equ. 5.24*	$\mu(q\|q_c)^{**}$ md/yr	$\sigma(x\|x_c)$ Equ. 5.33*	$\sigma(q\|q_c)^{**}$ md/yr
0.02	0.0021	0.0200	3.0884	0.0002	0.0309
0.04	0.0096	0.0399	6.1614	0.0014	0.2162
0.06	0.0200	0.0596	9.2034	0.0034	0.5250
0.08	0.0378	0.0790	12.1992	0.0061	0.9420
0.10	0.1045	0.0978	15.1023	0.0096	1.4824
0.13	0.2188	0.1229	18.9782	0.0176	2.7178
0.15	0.3643	0.1372	21.1864	0.0242	3.7370
0.1737	0.5010	0.1506	23.2557	0.0323	4.9878
0.19	0.6328	0.1578	24.3675	0.0381	5.8834
0.21	0.7432	0.1639	25.3094	0.0445	6.8717
0.23	0.8301	0.1682	25.9734	0.0490	7.5666
0.27	0.9443	0.1722	26.5911	0.0544	8.4004
0.31	0.9876	0.1734	26.7764	0.0571	8.8174
0.37	0.9992	0.1737	26.8228	0.0573	8.8483
0.42	0.9999	0.1737	26.8228	0.0575	8.8792
∞	1.0000	0.1737	26.8228	0.0579	8.9409

* Coefficients and constants for the Equ. come from Table 5.1

** $q_c = x_c * A\,\overline{\underline{P_s}}$, $A\,\overline{\underline{P_s}} = 154.42$ md/yr

$q = x * A\,\overline{\underline{P_s}}$ (Table 4.11 , for C456)

$\mu(q|q_c) = \mu(x|x_c) * A\,\overline{\underline{P_s}}$

$\sigma(q|q_c) = \sigma(x|x_c) * A\,\overline{\underline{P_s}}$

Table 5.4: $\mu(x|x_c)$ and $\sigma(x|x_c)$ for the South-going Canal

x_c	F_c	$\mu(x\|x_c)$ Equ. 5.24*	$\mu(q\|q_c)$** md/yr	$\sigma(x\|x_c)$ Equ. 5.33*	$\sigma(q\|q_c)$** md/yr
0.01	0.0072	0.0100	0.5774	0.0004	0.0231
0.02	0.0193	0.0198	1.1433	0.0013	0.0751
0.04	0.0996	0.0389	2.2461	0.0046	0.2656
0.06	0.1934	0.0559	3.2277	0.0102	0.5889
0.08	0.3301	0.0708	4.0880	0.0171	0.9874
0.09	0.3984	0.0772	4.4575	0.0208	1.2010
0.10	0.4580	0.0829	4.7866	0.0245	1.4146
0.1106	0.5264	0.0883	5.0984	0.0280	1.6167
0.13	0.6543	0.0961	5.5488	0.0351	2.0267
0.15	0.7441	0.1021	5.8953	0.0411	2.3731
0.18	0.8965	0.1075	6.1031	0.0483	2.7888
0.21	0.9561	0.1096	6.3283	0.0522	3.0140
0.23	0.9780	0.1102	6.3629	0.0534	3.0833
0.25	0.9921	0.1105	6.3803	0.0537	3.1006
0.32	0.9999	0.1106	6.3860	0.0546	3.1526
∞	1.0000	0.1106	6.3860	0.0544	3.1411

* coefficients and constants for the Equation come from Appendix B for catchment C123

** $q_c = x_c * A\,\underline{\overline{P_s}}$

$q = x * A\,\underline{\overline{P_s}}$

$\mu(q|q_c) = \mu(x|x_c) * A\,\underline{\overline{P_s}}$

$\sigma(q|q_c) = \sigma(x|x_c) * A\,\underline{\overline{P_s}}$

$A\,\underline{\overline{P_c}} = 57.74$ md/yr
(Table 4.11 for C123)

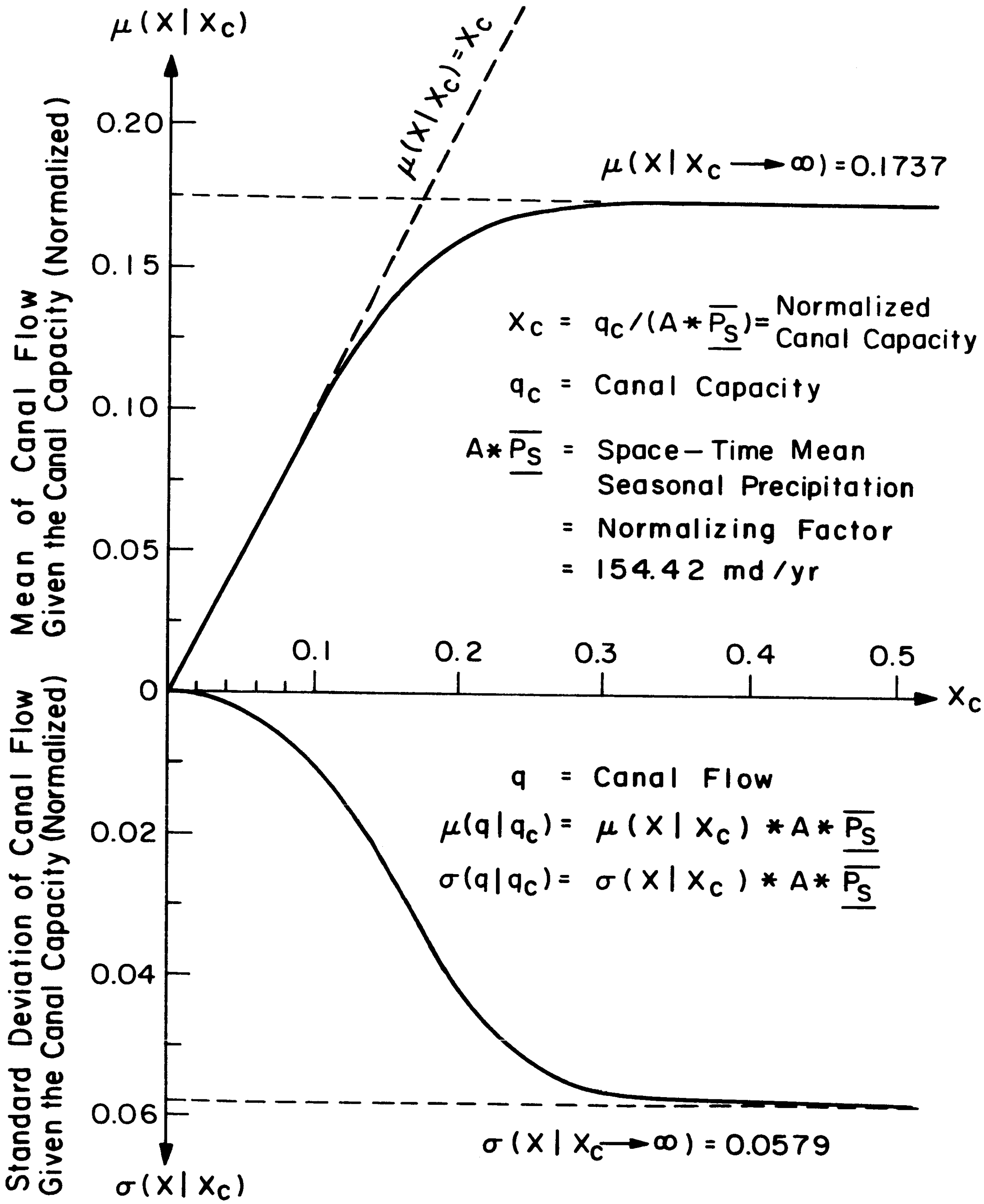

FIGURE 5.5

MEAN AND STANDARD DEVIATION OF ANNUAL CANAL FLOW GIVEN THE CANAL CAPACITY (NORTH-GOING CANAL) a very minor standard deviation. When the canal capacity is high, the mean and standard deviation of the canal flow are limited by the mean and standard deviation of the annual yield from the combined catchment.

In design, for example, if we choose $x_c = 0.08$ (Table 5.3), that is, a canal capacity of (0.08)(154.42) = 12.35 md/yr, we would expect to recover a mean canal flow of 12.20 md/yr, with a standard deviation of only 0.94 md/yr. The probability of having the capacity flow (12.35 md/yr) is given by Eq. (5.18) and Table 5.3 to be 1 - 0.0378 = 0.9622. The recurrence interval of this flow is given by $1/F_c = 26.46$ years. This means that on the average the annual canal flow will be lower than the canal capacity only once in twenty-six years.

5.3.3 Estimation of the Distribution, Mean and Variance of the Total Potential Water Recovery at Malakal due to Canal Inflows

The total potential water recovery (q_T) at Malakal is the sum of the canal flows from the north-going (q_N) and the south-going canal (q_S). Denoting their respective canal capacities as q_{CN} and q_{CS},

$$q_T = q_S + q_N \tag{5.39}$$

with

$$q_S = \begin{cases} A_S \, Y_A^{(S)} & , \quad A_S * Y_A^{(S)} < q_{CS} \\ q_{CS} & , \quad A_S * Y_A^{(S)} \geq q_{CS} \end{cases} \tag{5.40}$$

and

$$q_N = \begin{cases} A_N \, Y_A^{(N)} & , \quad A_N * Y_A^{(N)} < q_{CN} \\ q_{CN} & , \quad A_N * Y_A^{(N)} \geq q_{CN} \end{cases} \tag{5.41}$$

where

A_S = area of catchment C123

A_N = area of catchment C456

$Y_A^{(S)}$ = annual yield per unit area of catchment C123

$Y_A^{(N)}$ = annual yield per unit area of catchment C456

Normalizing Eq. (5.39),

$$\frac{q_T}{(A_s \, \underline{\overline{P}_s^{(S)}} + A_N \, \underline{\overline{P}_s^{(N)}})} = \frac{A_s \, \underline{\overline{P}_s^{(S)}}}{(A_s \, \underline{\overline{P}_s^{(S)}} + A_N \, \underline{\overline{P}_s^{(N)}})} \cdot \left[\frac{q_S}{A_s \, \underline{\overline{P}_s^{(S)}}}\right] + \frac{A_N \, \underline{\overline{P}_s^{(N)}}}{(A_s \, \underline{\overline{P}_s^{(S)}} + A_N \, \underline{\overline{P}_s^{(N)}})} \cdot \left[\frac{q_N}{A_N \, \underline{\overline{P}_s^{(N)}}}\right] \tag{5.42}$$

or

$$x_T = \alpha_S \, x_S + \alpha_N \, x_N \tag{5.43}$$

where

$A_s \, \underline{\overline{P}_s^{(S)}}$ = space-time mean seasonal precipitation on C123

= 57.74 md/yr (Table 4.11)

$A_N \, \underline{\overline{P}_s^{(N)}}$ = space-time mean seasonal precipitation on C456

= 154.42 md/yr (Table 4.11)

$$x_T = q_T/(A_s \, \underline{\overline{P}_s^{(S)}} + A_N \, \underline{\overline{P}_s^{(N)}}) = q_T/\alpha_T \tag{5.44}$$

= normalized total potential water recovery at Malakal

$$x_S = q_s/(A_s\,\overline{P}_{\underline{s}}^{(S)}) \tag{5.45}$$

= normalized canal flow from the south-going canal

$$x_N = q_N/(A_N\,\overline{P}_{\underline{s}}^{(N)}) \tag{5.46}$$

= normalized canal flow from the north-going canal

$$\alpha_T = (A_s\,\overline{P}_{\underline{s}}^{(S)} + A_N\,\overline{P}_{\underline{s}}^{(N)}) = 212.16 \text{ md/yr} \tag{5.47}$$

$$\alpha_S = A_s\,\overline{P}_{\underline{s}}^{(S)}/(A_s\,\overline{P}_{\underline{s}}^{(S)} + A_N\,\overline{P}_{\underline{s}}^{(N)}) = 0.2722 \tag{5.48}$$

$$\alpha_N = A_N\,\overline{P}_{\underline{s}}^{(N)}/(A_s\,\overline{P}_{\underline{s}}^{(S)} + A_N\,\overline{P}_{\underline{s}}^{(N)}) = 0.7278 \tag{5.49}$$

Normalizing Eq. (5.39) keeps the numerical values of x_T, x_S and x_N between 0 and 1, which is more manageable.

From Eqs. (5.40) and (5.45), we obtain

$$x_s = \begin{cases} A_s\,Y_A^{(S)}/(A_s\,\overline{P}_{\underline{s}}^{(S)}) = Y_A^{(S)}/\overline{P}_{\underline{s}}^{(S)} & , \quad Y_A^{(S)}/\overline{P}_{\underline{s}}^{(S)} < x_{CS} \\ q_{CS}/(A_s\,\overline{P}_{\underline{s}}^{(S)}) = x_{CS} & , \quad Y_A^{(S)}/\overline{P}_{\underline{s}}^{(S)} \geq x_{CS} \end{cases} \tag{5.50}$$

and from Eqs. (5.41) and (5.46),

$$x_N = \begin{cases} A_N\,Y_A^{(N)}/(A_N\,\overline{P}_{\underline{s}}^{(N)}) = Y_A^{(N)}/\overline{P}_{\underline{s}}^{(N)} & , \quad Y_A^{(N)}/\overline{P}_{\underline{s}}^{(N)} < x_{CN} \\ q_{CN}/(A_N\,\overline{P}_{\underline{s}}^{(N)}) = x_{CN} & , \quad Y_A^{(N)}/\overline{P}_{\underline{s}}^{(N)} \geq x_{CN} \end{cases} \tag{5.51}$$

Given the above form of x_T (Eqs. (5.43), (5.50), and (5.51)), it will be extremely difficult to derive in closed analytical forms the distribution, mean and variance of x_T given the normalized capacities x_{CS} and x_{CN}, especially when x_S and x_N are correlated. Before offering a procedure to solve this problem in general, we will first consider some special cases where approximate analytical solutions do exist.

When the canal capacity is very small (say, two standard deviations below the mean annual yield of its corresponding combined catchment), the canal flow will be very close to the canal capacity (see Table 5.3 and Figure 5.5), and will be relatively independent of the flows from other canal(s). Therefore, if either x_{CS} or x_{CN} is very small, or both are, we may treat x_S and x_N as independent (uncorrelated). Under such conditions, the mean of x_T may be obtained by taking the expected value of Eq. (5.43) as

$$E(x_T|x_{CS}, x_{CN}) = \alpha_S \, E(x_S|x_{CS}) + \alpha_N \, E(x_N|x_{CN})$$

or

$$\mu(x_T|x_{CS}, x_{CN}) = \alpha_S \, \mu(x_S|x_{CS}) + \alpha_N \, \mu(x_N|x_{CN}) \qquad (5.52)$$

where $\mu(x_S|x_{CS})$ and $\mu(x_N|x_{CN})$ are given by Eq. (5.24), using the constants and coefficients of C123 for the south-going canal (Appendix B), and those of C456 for the north-going canal (Table 5.1).

The variance of x_T is then,

$$\sigma^2(x_T|x_{CS}, x_{CN}) = \alpha_S^2 \, \sigma^2(x_S|x_{CS}) + \alpha_N^2 \, \sigma^2(x_N|x_{CN}) \qquad (5.53)$$

where $\sigma^2(x_S|x_{CS})$ and $\sigma^2(x_N|x_{CN})$ are given by Eq. (5.33).

The empirical distribution of x_T may be generated from Eq. (5.17) by the following steps:

Step 1: Generate 2 uniformly distributed random numbers (F_S, F_N) between 0 and 1.

Step 2: If $F_S = 1$, set $F_S = 0.99999$.

If $F_N = 1$, set $F_N = 0.99999$.

Step 3: Obtain x_S and x_N from Eq. (5.17), given F_S and F_N.

Step 4: Evaluate $x_T = \alpha_S\, x_S + \alpha_N\, x_N$ (Eq. 5.43).

Step 5: Repeat Steps 1 through 4 for M times.

Step 6: Compute $$\bar{x}_T = \frac{1}{M} \sum_{j=1}^{M} x_T(j) \tag{5.54}$$

$$\mathrm{Var}(x_T) = \frac{1}{M} \sum_{j=1}^{M} [x_T(j)]^2 - \bar{x}_T^2 \tag{5.55}$$

$$\delta_\mu(M) = [\bar{x}_T - \mu(x_T | x_{CS}, x_{CN})]/\mu(x_T | x_{CS}, x_{CN}) \tag{5.56}$$

$$\delta_\sigma(M) = [(\mathrm{Var}(x_T))^{1/2} - \sigma(x_T | x_{CS}, x_{CN})]/\sigma(x_T | x_{CS}, x_{CN}) \tag{5.57}$$

Step 7: If $|\delta_\mu(M)|$ and $|\delta_\sigma(M)|$ are less than some prescribed error bounds, stop and form the empirical CDF of x_T from the series $\{x_T(k)\}_{k=1}^{M}$.

Step 8: If the conditions in Step 7 are not met, increase M and repeat Steps 1 through 7.

It will be helpful to plot $|\delta_\mu(M)|$ and $|\delta_\sigma(M)|$ versus M to see that the former two indeed fall below the prescribed error bounds gradually as $M \to \infty$, instead of accidentally falling below them for some unexpected small M (say M = 100). Since Eq. (5.17) is a simple equation, it will not require much computer time even if we increase M to 50,000.

In general, for <u>any given capacities</u>, x_{CS} and x_{CN}, and <u>correlated flows</u>, x_S and x_N, the empirical distribution, mean and variance of x_T can be determined by the Monte Carlo simulation technique as described in Sections 4.4.2 and 4.4.3 (see Chapter 4). From the simulation, we obtain the annual catchment yield Y_A, as shown in Fig. 5.6. From Eqs. (4.38) and (4.40), we may write Eq. (5.50) as

$$x_S(j) = \begin{cases} Y_A^{(k)}(j)/\underline{\overline{P}_s^{(k)}} & , \quad Y_A^{(k)}(j)/\underline{\overline{P}_s^{(k)}} < x_{CS} \\ x_{CS} & , \quad Y_A^{(k)}(j)/\underline{\overline{P}_s^{(k)}} \geq x_{CS} \end{cases} \tag{5.58}$$

for

$k = (1, 2, 3)$ representing catchment C123

$j = 1, 2, 3, \ldots, 2000$

Similarly, for Eq. (5.51),

$$x_N(j) = \begin{cases} Y_A^{(k)}(j)/\underline{\overline{P}_s^{(k)}} & , \quad Y_A^{(k)}(j)/\underline{\overline{P}_s^{(k)}} < x_{CN} \\ x_{CN} & , \quad Y_A^{(k)}(j)/\underline{\overline{P}_s^{(k)}} \geq x_{CN} \end{cases} \tag{5.59}$$

for

$k = (4, 5, 6)$ representing catchment C456

$j = 1, 2, 3, \ldots, 2000$

And

$$x_T(j) = \alpha_s * x_s(j) + \alpha_N * x_N(j) \tag{5.60}$$

$$j = 1, 2, 3, \ldots, 2000$$

The empirical distribution of x_T can be formed from the series $\{x_T(j)\}_{j=1}^{2000}$. The mean and variance of x_T can be computed from Eqs. (5.54) and (5.55) with M = 2000 years. The empirical distribution,

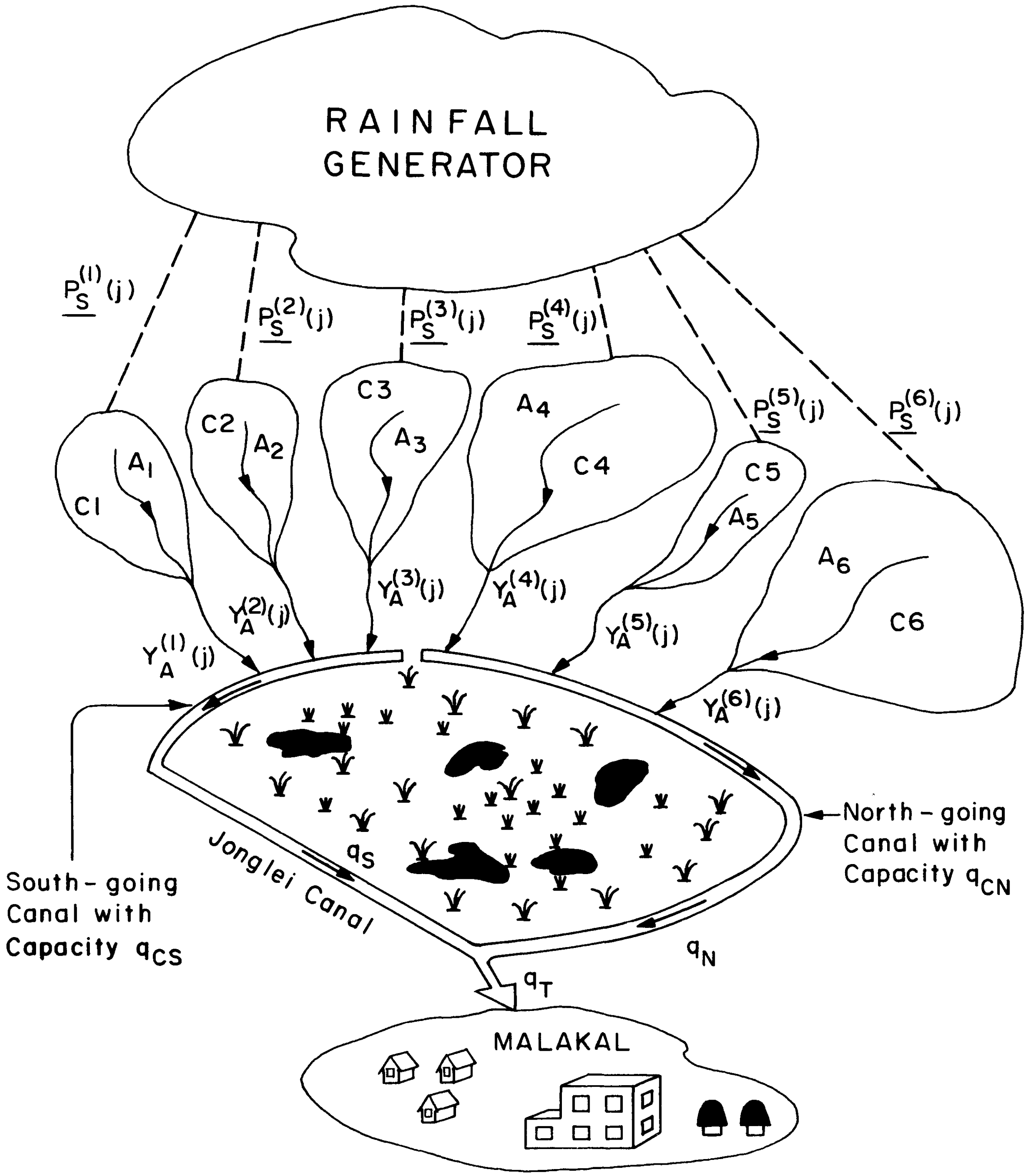

FIGURE 5.6

SIMULATION OF TOTAL CANAL INFLOWS AT MALAKAL mean and variance of the total potential water recovery (q_T) at Malakal can easily be retrieved from those of x_T using Eqs. (5.44) and (5.47).

5.4 Canal Cost-Capacity under Uncertain Canal Flows

5.4.1 Introduction

The purpose of this section is to demonstrate how the cost of canal work for different canal alternatives may be compared by using the distribution, mean and variance of normalized canal flows derived in Section 5.3. We do not intend to provide the actual cost estimates.

5.4.2 Determination of the Cost Function of Canal Work

For a trapezoidal, open-channel aqueduct, the construction costs include the fixed cost, the excavation cost and the lining cost. The fixed cost may include rights of way, surveying, canal head and tail flow regulators and navigation locks. In general, these costs will vary with the top width (w) of the canal very roughly as (41),

$$\text{Fixed cost per kilometer, } FC = k_o + k_1 w \tag{5.61}$$

$$\text{Excavation cost per kilometer, } EC = k_2 w^2 \tag{5.62}$$

$$\text{Lining cost per kilometer, } LC = k_3 w^{1.5} \tag{5.63}$$

Hence, the total construction costs (C_T) per unit length of canal is roughly a polynomial in w, as

$$C_T = k_o + k_1 w + k_2 w^2 + k_3 w^{1.5} \tag{5.64}$$

For a trapezoidal canal with constant channel bed slope and without a freeboard, the canal capacity (q_c) is roughly proportional to the canal top width (w) by (41)*

$$q_c = k_4 \, w^{2.7} \qquad (5.65)$$

Also, the depth of channel (H) is assumed proportional to the top width (w), by*

$$H = k_5 \, w \qquad (5.66)$$

To determine the total construction cost, the cost coefficients k_o, k_1, k_2 and k_3 in Eq. (5.64) need to be evaluated first. Table 5.5 (42) gives the actual construction costs for the Jonglei Canal, which may be used to estimate these cost coefficients.

From the Jonglei Canal project literature (4), the following data are obtained,

$$q_c = 27.5 \text{ Mm}^3/\text{day} = 27.5 \times 10^6 \text{ meter}^3/\text{day}$$

for

w = 76 meters

H = 4 meters

From Eq. (5.65), $k_4 = q_c/w^{2.7}$

---

*Equations (5.65) and (5.66) should <u>never</u> be used in <u>actual</u> capacity design, as the error involved may be quite large.

$$\therefore \quad k_4 = \frac{27.5 \times 10^6 \ m^3/day}{(76)^{2.7} \ m^{2.7}} = 229.69 \ m^{0.3}/day$$

From Eq. (5.66), $k_5 = H/w$

$$\therefore \quad k_5 = 4/76 = 0.0526$$

The canal capacity in Table 5.5 is 20 Mm^3/day. From Eq. (5.65), the top width of the canal is

$$w = (q_c/k_4)^{1/2.7}$$

$$= \left(\frac{20 \times 10^6 \ m^3}{229.69 \ m^{0.3}}\right)^{1/2.7} = 67.5 \text{ meters}$$

The Jonglei Canal is about 280 km long. The excavation cost is 16.7 million Sudanese pounds (Table 5.5, Item 1) or U.S. \$33.4 million, so the excavation cost per kilometer of the 20 Mm^3/day capacity canal is, by Eq. (5.62),

$$EC = \frac{\$33.4 \times 10^6}{280 \text{ km}} = k_2 \ (67.5 \text{ meters})^2$$

or

$$k_2 = \$26.18/m^2/km$$

The lining cost is not mentioned in Table 5.5, so we assume $k_3 = 0$ in Eqs. (5.63) and (5.64).

Two data points are required to determine the cost coefficients k_o and k_1 in Eq. (5.61). Items 3 and 4 in Table 5.5 suggest these two points.

Table 5.5 (42)

CONSTRUCTION COSTS FOR PHASE I OF THE JONGLEI CANAL PROJECT

	WORKS*	Cost (Sudanese Pounds)**
1.	Earth work in the excavation of the 20 Mm^3/day Jonglei Canal (1 Mm^3/day = 10^6 m^3/day)	16,700,000
2.	Construction of Jonglei Canal head regulator capacity 20 Mm^3/day, with navigation lock taking into account the presence of weeds and other elements	9,500,000
3.	Construction of the Canal tail regulator, capacity 20 Mm^3/day with navigation lock	9,500,000
4.	Construction of lower Atem regulator, capacity 60 Mm^3/day	12,000,000
5.	Training and banking of River Atem from its head to the Lower Atem regulator at Jonglei latitude to pass the maximum natural flows	6,000,000
6.	Local development projects, including an irrigation canal with a capacity of 5 Mm^3/day, appurtenant irrigation and drainage scheme network and the reclamations, construction and community development projects	18,000,000
	TOTAL	71,700,000
	Gross drainage works, reserve funds and contingencies	9,300,000
	GRAND TOTAL	81,000,000

* Period of construction: 1976-1982

** 1 Sudanese Pound ≡ 2.0000 U.S. Dollar

1 Egyptian Pound ≡ 1.4286 U.S. Dollar
as the market exchange rate in August, 1980 (43).

In Item 3, the fixed cost for the construction of the Canal tail regulator, capacity 20 Mm^3/day (w = 67.5 meters) with navigation lock is 9.5 million Sudanese pounds (U.S. $19 million). In Item 4, the fixed cost for the construction of lower Atem regulator of capacity 60 Mm^3/day amounts to 12 million Sudanese pounds (U.S. $24 million). For such a capacity, w is 101.5 meters (from Eq. (5.65)). Thus, from Eq. (5.61),

$$\$19 \times 10^6 = k_o + k_1 \text{ (67.5 meters)}$$
$$\$12 \times 10^6 = k_o + k_1 \text{ (101.5 meters)}$$

Solving these gives

$$k_o = \$5.102941 \times 10^6$$
$$k_1 = \$0.205882 \times 10^6\text{/meter}$$

In this application, the form of Eq. (5.61) is adopted for the fixed cost (instead of the fixed cost per kilometer). This is the cost connected primarily with the construction of a flow regulator. Since there are normally two flow regulators, one at the head and the other at the tail of the canal, the cost coefficients, k_o and k_1, are both multiplied by two.

Summarizing, the total construction cost (C_L) for an unlined canal, L kilometers long with a capacity of q_c cubic meters per day, is

$$C_L = 2k_o + 2k_1 w + k_2 Lw^2 \qquad (5.67)$$

where

$$w = (q_c/k_4)^{1/2.7} \text{ , from Eq. (5.65)}$$

and

$$k_o = \$5.102941 \times 10^6$$

$$k_1 = \$0.205882 \times 10^6/\text{meter}$$

$$k_2 = \$26.18/\text{meter}^2/\text{kilometer}$$

$$k_4 = 229.69 \text{ meter}^{0.3}/\text{day}$$

$$k_5 = 0.0526$$

5.4.3 Cost-Capacity Comparison of Canal Alternatives under Uncertain Canal Flows

The total construction costs are evaluated for various canal capacities, and are tabulated in Tables 5.6 and 5.7 for the north-going (840 km) and south-going (300 km) canal, respectively. Table 5.6 can be combined with Table 5.3, and Table 5.7 combined with Table 5.4, to prepare Figure 5.7 for cost-capacity design comparison of the two canals. In Fig. 5.7, $P(q = q_c)$ is the probability of $q = q_c$, which is obtained from Eq. (5.18) as $(1 - F_c)$.

To interpret Figure 5.7, we start with a design canal capacity, q_c, traveling up the graph, we determine the total construction costs, C_L, for such a capacity at a point on the $C_L - q_c$ curve. Going right from this point, we find the mean annual canal flow given the canal capacity $\mu(q|q_c)$ from a point on the $C_L - \mu(q|q_c)$ curve. Traveling downward from this point, we reach a point on the $\sigma(q|q_c) - \mu(q|q_c)$ curve which tells the standard deviation of the canal flow given the canal design capacity.

TABLE 5.6

COST-CAPACITY DESIGN (NORTH-GOING CANAL)

NORTH-GOING CANAL (L = 840 km)

x	q_c md/yr	q_c Mm^3/day	w meters	H meters	C_L U.S.$x10^6	C_L/L U.S.$x10^6/km
0.0200	3.0884	8.46	49.12	2.59	83.48	0.0994
0.0300	4.6326	12.69	57.07	3.00	105.34	0.1254
0.0400	6.1768	16.92	63.49	3.34	125.00	0.1488
0.0500	7.7210	21.15	68.96	3.63	143.18	0.1705
0.0600	9.2652	25.38	73.78	3.88	160.29	0.1908
0.0700	10.8094	29.61	78.11	4.11	176.56	0.2102
0.0800	12.3536	33.85	82.07	4.32	192.14	0.2287
0.0900	13.8978	38.08	85.73	4.51	207.15	0.2466
0.1000	15.4420	42.31	89.15	4.69	221.67	0.2639
0.1100	16.9862	46.54	92.35	4.86	235.78	0.2807
0.1200	18.5304	50.77	95.37	5.02	249.51	0.2970
0.1300	20.0746	55.00	98.24	5.17	262.91	0.3130
0.1400	21.6188	59.23	100.98	5.31	276.01	0.3286
0.1500	23.1630	63.46	103.59	5.45	288.85	0.3439
0.1600	24.7072	67.69	106.10	5.58	301.43	0.3588
0.1700	26.2514	71.92	108.51	5.71	313.80	0.3736
0.1800	27.7956	76.15	110.83	5.83	325.95	0.3880
0.1900	29.3398	80.38	113.07	5.95	337.91	0.4023
0.2000	30.8840	84.61	115.24	6.07	349.69	0.4163
0.2100	32.4282	88.84	117.34	6.18	361.30	0.4301
0.2200	33.9724	93.08	119.38	6.28	372.76	0.4438
0.2300	35.5166	97.31	121.36	6.39	384.06	0.4572
0.2400	37.0608	101.54	123.29	6.49	395.23	0.4705
0.2500	38.6050	105.77	125.17	6.59	406.27	0.4837
0.2600	40.1492	110.00	127.00	6.68	417.18	0.4966
0.2700	41.6934	114.23	128.78	6.78	427.97	0.5095
0.2800	43.2376	118.46	130.53	6.87	438.65	0.5222
0.2900	44.7818	122.69	132.24	6.96	449.22	0.5348
0.3000	46.3260	126.92	133.91	7.05	459.68	0.5472
0.3100	47.8702	131.15	135.55	7.13	470.05	0.5596
0.3200	49.4144	135.38	137.15	7.22	480.33	0.5718
0.3300	50.9586	139.61	138.72	7.30	490.51	0.5839
0.3400	52.5028	143.84	140.26	7.38	500.61	0.5960
0.3500	54.0470	148.07	141.78	7.46	510.62	0.6079
0.3600	55.5912	152.30	143.26	7.54	520.56	0.6197
0.3700	57.1354	156.54	144.73	7.62	530.41	0.6314
0.3800	58.6796	160.77	146.16	7.69	540.19	0.6431
0.3900	60.2238	165.00	147.57	7.77	549.90	0.6546
0.4000	61.7680	169.23	148.97	7.84	559.54	0.6661
0.4100	63.3122	173.46	150.33	7.91	569.11	0.6775
0.4200	64.8564	177.69	151.68	7.98	578.62	0.6888
0.4300	66.4006	181.92	153.01	8.05	588.06	0.7001
0.4400	67.9448	186.15	154.32	8.12	597.44	0.7112
0.1737	26.8227	73.49	109.37	5.76	318.31	0.3789

TABLE 5.7

COST-CAPACITY DESIGN (SOUTH-GOING CANAL)

SOUTH-GOING CANAL (L = 300 km)

x	q_c md/yr	q_c Mm^3/day	w meters	H meters	C_L U.S.\$x10^6	C_L/L U.S.\$x10^6/km
0.0100	0.5774	1.58	26.39	1.39	26.54	0.0885
0.0200	1.1548	3.16	34.12	1.80	33.40	0.1113
0.0300	1.7322	4.75	39.65	2.09	38.88	0.1296
0.0400	2.3096	6.33	44.10	2.32	43.64	0.1455
0.0500	2.8870	7.91	47.90	2.52	47.95	0.1598
0.0600	3.4644	9.49	51.25	2.70	51.94	0.1731
0.0700	4.0418	11.07	54.26	2.86	55.67	0.1856
0.0800	4.6192	12.66	57.01	3.00	59.21	0.1974
0.0900	5.1966	14.24	59.56	3.13	62.59	0.2086
0.1000	5.7740	15.82	61.93	3.26	65.82	0.2194
0.1100	6.3514	17.40	64.15	3.38	68.94	0.2298
0.1200	6.9288	18.98	66.25	3.49	71.96	0.2399
0.1300	7.5062	20.56	68.24	3.59	74.89	0.2496
0.1400	8.0836	22.15	70.14	3.69	77.73	0.2591
0.1500	8.6610	23.73	71.96	3.79	80.51	0.2684
0.1600	9.2384	25.31	73.70	3.88	83.21	0.2774
0.1700	9.8158	26.89	75.37	3.97	85.86	0.2862
0.1800	10.3932	28.47	76.99	4.05	88.46	0.2949
0.1900	10.9706	30.06	78.54	4.13	91.00	0.3033
0.2000	11.5480	31.64	80.05	4.21	93.50	0.3117
0.2100	12.1254	33.22	81.51	4.29	95.95	0.3198
0.2200	12.7028	34.80	82.93	4.36	98.36	0.3279
0.2300	13.2802	36.38	84.30	4.44	100.74	0.3358
0.2400	13.8576	37.97	85.64	4.51	103.08	0.3436
0.2500	14.4350	39.55	86.95	4.58	105.38	0.3513
0.2600	15.0124	41.13	88.22	4.64	107.66	0.3589
0.2700	15.5898	42.71	89.46	4.71	109.90	0.3663
0.2800	16.1672	44.29	90.67	4.77	112.12	0.3737
0.2900	16.7446	45.88	91.86	4.83	114.30	0.3810
0.3000	17.3220	47.46	93.02	4.90	116.47	0.3882
0.3100	17.8994	49.04	94.16	4.96	118.61	0.3954
0.3200	18.4768	50.62	95.27	5.01	120.72	0.4024
0.3300	19.0542	52.20	96.36	5.07	122.82	0.4094
0.3400	19.6316	53.79	97.43	5.13	124.89	0.4163
0.3500	20.2090	55.37	98.49	5.18	126.94	0.4231
0.1106	6.3860	17.50	64.28	3.38	69.13	0.2304

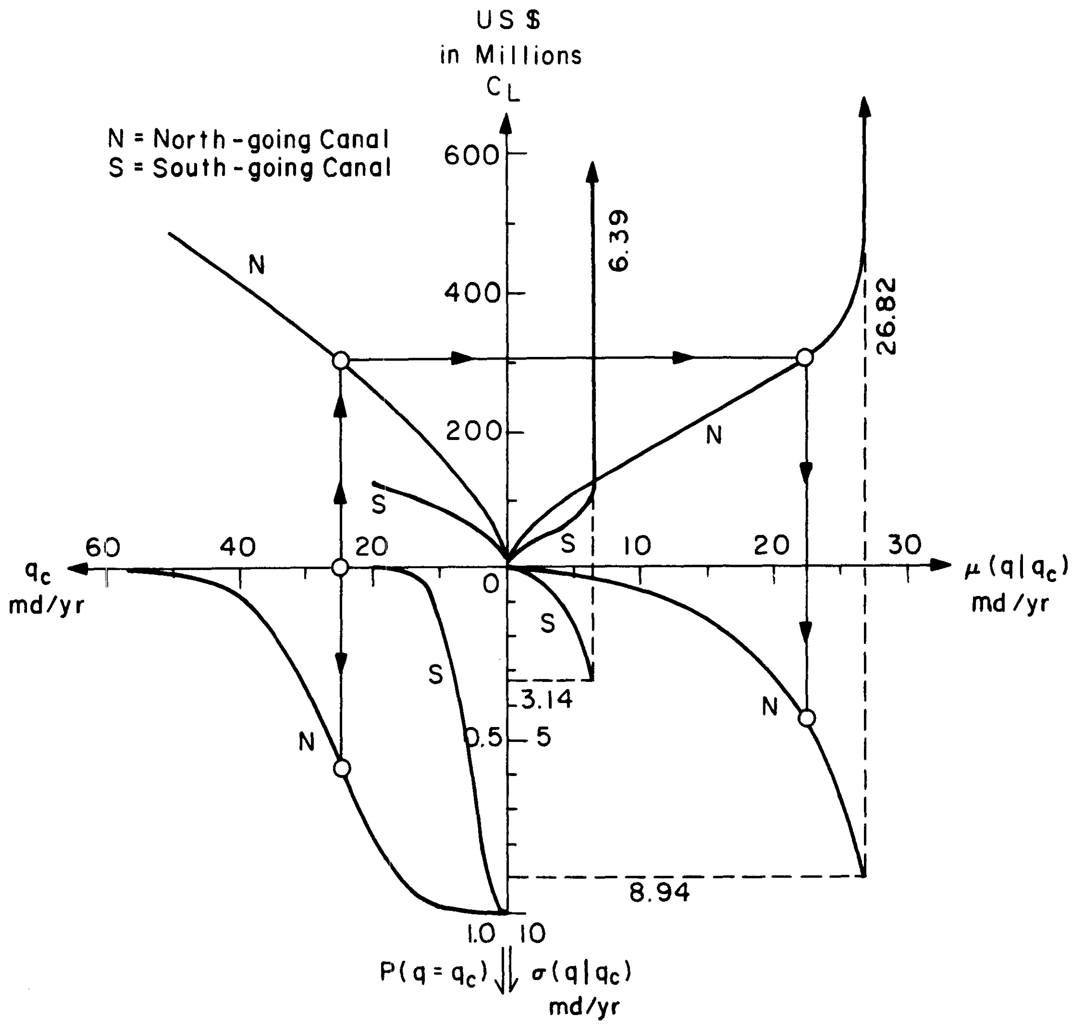

FIGURE 5.7

COST-CAPACITY COMPARISON OF CANAL ALTERNATIVES UNDER UNCERTAIN CANAL FLOWS

In comparing the canal alternatives, for example, for a mean canal flow $\mu(q|q_c)$ of 5 md/yr (Fig. 5.8), it will be cheaper to build the south-going canal. However, the standard deviation of the canal flow in this case is much higher than that of the north-going canal. A tradeoff exists between having cheaper canal construction costs but higher uncertainty of canal flows (higher $\sigma(q|q_c)$), and more expensive construction costs but smaller uncertainty of canal flows (smaller $\sigma(q|q_c)$). For a mean canal flow of higher than 6.39 md/yr, the north-going canal is the only choice because the south-going canal cannot yield a flow higher than 6.39 md/yr even for unlimited canal capacity.

5.5 Derivation of the Distribution, Mean and Variance of the Potential Canal Flow Given the Canal Capacity (A Refined Model)

5.5.1 Introduction

In the previous sections, only the annual flows are considered. We have assumed implicitly that a canal capacity capable of recovering a mean annual flow of 12 md implies a recovery of 1 md per month. This is not strictly correct because of the fluctuation of the mean monthly catchment yields. In this section, the monthly spillage will be considered, and the mean and variance of the annual potential canal flow given the constant monthly canal capacity will be derived in closed analytical form. Due to insufficient data of the mean monthly sub-catchment flows, application of the cost-capacity analysis will be left for future research.

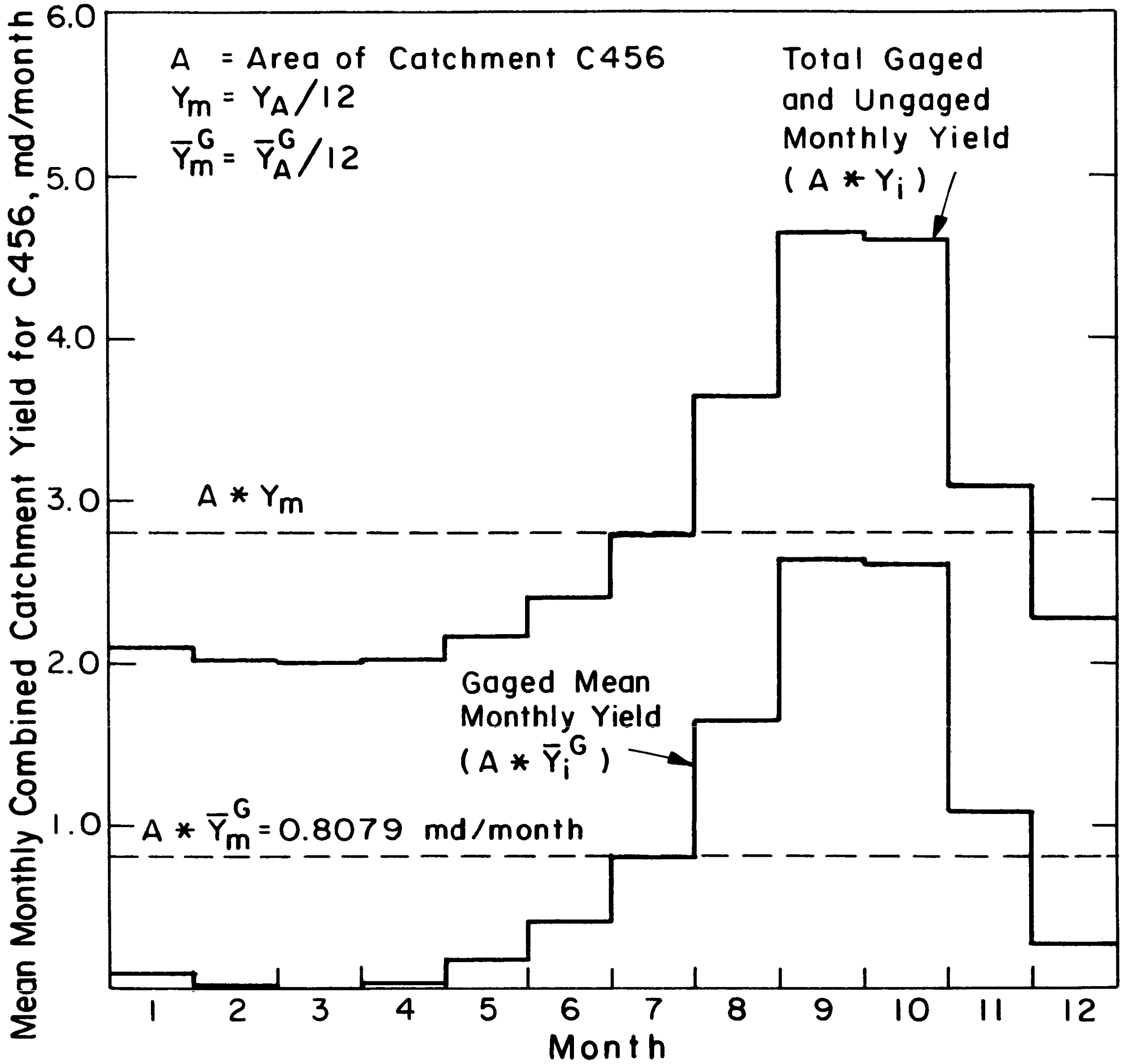

FIGURE 5.8 : MONTHLY COMBINED CATCHMENT YIELD

(AS PROPORTIONAL TO GAGED MEAN MONTHLY YIELD)

5.5.2 Derivation of the Distribution, Mean and Variance of the Monthly Potential Canal Flow Given the Monthly Canal Capacity

To facilitate our work, the fluctuation of the monthly combined catchment yield (gaged + ungaged), $A * Y_i$, is assumed to follow that of the gaged mean monthly combined catchment yield, $A * \bar{Y}_i^G$, as shown in Fig. 5.8. Here,

$$A * \bar{Y}_i^G = b_i * A * \bar{Y}_m^G \tag{5.68}$$

or

$$b_i = \bar{Y}_i^G / \bar{Y}_m^G \quad , \qquad i = 1, \ldots, 12 \tag{5.69}$$

where

A = area of combined catchment

$\bar{Y}_m^G = \bar{Y}_A^G/12$ = gaged mean annual monthly yield

Y_A = annual combined catchment yield

Y_i = monthly combined catchment yield for month i

b_i = ratio of gaged mean monthly yield to gaged mean annual monthly yield for the i^{th} month

The overbar signifies time average and the superscript "G" means "gaged discharge," and

$$AY_i = b_i * A * Y_m = b_i * A * (Y_A/12) \tag{5.70}$$

or

$$Y_i = a_i \, Y_A \tag{5.71}$$

$a_i = b_i/12, \; i = 1, \ldots, 12$

Y_i, Y_m, $\bar{Y}_i^G$, $\bar{Y}_m^G$ may be in m/month or cm/month. $A*Y_i$, $A*Y_m$, $A*\bar{Y}_i^G$, $A*\bar{Y}_m^G$ may be in m^3/month or Mm^3/month or md/month.

From Fig. 5.9(a), the monthly canal flow (q_i) is given by

$$q_i = \begin{cases} A * Y_i, & A * Y_i < q_{cm} \\ q_{cm} = q_c/12 \,, & A * Y_i \geq q_{cm} \end{cases} \tag{5.72}$$

with

q_{cm} = constant monthly canal capacity

q_c = annual canal capacity

Substituting Eq. (5.71) in (5.72) and normalizing by $(a_i A * \underline{\bar{P}_s})$, where a_i is the monthly proportionality factor and $A * \underline{\bar{P}_s}$ is the space-time mean seasonal catchment precipitation,

$$\frac{q_i}{a_i A * \underline{\bar{P}_s}} = \begin{cases} Y_A/\underline{\bar{P}_s} \,, & Y_A/\underline{\bar{P}_s} < q_{cm}/(a_i A * \underline{\bar{P}_s}) \\ q_{cm}/(a_i A * \underline{\bar{P}_s}) \,, & Y_A/\underline{\bar{P}_s} \geq q_{cm}/(a_i A * \underline{\bar{P}_s}) \end{cases}$$

$$i = 1, 2, \ldots, 12 \tag{5.73}$$

Let

$$x_i = q_i/(a_i A * \underline{\bar{P}_s}) \tag{5.74}$$

= normalized monthly canal flow for month i

$$x_{ci} = q_{cm}/(a_i A * \underline{\bar{P}_s}) \tag{5.75}$$

= normalized monthly canal capacity for month i

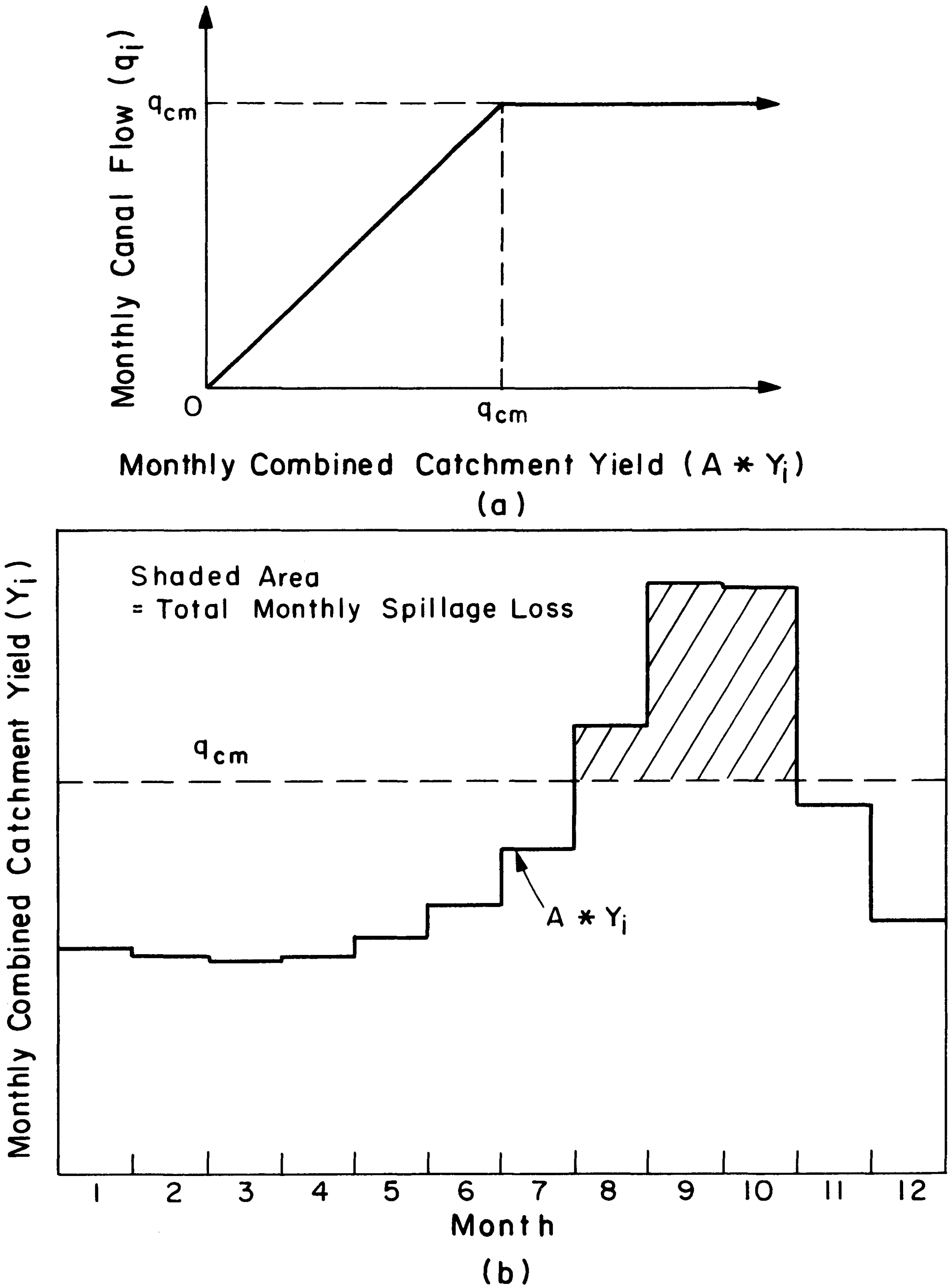

FIGURE 5.9 : RELATIONSHIP BETWEEN MONTHLY CANAL FLOW AND MONTHLY COMBINED CATCHMENT YIELD

(Notice that the capacity q_{cm} is the same constant for all the months, but the normalized capacity x_{ci} is different for different months because of the monthly factor a_i. This seemingly strange normalization allows easy application of previous derived formulas.)

Equation (5.73) can be written as

$$x_i = \begin{cases} Y_A/\overline{P}_s & , \quad Y_A/\overline{P}_s < x_{ci} \\ x_{ci} & , \quad Y_A/\overline{P}_s \geq x_{ci} \end{cases} \tag{5.76}$$

$$i = 1, 2, \ldots, 12$$

Equation (5.76) is almost identical to Eq. (5.16), except for the normalizing factor which is monthly specific. Therefore, Eqs. (5.17) through (5.38) are applicable to the normalized monthly canal flow (x_i). We only need to replace x, x_c, F and F_c in those equations (5.17 to 5.38) by x_i, x_{ci}, F_i and F_{ci}, respectively, to arrive at, from Eqs. (5.24) and (5.33),

$$\mu(x_i|x_{ci}) = \sum_{n=0}^{10} \frac{C_n F_{ci}^{n+1}}{(n+1)} + \frac{a}{(1-b)} [1 - (1-F_{ci})^{1-b}] + x_{ci}(1-F_{ci}) \tag{5.77}$$

and

$$\sigma^2(x_i|x_{ci}) = \left\{ \sum_{n=0}^{20} \frac{e_n F_{ci}^{n+1}}{(n+1)} + 2a*\Gamma(1-b) \sum_{n=0}^{10} \frac{C_n*\Gamma(n+1)}{\Gamma(n+2-b)} * I_{F_{ci}}(n+1, 1-b) \right.$$
$$\left. + \frac{a^2}{(1-2b)} [1 - (1-F_{ci})^{1-2b}] + x_{ci}^2(1-F_{ci}) - \mu^2(x_i|x_{ci}) \right\} \tag{5.78}$$

for

$$a > 0 \quad , \quad 0 < b < 1/2$$

$$e_o = c_o^2 \quad , \quad e_n = \sum_{k=0}^{n} c_k \, c_{n-k}$$

$$i = 1, 2, \ldots, 12 \quad , \quad n = 1, 2, \ldots, 20$$

where

$\mu(x_i|x_{ci})$ = mean monthly canal flow (normalized) given the monthly canal capacity (normalized)

$\sigma^2(x_i|x_{ci})$ = variance of monthly canal flow (normalized) given the monthly canal capacity (normalized)

From Eqs. (5.74) and (5.75), we obtain

$$\mu(q_i|q_{cm}) = a_i A * \underline{\bar{P}_s} * \mu(x_i|x_{ci}) \tag{5.79}$$

$$\sigma^2(q_i|q_{cm}) = (a_i A * \underline{\bar{P}_s})^2 * \sigma^2(x_i|x_{ci}) \tag{5.80}$$

which are the mean and variance of the monthly canal flow given the monthly canal capacity.

The distribution of q_i can be deduced from Eqs. (5.18), (5.22) and (5.23), as

$$\text{Prob}[q_i < q_i' | 0 \leq q_i' < q_{cm}] = F_i' = G^{-1}(x_i') \tag{5.81}$$

$$\text{Prob}[q_i = q_{cm}] = 1 - F_{ci} \tag{5.82}$$

$$\text{Prob}[q_i \leq q_{cm}] = 1 \tag{5.83}$$

Figure 5.9(b) shows the monthly spillage loss. This loss depends critically on the factor a_i, which determines whether q_i is higher or lower than q_{cm}.

5.5.3 Derivation of the Distribution, Mean and Variance of the Annual Potential Canal Flow Given the Monthly Canal Capacity

The annual canal flow (q_A) is the sum of the monthly canal flows (q_i), as

$$q_A = \sum_{i=1}^{12} q_i \tag{5.84}$$

From Eqs. (5.74) and (5.75) and (5.72)

$$q_i = a_i A * \underline{\overline{P}_s} * x_i \qquad (5.74)'$$

$$q_{cm} = a_i A * \underline{\overline{P}_s} * x_{ci} \qquad (5.75)'$$

and

$$q_c = 12 * q_{cm} \qquad (5.72)'$$

Taking the expected value of both sides of Eq. (5.84), given the constant monthly canal capacity, q_{cm},

$$E(q_A | q_{cm}) = E[\sum_{i=1}^{12} (q_i | q_{cm})] \tag{5.85}$$

which is equivalent to

$$\mu(q_A | q_c) = \sum_{i=1}^{12} a_i A * \underline{\overline{P}_s} * E(x_i | x_{ci})$$

$$= A * \underline{\overline{P}_s} * \sum_{i=1}^{12} a_i * \mu(x_i | x_{ci}) \tag{5.86}$$

where $\mu(q_A | q_c)$ is the mean annual canal flow given the canal capacity.

The variance of annual canal flow given q_{cm} is

$$\mathrm{Var}(q_A | q_{cm}) = \mathrm{Var}[\sum_{i=1}^{12} (q_i | q_{cm})] \tag{5.87}$$

or equivalently,

$$\sigma^2(q_A | q_c) = \mathrm{Var}[\sum_{i=1}^{12} (a_i A * \underline{\overline{P}_s} * x_i | x_{c1}, x_{c2}, \ldots, x_{c12})$$

$$= (A * \underline{\overline{P}_s})^2 \sum_{i=1}^{12} a_i^2 \sigma^2(x_i | x_{ci})$$

$$+ 2 * (A * \underline{\overline{P}_s})^2 \sum_{i=1}^{12} \sum_{j=i+1}^{12} a_i a_j * Z(i, j) \tag{5.88}$$

where Z(i, j) is the covariance term given by

$$Z(i, j) = \mathrm{COV}(x_i, x_j | x_{ci}, x_{cj})$$

$$= E[x_i * x_j | x_{ci}, x_{cj}] - \mu(x_i | x_{ci}) * \mu(x_j | x_{cj}) \tag{5.89}$$

Z(i, j) depends on the relative magnitude of a_i and a_j. There are three distinct cases:

Case 1: $a_j/a_i = 1$

This case implies $x_j = x_i$. Therefore, the covariance becomes the variance, as

$$Z(i, j) = \mathrm{COV}(x_i, x_i | x_{ci}, x_{ci})$$

$$= \sigma^2(x_i | x_{ci}) = \sigma^2(x_j | x_{cj}) \tag{5.90}$$

Case 2: $a_j/a_i > 1$

In this case, it can be seen that from Eq. (5.75), $x_{ci} > x_{cj}$.

The relation between x_{ci} and x_{cj} is shown in Fig. 5.10(a). There are three regions (I, II, III).

Region I is defined by $0 < (x_i, x_j) < x_{cj} < x_{ci}$. Here,

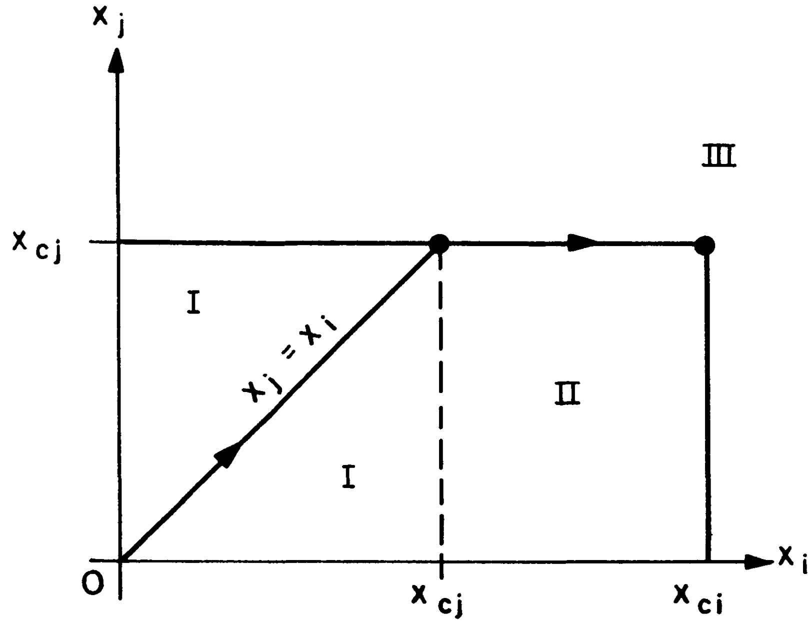

(a) For $a_j / a_i > 1$, $x_{ci} > x_{cj}$

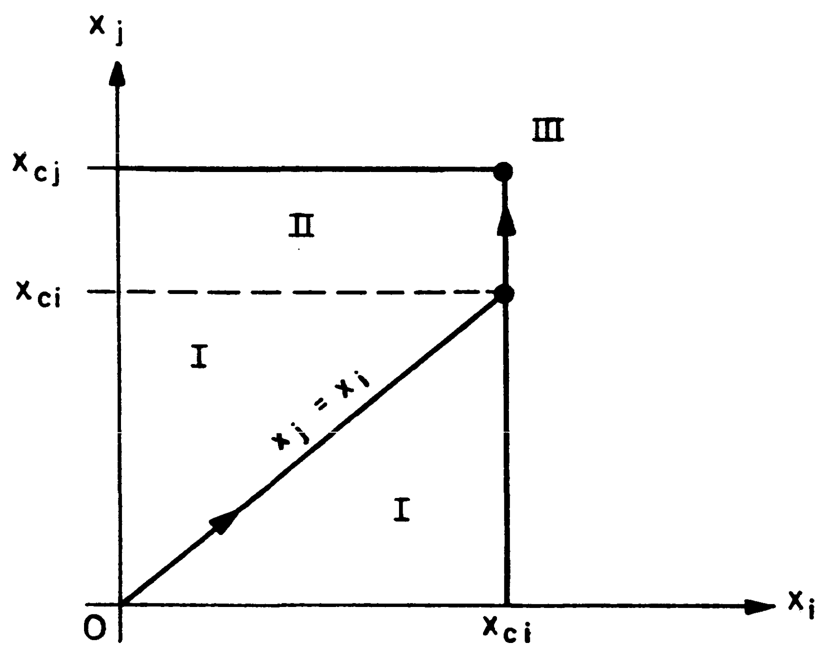

(b) For $a_j / a_i < 1$, $x_{cj} > x_{ci}$

FIGURE 5.10 : RELATIONSHIP BETWEEN THE NORMALIZED MONTHLY CANAL CAPACITIES FOR MONTHS i AND j

$$x_j/x_i = \frac{q_j/(a_jA * \underline{\overline{P}_s})}{q_i/(a_iA * \underline{\overline{P}_s})} = \frac{q_j\ a_i}{q_i\ a_j}$$

$$= \frac{(a_j\ Y_A)\ a_i}{(a_i\ Y_A)\ a_j} = 1 \qquad (5.91)$$

For Region II, since x_j is bounded by x_{cj}, we have

$$x_j = x_{cj} \text{ and } x_{cj} \leq x_i < x_{ci} \qquad (5.92)$$

For Region III,

$$x_j = x_{cj} \quad \text{and} \quad x_i = x_{ci} \qquad (5.93)$$

With the relationship between x_j and x_i in the three regions defined, the evaluation of the expectation term in Eq. (5.89) can now proceed.

$$E[x_i * x_j | x_{ci}, x_{cj}] = \int_o^{x_{cj}} x_i^2 f(x_i)\ dx_i + x_{cj} \int_{x_{cj}}^{x_{ci}} x_i f(x_i)\ dx_i$$

$$+ x_{cj}\ x_{ci} \int_{x_{ci}}^{\infty} f(x_i)\ dx_i \quad , \quad a_j/a_i > 1 \qquad (5.94)$$

where

$f(x_i)$ = PDF of x_i

The integrals in the above equation are similar to those of Eqs. (5.24) and (5.25), and the final form of Eq. (5.94) is

$$E[x_i * x_j | x_{ci}, x_{cj}] = \sum_{n=0}^{20} \frac{e_n F_{cj}^{n+1}}{(n+1)} + 2a*\Gamma(1-b) \sum_{n=0}^{10} C_n * \frac{\Gamma(n+1)}{\Gamma(n+2-b)}$$

$$* \; I_{F_{cj}}(n+1, 1-b) + \frac{a^2}{(1-2b)} [1 - (1-F_{cj})^{1-2b}]$$

$$+ x_{cj} \left\{ \sum_{n=0}^{10} \frac{C_n (F_{ci} - F_{cj})^{n+1}}{(n+1)} + \frac{a}{(1-b)} [(1-F_{ci})^{1-b} \right.$$

$$\left. - (1-F_{cj})^{1-b}] \right\} + x_{cj} \, x_{ci} (1 - F_{ci}) \quad \text{for the case } a_j/a_i > 1$$

$$(5.95)$$

where

$$e_o = C_o^2 \quad , \quad e_n = \sum_{k=0}^{n} C_k C_{n-k}, \quad n = 1, 2, \ldots, 20$$

$$a > 0, \qquad 0 < b < 1/2$$

$\Gamma(u)$ = Gamma function

$I_\alpha(u, v)$ = Incomplete Beta function (Eq. (5.29))

F_{ci} and F_{cj} can be obtained by replacing (x_c, F_c) in Eq. (5.20) by (x_{ci}, F_{ci}) and (x_{cj}, F_{cj}).

Equations (5.95) and (5.89) define the covariance term Z(i, j) in Eq. (5.88) for Case 2 where $a_j/a_i > 1$.

Case 3: $a_j/a_i < 1$

In this case, $x_{cj} > x_{ci}$.

In Region I (Fig. 5.10b),

$$x_j/x_i = 1 \quad \text{for} \quad 0 < (x_i, x_j) < x_{ci} < x_{cj} \qquad (5.96)$$

In Region II,

$$x_i = x_{ci} \text{ and } x_{ci} \leq x_j < x_{cj} \tag{5.97}$$

In Region III,

$$x_i = x_{ci} \text{ and } x_j = x_{cj} \tag{5.98}$$

and

$$E[x_i * x_j | x_{ci}, x_{cj}] = \int_o^{x_{ci}} x_j^2 f(x_j)\, dx_j + x_{ci} \int_{x_{ci}}^{x_{cj}} x_j f(x_j)\, dx_j$$

$$+ x_{ci}\, x_{cj} \int_{x_{cj}}^{\infty} f(x_j)\, dx_j, \quad a_j/a_i < 1 \tag{5.99}$$

Equation (5.99) is similar in form to Eq. (5.94) in which x_{cj} interchanges with x_{ci}, and F_{cj} interchanges with F_{ci}. Therefore, the solution to Eq. (5.99) is the same as Eq. (5.95), but with the prescribed variables interchanged.

Having determined the covariance Z(i, j) for the three cases ($a_j/a_i = 1$, $a_j/a_i \gtrless 1$), $\sigma^2(q_A|q_c)$ in Eq. (5.88) is defined.

In general, the distribution of the annual canal flow (q_A) given the canal capacity (q_{cm}) can be determined by the Monte Carlo simulation technique, as described in Sections 4.4.2 and 4.4.3. For each simulated annual combined catchment yield, the monthly canal flows can be computed by Eqs. (5.71) and (5.72), and the annual canal flows (q_A) by Eq. (5.84). After a long series of q_A has been obtained, its empirical

CDF can be formed.

Chapter 6

SOME ANTICIPATED IMPACTS OF CANAL PROJECTS

6.1 The Jonglei Canal Project

In 1946, the Governor-General of the Republic of the Sudan approved the appointment of the "Jonglei Committee" to study in detail all possible effects of water resource development proposals submitted by the Egyptian Government. In this way, the effects and remedies of the Jonglei Canal proposal became a seven year study (1946-53) of the Jonglei Investigation Team (JIT).

In 1959, the Permanent Joint Technical Commission (PJTC), an intergovernmental body between Egypt and the Sudan was established, with the authority to draw up plans, supervise and execute water resource development projects for the benefit of both countries.

The final version of the Jonglei Canal Project was issued by the PJTC in April, 1974. It consists of two phases. Phase I includes the dredging of a 20 Mm^3/day capacity canal to bypass the Jebel-Zeraf swamp (the Sudd). The water is to be diverted from Bahr el Jebel at Jonglei, and delivered to the White Nile at the mouth of the River Sobat south of Malakal (Fig. 1.4). Phase II includes controlling the headwater lakes (Victoria, Kyoga, and Albert) (see Fig. 1.1) to equalize their natural outflows, and widening of the first phase canal, or the excavation of a new canal so that the total canal capacity reaches 43 Mm^3/day. The anticipated increased Nile yield from Phase I amounts to 4.7 md at Malakal, and after Phase II, 9 md. Phase I is expected to be completed in seven years (1976-82), with a total cost of 162 million U.S. dollars (Table 5.5).

Since the Bahr el Ghazal swamp and the Jebel-Zeraf swamp share the same hydrologic and ecological regimes, the drainage impacts from the latter are transferable to the former. In the following sections, the anticipated impacts from draining the Bahr el Ghazal swamp are inferred from the study of the Jonglei Investigation Team (JIT) (4).

6.2 On Environmental Impacts

By intercepting the inflows to the Central Swampland through the north-going and the south-going canals, some adverse environmental impacts are to be expected.

Within the Central Swampland, many toich lands will be lost due to insufficient river spills. This will cause serious losses in the pasture for grazing. The livestock population now dependent on toich land may be greatly reduced.

Deprived of river spills, numerous lakes and pools within the Central Swampland will dry out. The fish population in these areas will be sharply diminished.

The canals will stand as barriers to wildlife migration, and to the movement of people and their stocks.

Since the inhabitants (Nilotic tribes) of the Central Swampland are living in a very delicate balance with their environment (Section 3.8), any disruption of their environment will surely affect their livelihood to a greater or lesser extent. The total population to be affected in one way or another amounts to more than one million people (page 111).

At present, the huge amount of silt carried down the Ghazal tributaries is being filtered out at the Ghazal swamp. In the future, the canals will carry this silt into the White Nile, which may seriously reduce its carrying capacity.

At this time, it is not possible to estimate with assurance either the magnitude or the extent of any climatic changes which may be triggered by the swamp drainage. Certainly, reduction of the evapotranspiration by such an amount will cause a rise in the local mean temperature and a decrease in local mean humidity. Depriving the atmosphere of this evaporate may result in a reduction of regional precipitation.

6.3 On Sociological Impacts

There is no doubt that the Bahr el Ghazal canal project will bring profound economic and social changes to the inhabitants of the area.

Along the routes of the canals, large scale resettlement may be unavoidable.

Reduction of pastural lands will also cause friction among the tribes in some areas. In the past, grazing across other tribal territories was usually tolerated, but due to future shortages of toich land in such areas, these rights will be severely curtailed.

In areas where alternate pastural lands cannot be found, agricultural remedies may have to be offered to the victims. This will completely change their mode of living.

The Nilotic people are, in general, self-sufficient even though on a subsistance level. They are contented with what they have, and are not impressed by western civilization. Their resistance to change may create serious problems in the implementation of the project. Because of their reluctance to use cattle as working animals, machinery may have to be introduced in order for farming to increase the crop yield. This will cause drastic changes in the redistribution of wealth among the people.

Chapter 7

SUMMARY, CONCLUSIONS AND RECOMMENDATIONS FOR FUTURE WORK

7.1 Summary and Conclusions

In an annual water balance of the Central Swampland (Fig. 4.3), by neglecting any deep seepage of groundwater, it is found that an ungaged inflow of 15.1 md is necessary in order to account for the large evapotranspiration. The total estimated gaged and ungaged inflows to the Central Swampland amounts to 27.8 md, which may be considered the minimum potential water recovery from swamp drainage.

In a complementary annual water balance of the tributary catchments (Fig. 4.8), the ungaged inflow to the Central Swampland is found to be 19.8 md. The total estimated gaged and ungaged inflows to the Central Swampland from this analysis amounts to 32.5 md, which may be considered the maximum potential water recovery from draining the Ghazal swamp.

The physical evidence for ungaged inflow to the Central Swampland is:

1) Before reaching the Central Swampland, all the Bahr el Ghazal tributaries start to spill onto their flood-plains during the rainy season (3), (26).
2) The sandy river bed on the Ironstone Plateau just south of the Central Swampland takes up much of the dry season flow through seepage (26).

3) Numerous ungaged small streams, either ephemeral or perennial, flow into the Central Swampland from the subcatchments (32).

The two dry catchments in the north (Bahr el Arab and Raqaba el Zarqa) are excluded in the analysis of tributary inflows because they apparently make an insignificant contribution to the hydrology of the Bahr el Ghazal swamp. Any ungaged outflows from these two catchments will contribute either to deep seepage or to the closure error of the water balance, or both.

Based on the above results, even though we cannot conclude definitely that deep seepage at the Central Swampland is insignificant, we can be sure that the huge water loss (27.8 md to 32.5 md) at the Central Swampland can be explained by evapotranspiration alone.

7.2 Future Work

7.2.1 Suggested Hydrologic Studies

Future work on the hydrology of the Bahr el Ghazal basin should include:

1) Onsite investigation of the ungaged flow and the soil parameters along the canal routes for the design of the interception system and for the estimation of seepage and conveyance losses.

2) Onsite investigation of the practicality of joining the River Jur to the south-going canal because this route to Malakal is much shorter than that of the north-going canal.

3) Addition of the yields from the Lau and the Gell catchments to the south-going canal flows, since the canal intercepts these two rivers before reaching the Bahr el Jebel at Jonglei.

4) Acquisition and analysis of periodic satellite and aerial mapping data to define swamp topography, vegetation, and the annual cycle of water surface area.

5) Study of the dynamics of the expanding and contracting flooded area in the Central Swampland including the drying transient which will follow tributary interception. This will be valuable in planning land reclamation.

6) Verification or modification of the equilibrium canopy density on the tributary catchments, by onsite observation, or by aerial photograph.

7) Study of the spillage loss of canal flows at the monthly level.

8) Water balance study of the Bahr el Arab and Raqaba el Zarqa catchments to further refine the possibility of significant deep seepage at the Central Swampland.

9) Estimation of the distribution, mean and variance of the sum of the Bahr el Jebel flows and the south-going canal flows, both at Jonglei, for capacity expansion design of the Jonglei Canal to accommodate the combined inflows.

7.2.2 Suggested Remedial Measures for Some Adverse Environmental Impacts

The major environmental impact comes from the reduction of toich lands for grazing at the Central Swampland. Therefore, remedial measures should include the provision of domestic water supply to existing pastures which are at present unused due to water shortage. Pasture lands can also be increased by clearing the brush on the edge of the Ironstone Plateau, and in some parts of the Flood Region.

Small fish-breeding ponds should be provided to replace the natural sites lost by drainage.

Cattle ramps and canal crossings should be adequately provided so that the movement of men and animals will not be unduly hindered by the canal.

7.2.3 Suggested Remedial Measures for Some Adverse Sociological Impacts

The major sociological impacts come from the necessary resettlement of people along the canal routes, and from the people's resistance to changing their mode of living (Section 6.3).

Of course, the only way to eliminate these adverse sociological impacts is to eliminate the canal itself. This seems to be highly unlikely, since the alternatives for increasing the current Nile flow are very few, and the sources of appreciable recoverable water are mainly the swampy regions of the Sudan.

If the canal project is inevitable, it is suggested that public hearings be included as part of the decision process. The logistics and communication difficulties in obtaining public inputs and in identifying victims may be reduced to a minimum if the victims of various groups can be represented by spokesmen. These spokesmen may be interpretors chosen by the tribes to speak for the victim groups, or government agents working with the problems of the victims. The public hearings should be held for the spokesmen instead of the individual victim because the latter is almost impossible to reach.

Large contingency funds should be made available, if necessary, as many victims may not be readily identified at the conclusion of the public hearings.

Our contention is that <u>if change is inevitable</u>, every remedial measure should be taken into consideration and carefully implemented so as to help the natives make a smooth transition from their old mode of living to the new.

REFERENCES

1. Rzoska, J., The Nile, Biology of an Ancient River, The Hague, 1976.

2. Sanderson and Porter, Inc., Power Sector Survey - Arab Republic of Egypt, System Planning Diagnostic Report, Section I, Cairo, April, 1977.

3. Hurst, H. E. and Phillips, P., The Nile Basin, Volume I, General Description of the Basin, Meteorology, Topography of the White Nile Basin; Ministry of Public Works, Egypt; Physical Department, Physical Department Paper No. 26, Government Press, Cairo, 1931.

4. The Equatorial Nile Project (and Its Effects in the Anglo-Egyptian Sudan), a Report by the Jonglei Investigation Team. Introduction and Summary, Page xx; Volume I, Page 25; Volume III, Page 973, 978.

5. Hurst, H. E. and Phillips, P., The Nile Basin, Volume V, The Hydrology of the Lake Plateau and Bahr el Jebel; Ministry of Public Works, Egypt; Physical Department, Physical Department Paper No. 35, Schindler's Press, Cairo, 1939, Pages 35, 52, 120, 185, Chapter VII.

6. Migahid, A. M., Further Observations on the Flow and Loss of Water in the "Sudd" Swamps of the Upper Nile, Cairo University Press, 1952.

7. Vowinckel, E. and Orvig, S., "The Water Budget and Potential Water Reserves of the East Africa Source Region of the Nile," Journal of Applied Meteorology, Vol. 18, No. 2, Feb. 1979, American Meteorological Society.

8. Balek, Jaroslav, Hydrology and Water Resources in Tropical Africa, Elsevier Scientific Publishing Company, 1977.

9. Hydrometeorological Survey of the Catchments of Lakes Victoria, Kyoga and Albert, Report prepared by the Governments of Burundi, Egypt, Kenya, Rwanda, Sudan, United Republic of Tanzania and Uganda by the World Meteorological Organization acting as Executive Agency for the United Nations Development Programme, Geneva, 1974, Vol. I, Page 505; Volume III, Page 150, 218.

10. Chapas, L. C. and Roes, A. R., "Evaporation and Evapotranspiration in Southern Nigeria," Quarterly Journal, Royal Meteorological Society, Vol. 89, Page 314, 1963.

11. Penman, H. L., Vegetation and Hydrology, Technical Communication No. 53, Commonwealth Bureau of Soils, Harpenden, Published by the Commonwealth Agricultural Bureau, Farnham Royal, Bucks, England, Page 4, 64, 1963.

12. Migahid, A. M., An Ecological Study of the "Sudd" Swamps of the Upper Nile, Proceedings of the Egyptian Academy of Sciences, 3, 57-86, 1947.

13. Eagleson, P. S., "Climate, Soil and the Water Balance," M.I.T. Department of Civil Engineering, 1977.

14. Eagleson, P. S., "Climate, Soil and Vegetation 1. Introduction to Water Balance Dynamics," Water Resources Research, Vol. 14, No. 5, 1978a.

15. Eagleson, P. S., "Climate, Soil and Vegetation 2. The Distribution of Annual Precipitation Derived from Observed Storm Sequences," Water Resources Research, Vol. 14, No. 5, 1978b.

16. Eagleson, P. S., "Climate, Soil and Vegetation 3. A Simplified Model of Soil Moisture Movement in the Liquid Phase," Water Resources Research, Vol. 14, No. 5, 1978c.

17. Eagleson, P. S., "Climate, Soil and Vegetation 4. The Expected Value of Annual Evapotranspiration," Water Resources Research, Vol. 14, No. 5, 1978d.

18. Eagleson, P. S., "Climate, Soil and Vegetation 5. A Derived Distribution of Storm Surface Runoff," Water Resources Research, Vol. 14, No. 5, 1978e.

19. Eagleson, P. S., "Climate, Soil and Vegetation 6. Dynamics of the Annual Water Balance," Water Resources Research, Vol. 14, No. 5, 1978f.

20. Eagleson, P. S., "Climate, Soil and Vegetation 7. A Derived Distribution of Annual Water Yield," Water Resources Research, Vol. 14, No. 5, 1978g.

21. Thomas, H. A., "Frequency of Minor Floods," J. Boston Soc. Civil Eng., 35, pp. 425-442, 1948.

22. Tellers, T. E. and Eagleson, P. S., "Estimation of Effective Hydrologic Properties of Soils from Observations of Vegetation Density," M.I.T., Department of Civil Engineering, Ralph M. Parsons Laboratory for Water Resources and Hydrodynamics, Technical Report No. 254, March 1980.

23. Operational Navigation Chart, prepared and published by the Defense Mapping Agency Aerospace Center, St. Louis Air Force Station, Missouri 63118 (Series: ONC, Sheets: K-4, L-4).

24. The Nile Basin, Volume IV, up to the 8th Supplement. Ten-Day Mean and Monthly Mean Discharges of the Nile and its Tributaries by Nile

Control Staff. Ministry of Irrigation, Egypt, Nile Control Department, Paper No. 27, Cairo. General Organization for Government Printing Offices, 1971.

25. Ibrahim, H., Shibeerny, F. and Mostafa, F., Bahr el Ghazal Water Development Project (unpublished report).

26. Natural Resources and Development Potential in the Southern Provinces of the Sudan, A Preliminary Report, by the Southern Development Investigation Team, Sudan Government, Pages 5, 6, 39, 48 and 115, 1954.

27. El Shazly, E. M. and Abdel-Hady, M. A., et al., Satellite Mapping - Regional Geology, Geomorphology, Structure, Drainage and Hydrology of Bahr El Jebel Area (Jonglei Canal Project Area) Southern Sudan, published by Remote Sensing Center, Academy of Scientific Research and Technology, Cairo, Egypt, April, 1978.

28. The Nile Basin, Volume VI, up to 7th Supplement. Monthly and Annual Rainfall Totals and Number of Rainy Days at Stations in and near the Nile Basin by Nile Control Staff. Arab Republic of Egypt, Ministry of Irrigation, Nile Control Department, Paper No. 33, 1972.

29. Landsberg, H. E., Lippman, H., Paffen, K. H. and Troll, C., World Maps of Climatology (3rd edition). Publication of the Geomedical Research Unit of the Heidelberg Academy of Science, 1966.

30. Balek, J. and Perry, J. E., "Hydrology of Seasonally Inundated African Headwater Swamps," Journal of Hydrology, 19, pp. 227-249, 1973.

31. Soil Resources and Potential for Agriculture Development in Bahr el Jebel Area, Southern Sudan (Jonglei Canal Project Area). A report published by Remote Sensing Center, Academy of Scientific Research and Technology, Cairo, Egypt, for the Permanent Joint Technical Commission for Nile Waters, April 1978.

32. General Drainage Map of Bahr el Ghazal Area, Southwestern Sudan, Sheet II (from the Interpretation of Landsat Satellite Images), published by Remote Sensing Center, Academy of Scientific Research and Technology, Cairo, Egypt, 1980.

33. Hewlett, J. D. and Hibbert, A. R.,"Factors Affecting the Response of Small Watersheds to Precipitation in Humid Areas," in International Symposium on Forest Hydrology, edited by W. E. Sopper and H. W. Lull, pp. 275-290, Pergamon Press, New York, 1967.

34. Permanent Joint Technical Commission (P.J.T.C.), Study of the Water Losses in River Jur, Bahr El Ghazal Basin, Ministry of Irrigation Press, Cairo, 1971.

35. Mobarek, I. E., Salem, M. H. and Dorrah, H. T., Hydrological Studies on the River Nile, Cairo University - Massachusetts Institute of Technology Technological Planning Program, Cairo, A.R.E., May 1979.

36. Matalas, N. C., "Mathematical Assessment of Synthetic Hydrology," Water Resources Research, Vol. 3, No. 4, pp. 937-945, 1967.

37. Valencia, D. R. and Schaake, J. C., Jr., "A Disaggregation Model for Time Series Analysis and Synthesis," M.I.T., Ralph M. Parsons Laboratory for Water Resources and Hydrodynamics, Technical Report No. 149, 1972.

38. Stochastic Modelling of Nile Inflows to Lake Nasser, The River Nile Project, Cairo University - Massachusetts Institute of Technology, Technological Planning Program, Cairo, A.R.E., Dec. 1977.

39. International Mathematical and Statistical Librarian, Inc. (IMSL), Library 2, Edition 6, 1977 (Subroutines RLFOTH and RLDOPM).

40. Shoup, T. E., A Practical Guide to Computer Methods for Engineers, Prentice-Hall, Inc., 1979.

41. Hall, W. A. and Dracup, J. A., Water Resources Systems Engineering, McGraw-Hill, New York, 1970.

42. Permanent Joint Technical Commission (P.J.T.C.), Jonglei Project, First Phase, Cairo, Nov. 1978 (Unpublished Report).

43. International Financial Statistics, Volume XXXIII, October 1980, No. 10, published monthly by the International Monthly Fund, Washington, D. C. 20431.

APPENDIX A

Hydrologic Parameters of the Bahr el Ghazal Basin

Table A1

Gaged Mean Monthly Discharges* (up to 1967), 10^6 m^3/month

	Naam	Maridi	Tonj	Jur	Pongo	Loll
	1	2	3	4	5	6
Month						
1	-	-	34.7	44.3	9.7	26.8
2	-	-	19.4	11.0	3.8	8.4
3	-	-	16.6	0.0	0.2	3.0
4	-	-	15.6	30.3	0.0	1.8
5	21.7	8.6	49.2	130.0	3.0	20.5
6	60.0	49.7	99.1	248.0	21.9	128.0
7	62.0	72.7	165.0	436.0	42.4	306.0
8	62.0	115.0	241.0	803.0	86.1	750.0
9	60.0	161.0	390.0	1310.0	147.0	1180.0
10	62.0	96.2	363.0	1380.0	154.0	1070.0
11	27.0	19.4	169.0	646.0	93.1	342.0
12	3.1	0.6	36.3	180.0	13.7	65.8
Yearly	-	-	1600	5220	575	3900

* From Reference (24)

Table A2

Mean Monthly Station Precipitation, mm/month (up to 1972)

	Aweil	Raga	Wau	Tonj	Rumbek	Amadi*	Yubo**	Maridi	Yambio
	1	2	3	4	5	6	7	8	9
Month									
1	0	0	1	3	0	3	10	11	14
2	1	3	5	1	6	16	22	24	26
3	8	17	23	21	26	48	77	71	95
4	32	57	69	83	83	124	129	156	150
5	115	140	135	124	137	171	198	189	183
6	152	178	169	176	154	144	210	176	160
7	195	220	195	200	168	179	158	189	167
8	202	267	217	193	194	174	222	194	198
9	146	204	169	168	140	157	216	164	177
10	47	95	130	76	74	125	165	148	181
11	2	9	14	12	15	37	54	61	73
12	0	1	0	0	0	5	18	14	18
Yearly (mm)	900	1191	1127	1057	997	1183	1479	1397	1442

* Years of Data (1924 - 1964)

** Years of Data (1928 - 1949)

Table A3

Mean Monthly Station Number of Rainy Days m'_{ν} (up to 1972)

Month	Aweil 1	Raga 2	Wau 3	Tonj 4	Rumbek 5	Amadi* 6	Yubo** 7	Maridi 8	Yambio 9
1	0.0	0.0	0.1	0.2	0.0	0.6	1.0	1.4	1.9
2	0.2	0.4	0.6	0.2	0.0	1.7	2.0	2.4	2.7
3	1.2	2.0	2.8	2.3	2.7	4.8	5.3	6.4	7.7
4	3.6	5.2	5.5	6.1	6.3	8.9	9.5	10.6	11.2
5	8.8	9.8	10.2	9.1	8.4	10.4	13.4	12.7	12.7
6	10.0	11.0	11.3	10.2	9.3	10.0	12.4	12.3	11.9
7	12.3	14.2	13.6	11.8	10.4	10.5	11.3	12.5	12.6
8	13.5	16.2	14.8	13.4	11.6	12.0	13.8	12.7	14.2
9	10.7	12.9	12.5	10.4	8.4	9.5	13.7	11.9	12.8
10	4.0	7.5	9.9	6.8	5.6	8.3	12.7	10.9	14.0
11	0.2	0.9	1.7	1.3	1.2	3.5	4.8	5.6	7.2
12	0.0	0.0	0.0	0.0	0.0	0.9	1.6	1.8	2.4
Yearly	64.5	80.1	83.0	71.8	64.5	81.1	101.5	101.2	111.3

* Years of Data (1924 - 1964)

** Years of Data (1928 - 1949)

Table A4

Mean Monthly Station Storm Depth*, m_H, mm

Month	Aweil 1	Raga 2	Wau 3	Tonj 4	Rumbek 5	Amadi 6	Yubo 7	Maridi 8	Yambio 9
1	0.0	0.0	10.0	15.0	0.0	5.0	10.0	7.9	7.4
2	5.0	7.5	8.3	5.0	6.0	9.4	11.0	10.0	9.6
3	6.7	8.5	8.2	9.1	9.6	10.0	14.5	11.1	12.3
4	8.9	11.0	12.5	13.6	13.2	13.9	13.6	14.7	13.4
5	13.1	14.3	13.2	13.6	16.3	16.4	14.8	14.9	14.4
6	15.2	16.2	15.0	17.3	16.6	14.4	16.9	14.3	13.4
7	15.9	15.5	14.3	16.9	16.2	17.0	14.0	15.1	13.3
8	15.0	16.5	14.7	14.4	16.7	14.5	16.1	15.3	13.9
9	13.6	15.8	13.5	16.2	16.7	16.5	15.8	13.8	13.8
10	11.8	12.7	13.1	11.2	13.2	15.1	13.0	13.6	12.9
11	10.0	10.0	8.2	9.2	12.5	10.6	11.3	10.9	10.1
12	0.0	1.0	0.0	0.0	0.0	5.6	11.3	7.8	7.5
Yearly (mm)	14.0	14.9	13.6	14.7	15.5	14.6	14.6	13.8	13.0

* Monthly Storm Depth = Monthly Precipitation/monthly number of rainy days

Table A5

Space-time Mean Monthly Catchment $\underline{m}'_{\nu}$

	Naam	Maridi	Tonj	Jur	Pongo	Loll
	1	2	3	4	5	6
Month						
1	0.8	0.5	0.9	0.9	0.2	0.0
2	1.7	0.8	1.5	1.7	0.8	0.4
3	5.0	3.8	4.8	5.0	2.9	1.9
4	9.1	7.6	8.7	8.7	5.9	4.9
5	11.0	9.8	11.2	12.3	10.5	9.6
6	10.8	10.3	11.3	11.9	11.3	10.8
7	11.3	11.2	12.1	12.1	13.1	13.8
8	12.2	12.1	13.2	14.1	14.7	15.7
9	10.3	9.7	11.5	13.0	12.6	12.5
10	8.8	7.4	9.6	11.9	9.3	6.8
11	3.9	2.6	3.9	4.3	2.0	0.8
12	1.1	0.6	1.1	1.3	0.3	0.0
Yearly	86.0	76.5	89.9	97.2	83.5	77.1
Seasonal	82.4	72.1	86.4	93.3	80.3	74.1

Table A6

Space-time Mean Monthly Catchment Storm Depth $\underline{m}_H$, mm

	Naam	Maridi	Tonj	Jur	Pongo	Loll
	1	2	3	4	5	6
Month						
1	5.2	4.0	10.8	9.9	7.2	0.0
2	9.0	7.2	7.9	9.7	8.3	7.0
3	10.4	10.0	10.6	12.3	9.2	8.2
4	14.1	13.7	14.0	13.3	12.0	10.6
5	15.8	15.6	14.3	14.3	13.7	14.0
6	14.8	15.9	15.6	15.9	15.5	16.0
7	16.1	15.9	15.6	14.2	14.6	15.6
8	15.3	16.0	14.8	15.2	15.2	16.2
9	15.4	15.7	14.9	14.9	14.3	15.4
10	14.1	13.1	12.5	12.9	12.9	12.5
11	11.1	11.7	10.1	10.2	9.3	10.0
12	5.4	2.5	4.6	7.3	2.2	0.8
Yearly Mean (mm)	12.2	11.8	12.1	12.5	11.2	10.5
Seasonal Mean (mm)	14.1	14.5	13.6	13.7	13.4	14.3

Table A7

Table for Theissen's Areal weights, a_{ij}, km^2

Catchment / Station		Naam 1	Maridi 2	Tonj 3	Jur 4	Pongo 5	Loll 6
Aweil	1	0	0	0	0	1073	13005
Raga	2	0	0	0	0	1275	52144
Wau	3	0	0	0	11559	4565	0
Tonj	4	0	1613	9006	4301	0	0
Rumbek	5	2419	8938	269	0	0	0
Amadi	6	4570	0	0	0	0	0
Yubo	7	0	0	1075	28092	1515	189
Maridi	8	4973	4839	8401	0	0	0
Yambio	9	0	0	2957	10753	0	0
	SUM	11962	15390	21708	54705	8428	65338

Table A8

Mean Monthly Station Insolation, $\bar{q}_i$, kcal/cm^2/month

Month	Aweil 1	Raga 2	Wau 3	Tonj 4	Rumbek 5	Amadi* 6	Yubo 7	Maridi 8	Yambio 9
1	12.9	11.9	12.8	13.0	12.8	12.8	13.2	12.8	12.6
2	13.8	12.9	13.5	13.4	13.3	13.3	13.4	13.3	13.2
3	15.3	14.4	14.5	14.3	14.3	14.0	13.5	13.6	13.4
4	15.3	15.2	14.5	14.1	13.9	13.5	13.1	13.0	13.0
5	14.8	14.6	13.9	13.6	13.4	13.2	12.8	12.9	12.7
6	13.7	13.8	13.1	12.9	12.8	12.6	12.4	12.4	12.3
7	13.0	13.2	12.5	12.3	12.3	12.1	12.0	11.9	12.0
8	12.8	13.1	12.4	12.3	12.3	12.2	12.1	12.0	12.0
9	13.0	13.4	12.8	12.8	12.6	12.5	12.4	12.3	12.3
10	13.4	13.6	13.1	13.1	12.9	12.7	12.5	12.5	12.4
11	13.2	13.0	13.1	13.2	13.0	12.9	12.8	12.7	12.5
12	12.7	12.0	12.8	13.0	12.6	12.8	12.9	12.9	12.5
SUM	164	161	159	158	156	154	153	152	151

* Average of Station Rumbek and Maridi

Table A9

Mean Monthly Station Air Temperature,* $\overline{T}_A$, °C

Month	Aweil 1	Raga 2	Wau 3	Tonj 4	Rumbek 5	Amadi** 6	Yubo 7	Maridi 8	Yambio 9
1	26.0	22.9	26.6	27.0	27.1	26.1	26.2	25.0	25.5
2	27.8	24.7	28.2	27.9	28.2	27.1	26.5	25.9	26.4
3	30.7	27.6	30.2	29.7	30.3	28.4	26.9	26.5	26.7
4	30.8	29.1	30.3	29.3	29.4	27.4	25.9	25.3	26.0
5	29.8	28.0	29.0	28.2	28.3	26.8	25.3	25.2	25.4
6	27.5	26.4	27.3	26.8	27.0	25.6	24.5	24.2	24.6
7	26.2	25.3	26.1	25.5	26.0	24.6	23.8	23.2	23.9
8	25.7	25.1	25.9	25.6	25.9	24.7	23.9	23.5	23.9
9	26.2	25.7	26.6	26.5	26.6	25.3	24.5	24.0	24.6
10	26.9	26.1	27.4	27.3	27.3	25.9	24.7	24.4	24.7
11	26.6	24.9	27.4	27.5	27.5	26.2	25.4	24.8	24.9
12	25.6	23.0	26.6	26.9	26.6	25.9	25.6	25.2	24.9
Yearly Mean	27.5	25.7	27.6	27.4	27.5	26.2	25.3	24.8	25.1

* From 10 to 20 years of data in (1950 - 1975)
** Average of Station Rumbek and Maridi

Table A10

Mean Monthly Station Relative Humidity,* $\overline{S}$, %

Month	Aweil 1	Raga 2	Wau 3	Tonj 4	Rumbek 5	Amadi** 6	Yubo 7	Maridi 8	Yambio 9
1	36.0	36.4	31.5	39.2	40.0	47.9	52.7	55.8	57.8
2	33.7	34.2	28.6	34.5	37.7	46.2	54.6	54.6	57.6
3	33.9	38.0	35.4	39.4	42.8	53.2	63.0	63.6	66.5
4	47.1	51.7	50.1	57.0	57.8	66.9	73.2	76.0	76.7
5	58.7	64.9	62.8	65.5	71.2	74.0	78.3	76.8	79.2
6	70.3	73.2	70.5	71.7	74.6	77.6	79.7	80.6	80.7
7	78.0	80.0	75.2	77.9	77.9	80.7	81.8	83.5	84.8
8	81.1	80.9	77.6	79.6	80.1	82.1	83.6	84.1	84.8
9	79.4	78.9	73.8	77.3	77.0	79.7	80.2	82.4	81.1
10	71.6	73.1	68.8	72.2	73.3	75.9	78.9	78.4	81.2
11	54.7	56.7	51.3	60.6	59.9	66.7	71.9	73.4	74.5
12	42.8	44.3	37.6	49.5	42.9	51.8	60.4	60.7	66.2
Yearly Mean	57.3	59.4	55.3	60.4	61.3	66.9	71.5	72.5	74.3

* From 12 to 21 years of data in (1950 - 1975)
** Average of Station Rumbek and Maridi

Table A11

Mean Monthly Station Cloud Cover*, $\bar{N}$, %

Month	Aweil 1	Raga 2	Wau 3	Tonj 4	Rumbek 5	Amadi** 6	Yubo 7	Maridi 8	Yambio 9
1	25.0	50.4	40.9	41.3	59.2	51.1	25.9	42.9	41.7
2	31.3	59.6	44.2	47.1	60.5	56.7	29.2	52.9	45.0
3	42.9	62.9	60.4	61.7	73.8	71.1	42.8	68.3	65.0
4	60.0	77.5	65.9	70.4	79.2	80.3	55.0	81.3	75.0
5	58.8	80.8	70.9	69.2	77.5	77.9	51.7	78.3	73.8
6	68.9	83.8	71.0	71.8	76.3	77.4	50.0	78.4	72.5
7	75.9	86.7	79.6	78.8	83.3	83.1	56.8	82.8	79.9
8	77.9	85.9	79.2	76.2	82.1	81.5	51.0	80.8	78.7
9	72.1	84.2	75.0	73.8	79.2	78.8	46.3	78.4	72.5
10	56.0	80.4	69.3	66.4	79.2	78.4	51.3	77.5	75.0
11	34.2	69.6	54.2	51.3	74.2	70.3	41.3	66.3	65.0
12	26.7	59.6	38.8	39.2	63.8	57.8	30.0	51.7	42.9
Yearly mean	52.5	73.5	62.5	62.3	74.0	72.0	44.3	70.0	65.6

* From 10 to 21 yrs. of data in (1950 - 1975)

** Average of station Rumbek and Maridi

Table A12

Space-time Mean Monthly Catchment Air Temperature, $\underline{\overline{T_A}}$, ^oC

Month	Naam 1	Maridi 2	Tonj 3	Jur 4	Pongo 5	Loll 6
1	25.8	26.4	26.0	26.2	25.9	23.5
2	26.8	27.5	26.9	27.0	27.3	25.3
3	28.0	29.0	27.9	27.8	29.3	28.2
4	26.9	28.1	27.1	27.1	29.4	29.4
5	26.4	27.3	26.5	26.3	28.3	28.4
6	25.3	26.1	25.4	25.3	26.7	26.6
7	24.3	25.1	24.3	24.4	25.6	25.5
8	24.4	25.1	24.5	24.5	25.4	25.2
9	25.0	25.8	25.2	25.1	26.0	25.8
10	25.6	26.4	25.7	25.5	26.7	26.3
11	25.9	26.7	26.0	26.0	26.6	25.2
12	25.8	26.2	25.9	25.8	25.8	23.5
Yearly Mean	25.9	26.6	26.0	25.9	26.9	26.1
Seasonal Mean	25.8	26.6	25.8	25.8	27.2	26.8

Table A13

Mean Monthly Station Potential Evaporation (Water Surface)*, $\bar{e}_{pw}$, mm/month

Month	Aweil 1	Raga 2	Wau 3	Tonj 4	Rumbek 5	Amadi 6	Yubo 7	Maridi 8	Yambio 9
1	130	117	135	136	139	131	126	123	120
2	150	136	152	148	150	143	132	136	133
3	178	161	170	166	170	157	133	143	139
4	180	177	169	164	161	148	128	135	135
5	166	164	155	147	147	140	118	132	128
6	146	150	139	135	135	129	111	123	121
7	135	139	131	126	129	123	107	116	117
8	131	137	128	125	127	122	104	117	116
9	134	142	134	132	133	127	109	121	121
10	134	145	139	136	139	132	113	124	122
11	131	135	139	137	142	134	118	125	122
12	124	118	132	131	135	131	119	126	115
Yearly	1739	1721	1723	1683	1707	1617	1418	1521	1489

* Albedo = 0.05

Table A14

Mean Monthly Station Potential Evaporation (Wet Soil Surface)*, $\bar{e}_p$, mm/month

Month	Aweil 1	Raga 2	Wau 3	Tonj 4	Rumbek 5	Amadi 6	Yubo 7	Marido 8	Yambio 9
1	122	110	127	128	131	123	118	115	112
2	140	128	143	140	142	135	123	128	125
3	167	152	160	156	160	147	124	134	130
4	169	167	159	155	152	139	119	126	127
5	156	155	146	139	138	131	110	124	120
6	137	141	131	127	127	122	104	116	113
7	127	131	123	118	121	115	99	109	110
8	123	129	121	117	119	115	97	110	109
9	125	134	126	124	125	120	102	114	113
10	125	136	130	128	130	124	105	117	114
11	122	127	131	128	134	126	110	117	114
12	116	111	124	122	127	123	110	118	107
Yearly	1629	1621	1621	1582	1606	1520	1321	1428	1394

* Albedo = 0.1

Table A15

Mean Monthly Station Piche Tube Evaporation* $\bar{e}_p$' (mm/month)

Month	Aweil 1	Raga 2	Wau 3	Tonj 4	Rumbek 5	Amadi** 6	Yubo 7	Maridi 8	Yambio 9
1	319	298	350	415	282	248	254	214	211
2	357	322	357	444	293	254	255	215	209
3	397	360	360	400	285	225	186	164	171
4	309	276	267	270	183	138	120	93	111
5	211	183	186	189	133	107	93	81	90
6	120	123	126	138	93	80	78	66	75
7	87	102	102	96	74	65	68	56	62
8	71	87	90	87	71	64	68	56	62
9	84	96	105	105	81	72	75	63	72
10	124	127	130	141	105	90	81	74	78
11	198	198	225	246	165	134	126	102	99
12	264	257	310	353	229	197	208	164	155
Yearly (mm/yr)	2541	2429	2608	2884	1994	1674	1612	1348	1395

* From 13 to 21 years of data in (1950 - 1975)
** Average of Station Rumbek and Maridi

Table A16

Space-Time Mean Monthly Catchment Piché Tube Evaporation, $\bar{e}'_p$, mm/month

Month	Naam 1	Maridi 2	Tonj 3	Jur 4	Pongo 5	Loll 6
1	241	275	300	278	321	302
2	246	284	312	282	333	329
3	212	259	265	237	333	367
4	128	164	171	161	247	282
5	101	123	128	120	172	188
6	77	89	98	92	116	122
7	63	71	74	76	94	99
8	62	68	70	73	83	84
9	70	78	82	83	96	94
10	86	99	103	95	120	126
11	127	154	163	151	200	198
12	190	222	244	231	278	258
Yearly (mm/yr)	1603	1884	2012	1880	2393	2449

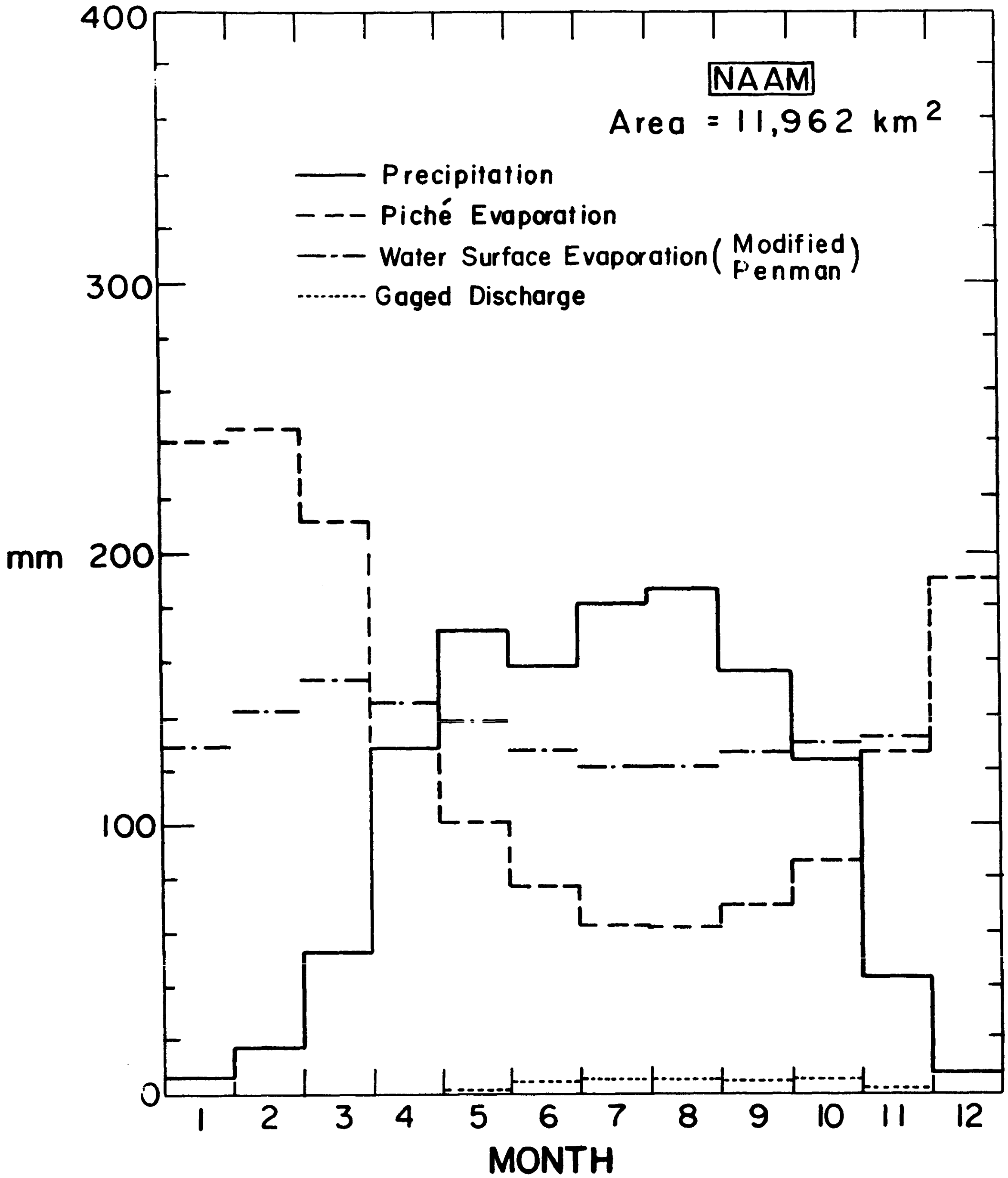

FIGURE A.1

MONTHLY DISTRIBUTIONS OF HYDROLOGIC PARAMETERS

(NAAM CATCHMENT)

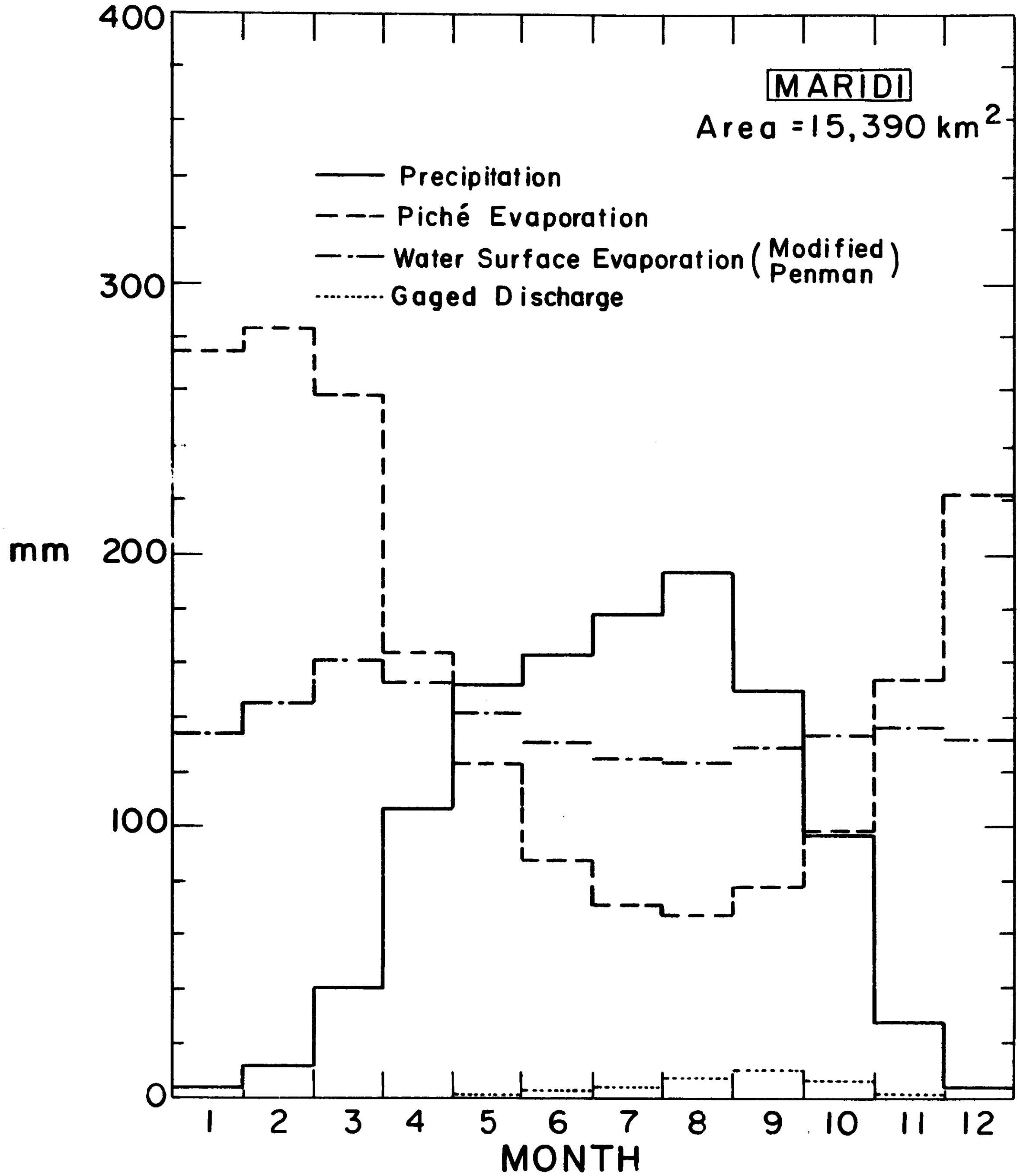

FIGURE A.2

MONTHLY DISTRIBUTIONS OF HYDROLOGIC PARAMETERS

(MARIDI CATCHMENT)

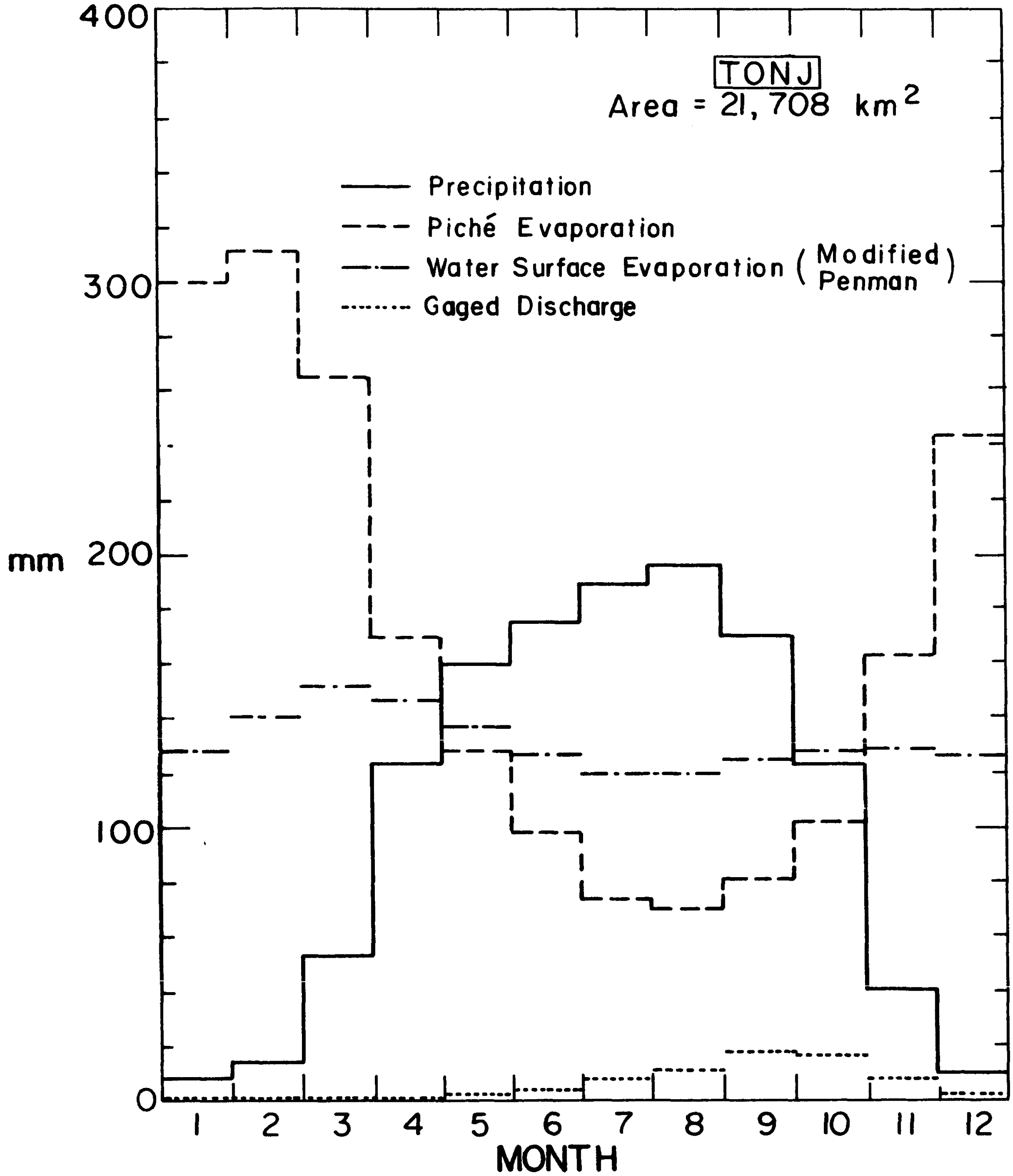

FIGURE A.3

MONTHLY DISTRIBUTIONS OF HYDROLOGIC PARAMETERS

(TONJ CATCHMENT)

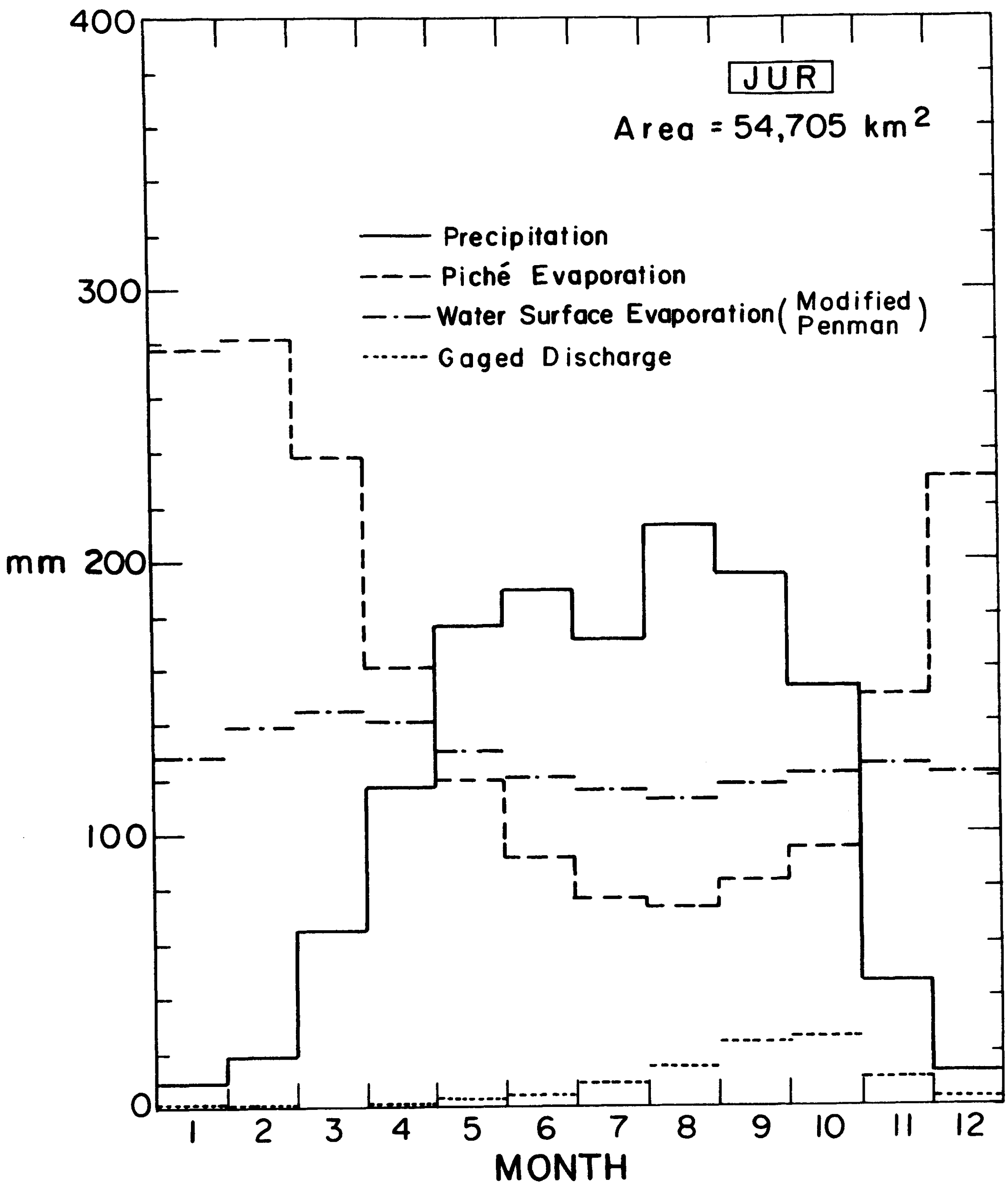

FIGURE A.4

MONTHLY DISTRIBUTIONS OF HYDROLOGIC PARAMETERS

(JUR CATCHMENT)

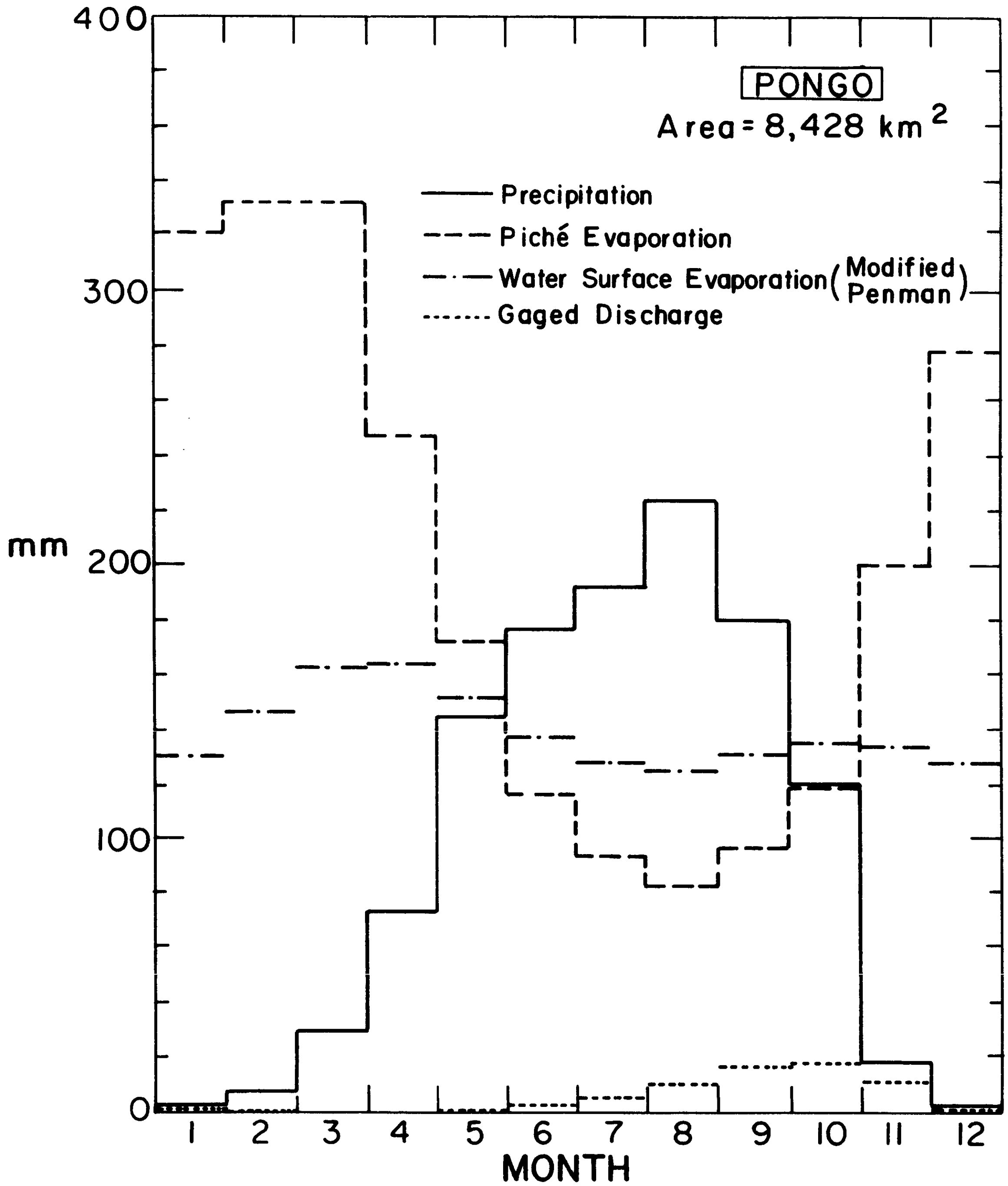

FIGURE A.5

MONTHLY DISTRIBUTIONS OF HYDROLOGIC PARAMETERS

(PONGO CATCHMENT)

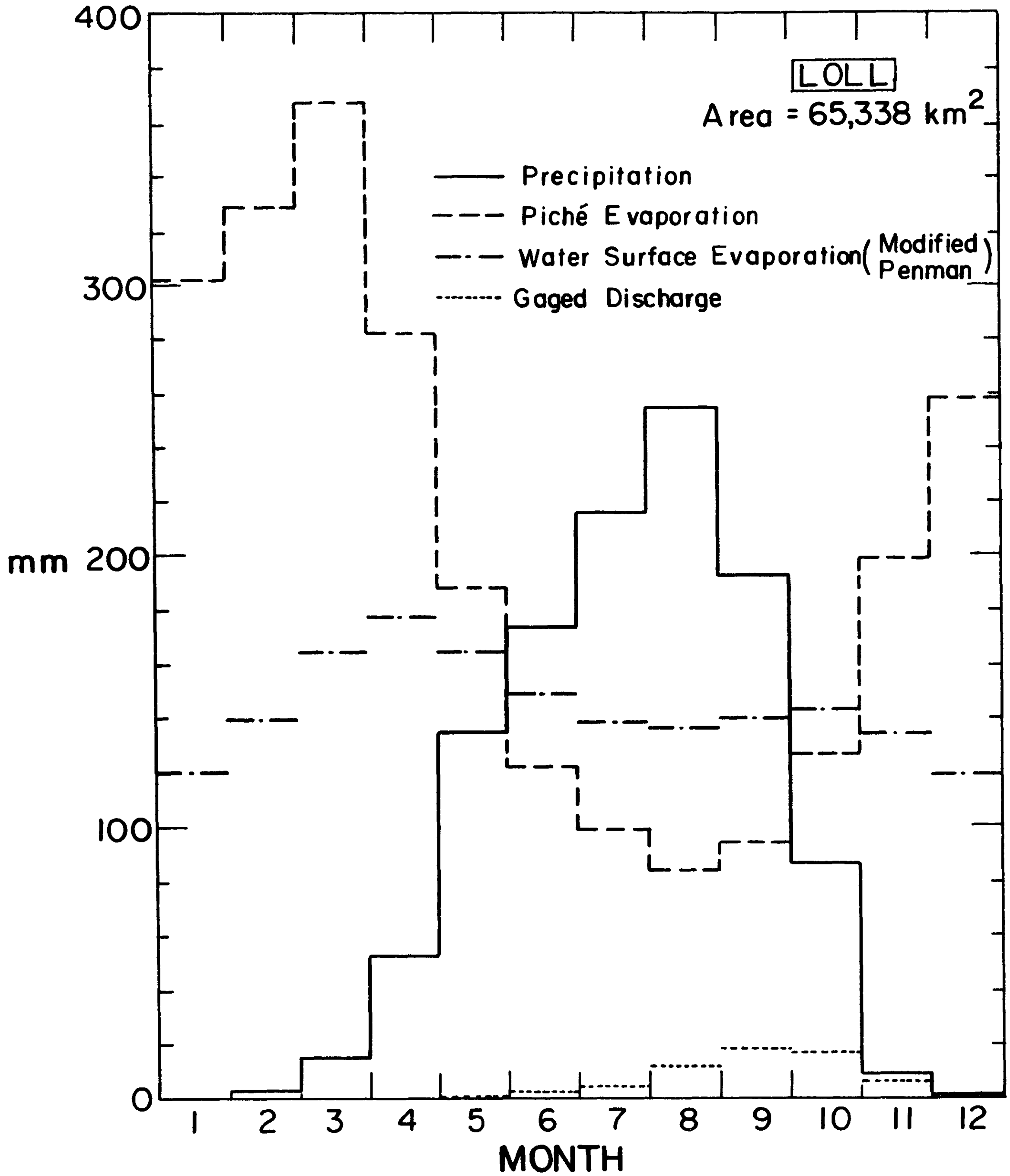

FIGURE A.6

MONTHLY DISTRIBUTIONS OF HYDROLOGIC PARAMETERS

(LOLL CATCHMENT)

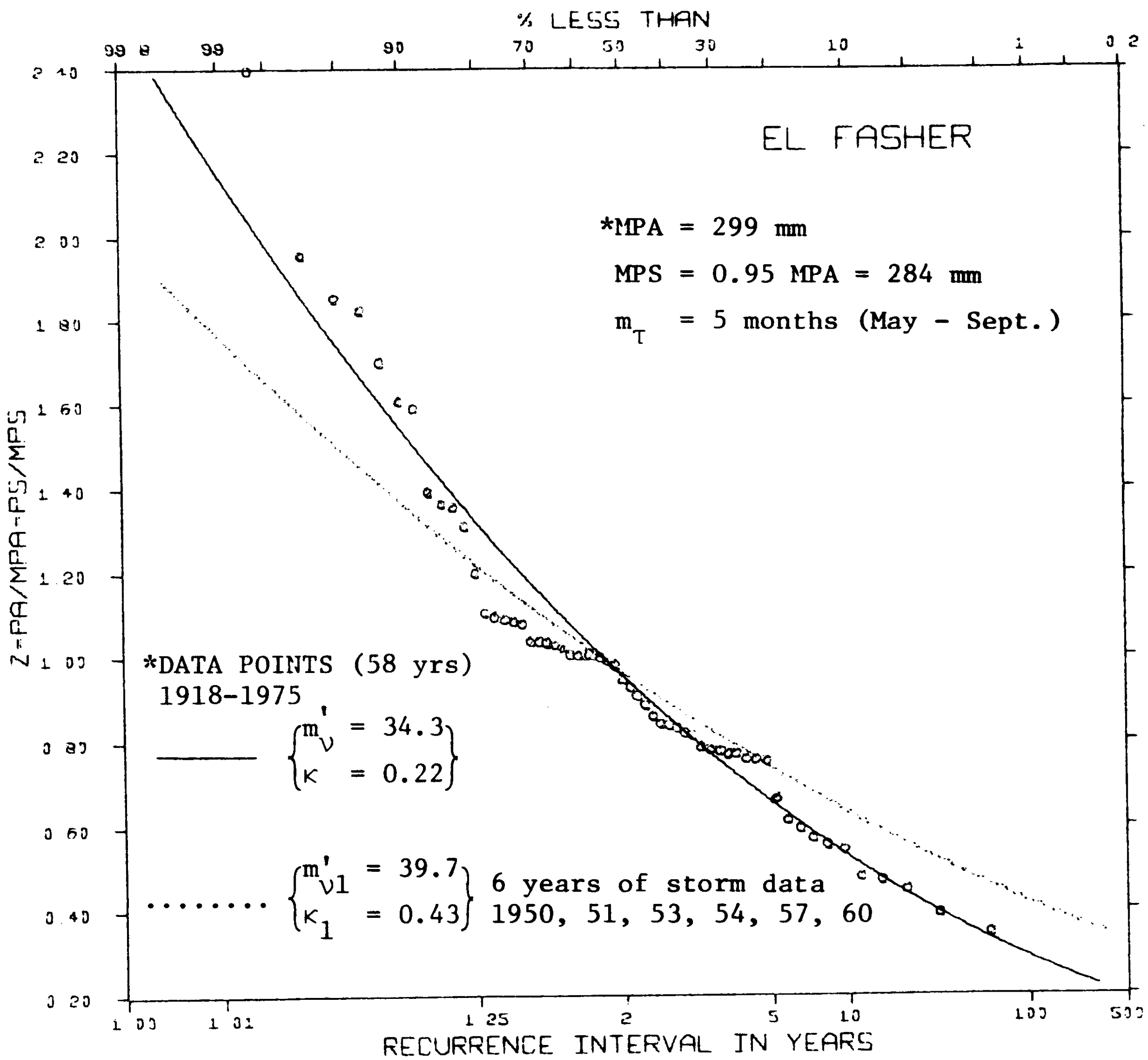

FIGURE A.7

FREQUENCY OF ANNUAL PRECIPITATION

(STATION EL FASHER)

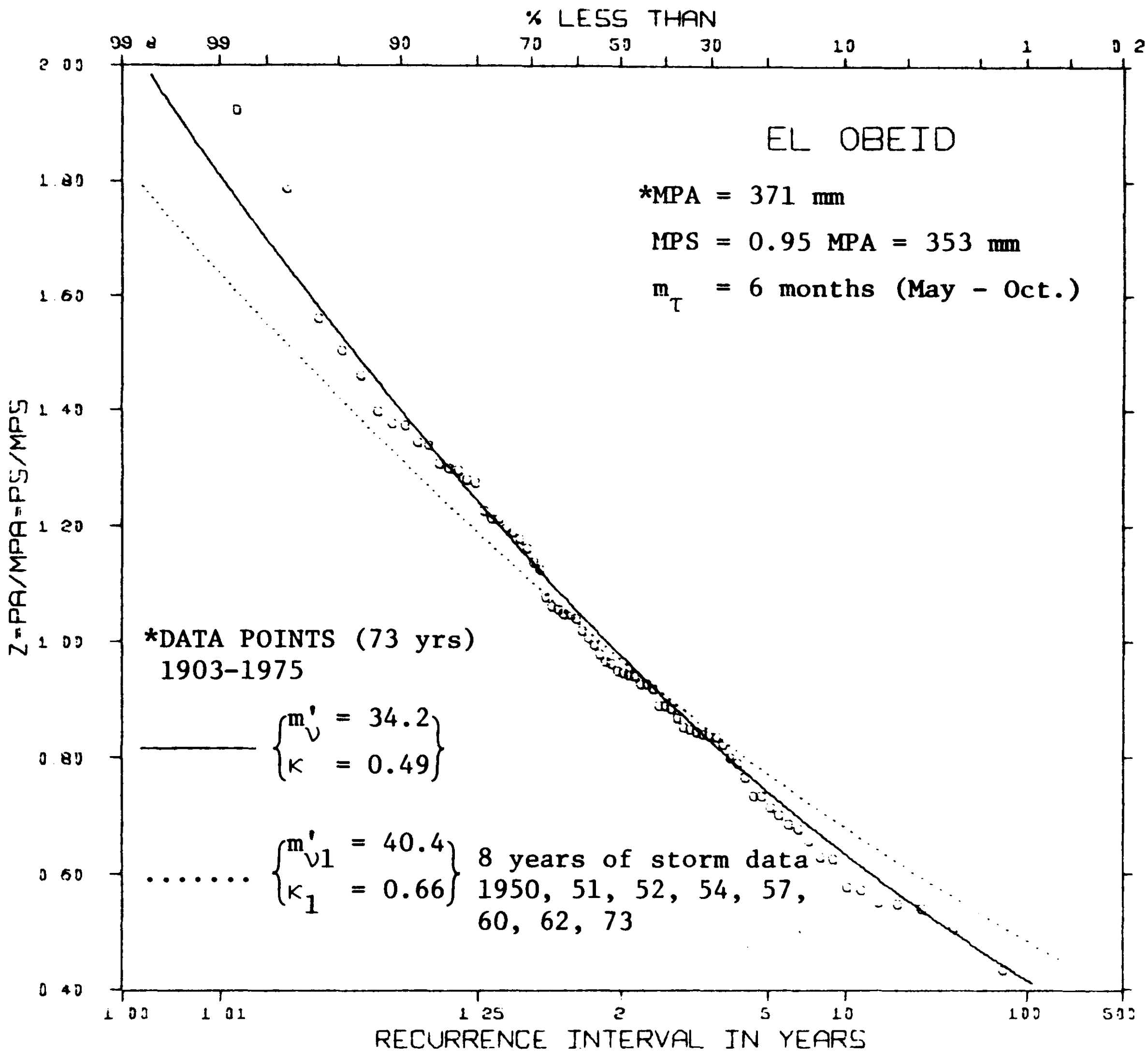

FIGURE A.8

FREQUENCY OF ANNUAL PRECIPITATION

(STATION EL OBEID)

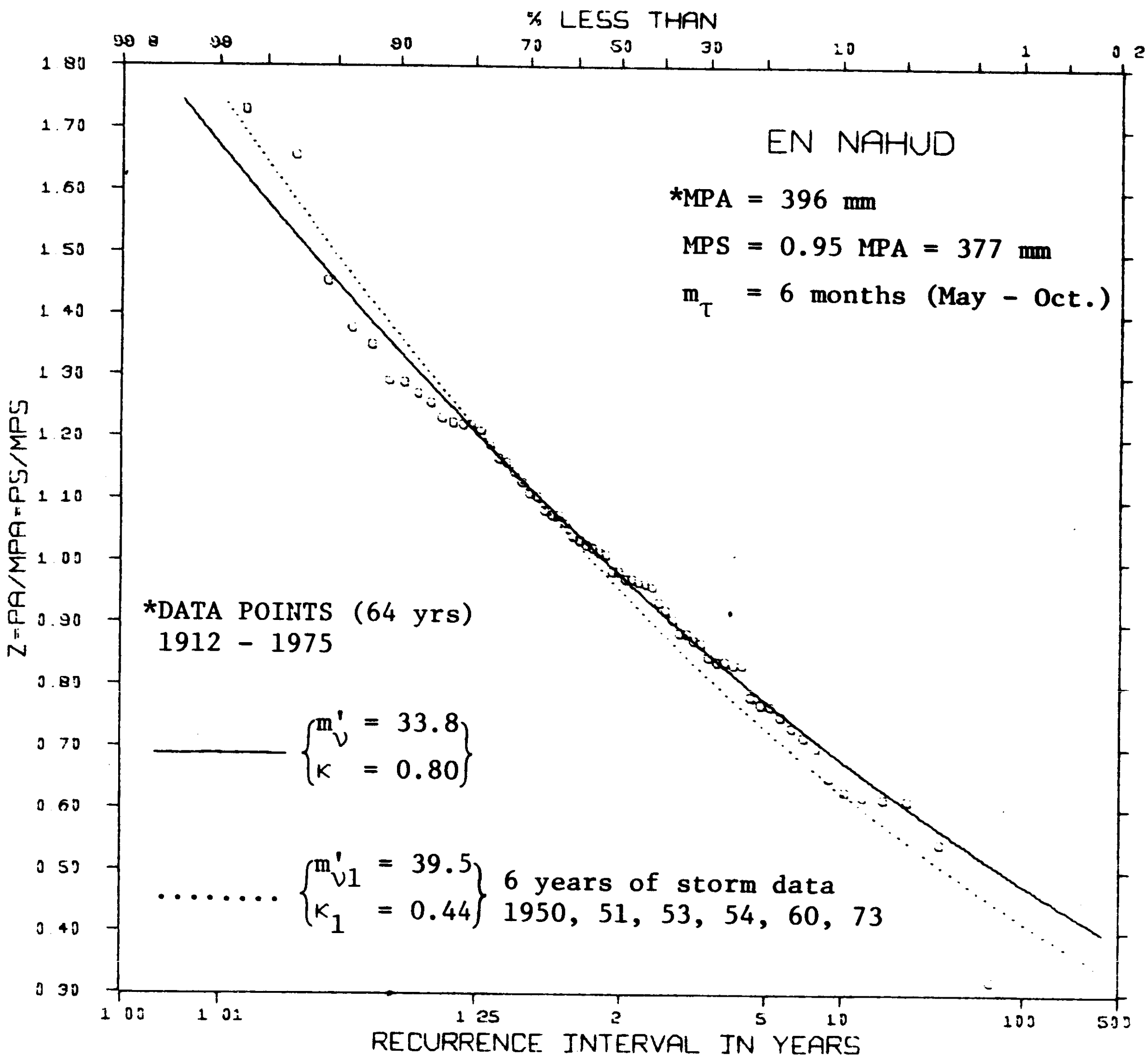

FIGURE A.9

FREQUENCY OF ANNUAL PRECIPITATION

(STATION EN NAHUD)

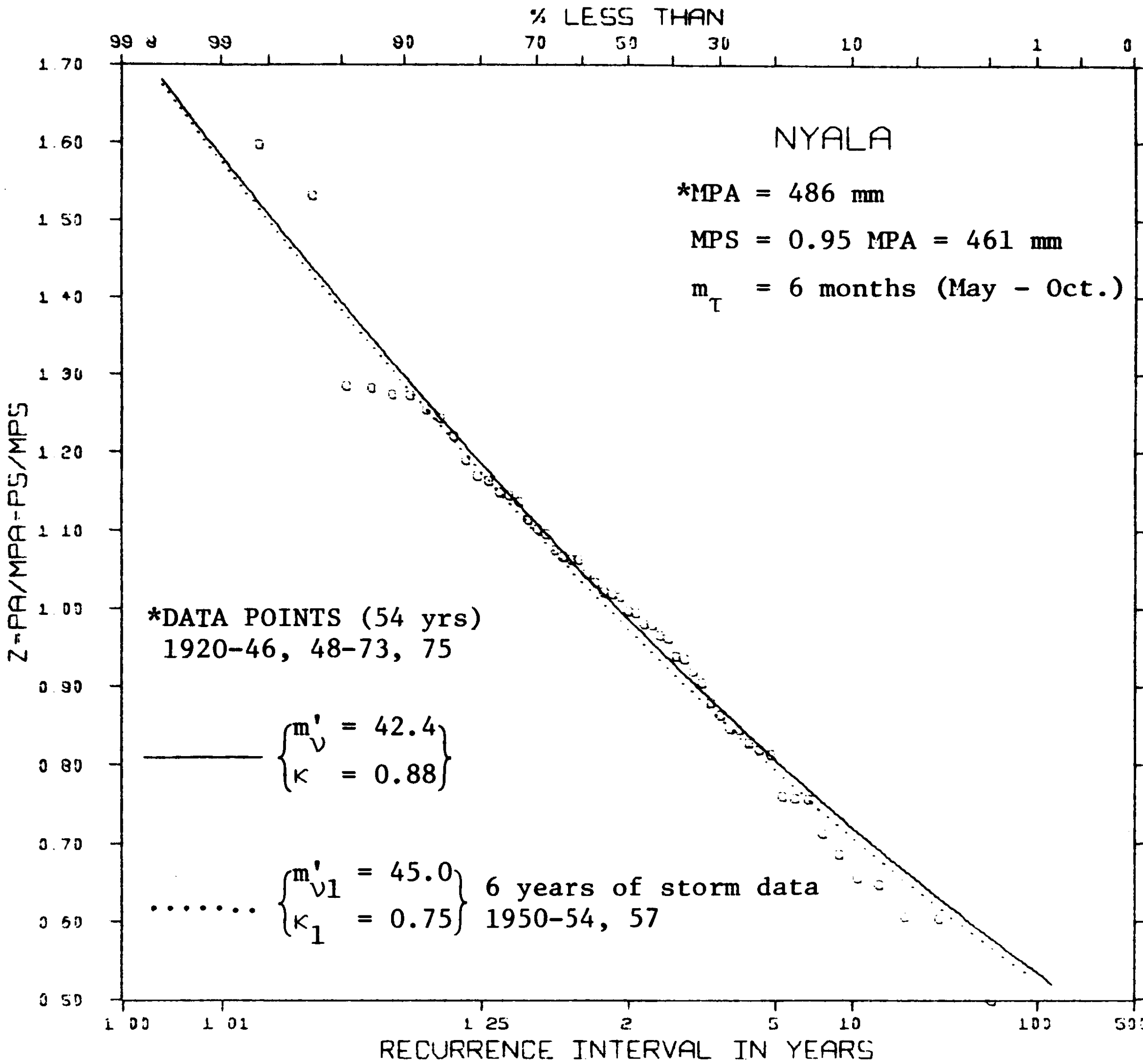

FIGURE A.10

FREQUENCY OF ANNUAL PRECIPITATION

(STATION NYALA)

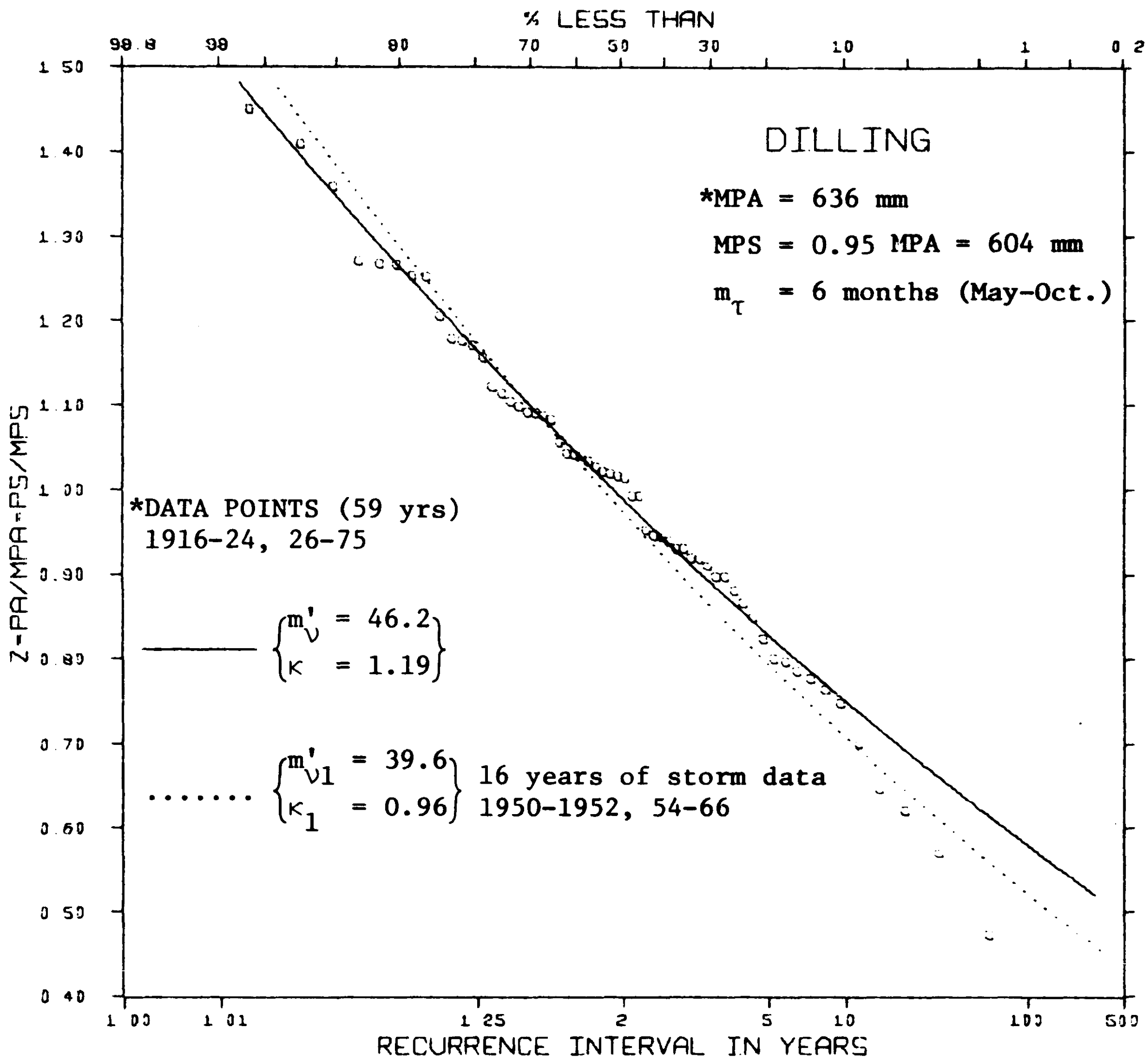

FIGURE A.11

FREQUENCY OF ANNUAL PRECIPITATION

(STATION DILLING)

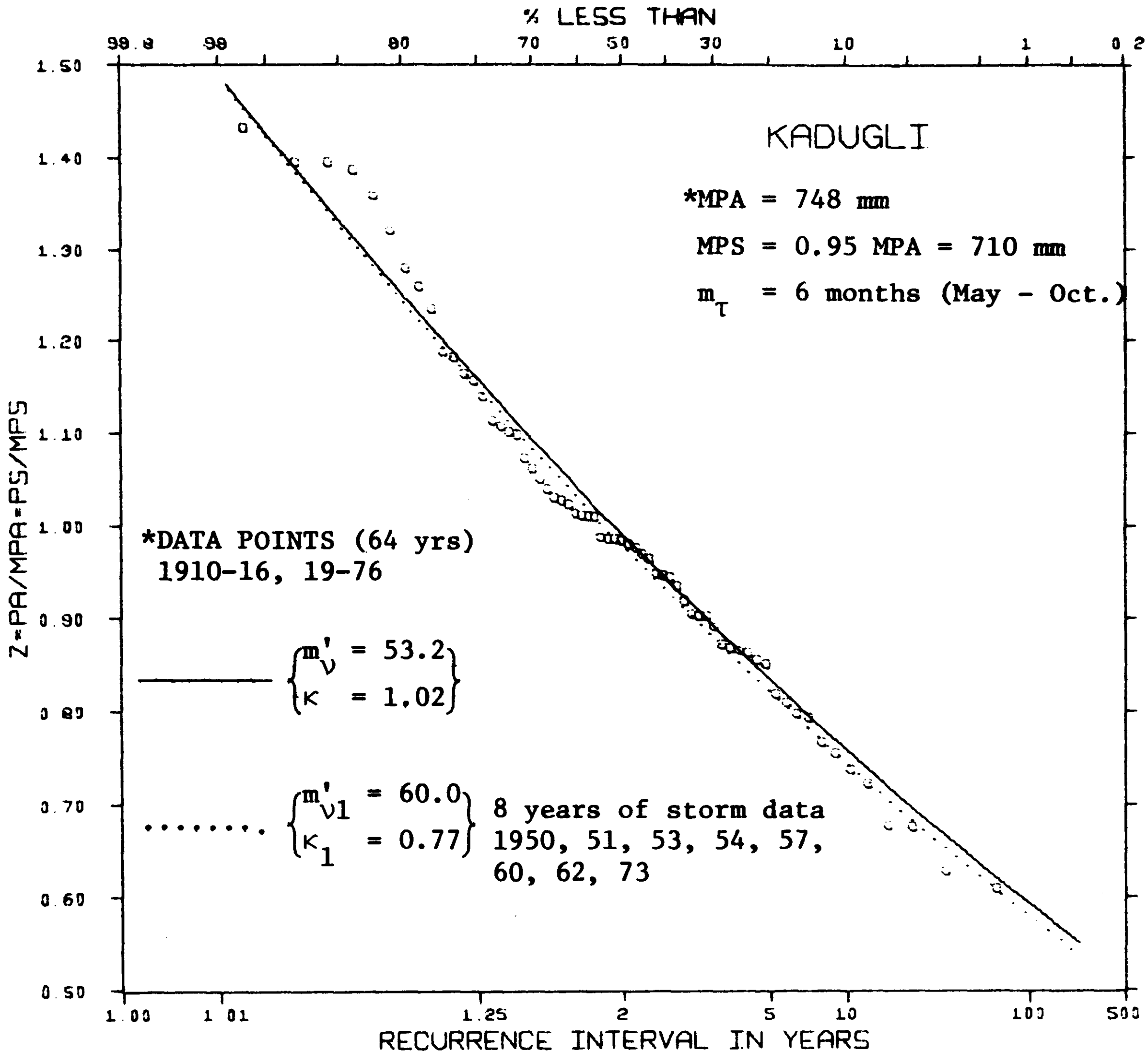

FIGURE A.12

FREQUENCY OF ANNUAL PRECIPITATION

(STATION KADUGLI)

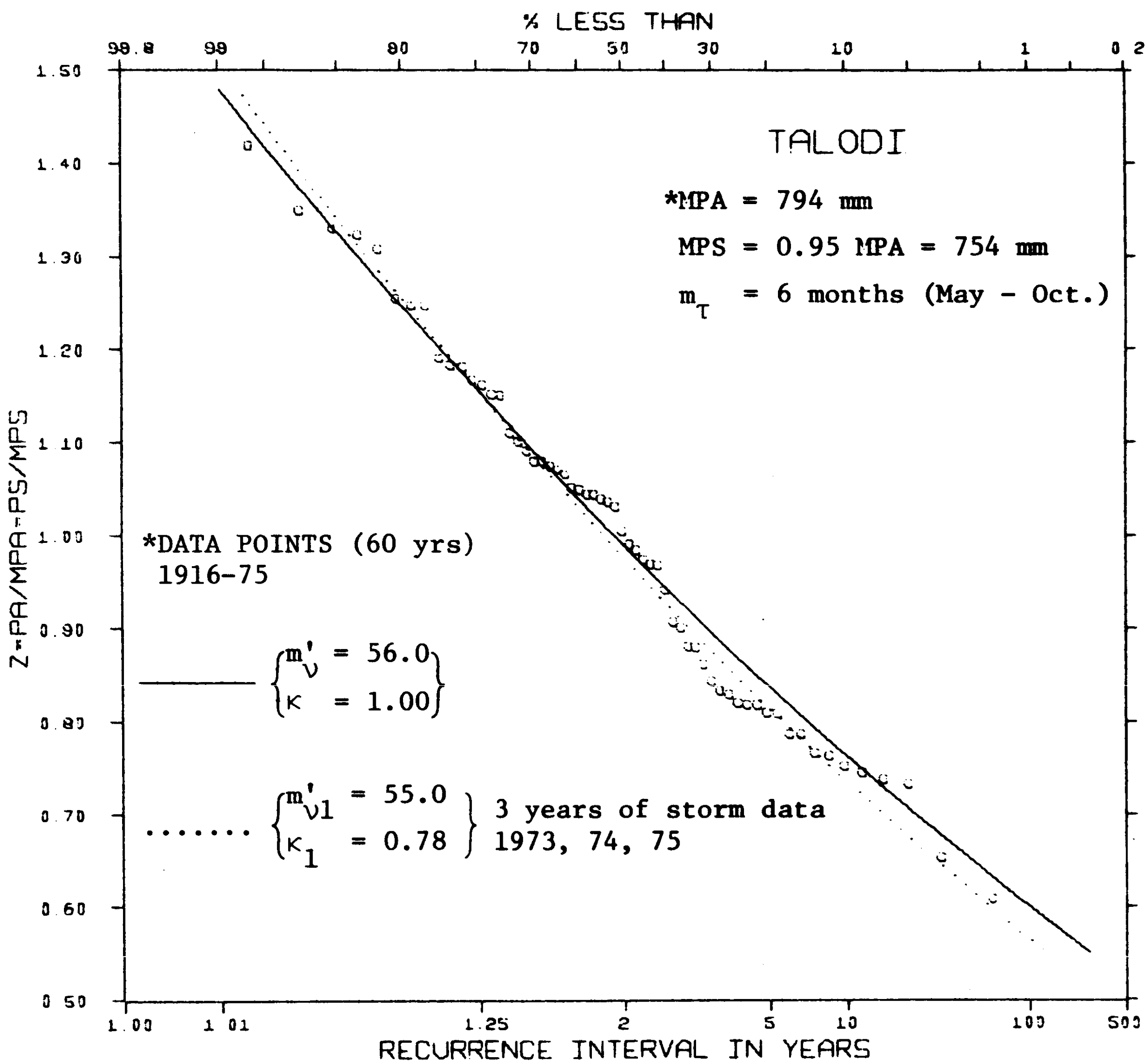

FIGURE A.13

FREQUENCY OF ANNUAL PRECIPITATION

(STATION TALODI)

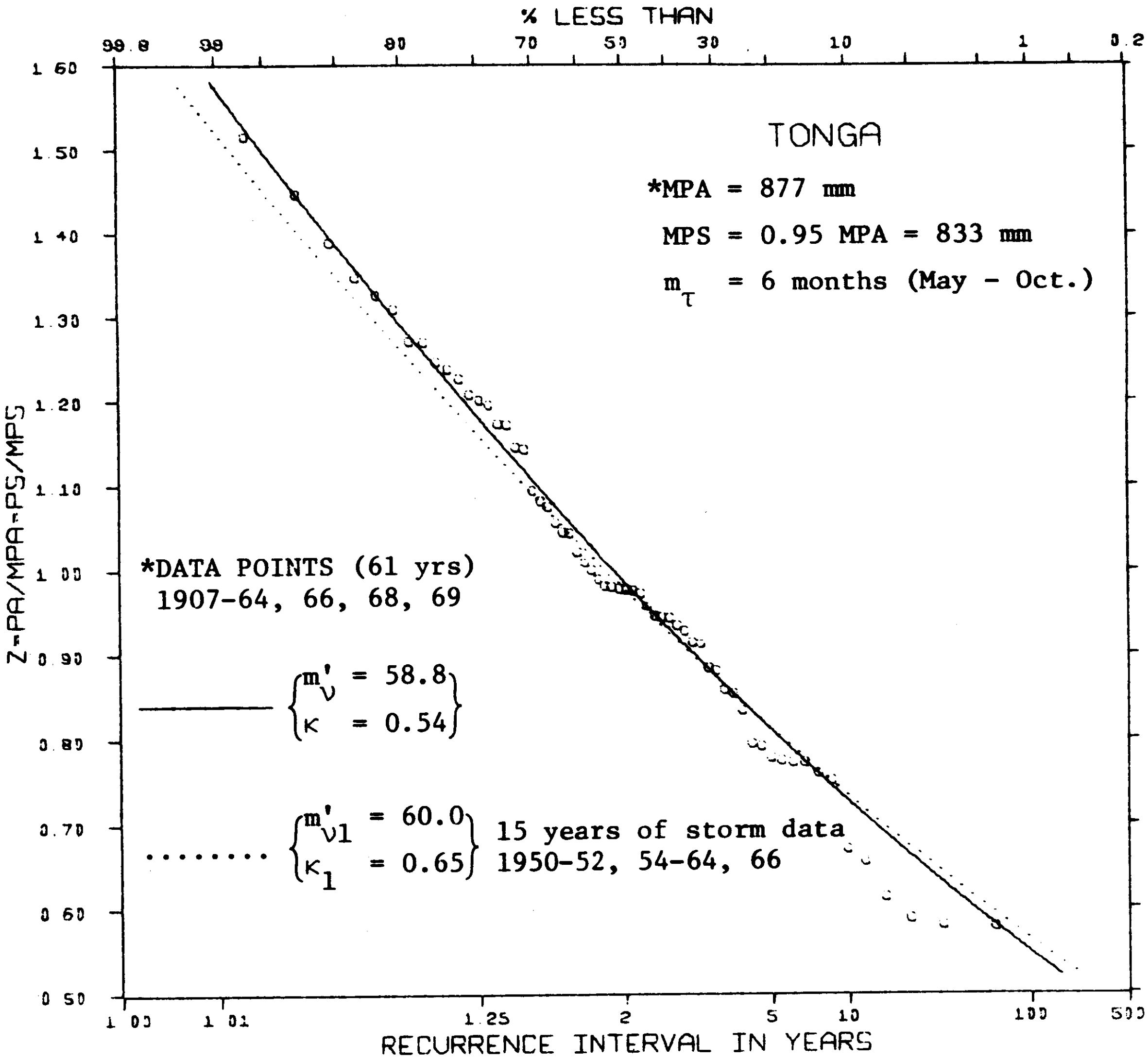

FIGURE A.14

FREQUENCY OF ANNUAL PRECIPITATION

(STATION TONGA)

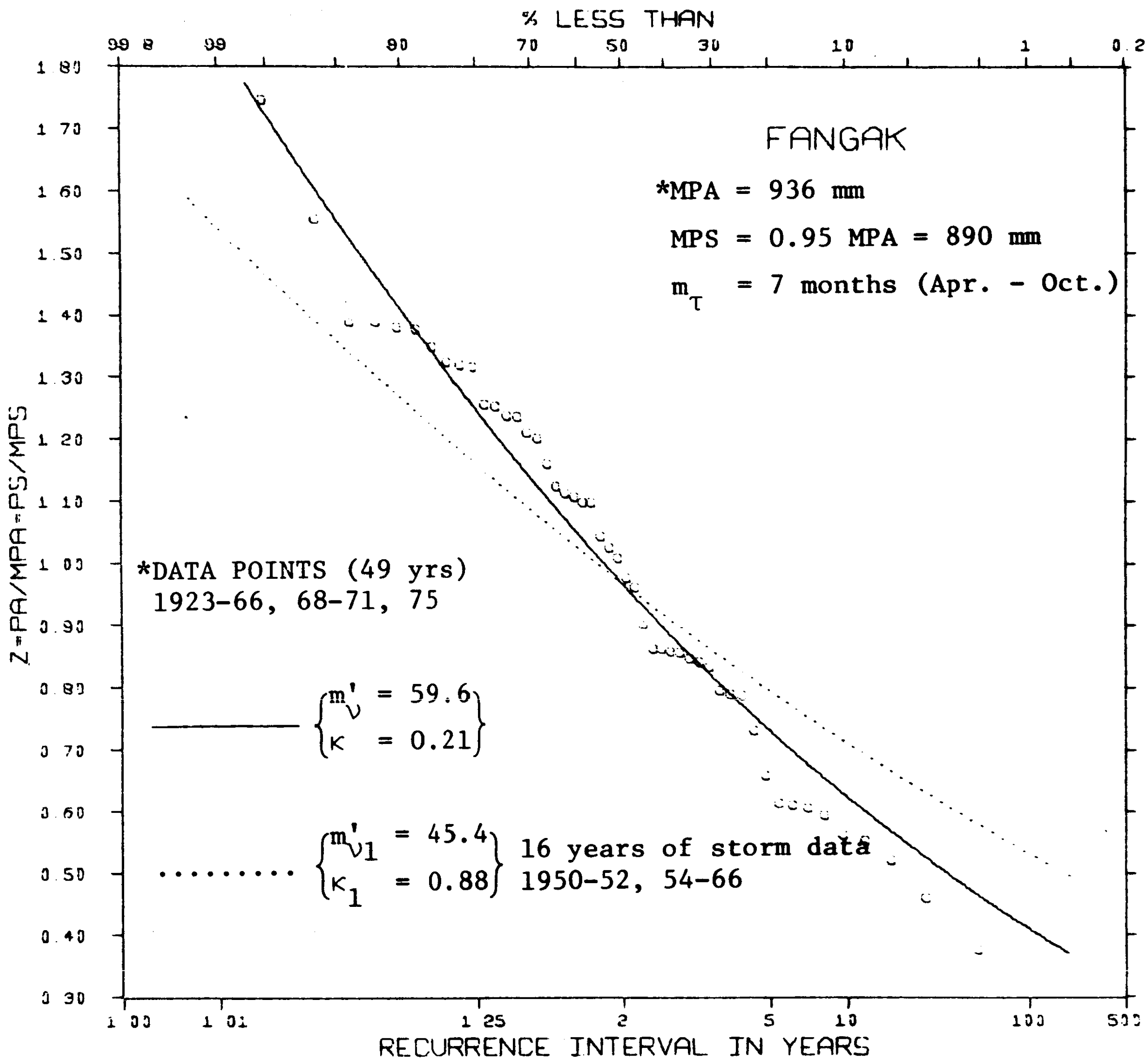

FIGURE A.15

FREQUENCY OF ANNUAL PRECIPITATION

(STATION FANGAK)

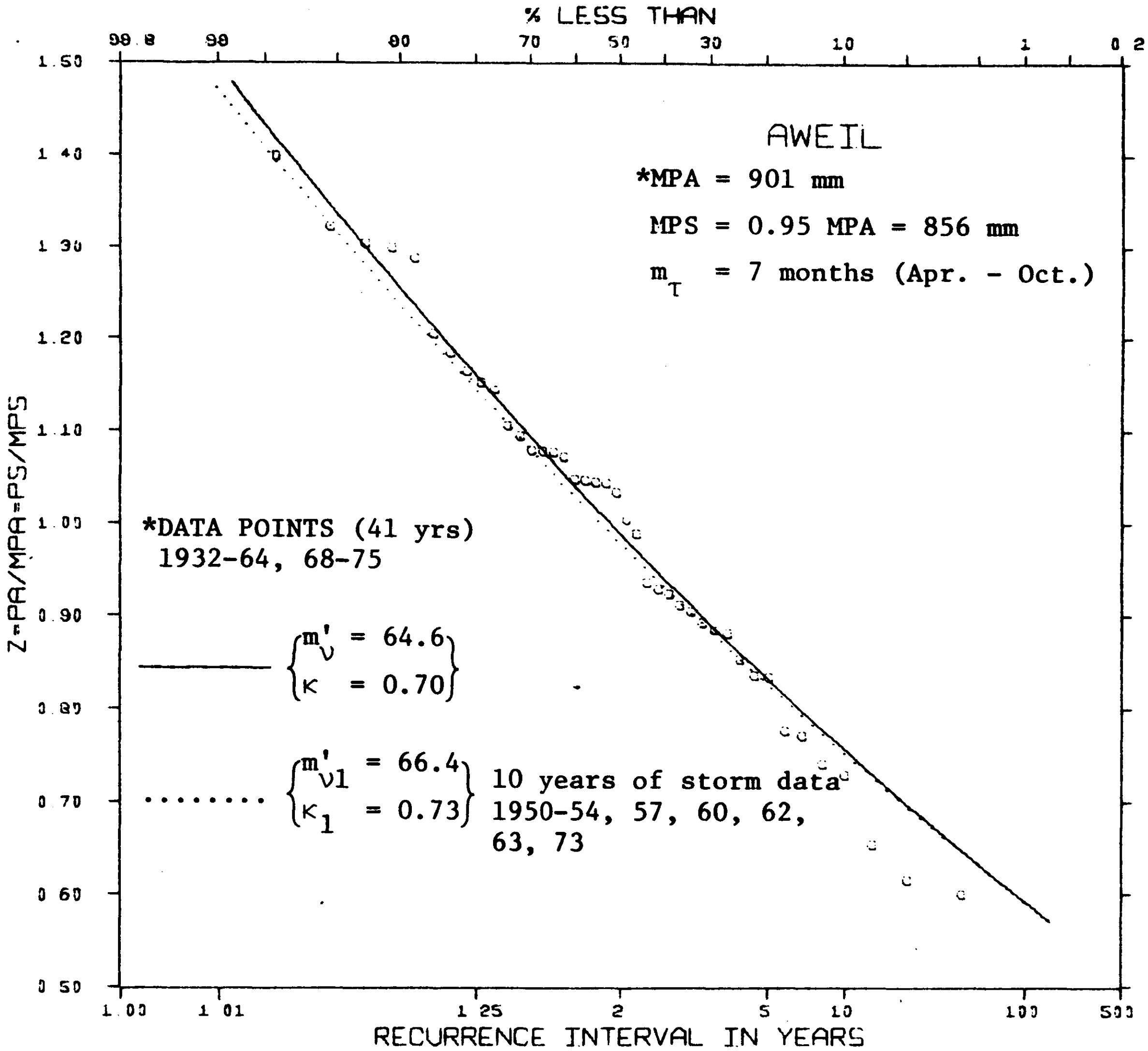

FIGURE A.16

FREQUENCY OF ANNUAL PRECIPITATION

(STATION AWEIL)

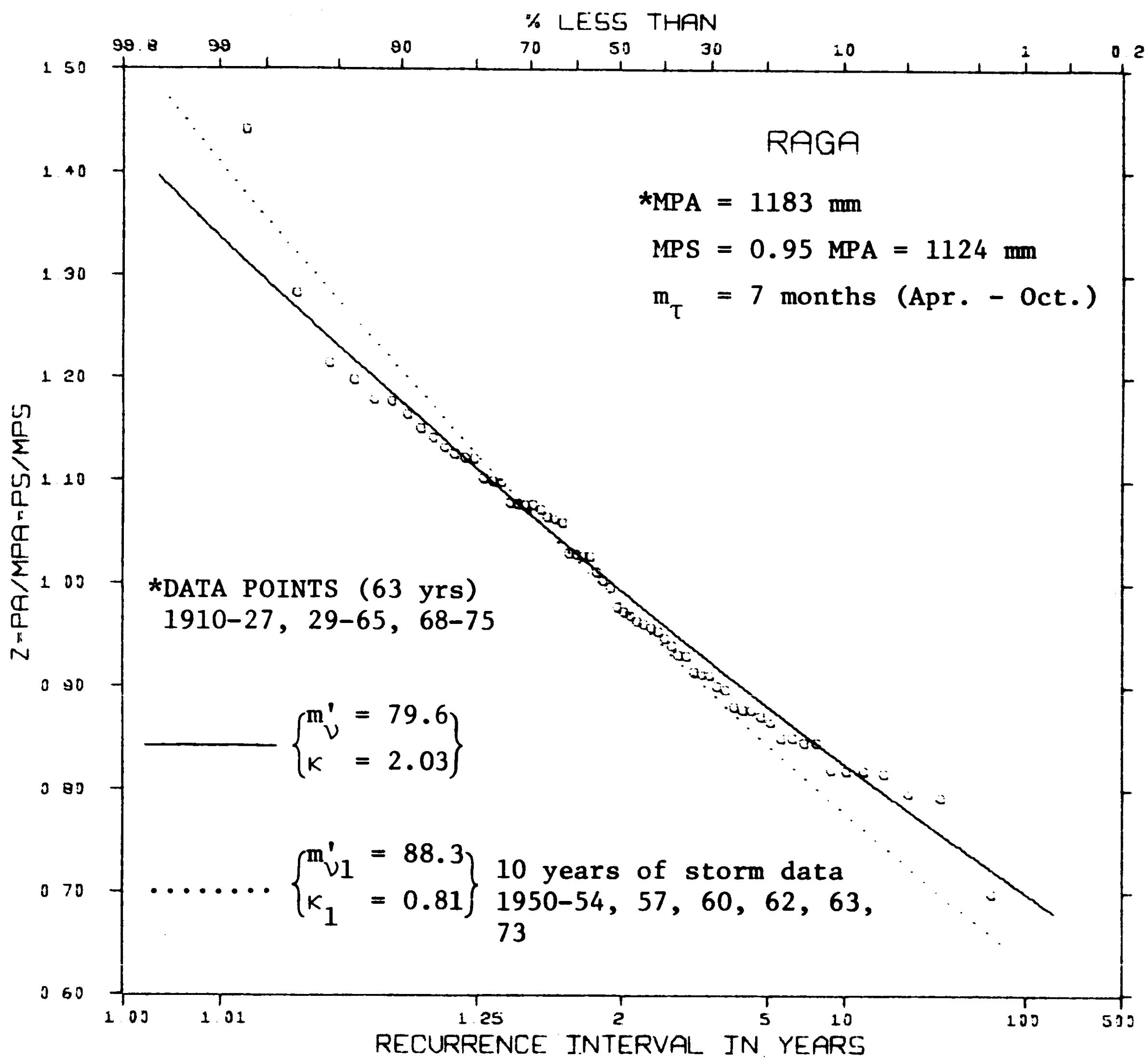

FIGURE A.17

FREQUENCY OF ANNUAL PRECIPITATION

(STATION RAGA)

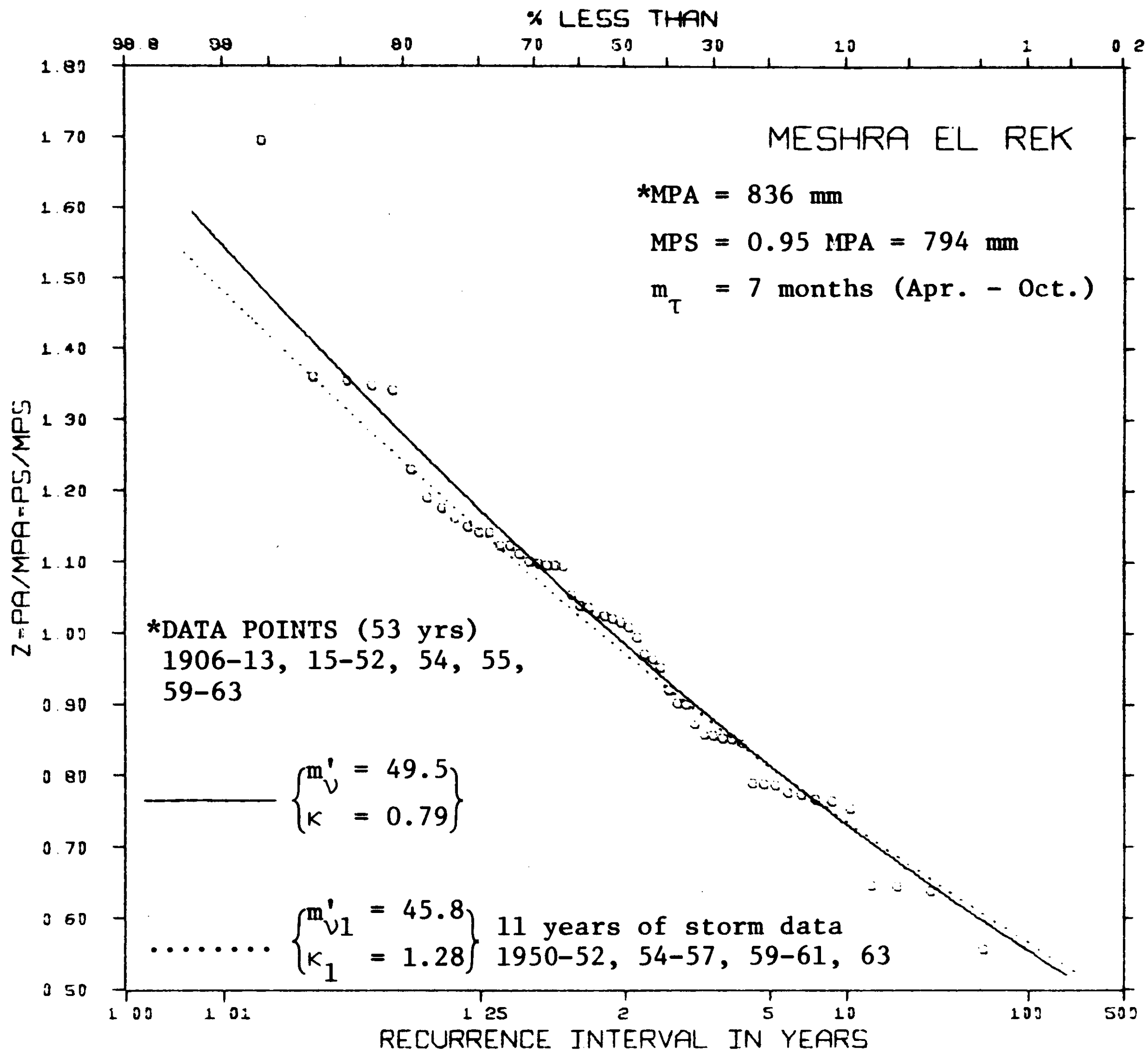

FIGURE A.18

FREQUENCY OF ANNUAL PRECIPITATION

(STATION MESHRA EL REK)

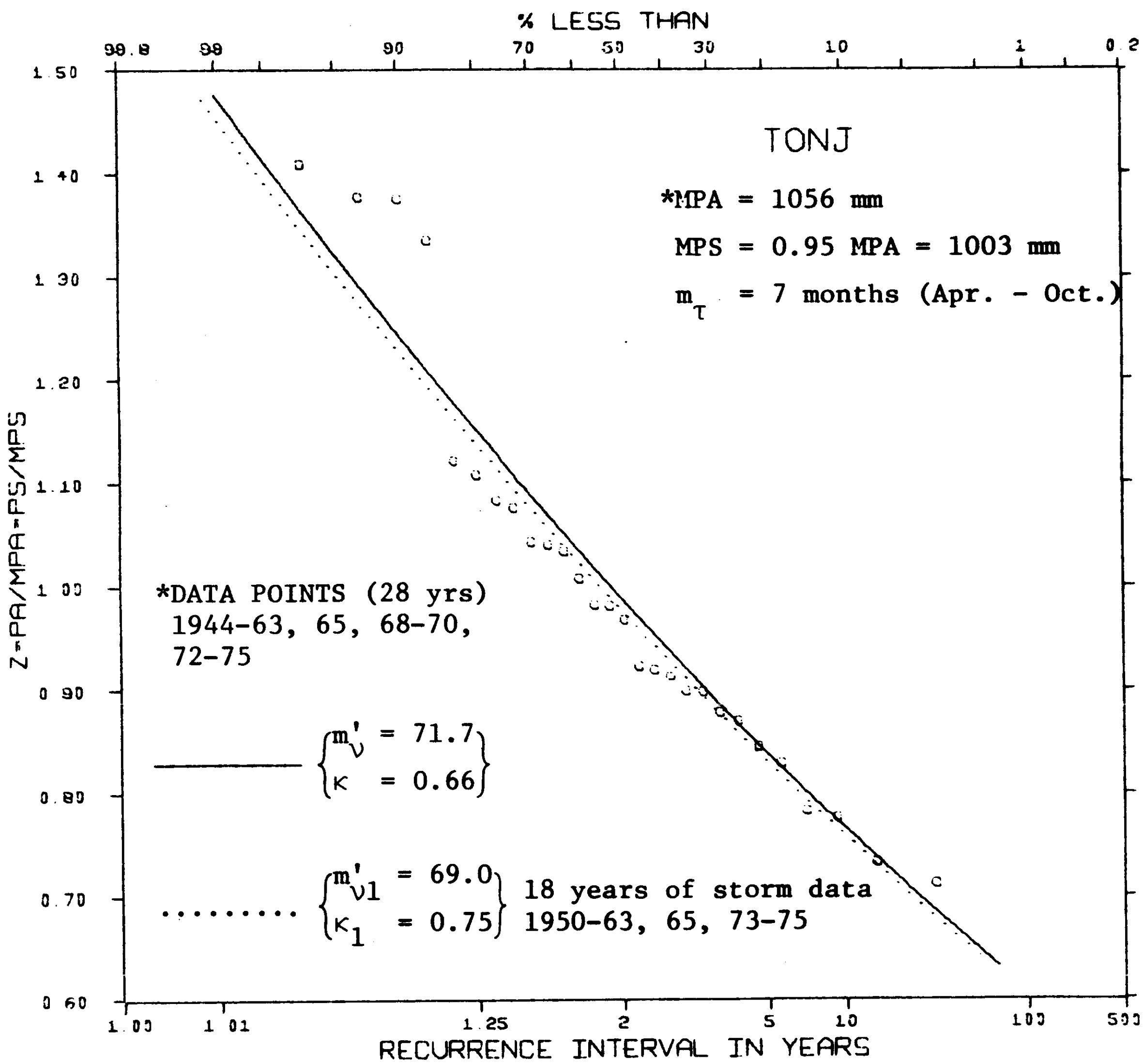

FIGURE A.19

FREQUENCY OF ANNUAL PRECIPITATION

(STATION TONJ)

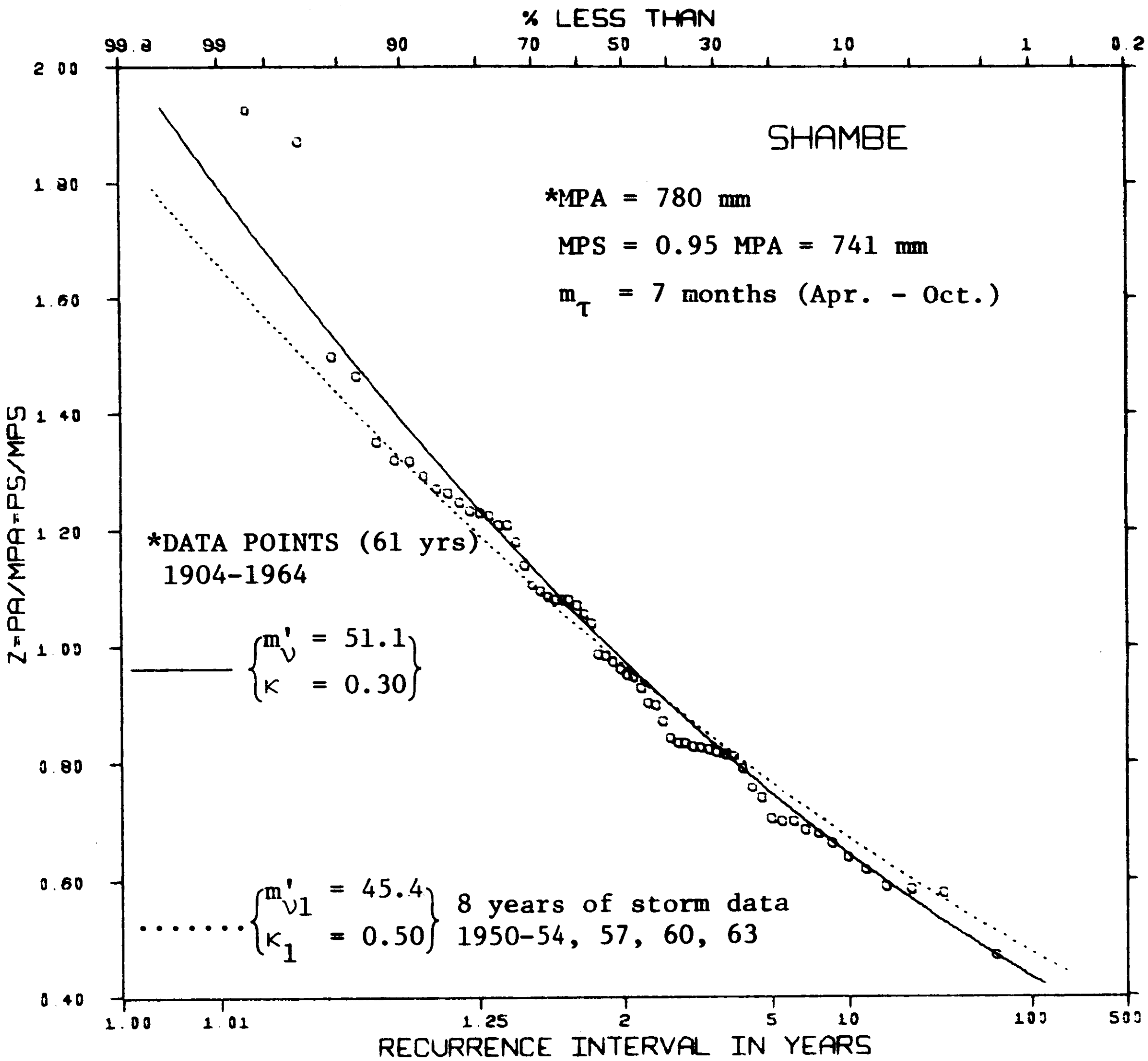

FIGURE A.20

FREQUENCY OF ANNUAL PRECIPITATION

(STATION SHAMBE)

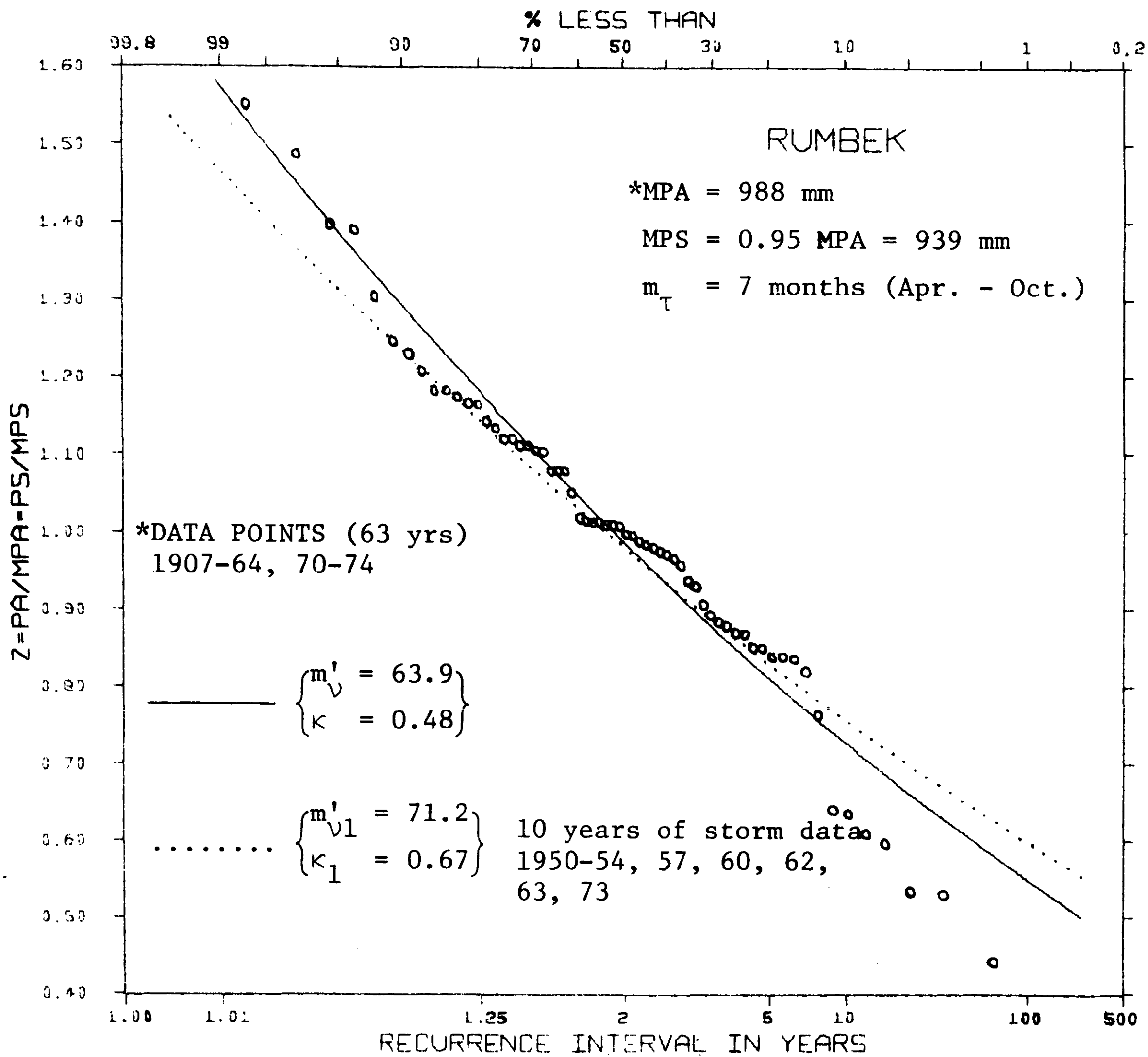

FIGURE A.21

FREQUENCY OF ANNUAL PRECIPITATION

(STATION RUMBEK)

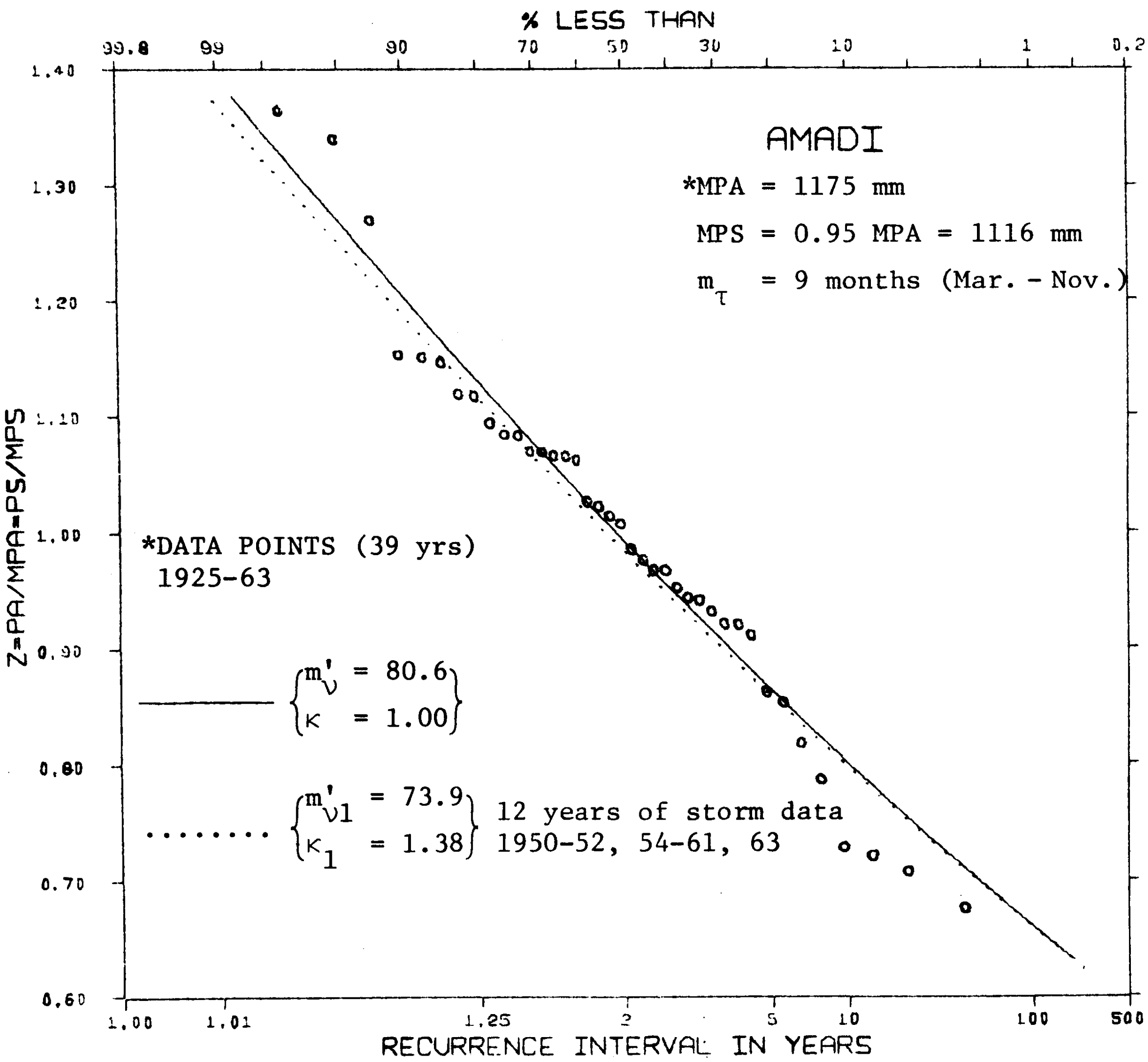

FIGURE A.22

FREQUENCY OF ANNUAL PRECIPITATION

(STATION AMADI)

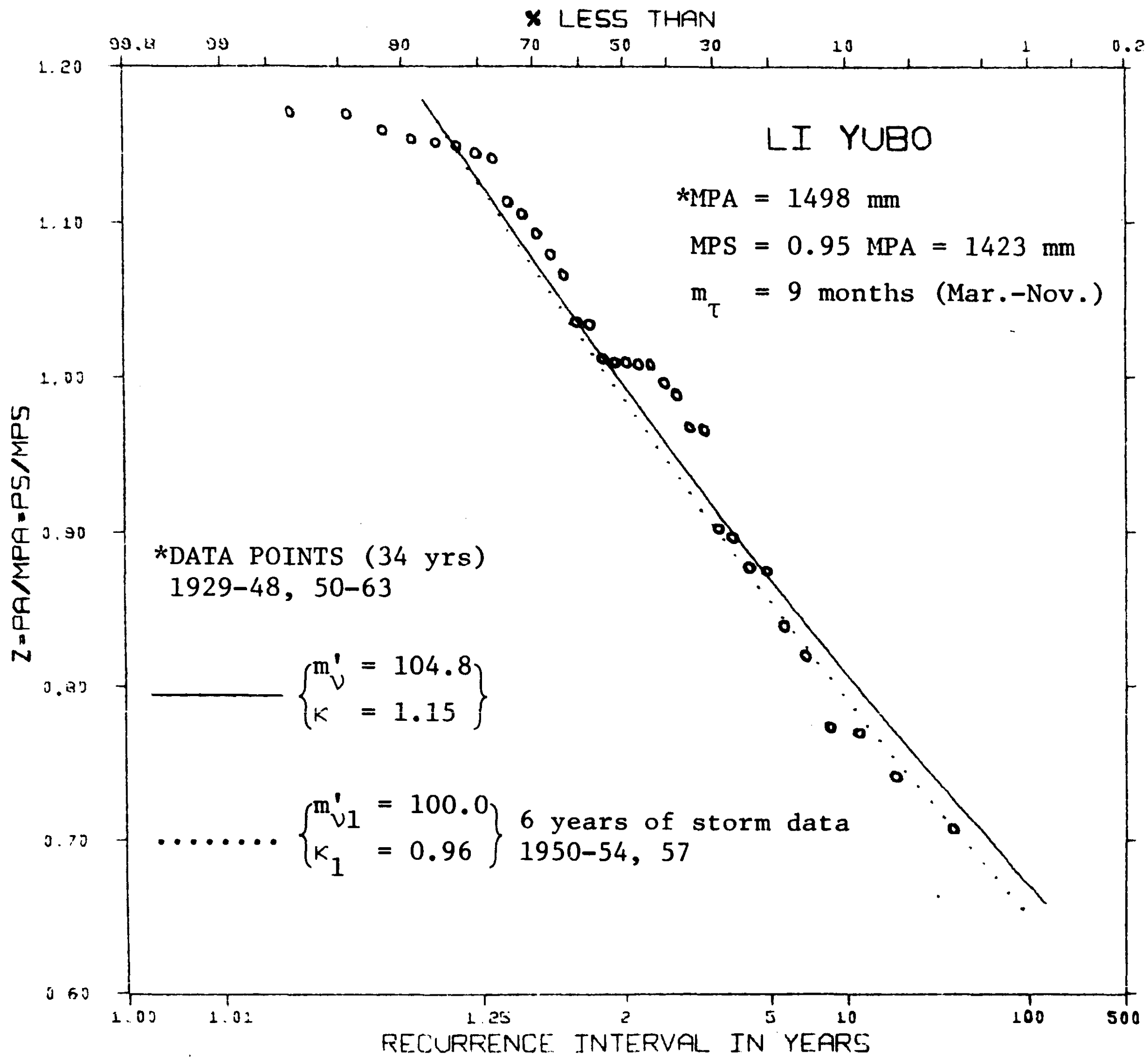

FIGURE A.23

FREQUENCY OF ANNUAL PRECIPITATION

(STATION LI YUBO)

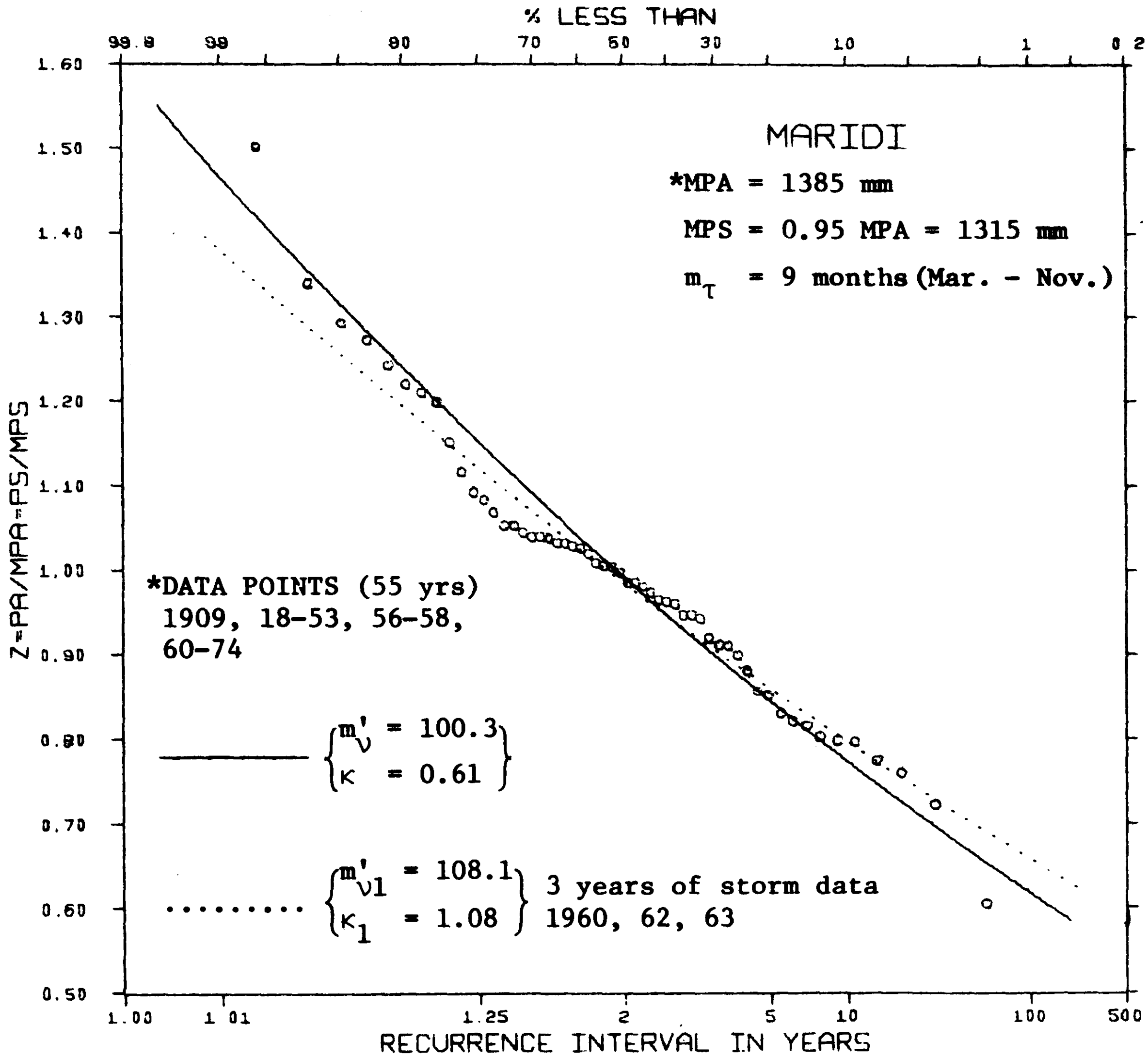

FIGURE A.24

FREQUENCY OF ANNUAL PRECIPITATION

(STATION MARIDI)

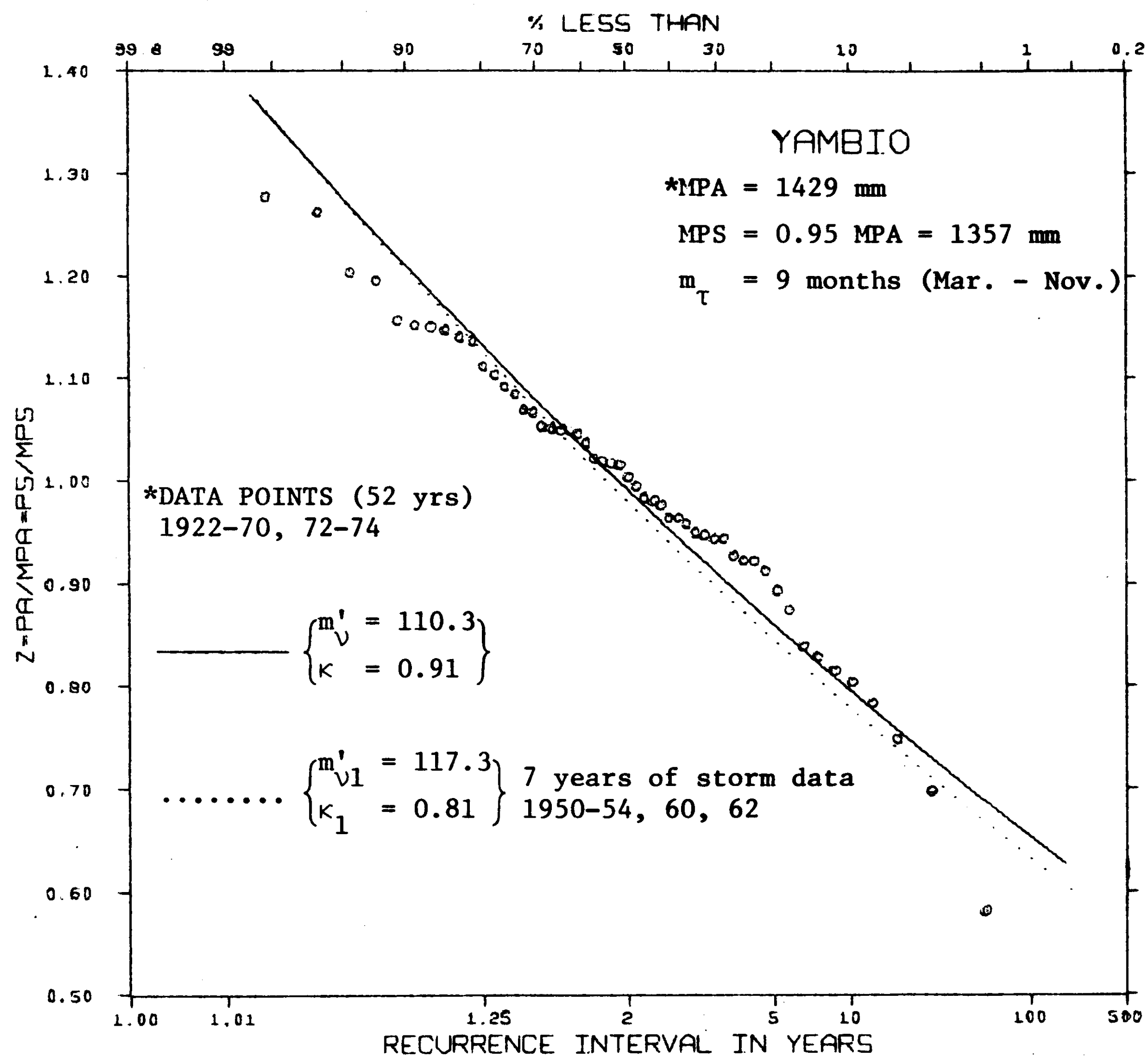

FIGURE A.25

FREQUENCY OF ANNUAL PRECIPITATION

(STATION YAMBIO)

APPENDIX B

Frequency Distribution of Catchment Precipitation and Catchment Yield

Table B1

Annual Observed Catchment Precipitation, mm
(1932 - 1963)

	NAAM	MARIDI	TONJ	JUR	PONGO	LOLL
	1	2	3	4	5	6
1	1217.	1270.	1179.	1450.	1175.	1103.
2	1129.	1054.	1208.	1515.	1195.	1232.
3	1246.	1106.	1155.	1130.	1103.	1212.
4	1221.	1067.	1259.	1358.	1107.	1062.
5	1237.	1044.	1345.	1544.	1298.	1113.
6	1282.	1077.	1359.	1444.	1127.	1261.
7	1212.	1117.	1279.	1399.	1317.	1351.
8	1383.	1113.	1209.	1387.	1298.	1578.
9	1103.	866.	1186.	1371.	1151.	1170.
10	1260.	1096.	1316.	1404.	1176.	1012.
11	1105.	1016.	1010.	1197.	1025.	1185.
12	947.	977.	981.	1145.	1005.	1206.
13	1195.	1133.	1165.	1440.	1316.	1079.
14	1215.	1169.	1266.	1400.	1064.	999.
15	1205.	1066.	1158.	1360.	1275.	1328.
16	1244.	1289.	1283.	1526.	1310.	1021.
17	1263.	1147.	1210.	1131.	1016.	969.
18	1292.	1091.	1250.	1365.	1191.	1096.
19	1304.	1264.	1421.	1362.	1357.	1154.
20	897.	887.	1017.	1230.	1058.	1216.
21	1201.	1199.	1198.	1519.	1203.	1105.
22	1064.	1008.	1100.	1141.	1183.	1210.
23	1139.	1268.	1449.	1426.	1182.	1108.
24	1176.	1169.	1227.	1196.	1238.	1235.
25	1274.	1202.	1209.	1437.	1156.	1116.
26	1196.	965.	1367.	1459.	1283.	1295.
27	1250.	901.	1353.	1489.	1335.	1204.
28	1208.	899.	1187.	1314.	1159.	1118.
29	1132.	949.	1488.	1590.	1226.	970.
30	1236.	1130.	1360.	1585.	1198.	1201.
31	1283.	1255.	1515.	1522.	1324.	1113.
32	1262.	1110.	1318.	1562.	1287.	1263.

Table B2

Frequency of Annual Observed Catchment Precipitation
(Naam Catchment)

NAAM

MEAN ANNUAL PRECIPITATION = 1199.   SDV = 97.

N	PA	Z	CDF
1	1383.	1.1531	0.9697
2	1304.	1.0873	0.9394
3	1292.	1.0770	0.9091
4	1283.	1.0701	0.8788
5	1282.	1.0693	0.8485
6	1274.	1.0622	0.8182
7	1263.	1.0535	0.7879
8	1262.	1.0524	0.7576
9	1260.	1.0504	0.7273
10	1250.	1.0420	0.6970
11	1246.	1.0391	0.6667
12	1244.	1.0371	0.6364
13	1237.	1.0311	0.6061
14	1236.	1.0307	0.5758
15	1221.	1.0176	0.5455
16	1217.	1.0145	0.5152
17	1215.	1.0129	0.4848
18	1212.	1.0104	0.4545
19	1208.	1.0068	0.4242
20	1205.	1.0049	0.3939
21	1201.	1.0012	0.3636
22	1196.	0.9971	0.3333
23	1195.	0.9967	0.3030
24	1176.	0.9806	0.2727
25	1139.	0.9500	0.2424
26	1132.	0.9441	0.2121
27	1129.	0.9416	0.1818
28	1105.	0.9212	0.1515
29	1103.	0.9200	0.1212
30	1064.	0.8874	0.0909
31	947.	0.7897	0.0606
32	897.	0.7478	0.0303

SDV = Standard Deviation of $\underline{P_A}$

$$Z = \underline{P_A} / \overline{\underline{P_A}} = \underline{P_s} / \overline{\underline{P_s}}$$

Table B3

Frequency of Annual Observed Catchment Precipitation
(Maridi Catchment)

MARIDI

MEAN ANNUAL PRECIPITATION = 1091.   SDV = 117.

N	PA	Z	CDF
1	1289.	1.1814	0.9697
2	1270.	1.1647	0.9394
3	1268.	1.1623	0.9091
4	1264.	1.1593	0.8788
5	1255.	1.1503	0.8485
6	1202.	1.1018	0.8182
7	1199.	1.0991	0.7879
8	1169.	1.0715	0.7576
9	1169.	1.0714	0.7273
10	1147.	1.0513	0.6970
11	1133.	1.0384	0.6667
12	1130.	1.0361	0.6364
13	1117.	1.0243	0.6061
14	1113.	1.0202	0.5758
15	1110.	1.0178	0.5455
16	1106.	1.0140	0.5152
17	1096.	1.0053	0.4848
18	1091.	1.0003	0.4545
19	1077.	0.9874	0.4242
20	1067.	0.9779	0.3939
21	1066.	0.9773	0.3636
22	1054.	0.9659	0.3333
23	1044.	0.9575	0.3030
24	1016.	0.9319	0.2727
25	1008.	0.9239	0.2424
26	977.	0.8958	0.2121
27	965.	0.8851	0.1818
28	949.	0.8699	0.1515
29	901.	0.8263	0.1212
30	899.	0.8239	0.0909
31	887.	0.8136	0.0606
32	866.	0.7941	0.0303

Table B4

Frequency of Annual Observed Catchment Precipitation
(Tonj Catchment)

TONJ

MEAN ANNUAL PRECIPITATION = 1251.   SDV = 127.

N	PA	Z	CDF
1	1515.	1.2114	0.9697
2	1488.	1.1897	0.9394
3	1449.	1.1583	0.9091
4	1421.	1.1361	0.8788
5	1367.	1.0926	0.8485
6	1360.	1.0875	0.8182
7	1359.	1.0861	0.7879
8	1353.	1.0819	0.7576
9	1345.	1.0754	0.7273
10	1318.	1.0538	0.6970
11	1316.	1.0522	0.6667
12	1283.	1.0259	0.6364
13	1279.	1.0225	0.6061
14	1266.	1.0121	0.5758
15	1259.	1.0064	0.5455
16	1250.	0.9991	0.5152
17	1227.	0.9810	0.4848
18	1210.	0.9672	0.4545
19	1209.	0.9667	0.4242
20	1209.	0.9665	0.3939
21	1208.	0.9658	0.3636
22	1198.	0.9573	0.3333
23	1187.	0.9491	0.3030
24	1186.	0.9480	0.2727
25	1179.	0.9427	0.2424
26	1165.	0.9311	0.2121
27	1158.	0.9256	0.1818
28	1155.	0.9234	0.1515
29	1100.	0.8797	0.1212
30	1017.	0.8130	0.0909
31	1010.	0.8078	0.0606
32	981.	0.7844	0.0303

Table B5

Frequency of Annual Observed Catchment Precipitation
(Jur Catchment)

JUR

MEAN ANNUAL PRECIPITATION = 1387.   SDV = 136.

N	PA	Z	CDF
1	1590.	1.1460	0.9697
2	1585.	1.1421	0.9394
3	1562.	1.1256	0.9091
4	1544.	1.1129	0.8788
5	1526.	1.0999	0.8485
6	1522.	1.0971	0.8182
7	1519.	1.0951	0.7879
8	1515.	1.0921	0.7576
9	1489.	1.0735	0.7273
10	1459.	1.0516	0.6970
11	1450.	1.0454	0.6667
12	1444.	1.0405	0.6364
13	1440.	1.0382	0.6061
14	1437.	1.0358	0.5758
15	1426.	1.0278	0.5455
16	1404.	1.0120	0.5152
17	1400.	1.0090	0.4848
18	1399.	1.0081	0.4545
19	1387.	0.9997	0.4242
20	1371.	0.9884	0.3939
21	1365.	0.9840	0.3636
22	1362.	0.9814	0.3333
23	1360.	0.9799	0.3030
24	1358.	0.9787	0.2727
25	1314.	0.9470	0.2424
26	1230.	0.8863	0.2121
27	1197.	0.8630	0.1818
28	1196.	0.8623	0.1515
29	1145.	0.8249	0.1212
30	1141.	0.8224	0.0909
31	1131.	0.8150	0.0606
32	1130.	0.8143	0.0303

Table B6

Frequency of Annual Observed Catchment Precipitation
(Pongo Catchment)

PONGO

MEAN ANNUAL PRECIPITATION = 1198.   SDV = 99.

N	PA	Z	CDF
1	1357.	1.1327	0.9697
2	1335.	1.1144	0.9394
3	1324.	1.1049	0.9091
4	1317.	1.0994	0.8788
5	1316.	1.0980	0.8485
6	1310.	1.0938	0.8182
7	1298.	1.0836	0.7879
8	1298.	1.0835	0.7576
9	1287.	1.0739	0.7273
10	1283.	1.0710	0.6970
11	1275.	1.0642	0.6667
12	1238.	1.0330	0.6364
13	1226.	1.0236	0.6061
14	1203.	1.0038	0.5758
15	1198.	1.0003	0.5455
16	1195.	0.9975	0.5152
17	1191.	0.9945	0.4848
18	1183.	0.9873	0.4545
19	1182.	0.9867	0.4242
20	1176.	0.9816	0.3939
21	1175.	0.9811	0.3636
22	1159.	0.9675	0.3333
23	1156.	0.9651	0.3030
24	1151.	0.9606	0.2727
25	1127.	0.9403	0.2424
26	1107.	0.9236	0.2121
27	1103.	0.9210	0.1818
28	1064.	0.8881	0.1515
29	1058.	0.8834	0.1212
30	1025.	0.8553	0.0909
31	1016.	0.8477	0.0606
32	1005.	0.8386	0.0303

Table B7

Frequency of Annual Observed Catchment Precipitation
(Loll Catchment)

LOLL

MEAN ANNUAL PRECIPITATION = 1165.   SDV = 123.

N	PA	Z	CDF
1	1578.	1.3542	0.9697
2	1351.	1.1597	0.9394
3	1328.	1.1396	0.9091
4	1295.	1.1117	0.8788
5	1263.	1.0841	0.8485
6	1261.	1.0824	0.8182
7	1235.	1.0599	0.7879
8	1232.	1.0576	0.7576
9	1216.	1.0433	0.7273
10	1212.	1.0404	0.6970
11	1210.	1.0385	0.6667
12	1206.	1.0349	0.6364
13	1204.	1.0335	0.6061
14	1201.	1.0306	0.5758
15	1185.	1.0167	0.5455
16	1170.	1.0037	0.5152
17	1154.	0.9908	0.4848
18	1118.	0.9596	0.4545
19	1116.	0.9575	0.4242
20	1113.	0.9550	0.3939
21	1113.	0.9549	0.3636
22	1108.	0.9510	0.3333
23	1105.	0.9487	0.3030
24	1103.	0.9469	0.2727
25	1096.	0.9409	0.2424
26	1079.	0.9263	0.2121
27	1062.	0.9113	0.1818
28	1021.	0.8765	0.1515
29	1012.	0.8687	0.1212
30	999.	0.8569	0.0909
31	970.	0.8326	0.0606
32	969.	0.8316	0.0303

Table B8

Frequency of Annual Derived Catchment Precipitation

Naam Catchment (m_ν=362, κ=0.73)		Maridi Catchment (m_ν=298, κ=0.54)	
Z^*	CDF	Z^*	CDF
0.65	0.0005	0.60	0.0003
0.70	0.0030	0.65	0.0014
0.75	0.0124	0.70	0.0061
0.80	0.0391	0.75	0.0204
0.85	0.0980	0.80	0.0546
0.90	0.2008	0.85	0.1203
0.95	0.3453	0.90	0.2241
1.00	0.5121	0.95	0.3610
1.05	0.6729	1.00	0.5140
1.10	0.8037	1.05	0.6611
1.15	0.8947	1.10	0.7840
1.20	0.9493	1.15	0.8742
1.25	0.9780	1.20	0.9329
1.30	0.9912	1.25	0.9671
1.35	0.9966	1.30	0.9850
1.40	0.9985	1.35	0.9936
1.45	0.9992	1.40	0.9972
		1.45	0.9987
		1.50	0.9992

$^* \; Z = \underline{P_A}/\overline{\underline{P_A}} = \underline{P_S}/\overline{\underline{P_S}}$

Table B9

Frequency of Annual Derived Catchment Precipitation

Tonj Catchment (m_ν=236, κ=0.70)		Jur Catchment (m_ν=208, κ=1.00)	
Z^*	CDF	Z^*	CDF
0.65	0.0006	0.65	0.0002
0.70	0.0033	0.70	0.0014
0.75	0.0133	0.75	0.0073
0.80	0.0410	0.80	0.0276
0.85	0.1009	0.85	0.0791
0.90	0.2039	0.90	0.1791
0.95	0.3474	0.95	0.3300
1.00	0.5124	1.00	0.5105
1.05	0.6713	1.05	0.6848
1.10	0.8010	1.10	0.8225
1.15	0.8920	1.15	0.9127
1.20	0.9472	1.20	0.9624
1.25	0.9767	1.25	0.9856
1.30	0.9905	1.30	0.9949
1.35	0.9963	1.35	0.9981
1.40	0.9984	1.40	0.9990
1.45	0.9991		

* $Z = \underline{P_A}/\underline{\overline{P_A}} = \underline{P_S}/\underline{\overline{P_S}}$

Table B10
Frequency of Annual Derived Catchment Precipitation

Pongo Catchment (m_ν=283, κ=1.07)		Loll Catchment (m_ν=141, κ=1.76)	
Z^*	CDF	Z^*	CDF
0.65	0.0002	0.65	0.0002
0.70	0.0012	0.70	0.0012
0.75	0.0065	0.75	0.0062
0.80	0.0256	0.80	0.0246
0.85	0.0756	0.85	0.0734
0.90	0.1749	0.90	0.1720
0.95	0.3269	0.95	0.3243
1.00	0.5102	1.00	0.5093
1.05	0.6872	1.05	0.6884
1.10	0.8262	1.10	0.8287
1.15	0.9161	1.15	0.9187
1.20	0.9647	1.20	0.9665
1.25	0.9868	1.25	0.9879
1.30	0.9954	1.30	0.9959
1.35	0.9983	1.35	0.9984
1.40	0.9991	1.40	0.9991

* $Z = \underline{P_A}/\underline{\overline{P_A}} = \underline{P_S}/\underline{\overline{P_S}}$

Table B 11: Observed Annual Gaged Discharges, md/yr (24)

Year	Tonj (Through Road Bridge)	Jur (At Wau)	Pongo (Downstream Road Bridge)	Loll (At Nyamlell)
1930	-	5.81	-	-
1942	(1.220)*	(4.195)	-	(0.596)
43	(0.717)	2.51	-	(0.628)
44	(1.527)	3.56	-	(0.294)
45	1.660	4.99	(2.965)	-
46	-	-	-	-
47	-	-	(3.577)	-
48	1.920	5.73	-	-
49	1.160	5.85	4.830	-
50	1.190	4.11	4.74	0.841
51	0.512	-	-	0.498
52	1.110	6.36	3.65	0.441
53	1.130	3.02	-	0.587
54	-	6.48	5.44	-
55	-	6.33	5.16	0.925
56	-	-	(4.047)	-
57	-	-	(3.032)	-
58	(2.258)	(7.025)	(1.870)	(0.627)
59	(1.690)	(3.347)	(1.034)	(0.435
60	-	-	-	-
1961	-	-	5.730	-
Years of Record	12	14	12	10

* Numbers inside brackets are estimates

Table B12

Frequency of Annual Derived Catchment Yield

NAAM CATCHMENT

I	CDF	YD*
1	0.9953	0.3097
2	0.9835	0.2654
3	0.9518	0.2248
4	0.8878	0.1879
5	0.7859	0.1541
6	0.6536	0.1233
7	0.5086	0.0953
8	0.3709	0.0697
9	0.2547	0.0464
10	0.1706	0.0267
11	0.1582	0.0262
12	0.1458	0.0257
13	0.1336	0.0252
14	0.1215	0.0247
15	0.1097	0.0242
16	0.0985	0.0237
17	0.0877	0.0233
18	0.0776	0.0229
19	0.0681	0.0224
20	0.0595	0.0220
21	0.0515	0.0216
22	0.0444	0.0212
23	0.0380	0.0208
24	0.0324	0.0205
25	0.0275	0.0201
26	0.0232	0.0197
27	0.0195	0.0194
28	0.0164	0.0191
29	0.0138	0.0187
30	0.0115	0.0184
31	0.0097	0.0181

MARIDI CATCHMENT

I	CDF	YD*
1	0.9960	0.3495
2	0.9873	0.3002
3	0.9655	0.2551
4	0.9218	0.2138
5	0.8503	0.1761
6	0.7517	0.1418
7	0.6340	0.1104
8	0.5098	0.0818
9	0.3915	0.0558
10	0.2882	0.0320
11	0.2659	0.0293
12	0.2507	0.0287
13	0.2351	0.0282
14	0.2194	0.0276
15	0.2037	0.0271
16	0.1879	0.0266
17	0.1724	0.0261
18	0.1573	0.0256
19	0.1426	0.0251
20	0.1285	0.0247
21	0.1152	0.0242
22	0.1027	0.0238
23	0.0910	0.0234
24	0.0802	0.0230
25	0.0704	0.0226
26	0.0615	0.0222
27	0.0536	0.0218
28	0.0465	0.0214
29	0.0402	0.0210
30	0.0348	0.0207
31	0.0300	0.0203
32	0.0259	0.0200
33	0.0223	0.0197
34	0.0193	0.0194
35	0.0167	0.0190
36	0.0144	0.0187

* $YD = Y_A/\overline{P_S}$

Table B13

Frequency of Annual Derived Catchment Yield

TONJ CATCHMENT			JUR CATCHMENT		
I	CDF	YD *	I	CDF	YD *
1	0.9980	0.4384	1	0.9978	0.5211
2	0.9939	0.3857	2	0.9909	0.4580
3	0.9821	0.3375	3	0.9676	0.4002
4	0.9555	0.2933	4	0.9110	0.3471
5	0.9070	0.2529	5	0.8093	0.2984
6	0.8331	0.2160	6	0.6670	0.2537
7	0.7364	0.1823	7	0.5062	0.2128
8	0.6248	0.1515	8	0.3541	0.1754
9	0.5093	0.1234	9	0.2300	0.1412
10	0.4000	0.0978	10	0.1401	0.1098
11	0.3039	0.0745	11	0.0810	0.0812
12	0.2244	0.0533	12	0.0450	0.0551
13	0.1619	0.0339	13	0.0255	0.0330
14	0.1420	0.0289	14	0.0244	0.0324
15	0.1333	0.0283	15	0.0232	0.0317
16	0.1247	0.0277	16	0.0221	0.0310
17	0.1161	0.0272	17	0.0210	0.0304
18	0.1077	0.0267	18	0.0198	0.0298
19	0.0995	0.0262	19	0.0187	0.0292
20	0.0916	0.0257	20	0.0176	0.0286
21	0.0840	0.0252	21	0.0165	0.0280
22	0.0768	0.0247	22	0.0154	0.0275
23	0.0699	0.0243	23	0.0143	0.0270
24	0.0635	0.0238	24	0.0133	0.0264
25	0.0575	0.0234	25	0.0123	0.0259
26	0.0519	0.0230	26	0.0113	0.0254
27	0.0468	0.0226	27	0.0104	0.0250
28	0.0421	0.0222	28	0.0096	0.0245
29	0.0379	0.0218	29	0.0088	0.0241
30	0.0340	0.0214	30	0.0080	0.0236
31	0.0306	0.0211	31	0.0073	0.0232
32	0.0275	0.0207	32	0.0067	0.0228
33	0.0247	0.0204	33	0.0061	0.0224
34	0.0223	0.0200	34	0.0055	0.0220
35	0.0201	0.0197	35	0.0050	0.0216
36	0.0181	0.0194	36	0.0045	0.0212
37	0.0164	0.0190	37	0.0041	0.0209
38	0.0149	0.0187	38	0.0038	0.0205
			39	0.0034	0.0202
			40	0.0031	0.0198

$* \ YD = Y_A/\overline{P_S}$

Table B14
Frequency of Annual Derived Catchment Yield

PONGO CATCHMENT			LOLL CATCHMENT		
I	CDF	YD*	I	CDF	YD*
1	0.9953	0.3226	1	0.9968	0.4372
2	0.9857	0.2842	2	0.9894	0.3815
3	0.9626	0.2489	3	0.9693	0.3304
4	0.9178	0.2167	4	0.9270	0.2836
5	0.8459	0.1871	5	0.8557	0.2407
6	0.7478	0.1601	6	0.7556	0.2016
7	0.6314	0.1354	7	0.6354	0.1658
8	0.5087	0.1129	8	0.5088	0.1331
9	0.3915	0.0922	9	0.3891	0.1032
10	0.2888	0.0734	10	0.2856	0.0760
11	0.2049	0.0563	11	0.2024	0.0511
12	0.1514	0.0443	12	0.1414	0.0293
13	0.1355	0.0435	13	0.1341	0.0288
14	0.1204	0.0427	14	0.1269	0.0282
15	0.1061	0.0420	15	0.1195	0.0276
16	0.0928	0.0412	16	0.1122	0.0271
17	0.0805	0.0405	17	0.1050	0.0265
18	0.0693	0.0398	18	0.0978	0.0260
19	0.0591	0.0391	19	0.0909	0.0255
20	0.0501	0.0384	20	0.0841	0.0250
21	0.0422	0.0377	21	0.0776	0.0246
22	0.0352	0.0371	22	0.0714	0.0241
23	0.0293	0.0365	23	0.0655	0.0237
24	0.0242	0.0359	24	0.0599	0.0232
25	0.0199	0.0353	25	0.0546	0.0228
26	0.0163	0.0347	26	0.0497	0.0224
27	0.0133	0.0341	27	0.0452	0.0220
28	0.0109	0.0336	28	0.0411	0.0216
29	0.0088	0.0330	29	0.0372	0.0212
			30	0.0338	0.0209
			31	0.0306	0.0205
			32	0.0278	0.0201
			33	0.0252	0.0198
			34	0.0229	0.0195
			35	0.0208	0.0191
			36	0.0190	0.0188

* $YD = Y_A/\overline{P_S}$

Table B15: Simulated Distribution of Annual Combined Catchment Yield for Catchment C12 and C56

C12		C56	
$Y_A/\overline{P}_s$	CDF	$Y_A/\overline{P}_s$	CDF
0.00	0.0000	0.00	0.0000
0.02	0.0295	0.02	0.0200
0.03	0.1215	0.03	0.0845
0.04	0.1820	0.04	0.1350
0.05	0.2475	0.05	0.1705
0.06	0.3235	0.06	0.2090
0.07	0.3940	0.07	0.2345
0.08	0.4580	0.08	0.2665
0.09	0.5150	0.09	0.3020
0.10	0.5730	0.10	0.3460
0.11	0.6230	0.11	0.3995
0.12	0.6710	0.12	0.4395
0.13	0.7280	0.13	0.4925
0.14	0.7810	0.14	0.5375
0.15	0.8234	0.15	0.5810
0.16	0.8624	0.16	0.6150
0.17	0.8879	0.17	0.6655
0.18	0.9134	0.18	0.7085
0.19	0.9309	0.19	0.7440
0.20	0.9464	0.20	0.7755
0.21	0.9619	0.21	0.8090
0.23	0.9799	0.22	0.8384
0.24	0.9849	0.23	0.8654
0.25	0.9894	0.24	0.8894
0.26	0.9914	0.25	0.9099
0.27	0.9924	0.26	0.9244
0.28	0.9964	0.27	0.9394
0.29	0.9969	0.28	0.9499
0.30	0.9979	0.29	0.9624
0.31	0.9989	0.30	0.9684
0.33	0.9994	0.31	0.9769
0.36	0.9999	0.32	0.9819
		0.33	0.9864
		0.34	0.9899
		0.35	0.9924
		0.36	0.9939
		0.38	0.9959
		0.39	0.9974
		0.40	0.9979
		0.41	0.9989
		0.42	0.9994
		0.44	0.9999

Table B16

Simulated Distribution of Annual Combined Catchment Yield
(Catchment C123)

CATCHMENT NAME
C123

COEFF. OF POLYNOMIAL IN ASCENDING ORDER

C(0)= -0.1989620E+00
C(1)= 0.1336679E+01
C(2)= -0.2420952E+02
C(3)= 0.2486388E+03
C(4)= -0.1427008E+04
C(5)= 0.4925684E+04
C(6)= -0.1062900E+05
C(7)= 0.1443311E+05
C(8)= -0.1197110E+05
C(9)= 0.5535289E+04
C(10)= -0.1092543E+04

A = 0.2004309E+00 B = 0.5112957E-01

I	F(I)	Y(I)	YFIT(I)	YERR(I)	YREL(I)
1	0.0	0.0	0.0015	0.0015	
2	0.0150	0.0200	0.0170	-0.0030	-0.1501
3	0.0560	0.0300	0.0330	0.0030	0.1011
4	0.0940	0.0400	0.0390	-0.0010	-0.0250
5	0.1405	0.0500	0.0483	-0.0017	-0.0346
6	0.1995	0.0600	0.0613	0.0013	0.0217
7	0.2575	0.0700	0.0709	0.0009	0.0128
8	0.3215	0.0800	0.0789	-0.0011	-0.0136
9	0.3940	0.0900	0.0893	-0.0007	-0.0073
10	0.4610	0.1000	0.1005	0.0005	0.0054
11	0.5310	0.1100	0.1112	0.0012	0.0111
12	0.5885	0.1200	0.1190	-0.0010	-0.0082
13	0.6460	0.1300	0.1287	-0.0013	-0.0097
14	0.7000	0.1400	0.1398	-0.0002	-0.0012
15	0.7430	0.1500	0.1502	0.0002	0.0016
16	0.7920	0.1600	0.1617	0.0017	0.0104
17	0.8409	0.1700	0.1699	-0.0001	-0.0007
18	0.8789	0.1800	0.1776	-0.0024	-0.0134
19	0.9129	0.1900	0.1853	-0.0047	-0.0248
20	0.9374	0.2000	0.1964	-0.0036	-0.0178
21	0.9544	0.2100	0.2063	-0.0037	-0.0175
22	0.9669	0.2200	0.2192	-0.0008	-0.0038
23	0.9729	0.2300	0.2257	-0.0043	-0.0187
24	0.9824	0.2400	0.2351	-0.0049	-0.0203
25	0.9874	0.2500	0.2479	-0.0021	-0.0084
26	0.9909	0.2600	0.2476	-0.0124	-0.0476
27	0.9959	0.2700	0.2615	-0.0085	-0.0316
28	0.9984	0.2800	0.2753	-0.0047	-0.0169
29	0.9994	0.2900	0.2894	-0.0006	-0.0022
30	0.9999	0.3200	0.3170	-0.0030	-0.0094

Table B17

Simulated Distribution of Annual Combined Catchment Yield
(Catchment C16)

CATCHMENT NAME
C16

COEFF. OF POLYNOMIAL IN ASCENDING ORDER

C(0)= -0.1893290E+00
C(1)= 0.3419068E+01
C(2)= -0.6347559E+02
C(3)= 0.6125542E+03
C(4)= -0.3308473E+04
C(5)= 0.1077599E+05
C(6)= -0.2200362E+05
C(7)= 0.2836010E+05
C(8)= -0.2240262E+05
C(9)= 0.9901406E+04
C(10)= -0.1875088E+04

A = 0.2023618E+00 B = 0.6485122E-01

I	F(I)	Y(I)	YFIT(I)	YERR(I)	YREL(I)
1	0.0	0.0	0.0130	0.0130	
2	0.0010	0.0100	0.0164	0.0064	0.6402
3	0.0035	0.0300	0.0243	-0.0057	-0.1902
4	0.0060	0.0400	0.0315	-0.0085	-0.2133
5	0.0095	0.0500	0.0404	-0.0096	-0.1918
6	0.0165	0.0600	0.0549	-0.0051	-0.0849
7	0.0355	0.0700	0.0776	0.0076	0.1086
8	0.0525	0.0800	0.0857	0.0057	0.0707
9	0.0800	0.0900	0.0896	-0.0004	-0.0042
10	0.1215	0.1000	0.0954	-0.0046	-0.0458
11	0.1670	0.1100	0.1084	-0.0016	-0.0150
12	0.2195	0.1200	0.1231	0.0031	0.0256
13	0.2890	0.1300	0.1318	0.0018	0.0141
14	0.3745	0.1400	0.1367	-0.0033	-0.0233
15	0.4625	0.1500	0.1499	-0.0001	-0.0008
16	0.5420	0.1600	0.1626	0.0026	0.0160
17	0.6165	0.1700	0.1698	-0.0002	-0.0014
18	0.6905	0.1800	0.1774	-0.0026	-0.0142
19	0.7620	0.1900	0.1908	0.0008	0.0041
20	0.8105	0.2000	0.1996	-0.0004	-0.0020
21	0.8609	0.2100	0.2085	-0.0015	-0.0070
22	0.9064	0.2200	0.2173	-0.0027	-0.0124
23	0.9364	0.2300	0.2257	-0.0043	-0.0185
24	0.9689	0.2500	0.2443	-0.0057	-0.0227
25	0.9824	0.2600	0.2562	-0.0038	-0.0145
26	0.9914	0.2700	0.2689	-0.0011	-0.0041
27	0.9939	0.2800	0.2765	-0.0035	-0.0125
28	0.9949	0.2900	0.2800	-0.0100	-0.0346
29	0.9974	0.3000	0.2970	-0.0030	-0.0099
30	0.9984	0.3100	0.3017	-0.0083	-0.0266
31	0.9989	0.3200	0.3133	-0.0067	-0.0209
32	0.9994	0.3300	0.3255	-0.0045	-0.0136
33	0.9999	0.3600	0.3640	0.0040	0.0110

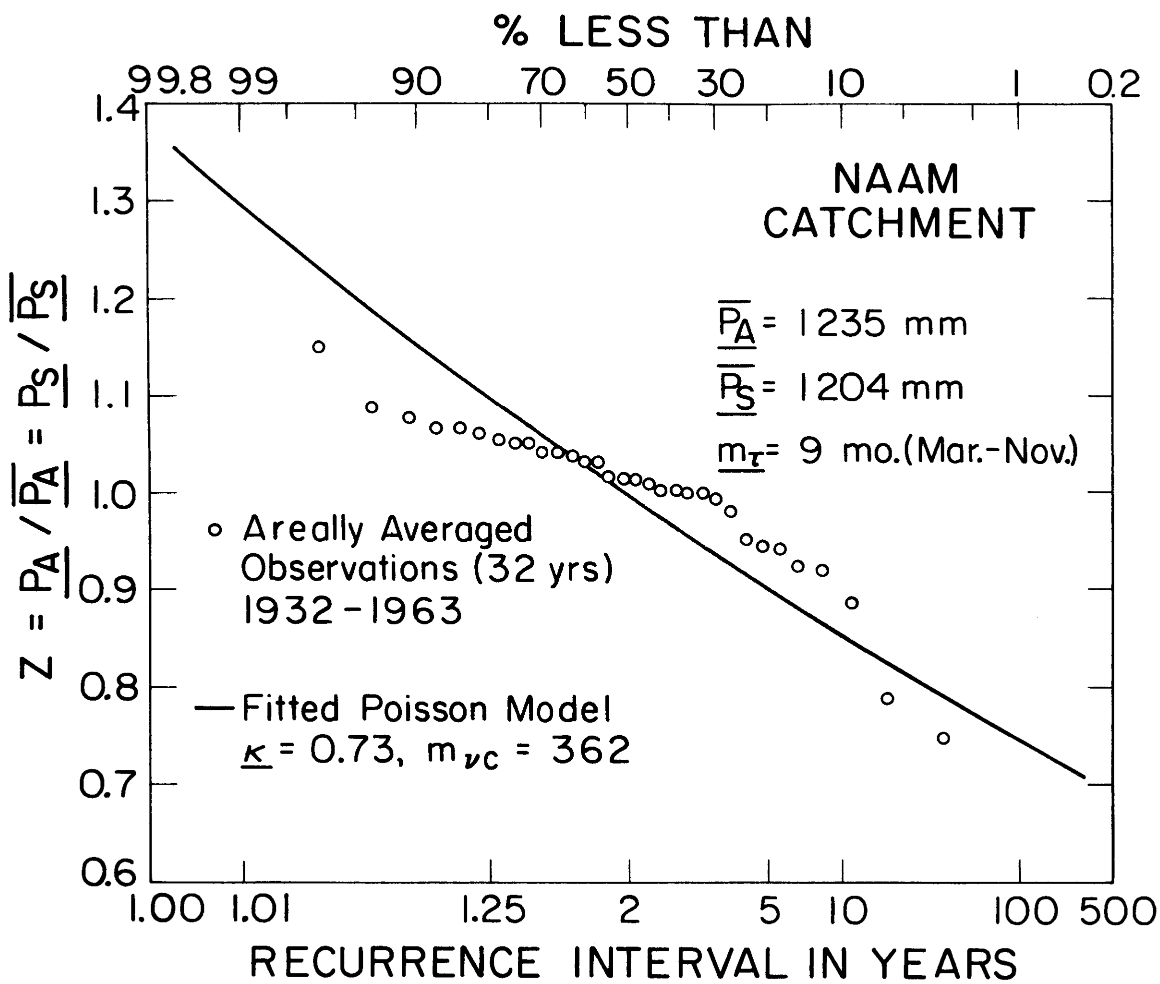

FIGURE B.1

FREQUENCY OF ANNUAL CATCHMENT PRECIPITATION

(NAAM CATCHMENT)

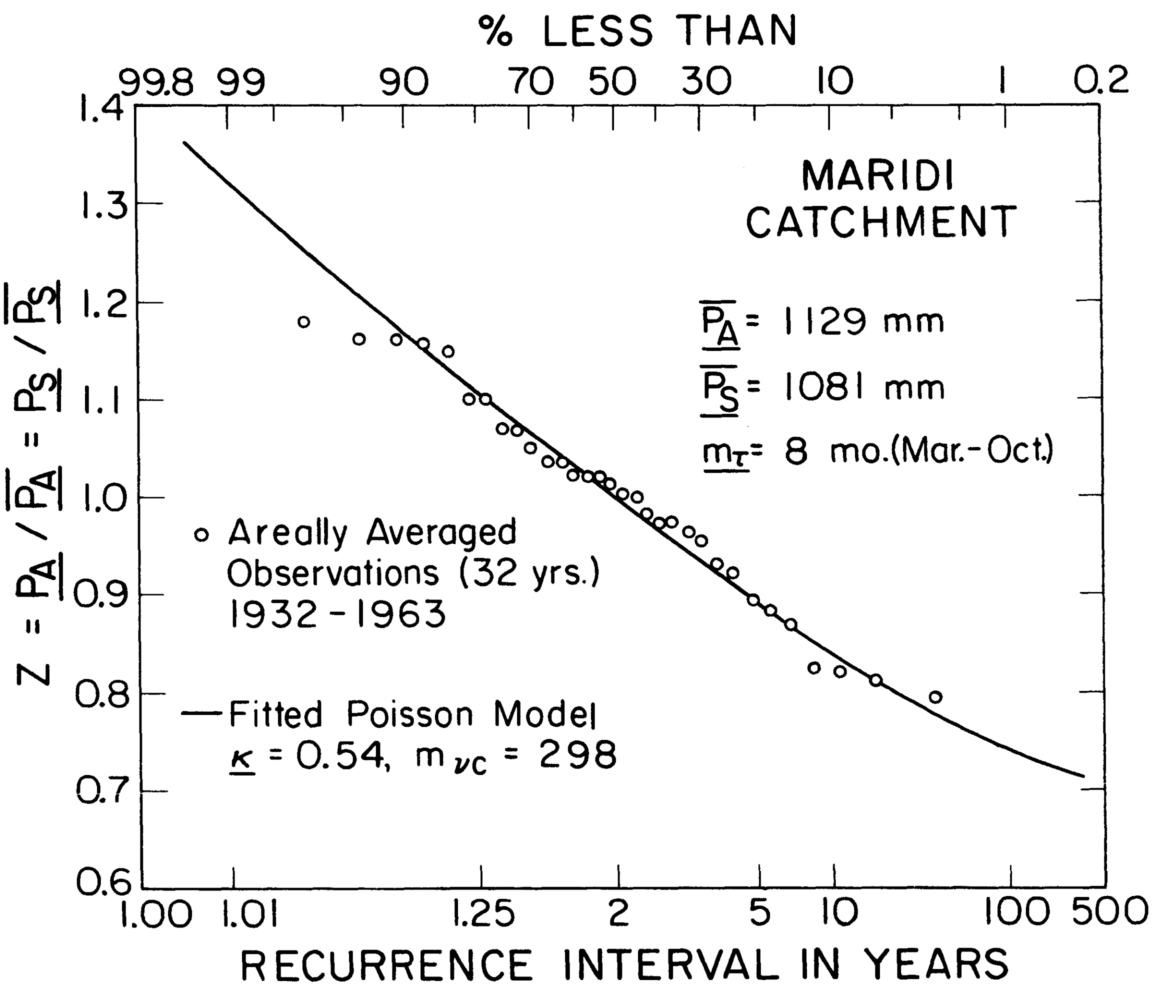

FIGURE B.2

FREQUENCY OF ANNUAL CATCHMENT PRECIPITATION

(MARIDI CATCHMENT)

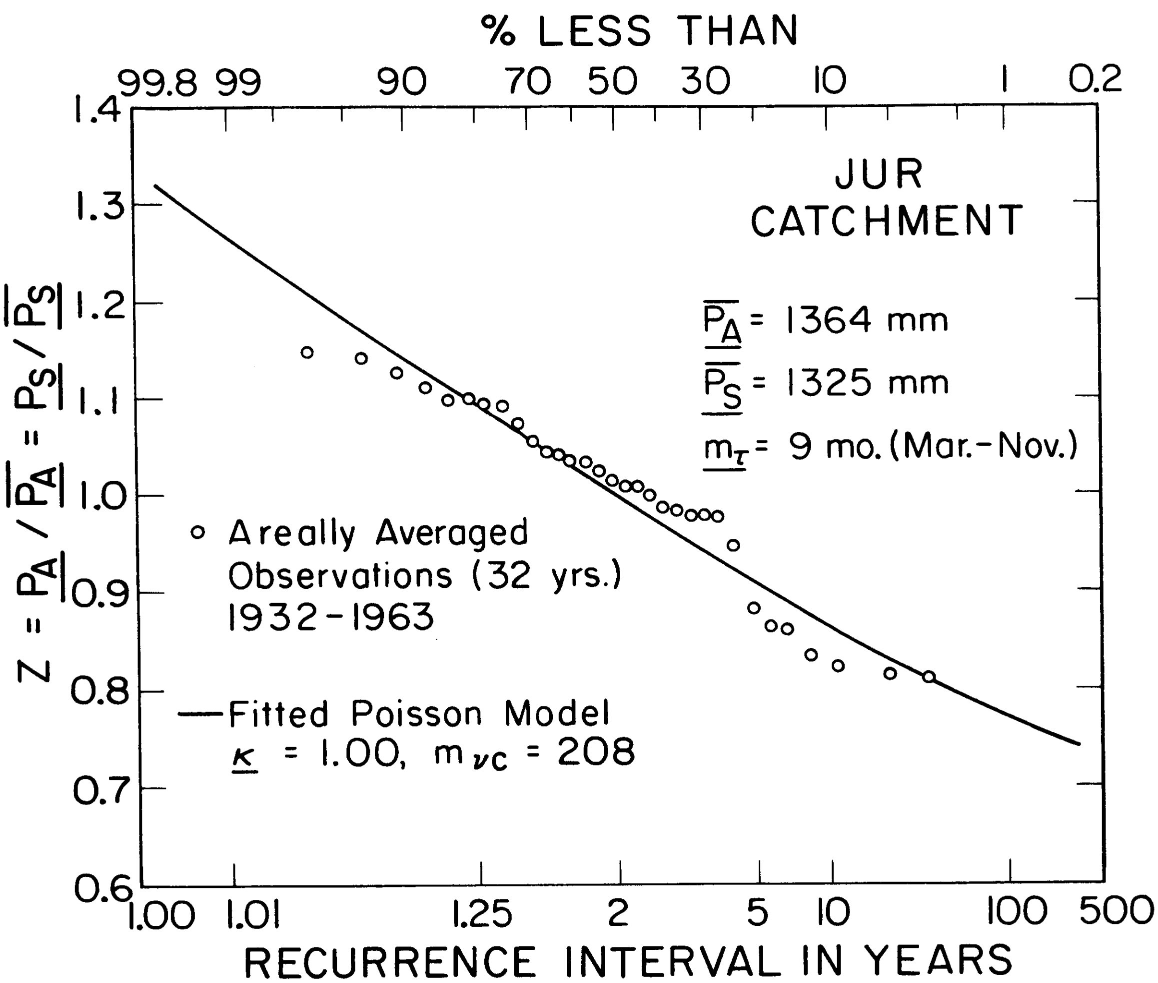

FIGURE B.3

FREQUENCY OF ANNUAL CATCHMENT PRECIPITATION

(JUR CATCHMENT)

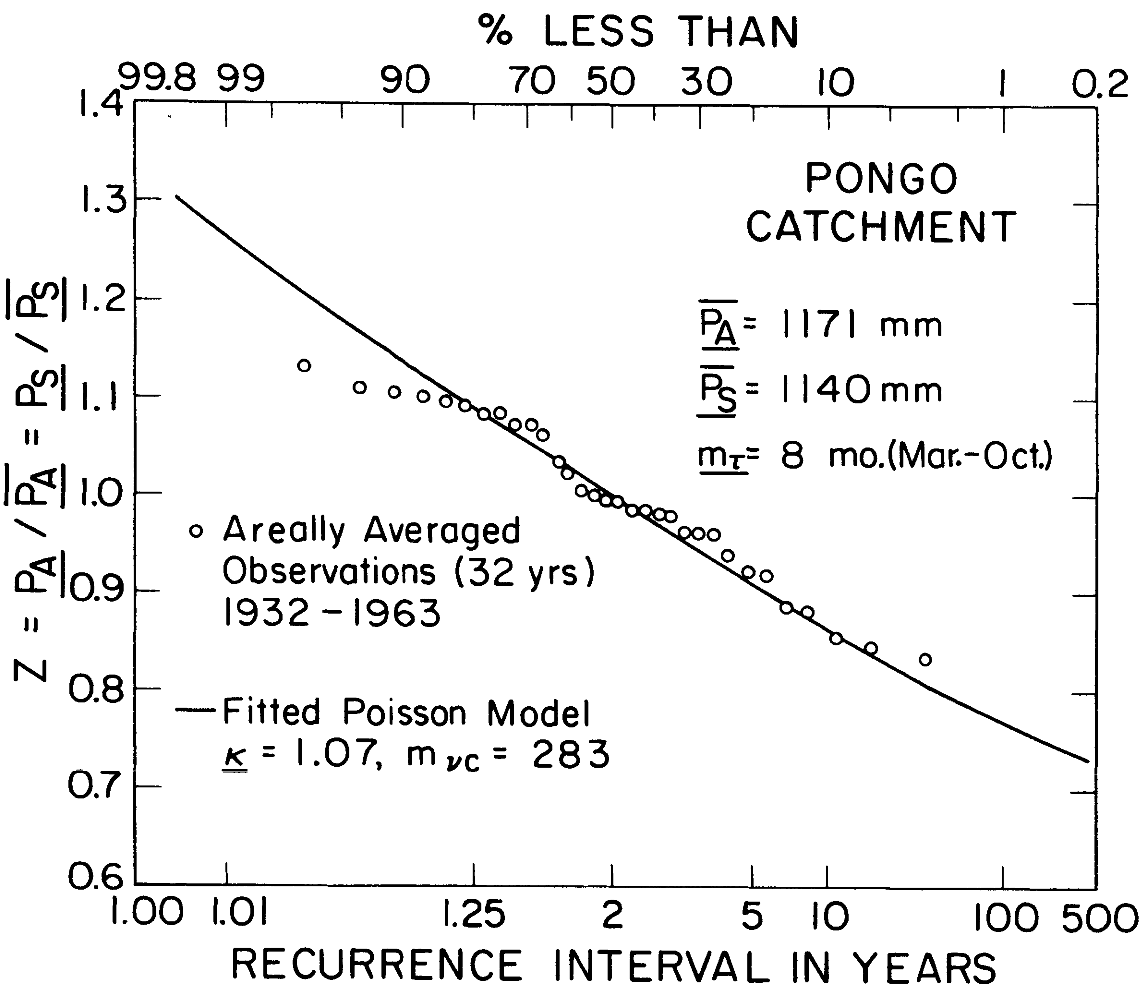

FIGURE B.4

FREQUENCY OF ANNUAL CATCHMENT PRECIPITATION

(PONGO CATCHMENT)

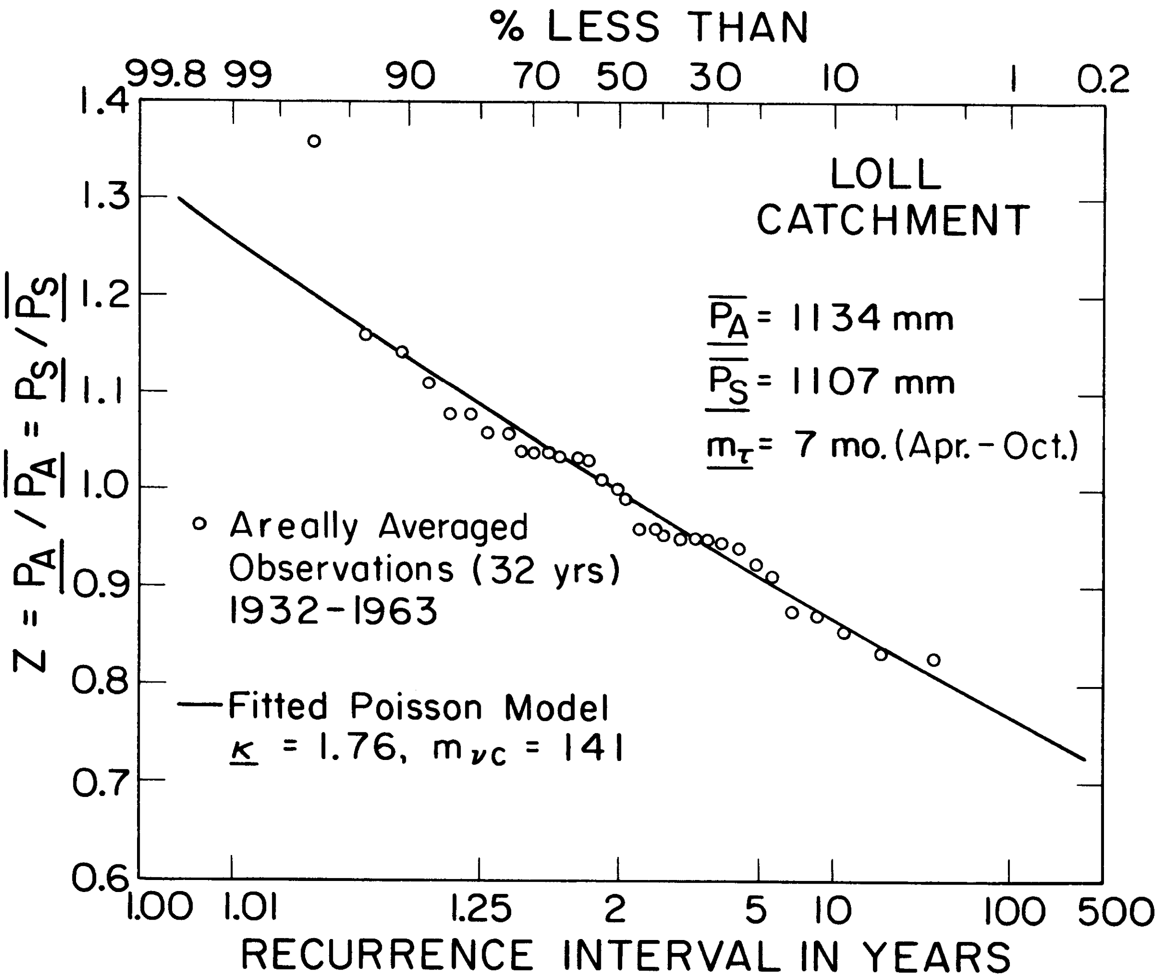

FIGURE B.5

FREQUENCY OF ANNUAL CATCHMENT PRECIPITATION

(LOLL CATCHMENT)

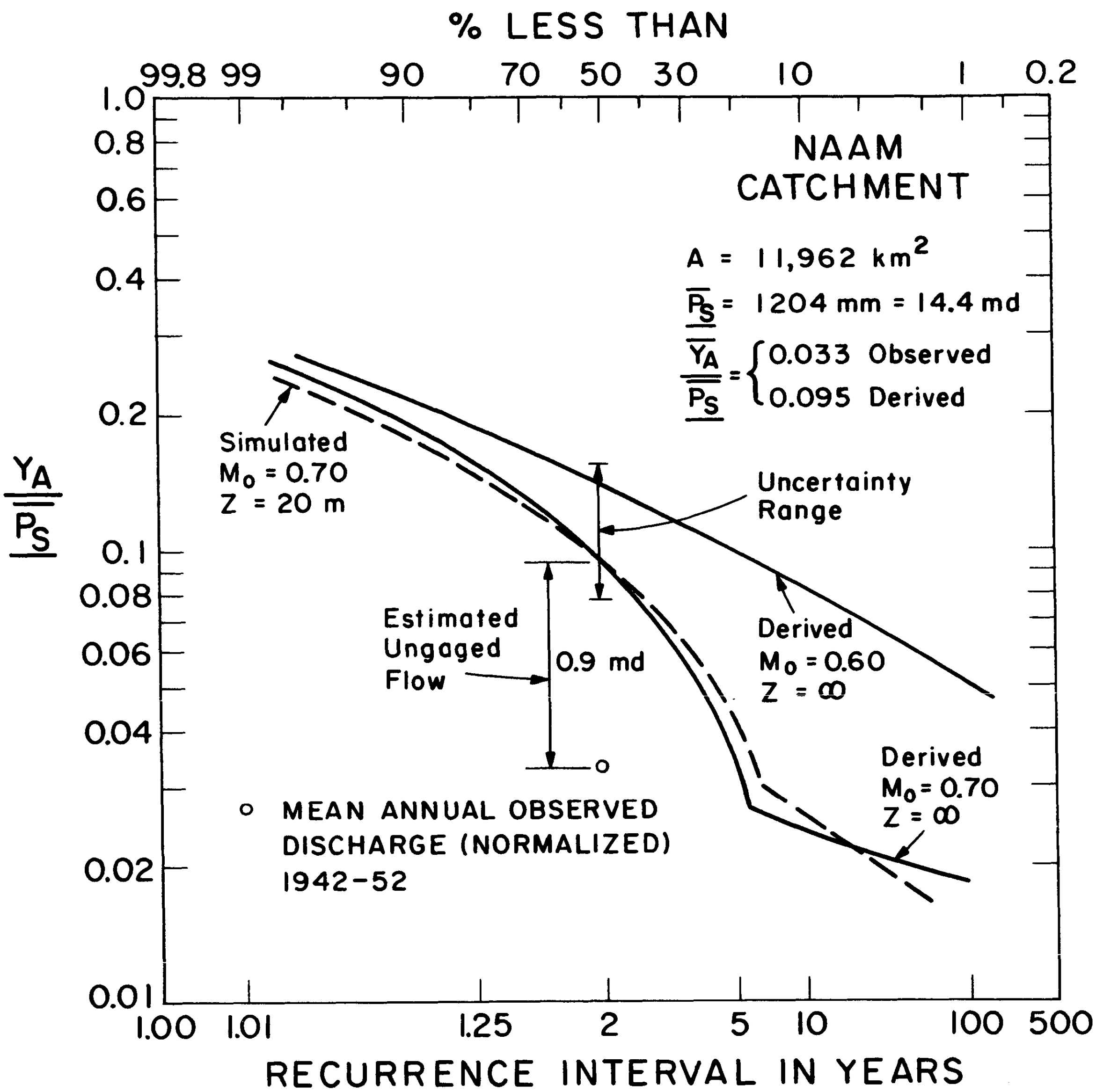

FIGURE B.6

FREQUENCY OF ANNUAL CATCHMENT YIELD

(NAAM CATCHMENT)

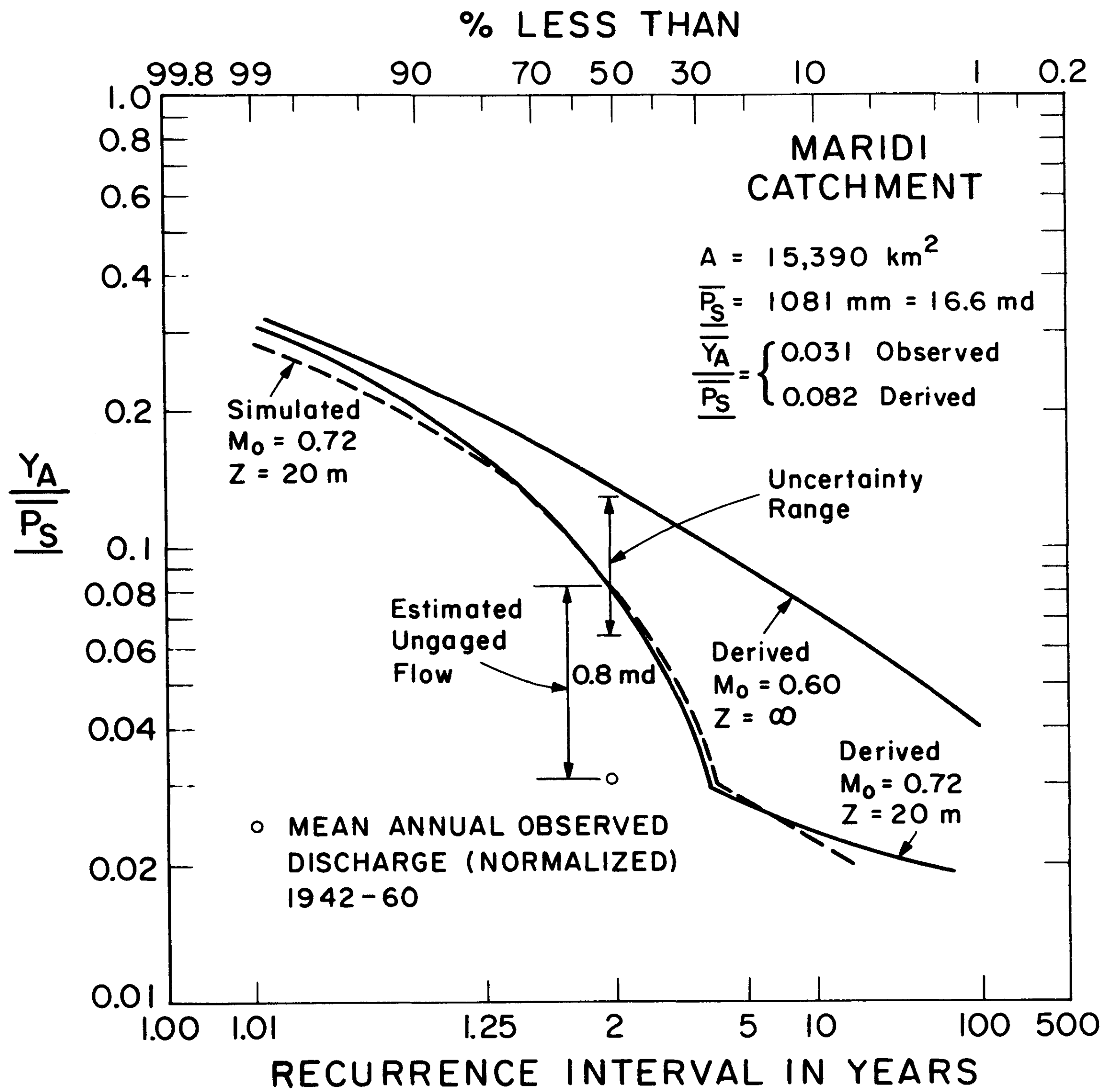

FIGURE B.7

FREQUENCY OF ANNUAL CATCHMENT YIELD

(MARIDI CATCHMENT)

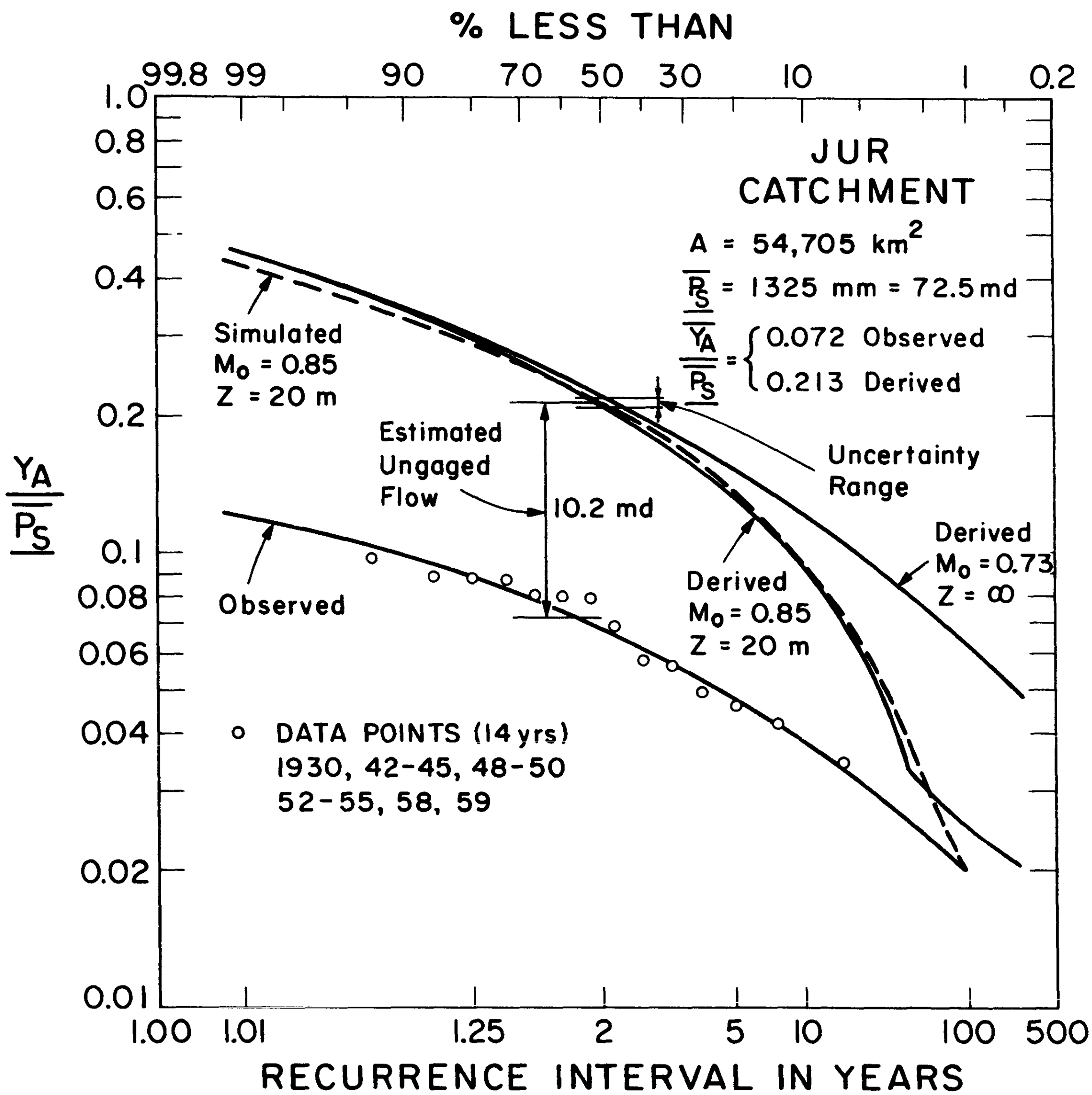

FIGURE B.8

FREQUENCY OF ANNUAL CATCHMENT YIELD

(JUR CATCHMENT)

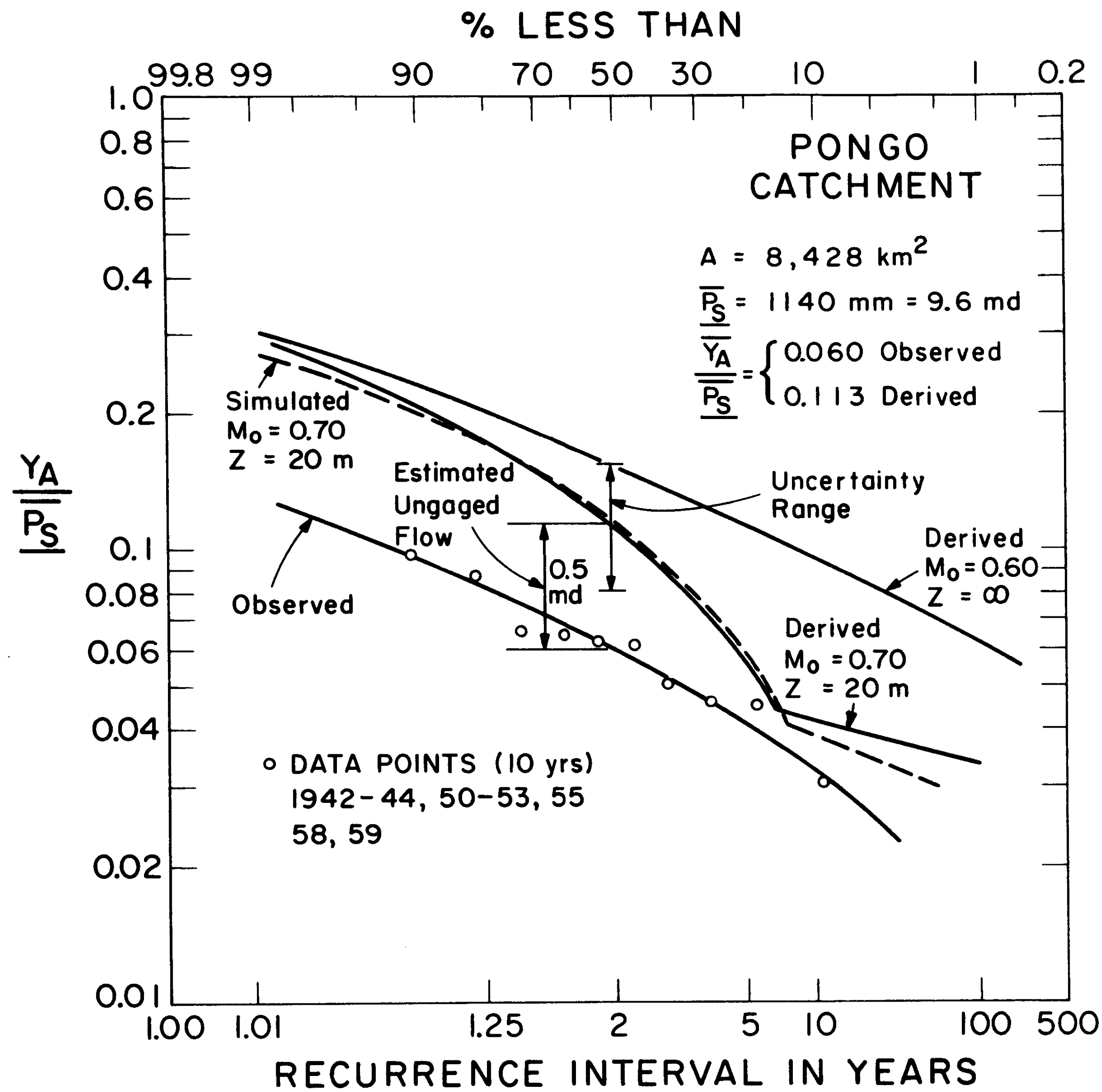

FIGURE B.9

FREQUENCY OF ANNUAL CATCHMENT YIELD

(PONGO CATCHMENT)

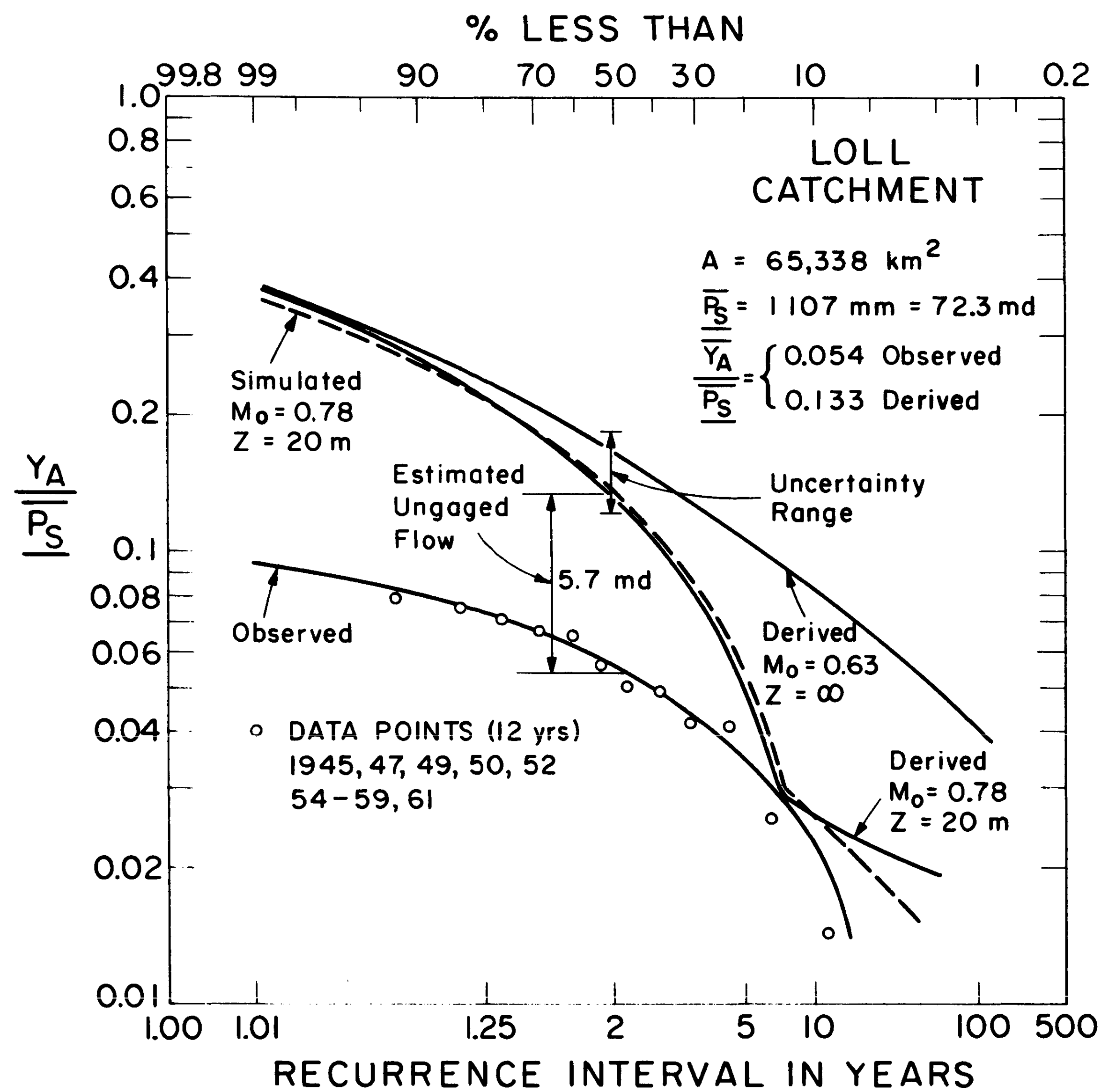

FIGURE B.10

FREQUENCY OF ANNUAL CATCHMENT YIELD

(LOLL CATCHMENT)

APPENDIX C

Computer Programs

```
C     THIS PROGRAM COMPUTES THE CDF OF NORMALIZED PRECIPITATION.
C     A LOGARITHMIC TRANSFORM IS USED IN ORDER TO AVOID EXPONENT
C     OVERFLOW OR UNDERFLOW PROBLEMS.
C     NAME     = NAME OF CATCHMENT (INPUT)
C     Z        = NORMALIZED PRECIPITATION
C              = SEASONAL PRECIPITATION / MEAN SEASONAL PRECIPITATION
C     ZL       = LOWER LIMIT OF Z (INPUT)
C     ZU       = UPPER LIMIT OF Z (INPUT)
C     INZ      = INCREMENT OF Z (INPUT)
C     M,VM     = MEAN NUMBER OF STORMS (INPUT)
C     V        = THE 'V'TH STORM
C     VMAX     = MAXIMUM NUMBER OF STORMS ALLOWED IN THE EVALUATION OF
C                CDF OF Z = 3*M
C     K        = PARAMETER OF GAMMA DISTRIBUTION, KAPPA, (INPUT)
C     FAC      = LOG OF 'V' FACTORIAL
C     DLGAMA   = LOG OF GAMMA DISTRIBUTION
C     GAMLID   = LOG OF INCOMPLETE GAMMA DISTRIBUTION
C     PROB     = CDF OF NORMALIZED PRECIPITATION (OUTPUT)
C     EPS      = RELATIVE ERROR IN COMPUTING THE INCOMPLETE GAMMA DISTRIB
C              = RELATIVE ERROR IN COMPUTING THE CDF OF Z
C                 (INPUT, 0.0001 IS COMMON)
C
C
      DIMENSION NAME(10)
      REAL*8 FAC(600)
      REAL*8 X,A,DLOG,DLGAMA,GAMLID,EPS
      REAL*8 M,K,W,T,Z,ZL,ZU,INZ,PROB
      REAL*8 XOLD,XSUM,SUM1,SUM2,TOT,VTOT,VOLD,VNEW
      INTEGER V,VM,VMAX
C
C     COMPUTE LOG OF V FACTORIAL
C
      DO 300 J=1,600
      VTOT=0.0D0
      DO 700 IV =1,J
  700 VTOT=VTOT+DLOG(DFLOAT(IV))
      FAC(J)=VTOT
  300 CONTINUE
C
C
  888 FORMAT('1',' INPUT ZL,ZU,INZ,EPS ')
      WRITE(6,888)
      READ(5,*)ZL,ZU,INZ,EPS
  900 WRITE(6,889)
  889 FORMAT('1',' INPUT NAME ')
      READ(5,3000)NAME
```

```
 3000 FORMAT(10A2)
      WRITE(6,3001)
 3001 FORMAT('1',' INPUT M,K ')
      READ(5,*)M,K
      IF(M.EQ.0.0)STOP
      WRITE(6,4000)NAME,M,K
 4000 FORMAT(1H0,10A2/' ',5X,'M=',F8.1,5X,'K=',F10.4//
     $9X,1HZ,6X,4HPROB/)
C
C     INITIALIZING VALUES
C
      Z=ZL
      VM=IFIX(SNGL(M))
      VMAX=IFIX(SNGL(3.*M))
 3    X=M*K*Z
      II =0
      JJ=1
      SUM1=0.0D0
      SUM2=0.0D0
 13   V=VM-II
      ICOUNT=V
      IF(V.EQ.0)GO TO 500
 23   IF(V.EQ.VMAX)GO TO 600
      IF(V.GT.600)GO TO 600
C
C     COMPUTE LOG INCOMPLETE GAMMA DISTRIBUTION
C
      A=DFLOAT(V)*K
      XOLD=1.0D0/A
      XSUM =1.0D0/A
      I=1
 100  XOLD=(XOLD/(A+I))*X
      XSUM=XSUM+XOLD
      IF((XOLD/XSUM).LE.EPS)GO TO 200
      I=I+1
      KCOUNT=I
      GO TO 100
 200  CONTINUE
      GAMLID=A*DLOG(X)-X+DLOG(XSUM)-DLGAMA(A)
C
C     COMPUTE THE SUMMATION OF ALL V TERMS
C
      VOLD=DFLOAT(V)*DLOG(M)-FAC(V)+GAMLID-M
      IF(VOLD.LE.-170.D0)VOLD=-170.D0
      VNEW=DEXP(VOLD)
      IF(V.GT.VM)GO TO 800
```

```
      SUM1=SUM1+VNEW
      IF((VNEW/SUM1).LE.EPS)GO TO 500
      II=II+1
      GO TO 13
  500 V=VM+JJ
      JCOUNT=V
      GO TO 23
  800 SUM2=SUM2+VNEW
      IF((VNEW/SUM2).LE.EPS)GO TO 600
      JJ =JJ+1
      GO TO 500
C
C     COMPUTE CDF OF NORMALIZED PRECIPITATION
C
  600 IF(M.GT.170.D0)M=170.D0
      PROB=SUM1+SUM2+DEXP(-M)
      WRITE(6,5000)Z,PROB
 5000 FORMAT(' ',F10.2,F10.5)
      IF(PROB.GT.0.999D0)GO TO 900
      Z=Z+INZ
      IF(Z.GT.ZU)GO TO 900
      GO TO 3
      END
```

```
C THIS PROGRAM COMPUTES THE WATER BALANCE COMPONENTS OF A CATCHMENT
C WITH A VARIABLE VEGETAL CANOPY
C
C
C      INPUTS :
C
C      NAME= NAME OF CATCHMENT
C      PAM = MEAN ANNUAL CATCHMENT PRECIPITATION, CM
C      MU  = MEAN NUMBER OF STORMS IN THE WET SEASON
C      MH  = MEAN STORM DEPTH, CM
C      MTR = MEAN STORM DURATION, DAYS
C      MTB = MEAN TIME BETWEEN STORMS, DAYS
C      TAU = MEAN LENGTH OF WET SEASON, DAYS
C      MI  = MEAN STORM INTENSITY, CM/HR
C
C      AK  = KAPPA, PARAMETER OF GAMMA DISTRIBUTION OF STORM DEPTH
C      AKV = POTENTIAL TRANSPIRATION EFFICIENCY
C      BMM = VEGETAL CANOPY DENSITY (INPUT NO. 0.1-0.9, NOT USED)
C      EPR = POTENTIAL EVAPORATION RATE OF WET SOIL SURFACE, CM/HR
C      HO  = SURFACE RETENTION CAPACITY, CM
C      TA  = MEAN AIR TEMPERATURE, DEGREE CENTIGRADE
C      WT  = AVERAGE DEPTH TO WATER TABLE, CM
C
C      N   = EFFECTIVE POROSITY OF SOIL
C      M   = PORE SIZE DISTRIBUTION INDEX
C      K1  = SATURATED EFFECTIVE HYDRAULIC CONDUCTIVITY, CM/SEC
C      SI1 = SOIL SUCTION, CM
C
C
C
C      OUTPUTS :
C
C      SO    = SPACE-TIME AVERAGE SOIL MOISTURE
C      J(E)  = EVAPOTRANSPIRATION FUNCTION
C      E     = EVAPORATION EFFECTIVENESS
C      RSA   = MEAN ANNUAL (SEASONAL) SURFACE RUNOFF, CM
C      RGA   = MEAN ANNUAL (SEASONAL) GROUND WATER RUNOFF, CM
C      EVAPO = MEAN ANNUAL (SEASONAL) EVAPOTRANSPIRATION, CM
C      ERN   = MEAN SURFACE RETENTION, CM
C      G     = GRAVITATIONAL INFILTRATION PARAMETER
C      SIGRF = CAPILLARY INFILTRATION PARAMETER
C      YIEP  = NORMALIZED MEAN ANNUAL CATCHMENT YIELD
C      W     = RATE OF CAPILLARY RISE FROM THE WATER TABLE, CM/HR
C
C
C
```

```
      REAL MTB,MTR,MH,MI,MU,M,N,K1,NU
      DIMENSION NAME(20)
      IO=6
      INP=5
C
C
      WRITE(6,566)
 566  FORMAT('1', ' INPUT STATION NAME ')
      READ(5,76)NAME
76    FORMAT(20A4)
C
C****************************************
C
C     ENTER CLIMATIC PARAMETERS
      WRITE(6,567)
 567  FORMAT('1', ' INPUT PAM,MU,MH,MTR,MTB,TAU,MI ')
      READ(5,*)PAM,MU,MH,MTR,MTB,TAU,MI
      WRITE(6,568)
 568  FORMAT('1', ' INPUT AK,AKV,BMM,EPR,HO,TA,WT ')
      READ(5,*)AK,AKV,BMM,EPR,HO,TA,WT
C
C     ENTER SOIL PARAMETERS
 123  WRITE(6,569)
 569  FORMAT('1', ' INPUT N, M, K1,SI1 ')
      READ(5,*)N,M,K1,SI1
      IF(N.EQ.0.0)STOP
C
C
C****************************************
C
C     COMPUTE M RELATED CONSTANTS
      C=3.+2./M
      FIC=10.0**(0.66+0.55/M+0.14/(M*M))
      DI=C-1./M-1.
      DE=2.+1./M
      D2=DE+2.
C
C*****************************
C
C
C     COMPUTE THE CAPILLARY RISE
      BK1=K1
      BZ= 1. + 1.5/(M*C-1.)
      WW=BZ*BK1*(SI1/WT)**(M*C)
      W=WW*3600.
C
```

```
C
C
C*****************************************
C
      WRITE(6,883)
 883  FORMAT(' ENTER CLIMATE/SOIL PROPERTIES')
      WRITE(6,763)NAME
 763  FORMAT(' ',20A4)
      WRITE(IO,1003)EPR,MTB,MTR,TAU,TA,K1,M,N,MH,MI,PAM,W,HO,
     1AK,WT,BMM,SI1,MU,AKV
 1003 FORMAT(' EPR=',F10.4/' MTB=',F10.4/' MTR=',F10.4/' TAU='
     1,F10.4/' TA =',F10.4/' K1 =',E10.4/' M =',F10.4/' N  ='
     2,F10.4/' MH =',F10.4/' MI =',F10.4/' PAM=',F10.4/
     3' W  =',F10.4/' HO =',F10.4/' AK =',F10.4/' WT =',E10.4/
     4' BMM=',F10.4/' SI1=',F10.4/' MU =',F10.4/' AKV = ',F7.2/)
      WRITE(6,777)
 777  FORMAT(5X,'BMM',5X,'PAM',7X,'SO',5X,'J(E)',8X,'E',6X,'RSA',
     16X,'RGA',4X,'EVAPO',4X,'ERN',11X,'G',7X,'SIGRF',8X,'YIEP')
C
C*****************************************
C
C---- COMPUTE WATER CONSTANTS
C     SUT=SURFACE TENSION
C     NU = VISCOSITY
C     GAMSW = SPECIFIC WEIGHT
      CALL WATCN(TA,SUT,NU,GAMSW)
C
C*****************************************
C
C     COMPUTE CLIMATIC PARAMETERS
      PA=PAM
      BM=BMM
      BETA=1./(24.*MTB)
      DELTA=1./(24.0*MTR)
      ETA=1./MH
      ALPHA=1./MI
      EPP=EPR*MU*MTB*24.
C
C*****************************************
C
C     COMPUTE SURFACE RETENTION CONSTANTS
      IF(HO.EQ.0.0)HO=1.E-7
      AL=AK /MH
      BLE=BETA/(AL*EPR)
      ALH=AL*HO
      BHE=BETA*HO/EPR
```

```
      GK1=1.-GAMT(AK,ALH)/GAMMA(AK)
      GK2=GAMT(AK,ALH+BHE)/GAMMA(AK)
      GK3=1.-GK1*EXP(-BHE)-GK2/(1.+BLE)**AK
      GK4=ALH
      GK5=BHE
      ERRV=ERSV(GK4,GK5,AKV,AK)
C
C*****************************
C
C     COMPUTE SOIL RELATED CONSTANTS
C
      FIED=FIE(DE)
      ECNST=2.*BETA*N*BK1*SI1/(3.1415927*M*EPR*EPR)*FIED*3600.
      SIGC=3000.*N*ETA*ETA*BK1*SI1/(3.1415927*DELTA*M)
C
C*****************************
C
      DO 255 KB=1,12
      BM=1.2-0.1*FLOAT(KB)
      IF(KB.EQ.1)BM=0.95
      IF(KB.EQ.2)BM=0.9
      IF(KB.EQ.3)BM=0.85
      IF(KB.EQ.12)BM=0.05
      SO=1.E-2
      DS=0.1
      ITER=1
C
C**************************************
C
C     COMPUTE SURFACE RETENTION
      ERN=(EPR/BETA)*((1.-BM)*GK3+BM*AKV*ERRV)
C
C*****************************
C
C
C     COMPUTE EVAPOTRANSPIRATION
      EPA=EPP*(1.-BM*(1.-AKV))
 10   E=ECNST*SO**D2
      EJE=EJ(E,BHE,ALH,BM,AKV,AK,W,EPR,BETA,BLE)
   12 ET =EPA*EJE
      ET1 =ET/PAM
C
C**************************************
C
C---- COMPUTE THE GROUNDWATER RUNOFF
      RGA=TAU*BK1*SO**C*86400.-365.*24.*W
```

```
      IF(RGA.LT.0.0)RGA=0.0
C
C*****************************************
C
C---- COMPUTE THE SURFACE RUNOFF
      FIID=FII(DI,SO)
      SIGRF=(SIGC*FIID*(1.-SO)*(1.-SO))**0.333333
      G=ALPHA*BK1*0.5*(1.+SO**C)*3600.-ALPHA*W
      RS1=EXP(-G-2.*SIGRF)*GAMMA(SIGRF+1.)*SIGRF**(-SIGRF)
      IF(RS1.LT.0.0)RS1=0.
      RSA=RS1*PAM
C
C********************************
C
C     COMPUTE WATER BALANCE COMPONENTS
      AWBAL=PA*(1.-RS1)-ET-RGA
      IF(ITER.EQ.1)GO TO 15
      IF(ABS(AWBAL).LE.PA*0.002)GO TO 50
      IF(AWBAL*OLD.LE.0.0)DS=-DS*0.5
   15 OLD=AWBAL
      SOLD=SO
      SO=SO+DS
      IF(SO.GT.1.)GO TO 254
      IF(SO.LE.0.)GO TO 254
      ITER=2
      GO TO 10
254   SO=0.0
      EJE=0.0
      GO TO 253
50    RG1=RGA/PAM
      YIEL1=RS1+RG1
      YIELD=RSA+RGA
      YIEP=YIELD/PAM
      PAZ=PA
C
C********************************
C
 253  WRITE(6,3127)BM,PAZ,SO,EJE,E,RSA,RGA,ET,ERN,G,SIGRF,YIEP
 3127 FORMAT(2F8.2,4F9.4,2F9.2,F7.2,3E12.4)
  255 CONTINUE
      GO TO 123
      END
C
C************************************************************************
C
      SUBROUTINE WATCN(TA,SUT,NU,GAMSW)
```

```
C     COMPUTE THE WATER CONSTANTS AT A GIVEN TEMPERATURE TA
      REAL NU,NUT
      DIMENSION SUTT(11),NUT(11),GAMST(11)
      DATA SUTT/75.6,74.9,74.2,73.5.72.0,72.1,71.4,70.7,70.0,69.3,68.6/,
     1 NUT/17.93E-3,15.18E-3,13.09E-3,11.44E-3,10.08E-3,8.94E-3,8.E-3,
     27.2E-3,6.53E-3,5.97E-3,5.94E-3/,
     3GAMST/0.99987,0.99999,0.99973,0.99913,0.99823,0.99708,0.99568,0.99
     4406,0.99225,0.99025,0.98807/
      IF(TA.GT.50.)GO TO 10
      ITA=IFIX(TA*0.2)+1
      FRAC=TA-FLOAT(IFIX(TA))
      ITA1=ITA+1
      SUT=(SUTT(ITA1)-SUTT(ITA))*0.2*FRAC+SUTT(ITA)
      NU=(NUT(ITA1)-NUT(ITA))*0.2*FRAC+NUT(ITA)
      GAMSW=((GAMST(ITA1)-GAMST(ITA))*0.2*FRAC+GAMST(ITA))*980.
      RETURN
   10 SUT=SUTT(11)
      NU=NUT(11)
      GAMSW=GAMST(11)*980.
      RETURN
      END
C
C*****************************************************************************
C
      FUNCTION ERSV(GK4,GK5,AKV,AK)
C     THIS FUNCTION COMPUTES THE VEGETATED SURFACE RETENTION
      GK6=GK4*AKV
      GK7=1.-GAMT(AK,GK6)/GAMMA(AK)
      GK8=GK5/GK6
      GK9=GAMT(AK,GK6+GK5)/GAMMA(AK)
      ERSV=1.-GK7*EXP(-GK5)-GK9/(1.+GK8)**AK
      RETURN
      END
C
C*****************************************************************************
C
      FUNCTION FIE(D)
C
C     THIS FUNCTION COMPUTES THE DESORPTION COEFFICIENT BY MEANS OF A
C     LOGARITHMIC INTERPOLATION OF THE VALUES GIVEN IN THE TABLE Y.
C
      DIMENSION Y(7)
      DATA Y/0.18,0.11,0.077,0.056.0.044,0.034,0.029/
      IF(D.GE.8.)GO TO 10
      X=D-1.
      I=IFIX(X)
```

```
      FRAC=X-FLOAT(I)
      Y1=ALOG(Y(I))
      Y2=ALOG(Y(I+1))
      FIE=EXP((Y2-Y1)*FRAC+Y1)
      RETURN
   10 FIE=0.029
      RETURN
      END
C
C***********************************************************************
C
C
C***********************************************************************
C
C***********************************************************************
C
      FUNCTION FII(D,SO)
C
C     THIS FUNCTION COMPUTES THE SORPTION COEFFICIENT BY MEANS OF AN
C     EMPIRICAL FIT
C
      POW=1.425-0.0375*D
      DEN=D*(1.-SO)**POW+1.666667
      FII=1./DEN
      RETURN
      END
C
C
C**********************************************************************
C
      FUNCTION EJ(E,BHE,ALH,BM,AKV,AK,W,EPR,BETA,BLE)
      LOGICAL UNFL
      WEP=W/EPR
      BMKV=BM*AKV
      GAMK=GAMT(AK,ALH)/GAMMA(AK)
      GAMA15 = GAMMA(1.5)
      CE=1.E10
      DBB=1.+BMKV-WEP
      BB=(1.-BM)/DBB+(BM*BMKV+(1.-BM)*WEP)/(2.*DBB*DBB)
      GAMK1=GAMT(AK,ALH+BHE)/GAMMA(AK)
      UNFL=BMKV.GT.0.0
      IF(BMKV-WEP.NE.0.0)CC=0.5/(BMKV-WEP)**2
      ES3=0.0
      ES4=0.0
      IF(UNFL)CE=CC*E
      UNFL=CE.LT.100.
```

```
      BE=BB*E
      IF(UNFL)GO TO 25
      GAMCE=GAMA15
      GO TO 27
25    GAMCE = GAMT(1.5,CE)
27    GAMBE = GAMT(1.5,BE)
      IF(UNFL)ES3=-EXP(-CE-BHE)*(WEP-BMKV-SQRT(2.*CC)*E)
      ES0=GAMK -(1.+BLE)**(-AK)*GAMK1*EXP(-BE)
       ES1=(1.-GAMK)*(1.-EXP(-BE-BHE)*(1.-WEP+BMKV+SQRT(
     22.*BB)*E)
     3+ES3
     4+SQRT(2.*E)*EXP(-BHE)*(GAMCE-GAMBE))
      ES5=(1.+BLE)**(-AK)*GAMK1
      ES6=EXP(-BE)*(WEP-BMKV-SQRT(2.*BB)*E)
      IF(UNFL)ES4=-EXP(-CE)*(WEP-BMKV-SQRT(2.*CC)*E)
      ESJ=ES0+ES1+ES5*(ES6+ES4+SQRT(2.*E)*(GAMCE-GAMBE))
      EVJ=AKV
30    EJ=((1.-BM)*ESJ+BM*EVJ)/(1.-BM*(1.-AKV))
      RETURN
      END
C
C*****************************************************************************
C
      FUNCTION GAMT(A,X)
C
C     THIS FUNCTION COMPUTES THE TRUNCATED GAMT DISTRIBUTION
C     ACCORDING TO THE ALGORITHM IN THE NATIONAL BUREAU OF STANDARDS
C     'HANDBOOK OF MATHEMATICAL TABLES'
       IF(X.EQ.0.0)GO TO 40
      IF(X.GE.100.)GO TO 50
      IO=6
      SUM=1./A
      AN=1.0
      OLD=SUM
   33 OLD=OLD*X/(A+AN)
      IF(OLD/SUM-1.E-6)20,10,10
   10 AN=AN+1.
      SUM=SUM+OLD
      IF(AN-300.)33,33,12
   12 WRITE(IO,100)X
  100 FORMAT('0NO CONVERGENCE FOR X=',E20.5)
   20 GAMT=EXP(A*ALOG(X)+ALOG(SUM)-X)
      GO TO 60
40    GAMT=0.0
      GO TO 60
   50 GAMT=GAMMA(A)
```

```
   60 RETURN
      END
C
C****************************************
```

```
C
C     THIS PROGRAM COMPUTES THE CDF OF YIELD FROM A CATCHMENT
C
C     INPUTS :
C
C     NAME= NAME OF STATION
C     PAM = MEAN SEASONAL PRECIPITATION, CM
C     MU  = MEAN NUMBER OF STORMS PER RAINY SEASON
C     MUC = MEAN CATCHMENT STORMS
C     MH  = MEAN STORM DEPTH, CM
C     MTR = MEAN STORM DURATION, DAYS
C     MTB = MEAN TIME BETWEEN STORMS, DAYS
C     TAU = MEAN SEASONAL LENGTH, DAYS
C     MI  = MEAN STORM INTENSITY, CM/HOUR
C     AK  = KAPPA, PARAMETER OF GAMMA DISTRIBUTION OF STORM DEPTH
C     AKV = POTENTIAL TRANSPIRATION EFFICIENCY
C     BMM = VEGETAL CANOPY DENSITY
C     EPR = POTENTIAL EVAPORATION(WET SOIL SURFACE), CM/HOUR
C     HO  = SURFACE RETENTION CAPACITY, CM
C     TA  = MEAN SEASONAL AIR TEMPERATURE, *C
C     WT  = AVERAGE DEPTH TO WATER TABLE, CM
C     N   = MEDIUM EFFECTIVE POROSITY
C     M   = PORE SIZE DISTRIBUTION INDEX
C     K1  = SATURATURED EFFECTIVE HYDRAULIC CONDUCTIVITY, CM/SEC
C     SI1 = SOIL SUCTION, CM
C     DSO = SOIL MOISTURE INCREMENT(0.002-0.05)
C     CYU =UPPER LIMIT USED FOR THE CDF OF YD
C     CYL = LOWER LIMIT USED FOR THE CDF OF YD
C     BYU = UPPER LIMIT USED FOR YD IN THE CDF
C     BYL = LOWER LIMIT USED FOR YD IN THE CDF
C
C
C
C     OUTPUTS :
C
C     YD  = NORMALIZED MEAN ANNUAL CATCHMENT YIELD = YIEP
C     SO     = SPACE-TIME AVERAGE SOIL MOISTURE
C     J(E)    = EVAPOTRANSPIRATION FUNCTION
C     E      = EVAPORATION EFFECTIVENESS
C     RSA    = ANNUAL (SEASONAL) SURFACE RUNOFF, CM
C     RGA    = ANNUAL (SEASONAL) GROUND WATER RUNOFF, CM
C     EVAPO  = ANNUAL (SEASONAL) EVAPOTRANSPIRATION, CM
C     ERN    = SURFACE RETENTION, CM
C     G      = GRAVITATIONAL INFILTRATION PARAMETER
C     SIGRF  = CAPILLARY INFILTRATION PARAMETER
C     W      = RATE OF CAPILLARY RISE FROM THE WATER TABLE, CM/HR
```

```
C      CDF    = CUMULATIVE DISTRIBUTION OF YD
C
C
C
C
       REAL MTB,MTR,MH,MI,MU,M,N,K1,NU,MUC
       INTEGER SWITCH
       DIMENSION ZPA(500),FZ(500),YD(500),NAME(20)
       REAL*8 FAC(900),ZPAD(500),VTOT,MUCD,AKD
       COMMON FAC
C
       IO=6
       INP=5
       WRITE(6,566)
 566   FORMAT('1', ' INPUT STATION NAME ')
       READ(5,76)NAME
76     FORMAT(20A4)
C
C*************************************
C
C      ENTER CLIMATIC PARAMETERS
       WRITE(6,567)
 567   FORMAT('1', ' INPUT PAM,MUC,MU,MH,MTR,MTB,TAU,MI ')
       READ(5,*)PAM,MUC,MU,MH,MTR,MTB,TAU,MI
       WRITE(6,568)
 568   FORMAT('1', ' INPUT AK,AKV,BMM,EPR,HO,TA,WT ')
       READ(5,*)AK,AKV,BMM,EPR,HO,TA,WT
C
C      ENTER SOIL PARAMETERS
       WRITE(6,569)
 569   FORMAT('1', ' INPUT N, M, K1,SI1,DSO ')
       READ(5,*)N,M,K1,SI1,DSO
C
C
C      ENTER CDF STOPPING CRITERIA
       WRITE(6,570)
 570   FORMAT('1',' INPUT CYU,CYL,BYU,BYL ')
       READ(5,*)CYU,CYL,BYU,BYL
C
C*************************************
C
C
C      COMPUTE LOG OF V FACTORIAL
C
       DO 30 J=1,900
       VTOT=0.0D0
```

```
      DO 40 IV=1,J
 40   VTOT=VTOT+DLOG(DFLOAT(IV))
      FAC(J)=VTOT
 30   CONTINUE
C
C*********************************************************************
C
C     COMPUTE M RELATED CONSTANTS
      C=3.+2./M
      FIC=10.0**(0.66+0.55/M+0.14/(M*M))
      DI=C-1./M-1.
      DE=2.+1./M
      D2=DE+2.
C
C******************************
C
C
C     COMPUTE THE CAPILLARY RISE
      BK1=K1
      BZ= 1. + 1.5/(M*C-1.)
      WW=BZ*BK1*(SI1/WT)**(M*C)
      W=WW*3600.
C
C
C
C****************************************
C
      WRITE(6,883)
 883  FORMAT(' ENTER CLIMATE/SOIL PROPERTIES')
      WRITE(6,77)NAME
 77   FORMAT(' ',20A4)
      WRITE(IO,1003)EPR,MTB,MTR,TAU.TA.K1.M.N.MH.MI.PAM.W.HO,
     1AK,WT,BMM,SI1,MU,AKV,MUC
 1003 FORMAT(' EPR=',F10.4/' MTB=',F10.4/' MTR=',F10.4/' TAU='
     1,F10.4/' TA =',F10.4/' K1 =',E10.4/' M =',F10.4/' N  ='
     2,F10.4/' MH =',F10.4/' MI =',F10.4/' PAM=',F10.4/
     3' W  =',F10.4/' HO =',F10.4/' AK =',F10.4/' WT =',E10.4/
     4' BMM =',F10.4/' SI1=',F10.4/' MU =',F10.4/' AKV = ',F7.2/
     5' MUC =',F10.4/)
      WRITE(6,777)
 777  FORMAT(5X,'BMM',5X,' PA',7X,'SO',5X,'J(E)',8X,'E',6X,'RSA',
     16X,'RGA',4X,'EVAPO',4X,'ERN',11X,'G',7X,'SIGRF',8X,'YIEP')
C
C****************************************
C
C---- COMPUTE WATER CONSTANTS
```

```
C      SUT=SURFACE TENSION                                              WAT01390
C      NU = VISCOSITY                                                   WAT01400
C      GAMSW = SPECIFIC WEIGHT                                          WAT01410
       CALL WATCN(TA,SUT,NU,GAMSW)                                      WAT01420
C                                                                       WAT01430
C****************************************                               WAT01440
C                                                                       WAT01450
C      COMPUTE CLIMATIC PARAMETERS                                      WAT01460
       PA=PAM                                                           WAT01470
       BM=BMM                                                           WAT01480
       BETA=1./(24.*MTB)                                                WAT01490
       DELTA=1./(24.0*MTR)                                              WAT01500
       ETA=1./MH                                                        WAT01510
       ALPHA=1./MI                                                      WAT01520
       EPP=EPR*MU*MTB*24.                                               WAT01530
C                                                                       WAT01540
C****************************************                               WAT01550
C                                                                       WAT01560
C      COMPUTE SURFACE RETENTION CONSTANTS                              WAT01570
       IF(HO.EQ.0.0)HO=1.E-7                                            WAT01580
       AL=AK /MH                                                        WAT01590
       BLE=BETA/(AL*EPR)                                                WAT01600
       ALH=AL*HO                                                        WAT01610
       BHE=BETA*HO/EPR                                                  WAT01620
       GK1=1.-GAMT(AK,ALH)/GAMMA(AK)                                    WAT01630
       GK2=GAMT(AK,ALH+BHE)/GAMMA(AK)                                   WAT01640
       GK3=1.-GK1*EXP(-BHE)-GK2/(1.+BLE)**AK                            WAT01650
       GK4=ALH                                                          WAT01660
       GK5=BHE                                                          WAT01670
       ERRV=ERSV(GK4,GK5,AKV,AK)                                        WAT01680
C                                                                       WAT01690
C******************************                                         WAT01700
C                                                                       WAT01710
C      COMPUTE SOIL RELATED CONSTANTS                                   WAT01720
C                                                                       WAT01730
       FIED=FIE(DE)                                                     WAT01740
       ECNST=2.*BETA*N*BK1*SI1/(3.1415927*M*EPR*EPR)*FIED*3600.         WAT01750
       SIGC=3000.*N*ETA*ETA*BK1*SI1/(3.1415927*DELTA*M)                 WAT01760
C                                                                       WAT01770
C******************************                                         WAT01780
C                                                                       WAT01790
       SO=1.E-2                                                         WAT01800
       DS=0.1                                                           WAT01810
       ITER=1                                                           WAT01820
       SWITCH=1                                                         WAT01830
       IP=1                                                             WAT01840
```

```
C
C**************************************
C
C      COMPUTE SURFACE RETENTION
       ERN=(EPR/BETA)*((1.-BM)*GK3+BM*AKV*ERRV)
C
C****************************
C
C
 113   CONTINUE
C
C      COMPUTE EVAPOTRANSPIRATION
       EPA=EPP*(1.-BM*(1.-AKV))
 10    E=ECNST*SO**D2
       EJE=EJ(E,BHE,ALH,BM,AKV,AK,W,EPR,BETA,BLE)
   12  ET =EPA*EJE
       ET1 =ET/PAM
C
C**************************************
C
C----  COMPUTE THE GROUNDWATER RUNOFF
       RGA=TAU*BK1*SO**C*86400.-365.*24.*W
       IF(RGA.LT.0.0)RGA=0.0
C
C**************************************
C
C----  COMPUTE THE SURFACE RUNOFF
       FIID=FII(DI,SO)
       SIGRF=(SIGC*FIID*(1.-SO)*(1.-SO))**0.333333
       G=ALPHA*BK1*0.5*(1.+SO**C)*3600.-ALPHA*W
       RS1=EXP(-G-2.*SIGRF)*GAMMA(SIGRF+1.)*SIGRF**(-SIGRF)
       IF(RS1.LT.0.0)RS1=0.
       RSA=RS1*PAM
C
C****************************
C
       IF(SWITCH.EQ.2)GO TO 25
C
C      COMPUTE WATER BALANCE COMPONENTS
       AWBAL=PA*(1.-RS1)-ET-RGA
       IF(ITER.EQ.1)GO TO 15
       IF(ABS(AWBAL).LE.PA*0.002)GO TO 50
       IF(AWBAL*OLD.LE.0.0)DS=-DS*0.5
   15  OLD=AWBAL
       SOLD=SO
       SO=SO+DS
```

```
      IF(SO.GT.1.)GO TO 254
      IF(SO.LE.0.)GO TO 254
      ITER=2
      GO TO 10
254   SO=0.0
      EJE=0.0
      GO TO 253
C
 50   SOM=SO
      SWITCH=2
      GO TO 113
 25   PA=ET+RSA+RGA
      YIELD=RSA+RGA
      YIEP=YIELD/PAM
      PAZ=PA
      ZPA(IP)=PA/PAM
      YD(IP)=YIEP
C********************************
C
 253  WRITE(6,3127)BM,PAZ,SO,EJE,E,RSA,RGA,ET,ERN,G,SIGRF,YIEP
 3127 FORMAT(2F8.2,4F9.4,2F9.2,F7.2,3E12.4)
C
C*******************************************************************
C
C     EVALUATE THE CDF OF YIELD
C
      ZPAD(IP)=DBLE(ZPA(IP))
      MUCD=DBLE(MUC)
      AKD=DBLE(AK)
      CALL CPREC(AKD,MUCD,ZPAD(IP),FZ(IP))
      IF(SO.GT.SOM)GO TO 123
      IF(FZ(IP).LT.CYL)SO=SOM+2*DSO
      IF(YD(IP).LT.BYL)SO=SOM+2*DSO
      IP=IP+1
      SO=SO-DSO
      GO TO 113
 123  CONTINUE
      IF(FZ(IP).GT.CYU)GO TO 234
      IF(YD(IP).GT.BYU)GO TO 234
      SO=SO+DSO
      IP=IP+1
      GO TO 113
C
C********************************************************************
C
C
```

```
 234  IPT=IP                                                            WAT02770
C                                                                       WAT02780
C     REARRANGE THE ARRAYS IN DECENDING ORDER                           WAT02790
C                                                                       WAT02800
      CALL SORT(FZ,IPT)                                                 WAT02810
      CALL SORT(YD,IPT)                                                 WAT02820
      WRITE(6,150)(I,FZ(I),YD(I),I=1,IPT)                               WAT02830
 150  FORMAT(//'    I            CDF          YD'//(I5,3X,2F11.4))      WAT02840
      STOP                                                              WAT02850
      END                                                               WAT02860
C***********************************************************************WAT02870
C                                                                       WAT02880
      SUBROUTINE WATCN(TA,SUT,NU,GAMSW)                                 WAT02890
C     COMPUTE THE WATER CONSTANTS AT A GIVEN TEMPERATURE TA             WAT02900
      REAL NU,NUT                                                       WAT02910
      DIMENSION SUTT(11),NUT(11),GAMST(11)                              WAT02920
      DATA SUTT/75.6,74.9,74.2,73.5,72.0,72.1,71.4,70.7,70.0,69.3,68.6/,WAT02930
     1 NUT/17.93E-3,15.18E-3,13.09E-3,11.44E-3,10.08E-3,8.94E-3,8.E-3,  WAT02940
     27.2E-3,6.53E-3,5.97E-3,5.94E-3/,                                  WAT02950
     3GAMST/0.99987,0.99999,0.99973,0.99913,0.99823,0.99708,0.99568,0.99WAT02960
     4406,0.99225,0.99025,0.98807/                                      WAT02970
      IF(TA.GT.50.)GO TO 10                                             WAT02980
      ITA=IFIX(TA*0.2)+1                                                WAT02990
      FRAC=TA-FLOAT(5*(ITA-1))                                          WAT03000
      ITA1=ITA+1                                                        WAT03010
      SUT=(SUTT(ITA1)-SUTT(ITA))*0.2*FRAC+SUTT(ITA)                     WAT03020
      NU=(NUT(ITA1)-NUT(ITA))*0.2*FRAC+NUT(ITA)                         WAT03030
      GAMSW=((GAMST(ITA1)-GAMST(ITA))*0.2*FRAC+GAMST(ITA))*980.         WAT03040
      RETURN                                                            WAT03050
   10 SUT=SUTT(11)                                                      WAT03060
      NU=NUT(11)                                                        WAT03070
      GAMSW=GAMST(11)*980.                                              WAT03080
      RETURN                                                            WAT03090
      END                                                               WAT03100
C                                                                       WAT03110
C***********************************************************************WAT03120
C                                                                       WAT03130
      FUNCTION ERSV(GK4,GK5,AKV,AK)                                     WAT03140
C     THIS FUNCTION COMPUTES THE VEGETATED SURFACE RETENTION            WAT03150
      GK6=GK4*AKV                                                       WAT03160
      GK7=1.-GAMT(AK,GK6)/GAMMA(AK)                                     WAT03170
      GK8=GK5/GK6                                                       WAT03180
      GK9=GAMT(AK,GK6+GK5)/GAMMA(AK)                                    WAT03190
      ERSV=1.-GK7*EXP(-GK5)-GK9/(1.+GK8)**AK                            WAT03200
      RETURN                                                            WAT03210
      END                                                               WAT03220
```

```
C
C*****************************************************************************
C
      FUNCTION FIE(D)
C
C     THIS FUNCTION COMPUTES THE DESORPTION COEFFICIENT BY MEANS OF A
C     LOGARITHMIC INTERPOLATION OF THE VALUES GIVEN IN THE TABLE Y.
C
      DIMENSION Y(7)
      DATA Y/0.18,0.11,0.077,0.056,0.044,0.034,0.029/
      IF(D.GE.8.)GO TO 10
      X=D-1.
      I=IFIX(X)
      FRAC=X-FLOAT(I)
      Y1=ALOG(Y(I))
      Y2=ALOG(Y(I+1))
      FIE=EXP((Y2-Y1)*FRAC+Y1)
      RETURN
   10 FIE=0.029
      RETURN
      END
C
C*****************************************************************************
C
C
C*****************************************************************************
C
C*****************************************************************************
C
      FUNCTION FII(D,SO)
C
C     THIS FUNCTION COMPUTES THE SORPTION COEFFICIENT BY MEANS OF AN
C     EMPIRICAL FIT
C
      POW=1.425-0.0375*D
      DEN=D*(1.-SO)**POW+1.666667
      FII=1./DEN
      RETURN
      END
C
C
C*****************************************************************************
C
      FUNCTION EJ(E,BHE,ALH,BM,AKV,AK,W,EPR,BETA,BLE)
      LOGICAL UNFL
      WEP=W/EPR
```

```
      BMKV=BM*AKV
      GAMK=GAMT(AK,ALH)/GAMMA(AK)
      GAMA15 = GAMMA(1.5)
      CE=1.E10
      DBB=1.+BMKV-WEP
      BB=(1.-BM)/DBB+(BM*BMKV+(1.-BM)*WEP)/(2.*DBB*DBB)
      GAMK1=GAMT(AK,ALH+BHE)/GAMMA(AK)
      UNFL=BMKV.GT.0.0
      IF(BMKV-WEP.NE.0.0)CC=0.5/(BMKV-WEP)**2
      ES3=0.0
      ES4=0.0
      IF(UNFL)CE=CC*E
      UNFL=CE.LT.100.
      BE=BB*E
      IF(UNFL)GO TO 25
      GAMCE=GAMA15
      GO TO 27
25    GAMCE = GAMT(1.5,CE)
27    GAMBE = GAMT(1.5,BE)
      IF(UNFL)ES3=-EXP(-CE-BHE)*(WEP-BMKV-SQRT(2.*CC)*E)
      ES0=GAMK -(1.+BLE)**(-AK)*GAMK1*EXP(-BE)
       ES1=(1.-GAMK)*(1.-EXP(-BE-BHE)*(1.-WEP+BMKV+SQRT(
     22.*BB)*E)
     3+ES3
     4+SQRT(2.*E)*EXP(-BHE)*(GAMCE-GAMBE))
      ES5=(1.+BLE)**(-AK)*GAMK1
      ES6=EXP(-BE)*(WEP-BMKV-SQRT(2.*BB)*E)
      IF(UNFL)ES4=-EXP(-CE)*(WEP-BMKV-SQRT(2.*CC)*E)
      ESJ=ES0+ES1+ES5*(ES6+ES4+SQRT(2.*E)*(GAMCE-GAMBE))
      EVJ=AKV
30    EJ=((1.-BM)*ESJ+BM*EVJ)/(1.-BM*(1.-AKV))
      RETURN
      END
C
C*******************************************************************
C
      FUNCTION GAMT(A,X)
C
C     THIS FUNCTION COMPUTES THE TRUNCATED GAMT DISTRIBUTION
C     ACCORDING TO THE ALGORITHM IN THE NATIONAL BUREAU OF STANDARDS
C     'HANDBOOK OF MATHEMATICAL TABLES'
       IF(X.EQ.0.0)GO TO 40
      IF(X.GE.100.)GO TO 50
      IO=6
      SUM=1./A
      AN=1.0
```

```
      OLD=SUM
   33 OLD=OLD*X/(A+AN)
      IF(OLD/SUM-1.E-6)20,10,10
   10 AN=AN+1.
      SUM=SUM+OLD
      IF(AN-300.)33,33,12
   12 WRITE(IO,100)X
  100 FORMAT('0NO CONVERGENCE FOR X=',E20.5)
   20 GAMT=EXP(A*ALOG(X)+ALOG(SUM)-X)
      GO TO 60
40    GAMT=0.0
      GO TO 60
   50 GAMT=GAMMA(A)
   60 RETURN
      END
C
C*****************************************
C
C
      SUBROUTINE CPREC(K,W,Z,PROB)
C     THIS PROGRAM COMPUTES THE CDF OF NORMALIZED PRECIPITATION.
C     A LOGARITHMIC TRANSFORM IS USED IN ORDER TO AVOID EXPONENT
C     OVERFLOW OR UNDERFLOW PROBLEMS.
C     Z        = NORMALIZED PRECIPITATION
C              = SEASONAL PRECIPITATION / MEAN SEASONAL PRECIPITATION
C     W        = MEAN NUMBER OF STORMS IN THE RAINY SEASON
C     M,VM     = MEAN NUMBER OF STORMS
C     V        = THE 'V'TH STORM
C     VMAX     = MAXIMUM NUMBER OF STORMS ALLOWED IN THE EVALUATION OF
C                CDF OF Z = 3*M
C     K        = PARAMETER OF GAMMA DISTRIBUTION
C     FAC      = LOG OF 'V' FACTORIAL
C     DLGAMA   = LOG OF GAMMA DISTRIBUTION
C     GAMLID   = LOG OF INCOMPLETE GAMMA DISTRIBUTION
C     PROB     = CDF OF NORMALIZED PRECIPITATION
C     EPS      = RELATIVE ERROR IN COMPUTING THE INCOMPLETE GAMMA DISTRIB
C              = RELATIVE ERROR IN COMPUTING THE CDF OF Z
C
C
      REAL*8 FAC(900)
      REAL*8 X,A,DLOG,DLGAMA,GAMLID,EPS
      REAL*8 M,K,W,Z,PROBD
      REAL*8 XOLD,XSUM,SUM1,SUM2,TOT,VTOT,VOLD,VNEW
      INTEGER V,VM,VMAX
      COMMON FAC
C
```

```
C
C
C     INITIALIZING VALUES
C
      M=W
      EPS=0.0001D0
      VM=IFIX(SNGL(M))
      VMAX=IFIX(SNGL(3.*M))
 3    X=M*K*Z
      II =0
      JJ=1
      SUM1=0.0D0
      SUM2=0.0D0
 13   V=VM-II
      IF(V.EQ.0)GO TO 500
 23   IF(V.EQ.VMAX)GO TO 600
C
C     COMPUTE LOG INCOMPLETE GAMMA DISTRIBUTION
C
      A=DFLOAT(V)*K
      XOLD=1.0D0/A
      XSUM =1.0D0/A
      I=1
 100  XOLD=(XOLD/(A+I))*X
      XSUM=XSUM+XOLD
      IF((XOLD/XSUM).LE.EPS)GO TO 200
      I=I+1
      GO TO 100
 200  CONTINUE
      GAMLID=A*DLOG(X)-X+DLOG(XSUM)-DLGAMA(A)
C
C     COMPUTE THE SUMMATION OF ALL V TERMS
C
      VOLD=DFLOAT(V)*DLOG(M)-FAC(V)+GAMLID-M
      IF(VOLD.LE.-170.D0)VOLD=-170.D0
      VNEW=DEXP(VOLD)
      IF(V.GT.VM)GO TO 800
      SUM1=SUM1+VNEW
      IF((VNEW/SUM1).LE.EPS)GO TO 500
      II=II+1
      GO TO 13
 500  V=VM+JJ
      IF(V.GT.900)GO TO 600
      GO TO 23
 800  SUM2=SUM2+VNEW
      IF((VNEW/SUM2).LE.EPS)GO TO 600
```

```
      JJ =JJ+1
      GO TO 500
C
C     COMPUTE CDF OF NORMALIZED PRECIPITATION
C
 600  IF(M.GT.170.D0)M=170.D0
      PROBD=SUM1+SUM2+DEXP(-M)
      PROB=SNGL(PROBD)
      RETURN
      END
C
C******************************************************************
C
C     THIS PROGRAM ARRANGES THE INPUTS IN ASCENDING ORDER
C
      SUBROUTINE SORT(P,N)
      REAL P(N),LARGE
      N1=N-1
      DO 100 I=1,N1
      JJ=N-I
      DO 100 J=1,JJ
      IF(P(J).GE.P(J+1))GO TO 100
      LARGE=P(J)
      P(J)=P(J+1)
      P(J+1)=LARGE
 100  CONTINUE
      RETURN
      END
```